The functional role of Mcl-1 in the dynamics of mitotic cell fate.

A thesis submitted to the University of Manchester for the degree of Doctor of Philosophy in the Faculty of Life Sciences

2015

Olivia Alice Sloss

Table of Contents

Word Count: 46, 797 words.

List of Figures

List of Tables

Table of Abbreviations

γH2A.X	H2A Histone family, member X
AID	Auxin-inducible degron
APC/C	Anaphase promoting complex/cyclosome
ATP	Adenosine Triphosphate
Bad	Bcl-2-associated death promoter
Bak	Bcl-2 homologous antagonist killer
Bax	Bcl-2-associated X protein
Bcl-2	B-cell lymphoma-2
Bcl-xL	B-cell lymphoma-extra large
Bid	BH3 interacting-domain death agonist
Bik	Bcl-2 interacting killer
Bim	Bcl-2-like protein 11
BMF	Bcl-2 modifying factor
Bub1	Budding uninhibited by benzimidazoles 1
Bub3	Budding uninhibited by benzimidazoles 1
DiM	Death in Mitosis
BSA	Bovine Serum Albumin
Caspase	Cysteine-aspartic proteases
Cdc20	Cell Division Cycle 20
Cdk1	Cyclin dependent kinase-1
CHX	Cycloheximide
CRISPR	Clustered regularly interspaced short palindromic repeats
dNTP	Deoxynucleotide triphosphates
Erk-1	Extracellular-signal regulated kinase-1
Fbw7	F-box/WD repeat-containing protein 7
GDP	Guanosine diphosphate
GFP	Green Fluorescent Protein
GSK-3	Glycogen Synthase Kinase 3
GST	Glutathione S-transferase
GTP	Guanosine triphosphate
IAA	Indole-3-acetic acid
JNK	c-Jun N-terminal kinase
Mad1	Mitotic arrest deficient-1
Mad2	Mitotic arrest deficient-2
MAPK	Mitogen-activated protein kinases
MCC	Mitotic checkpoint complex
Mcl-1	Myeloid cell Leukemia 1
mMcl-1	Mouse Myeloid cell Leukemia 1
Mdm2	Mouse double minute 2
MEF	Mouse embryonic fibroblasts
MEK	Mitogen-activated protein kinase kinase
MOMP	Mitochondrial outer membrane permeabilisation
MULE	Mcl-1 ubiquitin ligase E3
Noxa	Phorbol-12-myristate-13-acetate-induced protein 1
Plk-1	Polo-like kinase-1
PmD	Post mitotic Death
proTAME	Pro Tosyl-L-Arginine Methyl Ester
Puma	P53 upregulated modulator of apoptosis
qPCR	Quantitative Polymerase Chain Reaction

RNAi	RNA interference
SAC	Spindle assembly checkpoint
SCF	Skp, Cullin, F-box containing complex
SDS	Sodium dodecyl sulfate
Sgo1	Shugoshin-like 1
siRNA	Small interfering RNA
Tir1	Transport inhibitor response-1
TPR	Tetratricopeptide
TRF2	Telomeric repeat-binding factor-2
WT	Wild type

Abstract

The University of Manchester
Olivia Alice Sloss
Doctor In Philoshophy (Ph.D).
The functional role of Mcl-1 in the dynamics of mitotic cell fate.
27-09-2015

Drugs that alter microtubule dynamics are often used in chemotherapy regimes in combination with other agents in order to treat various cancers. Despite the success over many years, there remain problems in toxicity, resistance and predictability to the drugs. In order to overcome these problems, there is a need to gain an understanding of how these drugs kill cancer cells in cell culture. As microtubule function is particularly important for chromosome movement in mitosis, cells treated with these agents cause a mitotic arrest through activation of the spindle assembly checkpoint. Following induction of a mitotic arrest, cells can escape this arrest (mitotic slippage) or undergo mitotic death, determined in part by the response of the apoptotic network. Levels of an anti-apoptotic protein, Mcl-1, are often lost over time in mitosis. Using time-lapse analysis on a cell line unable to escape the mitotic arrest, this thesis shows that Mcl-1 protein contributes to cell death both in mitosis and the subsequent interphase in response to microtubule toxin, taxol. This suggests that inhibiting Mcl-1 may increase the efficacy of anti-mitotic agents. In addition, mitotic cell lines prone to mitotic slippage were found to have higher levels anti-apoptotic protein, Bcl-xL, in comparison to Mcl-1, indicating one way in which these cells can cope with loss of Mcl-1 during mitosis.

Secondly, an evaluation of the contribution of the previously identified interaction between Mcl-1 and mitotic E3 ligase complex, the APC/C-Cdc20, to the rate of mitotic death and mitotic slippage was assessed. Inhibition of APC/C-Cdc20 activity or mutation of a Mcl-1 motif (RxxL) thought to engage with the APC/C-Cdc20 complex did not have a substantial effect on Mcl-1 degradation or mitotic death, thereby questioning the functional significance of this interaction. However, it appears that Mcl-1 protein levels can influence the rate of mitotic slippage and this influence was affected via Mcl-1's RxxL motif within Mcl-1. This suggests that Mcl-1 protein may delay mitotic slippage via substrate competition for the APC/C-Cdc20 complex with Cyclin B1, whose degradation is required for mitotic exit. Further analysis of this effect showed that this interaction may not be a universal effect. This together with the specific functional effect on mitotic slippage rather than mitotic death, suggests that this is an indirect effect caused by network interference between the components of the death and slippage pathways.

Declaration

I hereby declare that no portion of the work referred to in the thesis has been submitted in support of an application for another degree or qualification of this or any other university or other institute of learning

Copyright notice

i. The author of this thesis (including any appendices and/or schedules to this thesis) owns certain copyright or related rights in it (the "Copyright") and he has given The University of Manchester certain rights to use such Copyright, including for administrative purposes.

ii. Copies of this thesis, either in full or in extracts and whether in hard or electronic copy, may be made only in accordance with the Copyright, Designs and Patents Act 1988 (as amended) and regulations issued under it or, where appropriate, in accordance with licensing agreements which the University has from time to time. This page must form part of any such copies made.

iii. The ownership of certain Copyright, patents, designs, trade marks and other intellectual property (the "Intellectual Property") and any reproductions of copyright works in the thesis, for example graphs and tables ("Reproductions"), which may be described in this thesis, may not be owned by the author and may be owned by third parties. Such Intellectual Property and Reproductions cannot and must not be made available for use without the prior written permission of the owner(s) of the relevant Intellectual Property and/or Reproductions.

iv. Further information on the conditions under which disclosure, publication and commercialisation of this thesis, the Copyright and any Intellectual Property and/or Reproductions described in it may take place is available in the University IP Policy (see http://documents.manchester.ac.uk/DocuInfo.aspx?DocID=487), in any relevant Thesis restriction declarations deposited in the University Library, The University Library's regulations (see http://www.manchester.ac.uk/library/aboutus/regulations) and in The University's policy on Presentation of Theses

Acknowledgements

Firstly I would like to thank my supervisor Stephen for his patience, relentless curiousity, integrity and enthusiasm for great science; I have learnt more than I ever thought possible. Thanks to my advisor Mark Ashe for all his help over the years. In addition, thank you to Andrew Holland for the myc-Tir1 cell lines for the AID-auxin work and Peter March for his help within the Bioimaging facility.

To my incredible dysfunctional lab family both past and present: you crazy lot have made the last three years most unforgettable. Thank you in particular to the wonderful Anthony who has provided me with an organised lab, amazing cakes, squash games, tolerance towards my madness and the occasional subtle innuendo! Thanks to Dr Topham/Ham Sandwich/Kazakhstan/genuine inspiration who has been my comedy centre, moral compass, and most importantly, my mentor. To Ailsa “alright” Bennett: you have been tolerated. Thank you to Louisa for putting up with sitting next to me for the last 3 years and to Sam for her constant energy and optimism. I send a special thank you to Michael Smith for his assistance with the RNA analysis and for being my scientific partner in crime over the years. Thank you to the rest of the Taylor team and members of adjacent labs for providing a great scientific environment. Also a massive thank you to Manchester Korfball Club for their support and friendship over the years. Finally to my role models, my parents for their unwavering encouragement and belief.

My gratitude goes out to the Wellcome Trust programme for funding.

This thesis is dedicated to my Nan,

Alice Caldecourt.

1. Chapter 1: Introduction

1.1 Overview

Cancer is a complex, multi-faceted cellular disease that causes uncontrolled and deregulated cell growth and division within an organism. It is estimated that around 400 people per 100,000 in the UK were diagnosed with cancer in 2011 (Cancer Research UK). Cancer cells have evolved the ability to channel fundamental cellular processes to confer a selective advantage over the environment they inhabit. As well as uncontrolled proliferation, resisting cell death is a well-established cancer hallmark and has provided an evolutionary step for cancer cells to handle major deregulated intrinsic changes in cell growth, genomic instability as well as sustaining resistance to therapy. Because of this, the need to find drugs that can both inhibit proliferation and drive cell death of cancer cells are at the forefront of medical research.

A plant screening program between 1961 and 1980 identified a bark extract compound from the pacific yew tree, *Taxus brevifolia*, that displayed anti-tumourigenic properties both *in vitro* and in tumour-mouse models (Schiff et al., 1979; Wani et al., 1971; Weaver, 2014). With annual global sales reaching over $4.5 billion, this drug has enjoyed huge success within the cancer-drug market. From extensive studies in cell culture, it is known that the class of drugs that taxol belongs to, the vinca alkaloids, are able to 'arrest' cells in the mitotic phase and in doing so they block the cell's ability to divide and continue through the cell cycle. This cell cycle arrest would thereby hinder the ability of cancer cells to sustain chronic proliferation and survival. This rationale has provided the basis of basic research into understanding how these drugs function on a molecular level. Additionally, since the discovery of the vinca alkaloids, the drugs have been used not only as agents to target tumours in cancer patients but have also been utilised for decades as an essential tool to understand the fundamental biology of mitosis in the laboratory.

Success of these drugs in patients however, is hampered by a variety of side effects. An important step to limit these side effects is by enhancing the ability of existing drugs to kill tumour cells so that a lower drug concentration can be administered. Additionally, as with most cancer

therapies, tumours exhibit a variety of resistance phenotypes in response to anti-mitotic drugs. Furthermore, the developments of recent technologies that allow the use of single-cell whole-population analysis have alluded to large-scale heterogeneity that exists both between and within tumours in terms of the ability to resist drug-induced cell death. A major factor that determines the efficiency of cell death is the balance between the pro- and anti-death components of the intrinsic apoptotic death network. Understanding the basic biology that underlies how the death network responds to anti-mitotic drug treatment and identifying how the apoptotic network provides resistance to these mitotic drugs may allow (1) prediction of patients that will respond best to the anti-mitotics and (2) improvement of efficacy through combination therapy.

This introduction aims to outline the current understanding into the way in which anti-mitotic drugs function as well as highlight the way in which the apoptotic network balance responds during an enforced mitotic arrest. To do this I will firstly provide a detailed explanation of the regulation of mitosis and how anti-mitotic drugs affect normal cell division.

Secondly, I will assimilate and evaluate current theories based on cell culture studies about how cells respond to the drugs on a molecular level, how these drugs can eventually lead to cell death and how these ideas may be exploited in a therapeutic setting. Finally, I will focus on a protein that this thesis will concentrate on, anti- apoptotic protein Mcl-1, and how it is involved in defining the cells' drug response.

1.2 Mitosis

Cell division (mitosis) is fundamental to the evolution and functioning of complex multicellular organisms. Mitosis provides an environment that allows the cell to segregate its duplicated genome and intracellular contents into two daughter cells. This process therefore enables proliferation and growth of cell populations as well as propagation of genetically identical cells, be that cells that normally function within an organism or those that abnormally function such as cancer cells. To ensure accurate transfer of genetic material, mitotic cells contain controls that inhibit division until accurate segregation can be achieved. It is these controls that are exploited by anti-mitotic drugs. This chapter aims to outline the process of mitosis and the controls in order to help understand how cells respond to these drugs.

1.2.1 Introduction to mitosis

In comparison to other characterized stages of the cell cycle (G1, G2 and S phase) (Figure 1.1A), the mitotic phase displays distinct morphological intracellular dynamics easily recognizable under the microscope (Figure 1.1B). As such, the term ‘mitoses was coined by Walther Flemming as early as 1881 by visualising longitudinal spitting of chromosomes (“threads”) during cell division (Flemming, 1881). The dynamic movement of chromosomes in mitosis has since been used to define and describe the various mitotic stages. Early mitosis is initiated in prophase during chromosome condensation, which is then followed by nuclear envelope breakdown in prometaphase, thus allowing the chromosomes to engage with the mitotic apparatus. At metaphase, sister chromatids align at the central region of the cell and detach from each other during the transition into anaphase, where separated sister chromatids are pulled simultaneously to opposite poles of the cell. To complete mitosis, the segregated sets of chromosomes begin to de-condense and are packaged into two daughter nuclei in telophase. Finally, cell division is mediated by cytokinesis when the cell membrane invaginates and ‘pinches’ off to separate the cytoplasm and all other cellular components.

Inaccurate segregation of the duplicated genome in mitosis leads to cells with an unbalanced number of chromosomes, known as chromosome instability. Chromosome staining

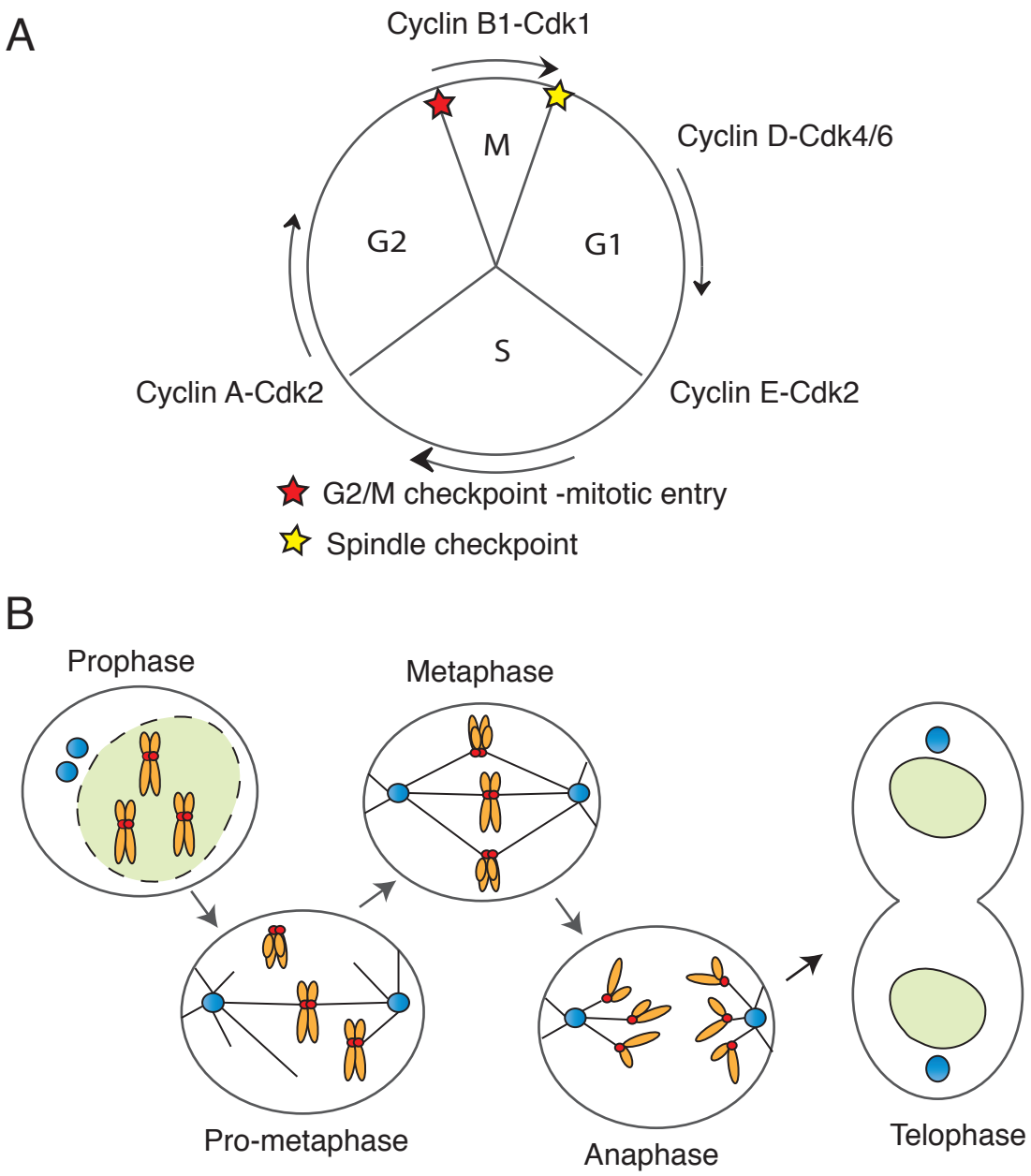

Figure 1.1. The Cell Cycle and Mitosis
(A) Cells cycle through rounds of cell division that can be broken up into distinct stages. Chromosomes are replicated during S phase and segregated in M phase, otherwise known as mitosis. These phases are separated in eukaryotic somatic cells by gap phases G1 and G2.
(B) The dynamic morphological changes during the stages of mitosis.

techniques (karyotyping) revealed that chromosome instability is a common occurrence within human cancers (Weaver and Cleveland, 2006). In addition, children born with various mental health conditions also display aneuploidy as a result of chromosome instability, for example those with Downs syndrome have an additional copy of chromosome 21 (Antonarakis et al., 2004). To safeguard against such irreversible errors in cells, chromosome segregation during the metaphase to anaphase transition is regulated by an internal control system, the spindle assembly checkpoint (SAC), that inhibits sister chromatid separation and cell division until all chromosomes are stably attached to the mitotic apparatus and are aligned at metaphase. The control of mitosis and chromosome movement by the SAC is fundamental to the fidelity of the transfer of genetic material.

1.2.2 Microtubule dynamics

Movement of condensed chromosomes around the cell during mitosis is mediated by attachments to long hollow cylindrical microtubule structures (Figure 1.2A). In mitosis, microtubules are organised within the cytoplasm by two multi-protein structures named centrosomes that associate with the minus end of the microtubules, creating a mitotic spindle structure. A single centrosome becomes duplicated in late G1 and each centrosome localises to opposite ends of the cell during prometaphase. Microtubules dynamically elongate and retract from these organising centres through the rapid association and dissociation of α-tubulin and β-tubulin heterodimers at the plus end, a characteristic known as dynamic instability. Tubulin heterodimers polymerise microtubules in a GTP-bound conformation, creating a 'GTP-cap' that is stable and enables end growth (Desai and Mitchison, 1997). However, upon tubulin binding, GTP becomes hydrolysed to GDP, changing its conformation and creating a strained structure that without the GTP cap, causes tubulin dissociation and microtubule catastrophe (Alushin et al., 2014). Thus, dynamic instability is caused by gain and loss of a 'GTP cap' structure at the plus end of microtubules.

Dynamic instability is particularly rapid during mitosis and enables 1) 'search and capture' mechanism for bi-attachment to chromosomes (each sister chromatid attached to a

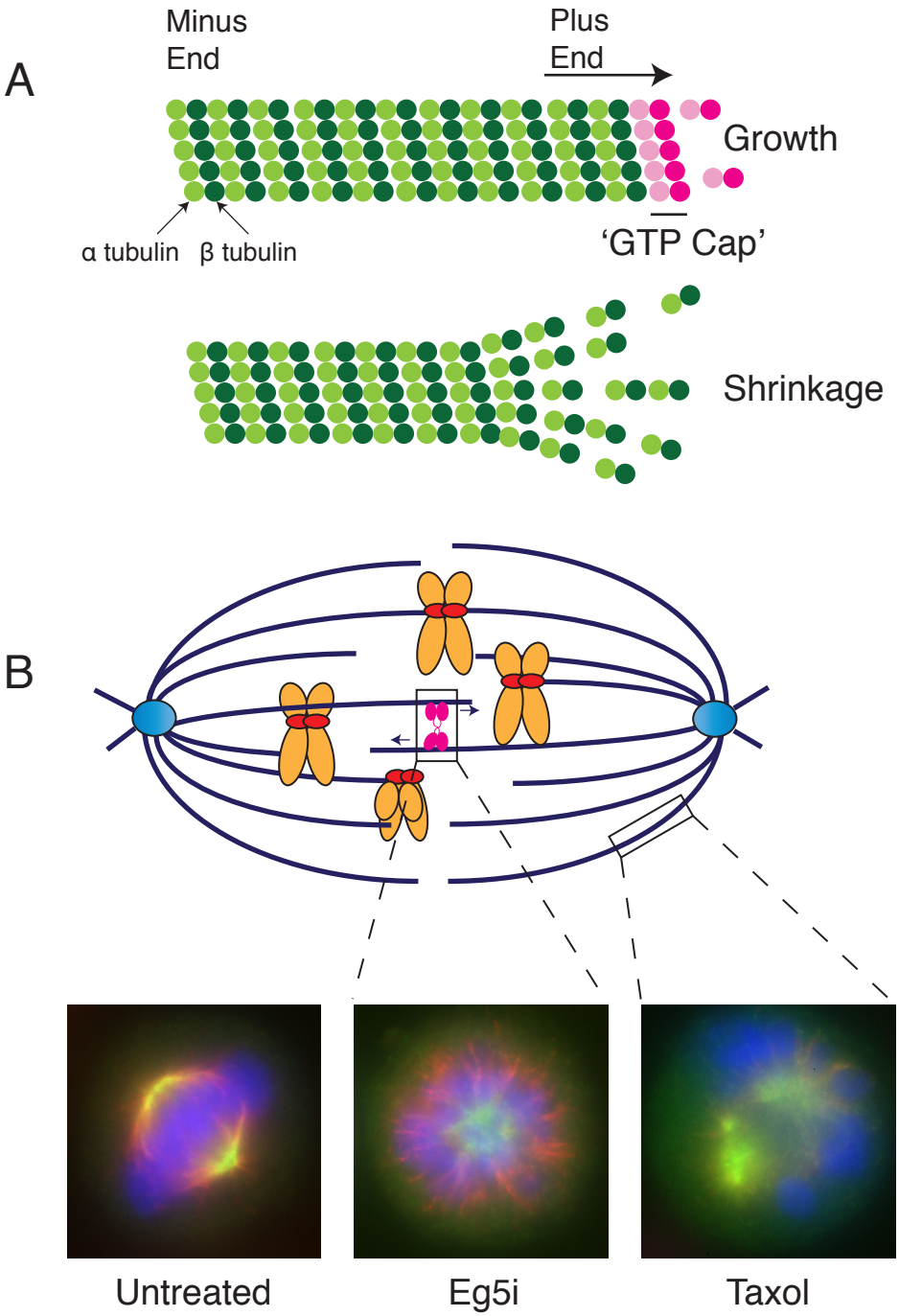

Figure 1.2. Microtubule dynamics and anti-mitotic drugs
(A) Dynamic instability of microtubules. Microtubules elongate following polymerisation of GTP-bound tubulin dimers at the plus end, forming a 'GTPcap'. When the rate of polymerisation is less than the rate of GTP hydrolysis, the cap is lost and the microtubule undergoes catastrophe.
(B) In mitosis under normal conditions, microtubules form a bipolar spindle. Eg5 is a kinesin required for centrosome separation by pushing apart microtubules originating from opposite poles. When Eg5 is inhibited, centrosome separation is supressed, characterised by a monopolar spindle. Inhibition of microtubule dynamics by addition of taxol results in an abnormal spindle. Pictures were taken with the help of Dr Anthony Tighe.

microtubule originating from opposite spindle poles), 2) the coordinated movement of chromosomes onto the metaphase plate and 3) the rapid movement of segregated chromatids at anaphase to opposite spindle poles, aided in part by the association of a variety of stabilising and destabilising proteins (Cross and McAinsh, 2014). As previously mentioned, it is important that separation of sister chromatids does not occur prematurely to ensure accurate segregation of the genome sets to opposite spindle poles. If anaphase is initiated before this time, unattached chromosomes would be unable to migrate towards the correct spindle pole, causing missegregation. In addition to this, during metaphase, kinetochores can become incorrectly attached, either by attachments of both chromatids to the same spindle pole (syntelic) or one kinetochore bound to microtubules from both poles (merotelic). Incorrect attachments can result in both sister chromatids migrating to the same spindle pole or chromatid breakage of lagging chromosomes that become trapped in the cytokinesis furrow (Godek et al., 2014).

The attachment status of a chromosome is monitored at the kinetochore: complex multi-protein structures assembled at the centromeric region of each sister chromatid. They comprise of around 80 different proteins, grouped into complexes that form the inner kinetochore that recognises and binds the centromere by interactions with CENP-A, a histone isotype, and the outer kinetochore (the KMN network comprising of Ndc80, Mis12 and Knl1) that interacts with microtubules (Foley and Kapoor, 2013). Kinetochore proteins are regulated by phosphorylation by aurora B kinase which destabilizes incorrect microtubule attachments (Lampson et al., 2004; Welburn et al., 2010). Bi-attachment of chromosomes increases tension and the distance between the centromere and the outer kinetochore network, suppressing aurora B-mediated phosphorylation of kinetochore proteins, and stabilising interactions leading to inhibition of the SAC and mitotic exit (Lampson and Cheeseman, 2011; Liu et al., 2009).

1.2.3 Control of Cyclin B1-Cdk1

Control of the cell cycle is mediated by several Cyclin-dependent kinases (Cdks) that require activation through association with a Cyclin co-factor protein (Figure 1.1A)(Hochegger et al., 2008). Cyclin binding drives a conformational change in Cdks that leads to alignment of residues required for enzyme catalysis in the active site (Jeffrey et al., 1995). The Cyclin

B1/Cdk1 complex, otherwise known as the maturing-promoting factor, was identified in *Xenopus* oocytes as a kinase complex made up of two proteins sufficient to direct an interphase-arrested cell into metaphase (Lohka et al., 1988). In mammalian cells, both Cdk1 and Cyclin B1 are essential genes and importantly Cdk1 activity is sufficient to drive mammalian cell cycles (Brandeis et al., 1998; Santamaría et al., 2007). The Cyclin B1/Cdk1 complex directly phosphorylates substrates that facilitate bipolar spindle assembly, organelle fragmentation, centrosome separation, and cytoskeleton rearrangement, as well as regulating mitotic exit and cytokinesis mechanisms (Blangy et al., 1995; Crasta et al., 2006; Estey et al., 2013; Nigg, 1995). For example, Cdk1 phosphorylates proteins GRASP65 and nuclear lamins that drive Golgi and nuclear envelope disassembly respectively (Dessev et al., 1991; Wang et al., 2003). Therefore, controlling Cyclin B1/Cdk1 activity is fundamental to mitosis.

Mitotic events are controlled by the regulation of the Cyclin B1/Cdk1 complex kinase activity at two checkpoints controlling entry into mitosis (G2/M transition) and mitotic exit (spindle assembly checkpoint (SAC)). Activation of Cyclin B1/Cdk1 at mitotic entry is controlled firstly by increased expression of Cyclin B1 and also by post-translational modification of Cdk1 (Nurse, 1990). Translation of Cyclin B mRNA is necessary for cells to enter into prophase (Minshull et al., 1989). Cyclin B1 expression increases during S phase and peaks shortly before entry into mitosis, providing sufficient co-activator levels for Cdk1 (Hwang et al., 1995). Once bound, Cyclin B1/Cdk1 is activated by phosphorylation on T161 by Cdk1 activating kinase (CAK) and dephosphorylation of T14 and T15 by Cdc25 (Lindqvist et al., 2009; Lolli and Johnson, 2005).

Following sister chromatid separation in anaphase, timely inactivation of Cdk1 activity through loss of Cyclin B1 is required for mitotic exit and cell cycle progression (Figure 1.3) (Oliveira et al., 2010; Rattani et al., 2014). Expression of a non-degradable Cyclin B1 mutant displayed an inability to initiate cytokinesis, disassemble the mitotic spindle, decondense chromosomes, and assemble the nuclear envelope (Wheatley et al., 1997). Reversal of Cyclin B1/Cdk1 phosphorylation reactions is performed by phosphatases for a successful exit from mitosis (Wurzenberger and Gerlich, 2011). In mammalian cells PP2A phosphatases have been identified as proteins that counteract Cdk1 activity

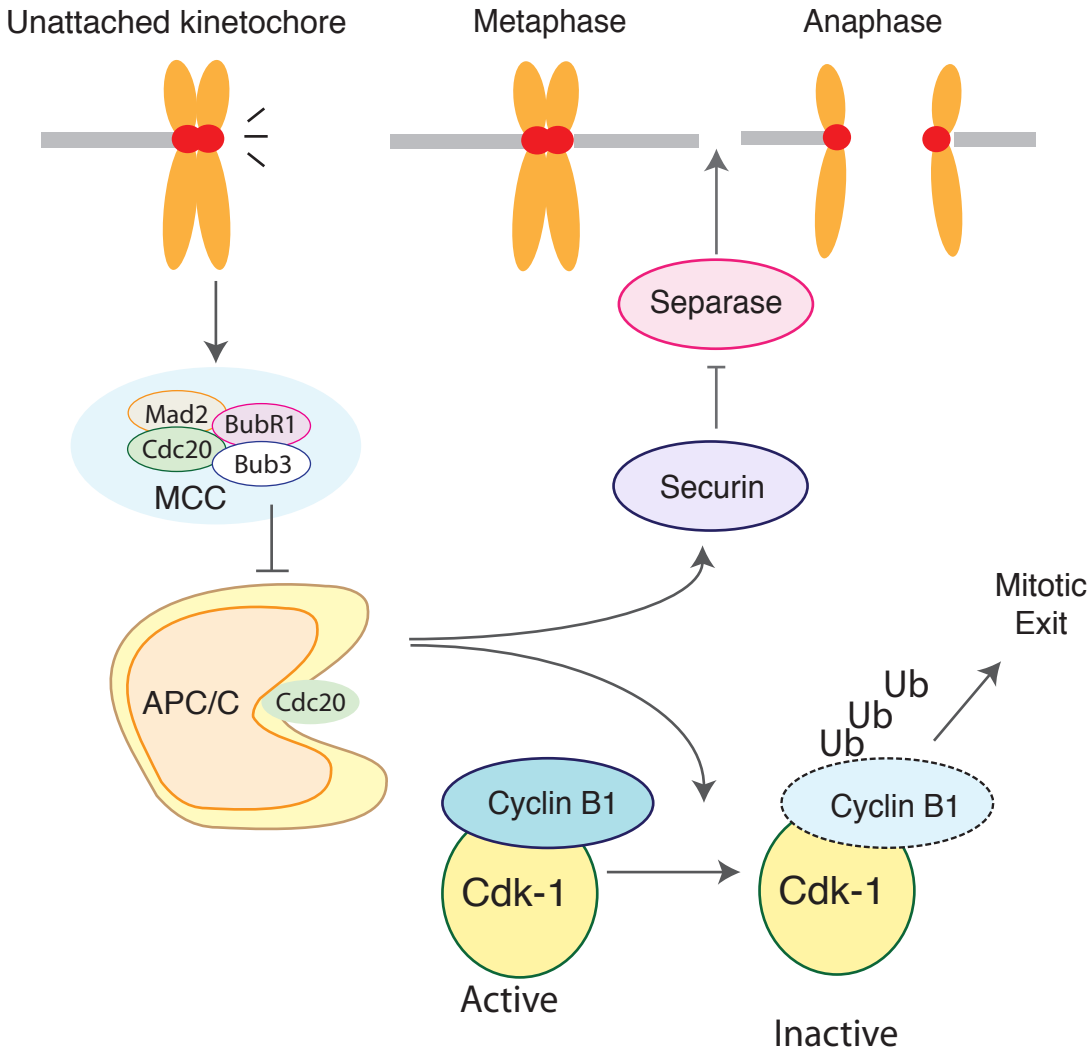

Figure 1.3. The role of APC/C-Cdc20 in mitotic exit.
An unattached kinetochore drives the formation of diffusable spindle checkpoint complex that inhibits the E3 ligase APC/C-Cdc20. Upon correct kinetochore attachment, this signal ceases, activating APC/C-Cdc20. This causes degradation of Cyclin B1 and securin, alleviating separase to cleave cohesin complexesforcing sister chromatid separation and anaphase.

(Agostinis et al., 1992; Mochida et al., 2009; Schmitz et al., 2010). PP2A-B55 is regulated indirectly through mitotic-phosphorylation by microtubule-like Serine/threonine kinase-like protein (MASTL or Greatwall kinase in Drosophila) that is activated by Cdk1 (Álvarez-Fernández et al., 2013; Burgess et al., 2010; Castilho et al., 2010; Manchado et al., 2010; Voets and Wolthuis, 2010). Upon anaphase onset when Cyclin B1 is degraded and Cdk1 activity is low, the phosphatases are rapidly activated to drive mitotic exit and reassembly of the nucleus in the daughter cells.

Loss of Cyclin B1 is driven by rapid ubiquitin-mediated proteolysis at the onset of anaphase (Glotzer et al., 1991). Ubiquitin is a small 8.5-kDa protein that becomes covalently attached to lysine residues within proteins targeted for degradation (Hershko, 2005). Following the addition of one ubiquitin molecule, subsequent ubiquitin molecules are added, creating a polyubiquitin chain that is recognized by the proteasome (Tokumoto et al., 1997). The proteasome is an ATP-dependent proteolytic holoenzyme complex that recognizes ubiquitinated proteins and cleaves the targeted polypeptides into shorter peptide sequences within its core (Finley, 2009). The transfer of ubiquitin onto targeted proteins is mediated by the concerted action of three enzymes (Burger and Seth, 2004; Hershko et al., 1983). In short, ubiquitin is transferred to an E2 ubiquitin conjugating enzyme in an ATP-dependent manner mediated by an E1 enzyme (ubiquitin-activating enzyme). Finally an E3 ligase enzyme is required to transfer the ubiquitin molecule from the E2 protein to the target substrate. Specifically, Cyclin B1 ubiquitination is catalyzed by E3 ligase APC/C at metaphase onset (Clute and Pines, 1999; Irniger et al., 1995; King et al., 1995; Sudakin et al., 1995). The APC/C is composed of 19 subunits forming a large 1.22 MDa protein complex that requires binding of co-activators Cdc20 and Cdh-1 to aid target substrate binding (Fang et al., 1998; Kramer et al., 1998; Sivakumar and Gorbsky, 2015; Weinstein et al., 1994). Co-activators interact with TPR motifs that are abundant on APC/C subunits Apc3 and Apc8 (Chang et al., 2014). APC/C-Cdc20 interaction is stabilised at the end of prophase by phosphorylation of the APC/C (Golan et al., 2002; Kraft et al., 2003; Kramer et al., 2000). Following stabilisation, Cyclin B1/Cdk1 is recruited to the APC/C complex in prometaphase aided by MASTL and Cdk cofactor proteins, Cks, but is not ubiquitinated until metaphase onset (Voets and Wolthuis, 2015; Van Zon et al., 2010). Additionally, two E2

enzymes that donate ubiquitin onto mitotic degradation substrates have been identified: E2S (or UbcH10), that initiates mono-ubiquitination, and Ube2S that catalyses ubiquitin chain elongation on lysines (Garnett et al., 2009; Jin et al., 2008; Williamson et al., 2009, 2011). Targeted ubiquitin-mediated proteolysis provides an efficient and precise way to regulate specific protein abundance as it is irreversible, thus stopping the re-occurrence of early mitotic events driven by Cdk1 activity and pushing the cell through the cell cycle in a singular direction.

1.2.4 APC/C function in anaphase

The metaphase to anaphase transition is a crucial point of cell division where accuracy is key to ensure production of two genetically identical daughter cells by sister chromatid separation (Figure 1.3). Inhibition of the APC/C both arrests the cell in mitosis and stalls sister chromatid segregation, showing that the APC/C also functions by targeting proteins for degradation that maintain sister chromatid cohesion in addition to Cyclin B1 (Holloway et al., 1993; Irniger et al., 1995). Sister chromatids are encircled at the centromeric region in mitosis by a multimeric protein ring structure, the cohesin complex that is bound and protected by phosphorylated Sgo1 complexed with phosphatase PP2A (Peters et al., 2008; Kitajima et al., 2006; Liu et al., 2013). Upon bi-attachment of the chromosome, Sgo1 becomes dephosphorylated and re-localises the complex away from the inner centromere (Higgins, 2013). At the onset of anaphase, cohesion subunit Scc1 is cleaved by a protease (separase) that alleviates the sister chromatids, allowing segregation to opposite spindle poles by microtubules (Uhlmann et al., 1999, 2000). Separase is inhibited by Securin, which, like Cyclin B1, is targeted by APC/C-Cdc20 for degradation following satisfaction of the spindle checkpoint (Hagting et al., 2002). Thus, by degrading Securin in a timely-manner, the APC/C also promotes anaphase by releasing separase to breakdown the interactions between the sister chromatids.

1.2.5 The Spindle Assembly Checkpoint

Cells are unable to enter anaphase until all chromosomes are bi-attached to microtubules and are aligned at metaphase. Indeed, lack of bi-attachment of just one chromosome is sufficient to delay anaphase onset (Rieder et al., 1994). Because of the

stochastic nature of microtubule movement, the time it can take for kinetochore attachment of all sister chromatids can be variable, causing a delay in chromosome-microtubule attachment. The delay in anaphase onset is mediated by the spindle assembly checkpoint (SAC) that monitors and responds to problems in kinetochore attachment by halting the onset of anaphase through inhibition of APC/C activity and Cyclin B1 degradation (Clute and Pines, 1999). The kinetochore acts as sensory machinery for bi-attachment that sends molecular signals to the checkpoint to indicate the attachment state. These inhibitory signals communicate a lack of correct bi-attachment, which halts anaphase onset. The unattached chromosomes then activate the SAC causing a prolonged mitotic arrest.

Genetic screens of *Saccharomyces cerevisae* identified components whose inhibition impaired the ability to halt the cell cycle in response to microtubule disruption (Hoyt et al., 1991; Li and Murray, 1991). These screens identified BubR1, Bub1, Bub3, Mad1 and Mad2. Mammalian counterparts of these proteins have since been discovered (Li and Benezra, 1996; Taylor and McKeon, 1997; Taylor et al., 1998). The precise mechanism of the spindle checkpoint is reviewed in detail in Lara-Gonzalez *et al.* 2012 (Lara-Gonzalez et al., 2012). To summarise, Bub1 is recruited to the kinetochore via Knl1 in early prophase and Mad2 bound to Mad1 is recruited to the unattached kinetochore via Mps1 activity (Hewitt et al., 2010; Lara-Gonzalez et al., 2012). The Mad1-Mad2 complex can change the conformation of another Mad2 molecule, allowing it to engage with Cdc20. The resulting Mad2-Cdc20 complex at the kinetochores binds sub-complex BubR1-Bub3 to generate the mitotic checkpoint complex MCC (De Antoni et al., 2005). The MCC binds and inhibits the APC/C by blocking ubiquitination of APC/C substrates including Cyclin B1 and Securin (Sudakin et al., 2001). When full chromosome alignment is achieved, the signal activating the SAC at the kinetochore ceases. The MCC is disassembled, mediated in part by $p31^{comet}$ and APC/C subunit APC15 that extracts Mad2 from free MCC and MCC bound to the APC/C respectively (Mansfeld et al., 2011; Uzunova et al., 2012; Westhorpe et al., 2011). Disassembly of the MCC liberates co-factor Cdc20 causing activation of APC/C for progression into anaphase.

1.2.6 APC/C degrons.

As well as Cyclin B1 and Securin, the APC/C mediates the degradation of many other mitotic substrates. These include Cyclin A, Nek2A, Cdc20, Plk1 and the aurora kinases (Sivakumar and Gorbsky, 2015). Specificity is provided by specific motifs within the substrate proteins that facilitate both binding of substrates to the APC/C and degradation. Many substrates contain a D-box motif (RXXL) or a KEN-box motif (KEN) (Pfleger and Kirschner, 2000). Both Cyclin B1 and Securin contain a well-characterised D-box in the N-terminus, and the RxxL destruction box of Cyclin B1 is highly conserved between species (Glotzer et al., 1991; Pines, 2011). In addition, structural studies show that other non-canonical sequences may be able to bind APC/C-Cdc20 sites in a similar way to D-box and KEN-box substrates (He et al., 2013). These motifs interact with the WD40 domain present in APC/C co-activators Cdc20 and Cdh1 which then position the substrate protein near the catalytic core of the APC formed by subunits Apc2 and Apc11 for ubiquitin transfer (Barford, 2015; Chao et al., 2012; Kraft et al., 2005). This method of binding is utilized by the SAC as two MCC components, Mad3 and BubR1, contain KEN boxes that appear to act as 'pseudosubstrates', thus blocking the binding and recognition of KEN-box and D-box containing substrates ubiquitinated by the APC/C, including Cyclin B1 and Securin, and halting anaphase onset (Acquaviva et al., 2004; Chao et al., 2012; Lara-Gonzalez et al., 2011).

However, these motifs are not always necessary for APC/C-mediated degradation. For example some *bona fide* APC/C substrates containing D-box and KEN-box motifs, Cyclin A and Nek2A, are degraded during a mitotic arrest despite activation of the spindle checkpoint (den Elzen and Pines, 2001; Geley et al., 2001; Hayes et al., 2006). Cyclin A has a high affinity for Cdc20 and out-competes checkpoint components for APC/C-Cdc20 binding via its N-terminus, an interaction mediated by Cks (Di Fiore and Pines, 2010; Wolthuis et al., 2008). Nek2a is a kinase involved in centrosome separation (Fry et al., 1998). Nek2a degradation during a mitotic arrest is dependent on an MR tail and only when mutated does Nek2a degradation depend on checkpoint release mediated by a KEN box motif (Boekhout and Wolthuis, 2015). MR or IR motifs are also present on other APC/C substrates that aids binding to the APC/C (Hayes et al., 2006; Sedgwick et al., 2013; Vodermaier et al., 2003). The existence of several mechanisms by

which the APC/C binds and degrades substrates highlights the potential for discovery of other substrates destined for APC/C-mediated degradation in mitosis.

1.3 Anti-mitotic drugs

Studying the control of mitosis has proven vital from a basic cell biology perspective to the understanding of fundamental organismal processes. More recently, this kind of research has attracted researchers from a translational cancer biology background for several reasons. Firstly, an abnormal mitosis resulting in missegregation of a chromatid leads to aneuploidy, a known characteristic of many tumours (Lengauer et al., 1998). More relevant to this thesis, the second reason lies in understanding how cancer cells respond to cancer treatments used in the clinic. Several routine drugs that target microtubules have been shown in cell culture to arrest cells specifically in M phase. Understanding how these cells move from a mitotic arrest to cell death or cell resistance in response to these drugs may aid the development of better therapies as well as predict those who are able to respond.

1.3.1 Mechanism of anti-mitotic drugs

Anti-mitotic drugs affect microtubule dynamics by binding to tubulin either within the microtubule structure or in a monomer form. These anti-mitotics have displayed anti-tumourogenic properties, and as such are used in the clinic to treat a variety of cancers such as breast, ovarian, non-small cell lung cancer and Kaposi's sarcoma (Chang et al., 2003; Dumontet and Jordan, 2010; Markman, 2008; Pajk et al., 2008). These drugs are normally administrated in combination with a range of other targeted and DNA intercalating chemotherapies including herceptin, epirubicine and carboplatin (Glück et al., 2012; Markman, 2008; Stickeler et al., 2011). Despite extensive use of these drugs, it is unclear exactly how they work in patient tumours, and much current knowledge has been built on *in vitro* studies (Gascoigne and Taylor, 2009; Weaver, 2014). Part of this is due to the function of microtubules in many cellular processes including protein trafficking, cell migration and mitosis, meaning it is difficult to pinpoint the exact process where anti-mitotic drugs have the most impact (Komlodi-Pasztor et al., 2011; Mitchison, 2012). However, microtubule dynamics are particularly rapid during mitosis and as such, addition of anti-mitotics to cells in culture causes spindle defects (Figure 1.2B)(Rusan et al., 2001; Saxton et al., 1984; Zhai et al., 1996). This results in a prolonged mitotic arrest induced by activation of

the SAC, as the drugs affect the ability of microtubules to search and bind kinetochores, resulting in unattached chromosomes (Jordan et al., 1993, 1991).

Anti-mitotics can be classified into two groups: microtubule-destabilising agents and microtubule-stabilising agents. At high concentrations, drugs in the first group (nocodazole, colchicine and the Vinca alkaloids-vinblastine and vincristine amongst others) inhibit microtubule polymerization and growth. At lower concentrations, these drugs, like the microtubule-stabilising agents, suppress microtubule dynamics (Jordan and Wilson, 2004). These drugs can bind either along the microtubule itself or directly to soluble tubulin. Whereas the Vinca alkaloids bind primarily at the ends of microtubules, structural analysis has mapped out the taxol binding site to β-tubulin within the inner surface of the microtubule (Alushin et al., 2014; Nogales et al., 1995). The binding of taxol causes hydrolyzed tubulin to adopt a conformation as if bound to GTP, thus reducing strain and mitotic catastrophe (Alushin et al., 2014). Unlike other drugs, paclitaxel treatment is not easily reversed, a property that may explain its success in the clinic, as cells accumulate the drug intracellularly over time (Jordan et al., 1996; Zasadil et al., 2014).

Despite the efficacy of these drugs, patients display a variety of severe side-effects including neutropeania and myeloid toxicity (Dumontet and Jordan, 2010) Most notably, neuropathy has been observed in patients, a damaging nerve condition resulting in problems to the sensory, motor and automatic nervous system. As a result, second-generation anti-mitotic drugs targeting alternative mitotic protein families including the aurora kinases, polo-like kinases and microtubule kinesins were developed, in the hope of targeting mitosis without inducing similar side effects in patients. However, these drugs have thus far failed to show positive results in clinical trials (Lens et al., 2010; Rath and Kozielski, 2012). Recently, several clinical trials using Eg5 inhibitors have shown good tolerance by patients (Gerecitano et al., 2013; Hollebecque et al., 2013; Jones et al., 2013; Wakui et al., 2014). Eg5 is a motor protein required for centrosome separation and inhibition of its activity results in a monopolar spindle, lack of tension at the kinetochore and a prolonged mitotic arrest (Figure 1.2B) (Blangy et al., 1995; Gascoigne and Taylor, 2008; Mayer et al., 1999). Eg5 is one of the kinesin-5 family that contain two pairs of motor proteins separated by a α helical coiled rod structure and each end interacts with microtubules protruding from the two centrosomes. Using ATP-hydrolysis, the motor protein

moves along the microtubule, forcing separation of the spindle poles and formation of a bipolar spindle (Kapitein et al., 2005; Rath and Kozielski, 2012). However, like the other second-generation anti-mitotics, Eg5 inhibitors have yet to show efficacy. Taken together, this could reflect a lack of understanding into exactly how anti-mitotics cause cancer cell toxicity. However, this may also expose the need for clinical trials that carefully select patients based on the genetic makeup to show efficacy for these drugs. For example, non-small-cell lung cancer patients containing mutations in the TK domain region of EGFR are more likely to respond to gefitinib and erlotinib (Gazdar, 2009).

1.3.2 Response to anti-mitotic drugs.

A prolonged mitosis, whereby the cell cannot achieve full chromosome alignment over time, may be caused naturally by the inability of the stochastic 'search and capture' nature of microtubules to efficiently and accurately bind the kinetochores, or can be caused artificially by the described anti-mitotic drugs. However, cells are unable to maintain this mitotic state indefinitely and eventually adopt one of several states (Figure 1.4). In the mid-2000s, several of these states following this prolonged arrest were identified using flow cytometry and western blotting. Whilst one group described death in mitosis (DiM) following anti-mitotic treatment, others observed cells exiting mitosis without dividing despite an intact SAC and therefore unattached chromatids, a phenotype named mitotic slippage (Rieder and Maiato, 2004; Weaver and Cleveland, 2005). Equally, overriding the SAC in the presence of anti-mitotics also leads to a similar phenotype (Taylor and McKeon, 1997). Mitotic slippage produces abnormal cells often characterised by the presence of multiple nuclei (Jordan et al., 1996). These 'slipped' cells can undergo different post-mitotic responses: post-mitotic death (PmD), arrest in interphase or carry on through multiple cell cycles (Rieder and Maiato, 2004). In response to agents that perturb mitosis, failure to undergo death in mitosis (DiM) and/or failure to efficiently engage post-mitotic responses can lead to proliferation of cells with highly abnormal genomes (Dewhurst et al., 2014; Fujiwara et al., 2005). A systematic analysis of 15 cell lines using time-lapse microscopy that took phase contrast images every 10 minutes (Figure 1.5A) showed that different cell lines have variable responses to both the same drug as well as different anti-mitotic drugs, highlighting the complexity of cell responses to anti-mitotic drugs (Gascoigne and Taylor, 2008).

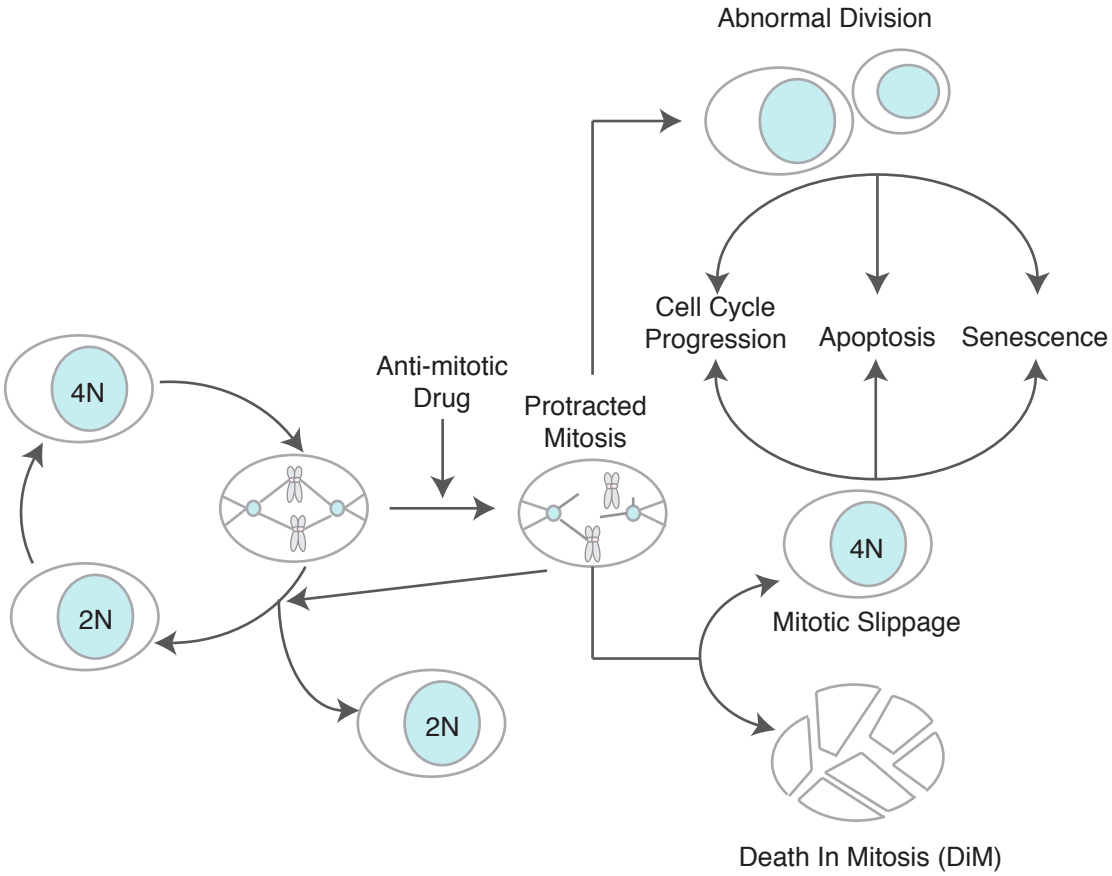

Figure 1.4. Cell Fate response to anti-mitotic drugs
Treatment of cells with anti-mitotics cause a protracted mitotic arrest. After a prolonged arrest, a cell can either commit to normal division, division, mitotic slippage or 'death-in-mitosis' (DiM). Following mitotic exit, a cellcan undertake a variety of post-mitotic responses: cell cycle progression, post-mitotic death (PmD) or senescence. Adapted from Gascoigne and Taylor 2009.

This analysis also utilised a single-cell approach that uncovered the varying cell heterogeneity toward drug response that exists within cell lines by evaluating the cell fate of 100 individual cells within each cell line population. This heterogeneity reflects the large-scale heterogeneity that exists within a tumour in patients that importantly plays a large role in conferring resistance to treatment (Burrell et al., 2013). Cell fate profiles are used as a way to visualise the intraline heterogeneity of cell fate within a population. These profiles are made up of individual lines signifying a single cell; the colour of the line depicts its fate and length of the line represents the amount of time the cell has taken to commit to that respective fate (Figure 1.5B). For example in a cell fate profile depicting RKO cells, all but two of the 100 cells analysed committed to DiM, each depicted by a single red line on the profile. Additionally, the time to DiM in each individual cell from the point of mitotic entry (T=0) can be measured (Figure 1.6A, right panel). Using a cell fate profile, it is easy to see that within a cell population, a variety of cell fates can be undertaken by different proportions of the cell populations. For example in this DLD-1 cell population treated with 0.1 μM taxol, 4 cells do not enter mitosis during the time period, 8 cells die before entering mitosis, 4 cells quickly commit to DiM, 8 cells divide and the rest commit to mitotic slippage (Figure 1.6A, left panel). Of the cells that slipped out of mitosis a variety of post-mitotic responses can be analysed. In the DLD-1 population, four cells re-entered a second mitosis and undertook DiM, 26 cells re-entered and slipped out of mitosis for a second time and the rest remained in interphase. However, it the HCT-116 cell line, many of the slipped cells commit to post-mitotic death (Figure 1.6A, middle panel). In addition, one can also use cell fate profiles to identify subtle population shifts towards one fate over another and can be used to accurately measure the kinetics of cell fate accumulation. This thesis routinely uses cell fate profiles as a way to not only observe the abundance of each cell fate response to anti-mitotic drugs and to also compare the rate that cells are able to commit to a fate.

Furthermore, by artificially delaying either DiM or mitotic slippage, the authors showed that cells contained the capacity to undertake either fate but the dominant fate in each cell line is caused by the rate of signalling to drive either phenotype. The competing networks model proposed that both DiM and mitotic slippage had a hypothetical threshold that the opposing signalling networks needed to attain during a prolonged mitotic arrest in order for the cell to

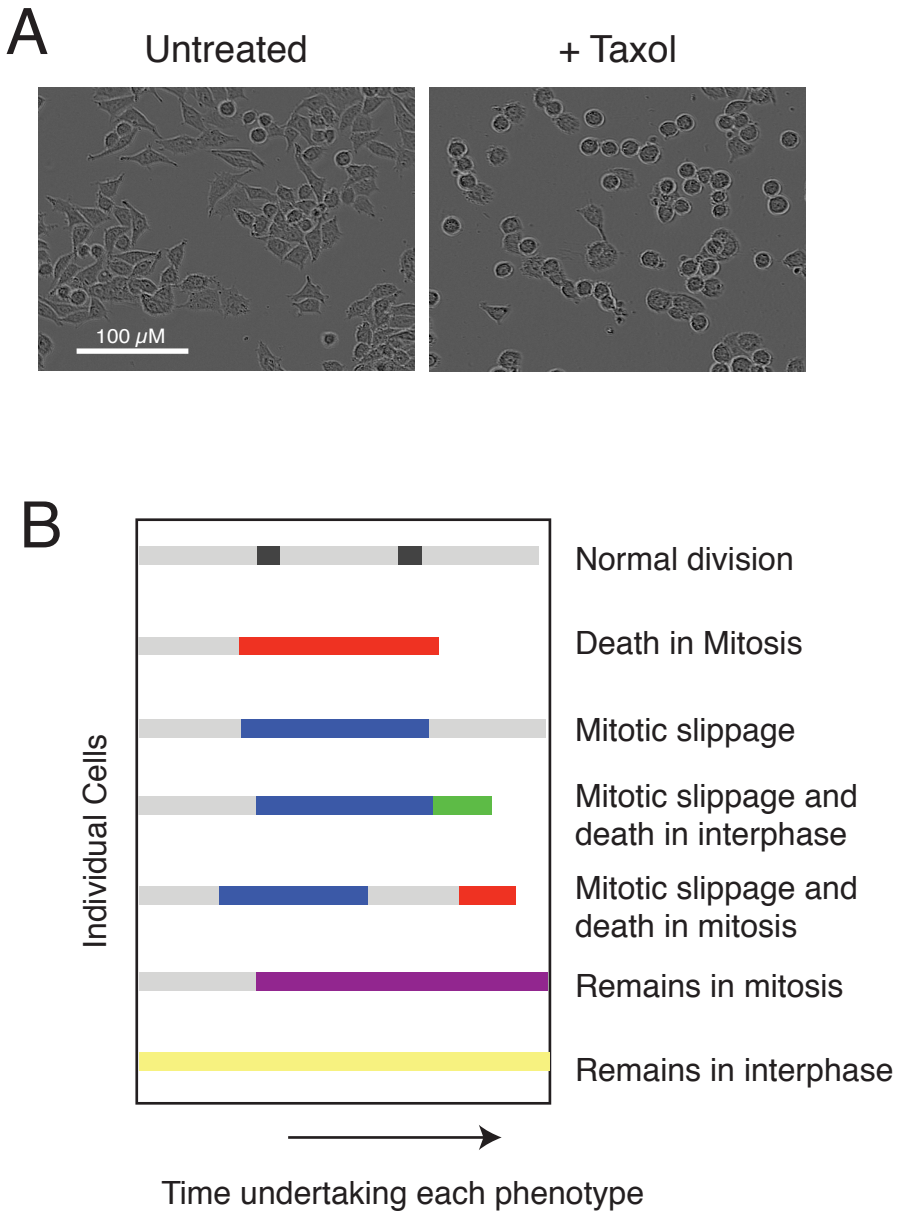

Figure 1.5 Creating cell fate profiles from time-lapse microcopy.
(A) Representative images of untreated (interphase, left) and taxol-treated (mitotic, right) RKO cells.
(B) Representative diagram of analysis of cell fate.

commit to the fate. The cell would therefore undertake the fate of the threshold that was reached first (Figure 1.6B). For example in the RKO cell line, the prediction is that the time to DiM is much faster than the time to mitotic slippage, hence why the majority of cells undertake the death in mitosis phenotype.

This model has since been used to explain both variations in drug responses between cell lines and within a cell line. As the genetic background can differ between cell lines, one can imagine that this influences the rate of signalling of both networks and the threshold required to breach. For example, the rate of mitotic slippage is slower in RKO cells than DLD-1 cells, hence why RKO cells are more able to undertake DiM due to an extended amount of time in which to do so. In contrast, it was shown that intra-cell variation was driven by non-genetic elements, meaning that differences in post-translational processes are likely to play a role in explaining the differences in the time to a particular fate of individual cells within a population. Since the competing networks model was first proposed, many post-transcriptional processes have been attributed as contributing factors to the rate of both networks. The rest of this introduction concentrates on the factors that contribute to the rates of both signalling networks.

1.3.3 Mitotic slippage and Cyclin B1 degradation

The factors influencing the rate of slippage are well defined. Slippage is characterised by residual Cyclin B1 degradation (Brito and Rieder, 2006). Overexpression of Cyclin B1 suppressed slippage and increased DiM in slippage-prone cells (Sakurikar et al., 2012). Conversely, Cdk1 inhibition reduced DiM in a death-prone cell line (Sakurikar et al., 2012). Using a tetracycline-induced reporter system, it was observed that cells that slipped out of mitosis displayed faster Cyclin B1 degradation kinetics than cells that died in mitosis (Gascoigne and Taylor 2008). Furthermore, a high destruction rate of mCherry fluorescent reporter fused to D-box, the motif within the N-terminus of Cyclin B1 recognised by the APC/C for ubiquitination, correlated with increased numbers of cells undergoing slippage in response to anti-mitotics (Gascoigne and Taylor, 2008; King et al., 1996). According to the competing networks model, in situations in which slippage is delayed, more time is also provided for the death signal to accumulate. Equally, in situations that accelerate Cyclin B1 degradation in a mitotic arrest, there

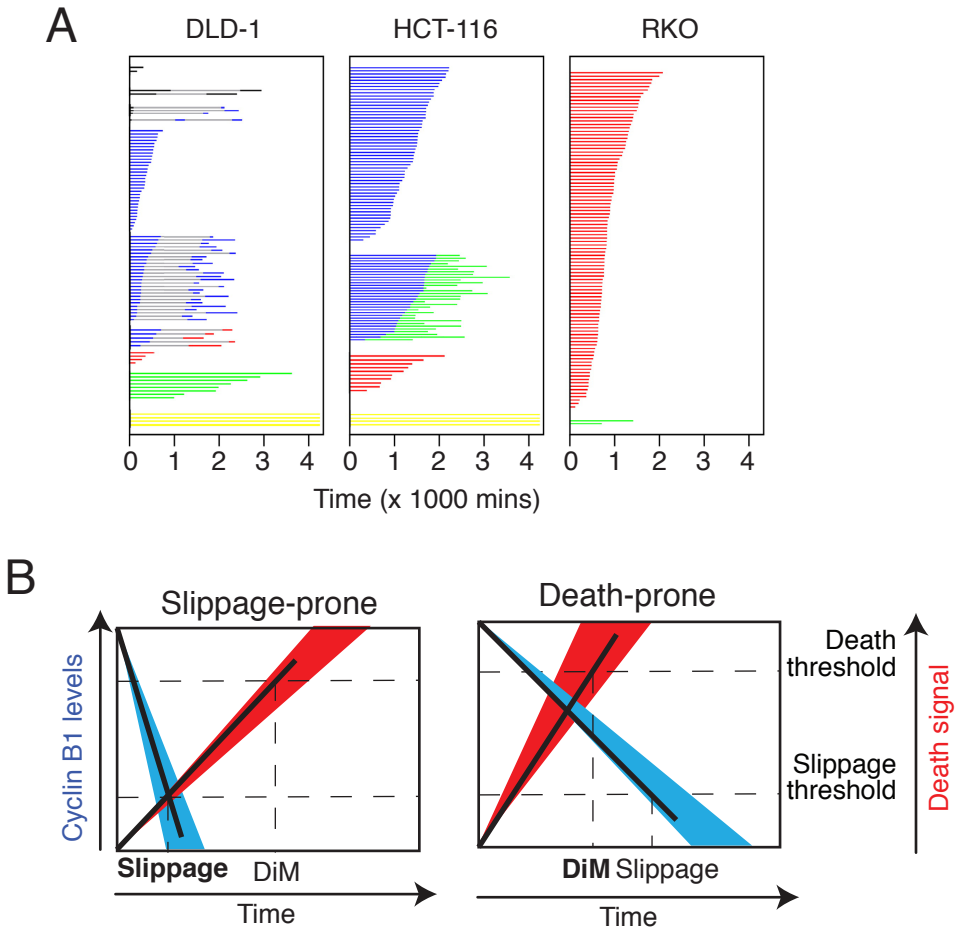

Figure 1.6. The Competing Networks Model
(A) Taken from Gascoigne and Taylor 2008, the panels represent cell fate profiles of the fate of 100 cells within DLD-1, HCT-116 and RKO cell lines treated with 0.1 μM taxol.
(B) The fate of a cell following a prolonged mitotic arrest is dictated by the relative rates of mitotic slippage (Cyclin B1 degradation) and death. Commitment to a fate is therefore dependent on which threshold is breached first. In death-prone cells, the death threshold is breached first and the opposite is true for slippage-prone cells Adapted from Gascoigne and Taylor 2008.

is less time for the death signal to accumulate and a greater proportion of cells will slip out of mitosis. A prime example of this is checkpoint override, and as such, SAC genes frequently manifest in anti-mitotic siRNA survival screens (Díaz-Martínez et al., 2014; Swanton et al., 2007; Topham et al., 2015; Tsui et al., 2009). Altogether this means that the rate of slippage is determined by the factors that control Cyclin B1 degradation.

Despite the presence of an active SAC signal, a primary factor in the rate of Cyclin B1 degradation is the rate of APC/C-Cdc20-mediated ubiquitination of Cyclin B1. Cdc20 depletion by RNAi completely abolished mitotic slippage and increased DiM, as residual Cyclin B1 degradation was no longer able to reach the slippage threshold (Huang et al., 2010, 2009; Sakurikar et al., 2012). Cdc20 is both targeted for degradation by the APC/C (followed by MCC disassembly by $p31^{comet}$) and is synthesized in mitosis, suggesting that Cdc20 turnover creates a small pool of newly-formed APC/C-Cdc20, causing residual Cyclin B1 degradation before SAC inhibition (Nilsson et al. 2008; Varetti et al. 2011; Westhorpe et al. 2011). Secondly, the net rate of ubiquitination of Cyclin B1 is dependent on the equilibrium between APC/C-Cdc20 activity and the activity of counteracting deubiquitinases. An shRNA screen found deubiquitinase USP44 (ubiquitin-specific protease 44) as a negative regulator of mitotic exit in response to taxol (Stegmeier et al., 2007). Finally, treatment of mitotic cells with the translation inhibitor cycloheximide accelerated slippage, as well as increased the rate of both Cyclin B1 and Cdc20 loss. Although not fully understood, this indicates that as well as Cdc20, Cyclin B1 is also synthesised in mitosis. This means that the rate of residual Cyclin B1 loss may depend in part on the rate of Cyclin B1 synthesis.

1.4 Apoptosis in Mitosis

The death-in-mitosis signal is less defined than the mitotic slippage signal. This is explained in part by the many mechanisms through which a cell can commit to death. These include necrosis, a form of cell death characterised by cellular swelling that is traditionally thought of as a non-regulated process of passive cell death (Elmore, 2012). However, little is known whether this plays a large physiological role in anti-mitotic-mediated cell death. More recently it was shown that reduced metabolic capacity activation of autophagy resulted in a reduction of mitochondria due to mitophagy, reduced ATP levels and increased mitotic cell death (Doménech et al., 2015).

Despite the many routes to cell death, several studies inhibiting the downstream components of the apoptotic pathway, the caspases, revealed the importance of the apoptotic network to DiM (Doménech et al., 2015; Gascoigne and Taylor, 2008; Shi et al., 2008). Furthermore, caspase staining of conditional Cdc20-null histological mouse samples suggests that apoptosis is an underlying factor driving cell death (Manchado et al., 2010). Therefore, to understand how anti-mitotics kill cells, an understanding of the apoptotic network and how it functions in mitosis is vital.

1.4.1 Introduction to apoptosis

The term apoptosis and the morphological definition was coined in 1971 and using electron microscopy and immunostaining techniques, researchers visualised the condensation and fragmentation of cytoplasmic and nuclear fragments into an apoptotic body, that was subsequently phagocytosed by neighboring cells (Fadeel and Orrenius, 2005). Programmed cell death through apoptosis has equipped tissues with the ability to regulate and maintain cell homeostasis. As such, many of the components of the apoptotic network were first identified during development studies in the nematode worm *Caenorhabditis elegans* (Elmore, 2012). The intrinsic apoptotic network has provided the cell with an ability to self-destruct in response to internal stresses and abnormalities. Whilst the effect of external signalling has not been ruled out, during a prolonged mitotic arrest, DNA damage and other intracellular stresses accumulate,

which signal to the intrinsic apoptotic machinery to co-ordinate the death response pathways. Furthermore, the ability of a cell to evade apoptosis became one of the original hallmarks of cancer (Hanahan and Weinberg, 2000). Since then, it has been shown that the physiological expression and function of several members of the apoptotic network are deregulated in human cancers (Adams and Cory, 2007; Beroukhim et al., 2010). A shift in the balance of the apoptotic network towards survival means that the network response is suppressed to abnormal/deleterious signals caused by accumulation of mutations. Furthermore, it makes cells less susceptible to cancer treatment attempts to induce cellular stresses. Understanding how the deregulated network responds to stresses will aid the development of targeted therapies. This section focuses on the molecular components of the apoptotic network and how the network responds to antimitotic drugs in cell culture.

1.4.2 The intrinsic apoptotic network

The apoptotic network is a regulated signalling balance of pro- and anti-apoptotic Bcl-2 family proteins (Figure 1.7). These signals eventually converge on the mitochondria and can result in mitochondrial outer membrane permeabilisation (MOMP) and the release of cytochrome C into the cytoplasm. Cytosolic cytochrome C is necessary to drive the downstream apoptotic program by causing the processing of a cysteine protease family of proteins, the caspases, whose cleavage catalysis irreversibly commits a cell to cell death (Liu et al., 1996). MOMP is caused by the homo- and heterodimerisation of pro-apoptotic effectors Bak and Bax. Under normal conditions, Bak and Bax localization fluctuates between the cytoplasm and the mitochondrial membrane but accumulates at the membrane upon apoptotic stimulation (Schellenberg et al., 2013; Todt et al., 2015). Upon receipt of pro-death signalling, Bak and Bax translocate to the mitochondrial membrane and oligomerise, forming channels that permeabilise the mitochondrial membrane.

To stop unwanted caspase activation and mitosis, the Bcl-2 anti-apoptotic proteins (Bcl-2, A1, Mcl-1, Bcl-W and Bcl-xL) bind and sequester Bak and Bax, blocking MOMP. These proteins form a hydrophobic groove out of several α helices that is bound by the BH3 domain of Bak and Bax (Chipuk et al., 2010). This repressive interaction between Bak/Bax and the Bcl-2

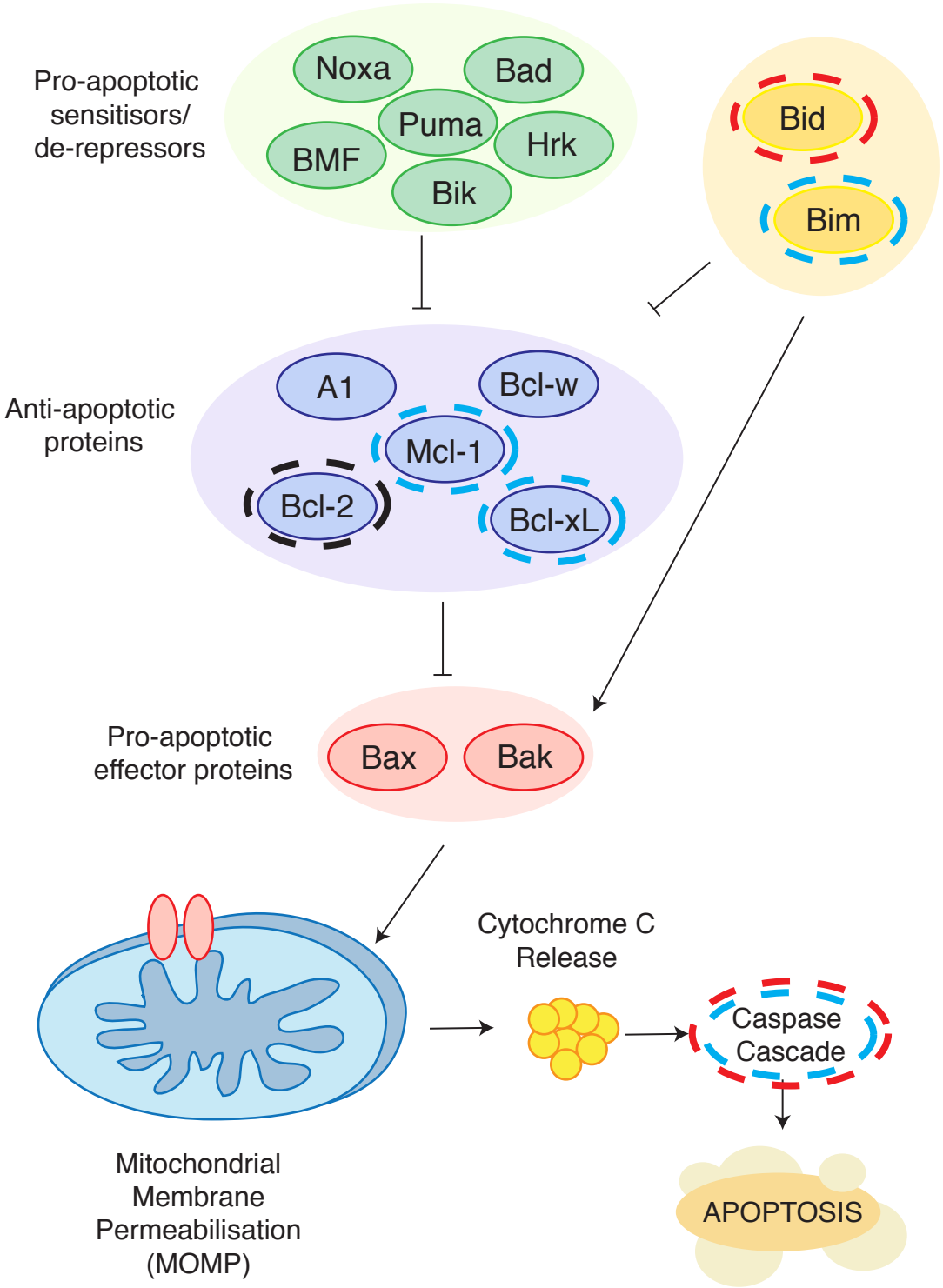

Figure 1.7. The Intrinsic apoptotic network
The network is made up of groups of pro- and anti-apoptotic proteins whose binding ultimately influences the ability of Bak and Bax to penetrate the mitochondrial membrane. Bak and Bax form channels in the mitochondrial membrane causing release of cytochrome C that drives a caspase cleavage cascade inducing apoptosis. Coloured circle denote mitosis-specific modification of protein, red indicates a gain of function, blue indicates a loss of function.

family proteins can be alleviated by the BH3-only proteins (BMF, Noxa, Bad, Hrk, Bik, Bid and Bim). As the name suggests, the BH3-only proteins only contain the BH3 domain that, when activated, compete with Bak and Bax for binding to anti-apoptotic proteins, thus sensitising the cell to MOMP. Moreover, the BH3-only proteins have varying affinities for the different anti-apoptotic Bcl-2 proteins they can bind (Chen et al., 2005). For example, where Bid, Bim and Puma bind all anti-apoptotic members, Noxa binding is specific only for Mcl-1, and Hrk is specific for Bcl-xL. Additionally, both Bid and Bim can directly interact and activate Bak and Bax. These interactions between the pro- and anti-apoptotic proteins define the network response to stimuli.

How a cell responds to apoptotic signaling depends on the ability of the apoptotic network to drive the downstream caspase cascade. The responsiveness of the network to drive apoptosis can be tested by BH3 profiling that measures the amount of cytochrome c release from extracted mitochondria following treatment with peptides corresponding to the various BH3 only proteins (Certo et al 06). A more recent method using a permeable JC-1 dye has been used in live cells as a marker for mitochondrial depolarisation (Ryan and Letai, 2013). Using these methods, it has been shown that the ability of these sensitiser peptides to induce MOMP is variable under certain contexts leading to the idea that the network can be 'primed' for apoptosis, or in other words, lowering the threshold required to initiate the irreversible apoptotic process. One way cells are primed is through the expression of activator BH3 only proteins (Bid and Bim) which become displaced from bound anti-apoptotic proteins by sensitiser BH3-only proteins following apoptotic stimuli to activate Bak and Bax oligomerisation (Certo et al., 2006). BH3-only profiling can also be used to determine the dependency of a cell line to certain anti-apoptotic proteins by determining which specific BH3 peptides can initiate cytochrome c release/MOMP (Certo et al 06, Deng et al 2007). Many of the apoptotic members are now known to undertake mitosis-specific phosphorylation, which has been shown to influence protein function within the network (see Chapter 1.4.3). These mitosis-specific modifications have been described as another way to 'prime' the apoptosis network to respond to signalling stimuli. Indeed, in comparison to interphase, the mitotic phase is more susceptible to cell death when stressed (Rieder and Maiato, 2004).

1.4.3 Pro-apoptotic proteins relevant to mitosis

The pro-apoptotic members within the network include the apoptotic effectors Bak and Bax but most post-translational changes currently discovered thus far are associated with the BH3-only proteins. As Bak and Bax are the downstream pro-apoptotic effectors it is unsurprising that these two proteins are vital for the co-ordination of cell death in response to anti-mitotic drugs. Co-knockout Bak and Bax MEFs fail to induce death following treatment with paclitaxel or Cdc20 RNAi (Miller et al., 2013; Wan et al., 2014). Specifically, Bak knockout MEFs conferred more death suppression compared to Bax knockout MEFs, breast cancer cells and fibroblasts, and HeLa cells, suggesting that Bak is the primary apoptotic effector (Miller et al., 2013; Upreti et al., 2008a). However, no mitotic-specific modifications to Bak or Bax have been identified.

However, several mitosis-specific changes have been identified in both the caspases and BH3-only proteins that affect the pro-death function of these proteins. In terms of the former group of proteins, mitosis-specific phosphorylations of two caspase proteins have been identified. Firstly, caspase 9 is phosphorylated at Thr125 in mitosis by Cyclin B1/Cdk1 and expression of a non-phosphorylatable mutant increases levels of apoptosis in response to nocodazole (Allan and Clarke, 2007). This suggests that phosphorylation of caspase 9 in mitosis counteracts apoptotic function. This appears also true for caspase 2. In *Xenopus* mitotic egg extracts, Caspase 2 is phosphorylated at Serine 208 (corresponding to S240 in humans) by Cdk1 *in vitro* and this phosphorylation suppresses caspase 2 processing and cleavage, (Andersen et al., 2009). Although the activity of caspase 2 appears suppressed in mitosis, knockout caspase 2 MEFs suppress death in response to paclitaxel treatment, questioning the importance of this phosphorylation (Dorstyn et al., 2012; Ho et al., 2008).

In addition to the caspases, BH3-only protein Bid becomes phosphorylated on Serine 66 specifically in mitosis. However, unlike the loss-of function caused by phosphorylation of the caspase proteins, phosphorylation of Bid increases that apoptotic response in RKO cells to paclitaxel and monastrol, indicating that this modification is involved in priming the network to mitotic death (Wang et al., 2014). Furthermore, knockdown of Bid and knockout Bid MEFs reduced apoptosis in response to taxol treatment in death-prone cell line RKO, further supporting

the importance of this protein to the mediating cell death in response to anti-mitotic drugs (Wang et al., 2014).

The function of two other BH3-only proteins, Bim and Noxa, are regulated by a decline in protein levels during mitosis. It was recently shown that Bim levels were reduced in mitosis and that Bim interacts with the WD40 motif of Cdc20 *in vitro* by expressing tagged proteins in HeLa cells (Wan et al., 2014). Mutation of two D-box like motifs in Bim stabilised it, and further sensitised cells to taxol, presumably through increased Bim levels (Wan et al., 2014). Like Bim, Noxa is also degraded during mitotic arrest although thus far the degradation mechanism is unknown (Haschka et al., 2015). Noxa is a BH3 only protein that specifically recognizes anti-apoptotic protein Mcl-1. Depletion of Noxa in cells treated with anti-mitotics decreases DiM and increases mitotic slippage, which may reflect the dependency of some cell lines on Mcl-1 to act as the dominant survival factor (Díaz-Martínez et al., 2014; Haschka et al., 2015). Although the effect of Noxa appears straight forward, the evidence surrounding the contribution of Bim to the apoptotic response to anti-mitotics is mixed. Whereas stable suppression of Bim by shRNA had no major effect on cell death (Tang et al., 2011), other reports using Bim RNAi showed that Bim had a pro-apoptotic role in antimitotic-mediated cell death (Haschka et al., 2015; Kawabata et al., 2012; Kutuk and Letai, 2010; Li et al., 2005). Interestingly, Bim RNAi could slow down DiM in HeLa cells (Haschka et al., 2015). Equally, there are conflicting reports about the response of Bim knockout cells to anti-mitotics (Miller et al., 2013; Tan et al., 2005). Furthermore, it appears that the MAPK signalling pathway can block cell death in response to antimitotics in part by phosphorylation-mediated degradation of Bim (Kawabata et al., 2012; Luciano et al., 2003; Tan et al., 2005). These discrepancies are likely to reflect either the extent of BH3-only protein redundancy that exists and the context-dependency of different cell lines for the BH3-only proteins.

1.4.4 Anti-apoptotic Bcl-2 family members relevant to mitosis

Mitotic-specific modifications are not limited to the pro-apoptotic proteins as several pro-survival factors are also modified in mitosis. For example Bcl-2, the first anti-apoptotic protein identified as a pro-survival gene in haemopoietic cells (Vaux et al., 1988), hence why the group

of proteins are known as the Bcl-2 family, is phosphorylated in mitosis (Haldar et al., 1995; Terrano et al., 2010). Overexpression of Bcl-2 suppresses apoptosis in MCF7 cells in response to paclitaxel (Kutuk and Letai, 2008). Expression of Bcl-2 with multiple mutations at phosphorylation sites (T69A, S70A, S87A and T56A) confers additional partial protection against apoptosis in response to nocodazole, suggesting phosphorylation suppresses Bcl-2 function (Deng et al., 2004; Haschka et al., 2015). However, knockdown of Bcl-2 has no effect on sensitivity to anti-mitotics in numerous cell lines, suggesting that Bcl-2 is not a vital survival factor during a mitotic arrest (Li et al., 2005; Shi et al., 2011).

Despite the neutral role Bcl-2 appears to have in a prolonged mitosis, high levels of another pro-survival Bcl-2 family member, Bcl-xL, correlated with a lower survival rate in breast cancer patients treated with paclitaxel in combination with cyclophosphamide (Flores et al., 2012). Further to this, depletion of Bcl-xL sensitised many cell lines to DiM (Bah et al., 2014; Shi et al., 2011). Bcl-xL is phosphorylated at serine 62 in a mitotic arrest, which does not affect the ability of Bcl-xL to localize to the mitochondria but hinders the ability of Bcl-xL to bind Bax, thus indicating that this phosphorylation has a loss-of-function effect on Bcl-xL, thus potentially contributing to the 'primed' state of the apoptotic network in mitosis (Bah et al., 2014; Du et al., 2005; Poruchynsky et al., 1998; Upreti et al., 2008b). *In vitro* studies have since identified the Cyclin B1/Cdk1 complex as a mitotic kinase that targets Bcl-xL (Terrano et al., 2010). Put together, this indicates that the level of Bcl-xL activity may be a primary determinant of mitotic fate. However, other studies focusing on another Bcl-2 family pro-survival factor, Mcl-1, suggest that this protein also plays a role in mitotic fate (see Chapter 1.5 for more detail). This may suggest a context-dependent role for the pro-survival proteins in a mitotic arrest.

1.4.5 Pro-apoptotic stimulus in mitosis

As shown above, many members of the apoptosis pathway undergo mitosis-specific modification. These changes have been described as 'priming' the apoptotic network towards pro-death (Wang et al., 2014). 'Priming' the network could make the network more responsive to pro-death stimuli. Equally, this could mean that the mitosis-specific changes in the apoptotic network are sufficient to drive DiM alone, without the need for a further stimulus.

Very little is known about the stimuli that can induce apoptosis in mitosis. A likely candidate to act as an initial pro-apoptotic stimulus is DNA damage that has been shown to accumulate during a prolonged mitotic arrest (Orth et al., 2012). However, blocking caspase activity or suppressing Mcl-1 in mitosis decreases the number of γH2A.X foci, suggesting that partial activation of apoptosis can lead to DNA damage (Colin et al., 2015; Orth et al., 2012). Accumulation of DNA damage through this pathway could cause a feed-forward loop through genotoxic stress signalling back to the apoptotic network. This was attributed to caspase-mediated cleavage of inhibitor of caspase-activated DNase (ICAD), enabling CAD to drive DNA fragmentation (Enari et al., 1998; Orth et al., 2012; Tang and Kidd, 1998). Additionally CAD is stabilised by Myc in a mitotic arrest (Topham et al., 2015).

Conversely, another group suggested that DNA damage may act as the initial apoptotic mediator by reporting that in mitosis the DNA damage signal originates from the deprotection of telomeres through the dissociation of TRF2 protein, causing a unique double-stranded DNA damage response that activates p53 in the subsequent interphase (Cesare et al., 2013; Hayashi et al., 2012). Although this did not appear to be relevant to mitotic death, follow-up reports showed that loss of TRF2 increased DIM and overexpression of TRF2 reduced DiM in Bcl-xL/Mcl-1 RNAi-treated cells, suggesting that this mechanism does also contribute to death in mitosis (Hayashi et al., 2015; Topham et al., 2015). Although the relative contribution of each mechanism to cell death remains unresolved, it is clear that the interplay between the DNA damage and apoptotic networks are important in determining the rate of DiM.

1.4.6 Myc and redundancy in apoptosis

Although many members of the network are modified in mitosis, it is important to point out that it is the net effect of the apoptotic network that determines the rate of DiM. There is a degree of functional overlap that exists between the apoptotic members due to the high level of structural conservation that exists between the members. For example, all BH3-only proteins except for Noxa can bind Bcl-xL. Conversely, Bid, Bim and Puma appear to be able to bind all Bcl-2 family members (Chipuk et al., 2010). This means that other members of the network may

be able to compensate for a loss in function of one protein. However, the BH3-only proteins respond to different stimuli, suggesting that there is a context-dependent nature of the apoptotic machinery that may play a role in driving differential responses of different cell lines during a mitotic arrest. For example, whereas Bim is required to drive apoptosis in B and T cells, Noxa and Puma are up-regulated in response to DNA damage (Bouillet et al., 1999; Nakano and Vousden, 2001; Oda et al., 2000). This BH3 redundancy is therefore likely to depend on the requirement of a particular cell line on different members of the apoptotic network, both pro-death and anti-death. This may also influence how that cell line responds to various changes in the apoptotic network

This redundancy was highlighted in a recent genome-wide siRNA screen completed in the lab that was performed with the intention of identifying the primary components that were required for death-in-mitosis. Despite suppressing all the protein members, none of the individual components of the apoptotic network were identified from the screen, which is likely to reflect the large scale of redundancy that exists. Instead, the screen identified transcription factor Myc as a major mediator of DiM (Topham et al., 2015). Further transcript analysis showed that Myc regulated several members of both the anti-apoptotic and pro-apoptotic families. Interestingly, loss of each of the four BH3-only proteins (Bid, Bim and Noxa) down regulated by loss of Myc protein had no effect on DiM or slippage. However, only upon loss of all four by RNAi was increased slippage observed. The SAC is evolutionary-conserved rheostat mechanism that responds to the degree of unattached kinetochores by regulating Mad2 recruitment to the kinetochore, is driven by a single input of unattached kinetochores (Westhorpe 2010, Collin, 2014). In contrast, the apoptotic network is far less conserved, responds to a multitude of inputs and can be “fine-tuned” depending on the context required due to the plethora of proteins available (Figure 1.8)(Topham et al., 2015). This makes overall interpretation of the function of each individual member of the network difficult.

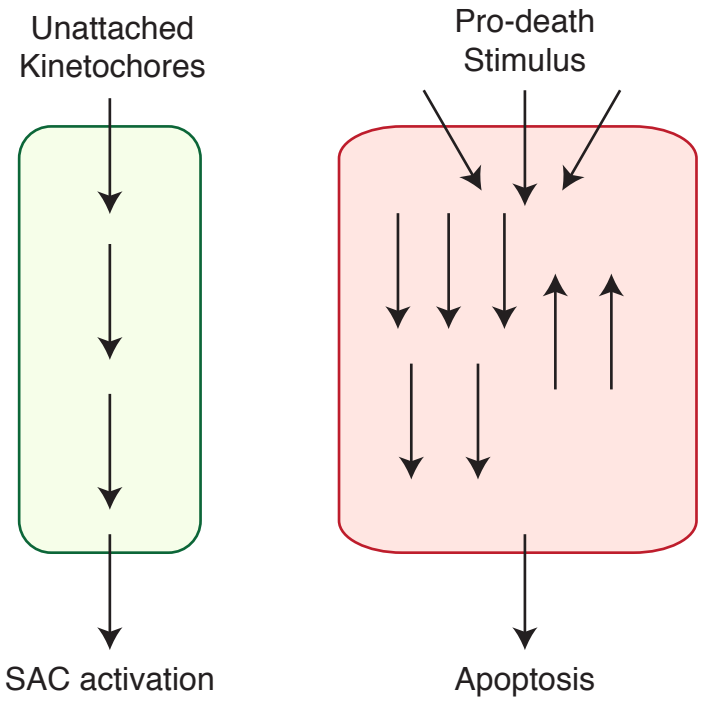

Figure 1.8. The nature of slippage versus apoptotic signalling networks.
The SAC responds to a single input, unattached kinetochores, and signals through a relatively linear signalling mechanism in order to cause SAC activation. In contrast, the apoptotic network network responds to a variety of pro-death stimuli and the net output is caused by how the individual components of the network respond as a whole to the stimulus.

1.5 Post-mitotic response

When talking in terms of the overall response to anti-mitotic drugs, it is also important to discuss a secondary effect of anti-mitotics in the subsequent interphase following escape from a mitotic arrest and DiM, and how the cells respond. Interphase cells that have undertaken mitotic slippage are characterised by the presence of micronuclei and tetraploidy. Although spontaneous tetraploidy is tolerated in some tissues, tetraploidy leads to increased chromosome instability. It has been previously proposed that chromosome instability in tetraploid cells is caused by an abnormal number of centrosomes generating an abnormal mitotic spindle in the subsequent M phase, thus causing an abnormal mitosis (Andreassen et al., 1996; Storchova and Pellman, 2004). Interestingly, tumor formation could be initiated by cytokinesis failure of p53-null cells *in vivo*, suggesting that tetraploidy could be a tumourgenesis driver (Fujiwara et al., 2005). It was proposed that cells evolved a checkpoint that suppresses cell cycle progression in the presence of tetraploidy, the tetraploidy checkpoint, which involves activation of p53 (Andreassen et al., 2001a; Margolis et al., 2003). Since its discovery, this theory has been debunked (Uetake and Sluder, 2004). Nonetheless, a decision point exists following mitotic exit that leads to cell cycle arrest, post-mitotic death (PmD) or continual cell cycling (Figure 1.4). Although this might not be caused by tetraploidy itself, it could be caused by other cellular damage that occurs during a mitotic arrest.

An interesting early observation was that p53-null fibroblasts were much more tolerant to chromosomal abnormalities, which suggested that p53 functions to arrest and drive cell death in tetraploid cells (Harvey et al., 1993). P53 is a global transcription factor and as such regulates several processes such as cell cycle arrest, senescence, invasion and apoptosis (Bieging et al., 2014). Importantly, when p53-null MEFs were exposed to either taxol or colcemid, cells failed to arrest in G1 and instead entered S phase and replicated the genome, creating octoploid cells (Cross et al., 1995; Lanni and Jacks, 1998; Di Leonardo et al., 1997; Woods et al., 1995). Moreover, p53 is not expressed in mitosis, indicating that its function is limited to the post-mitotic response (Minn et al., 1996). However in G1, p53 expression is switched on which leads to expression of p21, a Cdk inhibitor, and retinoblastoma protein (pRb) which inhibit cell cycle progression (Andreassen et al., 2001b; Borel et al., 2002; Lanni and Jacks, 1998). Under non-

stimulated conditions, p53 activity is suppressed by Mdm2. Mdm2 binds p53 in its transactivation domain and mediates its ubiquitination, thus inhibiting p53-dependent transcription through competitive binding to the active site and degradation (Haupt et al., 1997; Kubbutat et al., 1997; Momand et al., 1992; Oliner et al., 1993). P53 is activated by phosphorylation that relieves the inhibitory p53-Mdm2 interaction (Chehab et al., 1999; Shieh et al., 1997).

The ability of a tetraploid cell to commit to cell death following a G1 arrest caused by p53 activation is likely to depend on signalling to the intrinsic apoptotic network. This first became apparent when the abundance of tetraploid cells in culture increased upon overexpression of Bcl-xL (Minn et al., 1996). Consistent with this notion, loss of Bcl-xL in taxol-treated cells increased the number of slipped cells to commit to PmD (Topham et al., 2015). P53 activates transcription of BH3-only genes PUMA and NOXA, thus sensitising the apoptotic network to death (Nakano and Vousden, 2001; Oda et al., 2000; Yu et al., 2001). Interestingly, the amount of p53 protein may dictate whether a G1 arrest leads to apoptosis or not, indicating that there is a apoptotic threshold for p53-mediated apoptosis in G1 (Kracikova et al., 2013). It is therefore important to understand the factors that trigger p53 stabilisation and accumulation following a prolonged mitotic arrest that enable this threshold to be broken.

One such trigger, DNA damage, causes a p53-dependent G1 arrest (Kastan et al., 1991, 1992; Kuerbitz et al., 1992). It has been shown that DNA damage increases over time in mitosis (Colin et al., 2015; Hayashi et al., 2012). Importantly, a positive correlation has been shown between the duration of a mitotic arrest and the likelihood of G1 arrest (Uetake and Sluder, 2010). Although increased apoptosis correlates with mitotic duration, it is not clear whether cell death occurs during mitosis, post-mitosis or both (Colin et al., 2015; Zhu et al., 2014). Altogether this indicates that the post-mitotic response is in part dependent on the accumulation of DNA damage which occurs over time during a prolonged mitotic arrest (Colin et al., 2015). Another hypothesis linking the duration of mitotic arrest and apoptosis is an increased number of micronuclei triggering DNA damage and apoptosis (Zhu et al., 2014). Micronuclei are sites of replicative defects, chromothripsis and DNA damage, suggesting that a *de novo* damage signal following the formation of micronuclei may contribute to cell death (Crasta et al., 2012; Zhang et

al., 2015). However, the driver that connects mitotic duration and number of micronuclei has not been identified.

1.6 Mcl-1

Although there is likely to be redundancy in protein function within the apoptotic network, it is important to understand the individual units of the network in order to appreciate how the network responds as a whole during a mitotic arrest. One pro-survival member of the apoptotic network, Mcl-1, is degraded in mitosis. Although this appears to sensitise cells to DiM, it is not fully clear whether this is due to acceleration of DiM signalling or a delay in mitotic slippage. In addition, there are unresolved questions in regards to the nature of the mechanism driving Mcl-1 degradation and mitotic cell fate due to discrepancies in the literature that this thesis aims to answer. This chapter provides a detailed introduction into the regulation of Mcl-1, with particular focus on its regulation and function in mitosis.

1.6.1 Introduction to Mcl-1

Mcl-1 was first discovered as an early-induction gene expressed in differentiating human myeloid leukemia cells (Kozopas et al., 1993). Further overexpression studies in Chinese Hamster ovary cells confirmed an anti-apoptotic function for Mcl-1 (Reynolds et al., 1994). Moreover, Mcl-1 knockout mice are embryonic lethal and display a more severe phenotype when compared to knockout of other Bcl-2 family members (Chem et al., 1995; Rinkenberger et al., 2000; Veis et al., 1993). Mcl-1 is expressed in many tissues and is required for the survival and maintenance of many cell lineages (Krajewski et al., 1995; Thomas et al., 2010). As Mcl-1 contains three out of the four BH domains found in Bcl-2 family members in its C-terminus, Mcl-1 shares a large degree of structural homology with other Bcl-2 family members (Figure 1.9) (Thomas et al., 2010). Although Mcl-1 resides primarily in the cytoplasm, Mcl-1 also has a transmembrane domain in the C-terminus, which is required for mitochondrial localization of Mcl-1 (Akgul et al., 2000). Instead of a BH4 domain, Mcl-1 contains a larger N-terminus region, making Mcl-1 a larger protein of 350 residues. This N-terminal region contains motifs recognised by signalling networks in order to modulate the activity of Mcl-1. Deletion of the N-terminus impairs the ability of Mcl-1 to function as an anti-apoptotic factor, as well as to localise to the mitochondria. This suggests that mitochondrial localisation is required for it to antagonize Bak and Bax (Germain and Duronio, 2007).

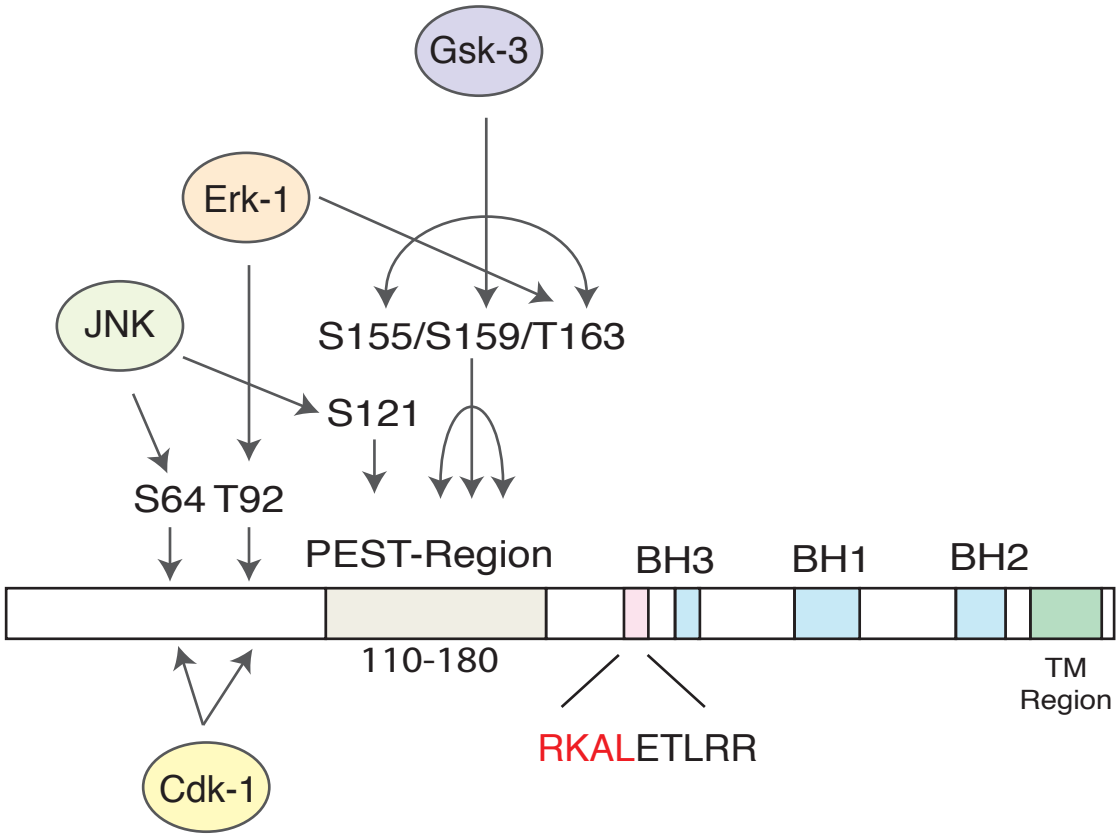

Figure 1.9. Regulation of Mcl-1.
Schematic of Mcl-1. Like other Bcl-2 family proteins, Mcl-1 contains three BH domains. Mcl-1 has a transmembrane region in the C-terminus and an extended N-terminus that is subject to phosphorylation by multiple kinase signalling cascades. The RxxL motif lies at amino acids 207-210.

Mcl-1 binds to the BH3 domain of Bak and Bax, thus inhibiting mitochondrial permeabilisation and caspase activation (Cuconati et al., 2003; Willis et al., 2005). These interactions can be displaced by BH3 only proteins Bid, Bim, Puma, Bik, Bmf and Noxa (Chipuk et al., 2010). Unlike the others, Noxa displays high specificity for Mcl-1 (Chen et al., 2005). Structural analysis of Mcl-1 C-terminal showed that Mcl-1, like other Bcl-2 family members, forms a hydrophobic groove of several α-helices with an electrostatic surface for binding of BH3 domain-containing substrates and upon binding, undergoes a conformational change (Day et al., 2005, 2008).

1.6.2 Mcl-1 in cancer progression.

As the ability of cancer cells to evade apoptosis is a fundamental characteristic of cancers, it is no surprise that Mcl-1 is deregulated in cancer cells (Hanahan and Weinberg, 2000). Enhanced protein expression is observed in a number of cancer types (Fleischer, 2006; Song et al., 2005). More recently, whole genome analysis of copy-number variation identified Mcl-1 gene amplification across multiple cancer types and interestingly, cells displaying Mcl-1 amplification are dependent on Mcl-1 for survival (Beroukhim et al., 2010). Loss of Mcl-1 by RNAi has been used to sensitise cancer cells to death, in combination with other agents in cell culture (Breitenbuecher et al., 2009; Cuconati et al., 2003; Henson et al., 2006; Nijhawan et al., 2003; Thallinger et al., 2004; Wei et al., 2008). Importantly, loss of Mcl-1 sensitises cells to antimitotic agents (Song et al., 2005; Tunquist et al., 2010).

Additionally Mcl-1 expression was associated with resistance to BH3 mimetics ABT-737 and ABT-263 (otherwise known as navitoclax), small peptides that neutralize the ability of Bcl-2 and Bcl-xL to bind pro-apoptotic factors by acting as a competitive inhibitor, by itself or in combination with anti-mitotics (Bah et al., 2014; Kutuk and Letai, 2008; Nakajima et al., 2014; Oltersdorf et al., 2005; Shi et al., 2011). This suggests not only that there is a level of functional redundancy between the Bcl-2 family proteins, but that cell lines dependent on Mcl-1 are unlikely to respond to BH3 mimetics. Recently, much work has gone into developing small molecule inhibitors targeting Mcl-1 (Belmar and Fesik, 2015). A small molecule inhibitor has been tested *in*

vitro that disrupts the Mcl-1-Bim complex, so reducing survival in Mcl-1-dependent cell lines, and further sensitises cells to death in combination with ABT-263 (Leverson et al., 2015).

1.6.3 Regulation of Mcl-1

Mcl-1 is subject to phosphorylation by different signalling cascades at its N-terminus, as it contains several PEST sequences (amino acids proline, glutamic acid, serine and threonine) which provides a platform for phosphorylation (Kozopas et al., 1993; Rogers et al., 1986). Thus far, phosphorylation sites have been identified in serine 63, threonine 92, serine 121, serine 155, serine 159 and threonine 163 (Ding et al., 2008; Domina et al., 2004; Inoshita et al., 2002; Kobayashi et al., 2007; Kodama et al., 2009; Maurer et al., 2006; Morel et al., 2009). Several kinases have been reported to phosphorylate Mcl-1 including Erk-1 (T92/T163), JNK (S64/S121), glycogen synthase kinase-3 (GSK-3)(S155/S159/T163) and Cdk1 (S64/T92) (Ding et al., 2008; Domina et al., 2004; Inoshita et al., 2002; Kobayashi et al., 2007; Kodama et al., 2009; Maurer et al., 2006; Morel et al., 2009). Each phosphorylation event has diverse effects on the stability and function of Mcl-1. Co-phosphorylation of both T92 and T163 stabilised the protein whereas phosphorylation at S155, S159 and T163 de-stabilised Mcl-1 (Ding et al., 2007, 2008). Furthermore it was shown that phosphorylation at T163 'primed' Mcl-1 for phosphorylation at S159 (Morel et al., 2009). Thus far there is conflicting evidence as to the effect of the double S121/T163 mutant on Mcl-1 stability and function (Inoshita et al., 2002; Kodama et al., 2009). More recently, mutation of T163 resulted in nuclear localization of Mcl-1, reduced stability and decreased apoptotic function although the mechanism is unclear (Thomas et al., 2012).

One of the best well-characterised mechanisms to suppress activity is Mcl-1 degradation. Mcl-1 protein decline was first discovered following exposure of HeLa cells to UV treatment indicating that Mcl-1 is a labile protein with a short half-life (Nijhawan et al., 2003). Several E3 ligases have been implicated in the targeted degradation of Mcl-1. These include Mcl-1 Ubiquitin Ligase E3 (MULE- the first E3 ligase identified), beta transducing-containing protein (β-TrCp) following phosphorylation of Mcl-1 by GSK-3, SCF-Fbw7 and APC/C-Cdc20 (Ding et al., 2007; Harley et al., 2010; Inuzuka et al., 2011; Wertz et al., 2011; Zhong et al.,

2005). However, the effect that targeted degradation has on Mcl-1 is unclear as one group found no difference in the stability of wild type Mcl-1 and a Mcl-1 lacking all the lysine residues that are required for ubiquitination (Stewart et al., 2010). Moreover, in a controlled *in vitro* system, the proteasome was sufficient to mediate Mcl-1 degradation (Stewart et al., 2010). It is likely that the cell type and genetic background play a large part in determining the importance of each mechanism of Mcl-1 degradation. Further to the role of Noxa as a pro-death BH3-only protein, Noxa can promote the degradation of Mcl-1 and sensitises cells treated with ABT-737 (Chen et al., 2005; Nakajima et al., 2014; Willis et al., 2005).

1.6.4 Mcl-1 protein during a mitotic arrest

Mcl-1 loss during mitosis is the most well characterised change to an apoptotic protein during a mitotic arrest (Millman and Pagano, 2011). Mcl-1 degradation in a mitotic arrest was first observed by Harley *et al.* who showed that Mcl-1 was degraded in a proteasome-dependent manner (Harley et al., 2010). As Mcl-1 loss is a characteristic molecular signature following the induction of other stresses (see above), one could suspect that Mcl-1 is a rapidly turned-over protein and that loss of Mcl-1 is just an indirect effect of suppression of synthesis mechanisms in mitosis. Indeed, cells treated with transcriptional repressors reduce Mcl-1 levels (Wei et al., 2012). However, certain observations have lead to the belief that mitotic Mcl-1 degradation is regulated by mitosis-specific mechanisms (Figure 1.10). Firstly, loss of Cdc20 and APC subunit APC3 stabilised Mcl-1 in mitosis in U20S cells (Harley et al., 2010). Furthermore, Mcl-1 contains a D-box-like RxxL motif, thus leading to the idea that Mcl-1 interacts with the APC/C-Cdc20. Indeed an interaction between Mcl-1 and Cdc20 was identified and mutation of the RxxL motif in Mcl-1 stabilised the protein (Harley et al., 2010).

Additionally, phosphorylation of Mcl-1 (Serine 64) was first identified by mass spectrometry. This phosphorylation was blocked following treatment with Cdk1 inhibitors suggesting that it was a mitosis-specific phosphorylation. Mutation of this residue did not affect the half-life of Mcl-1, failed to protect cells from apoptotic stimuli and displayed reduced binding to Bim, Noxa and Bak (Kobayashi et al., 2007). In addition, a separate mass spectrometry analysis identified mitosis-specific phosphosites of Mcl-1 at S64, S121, S159 and T163

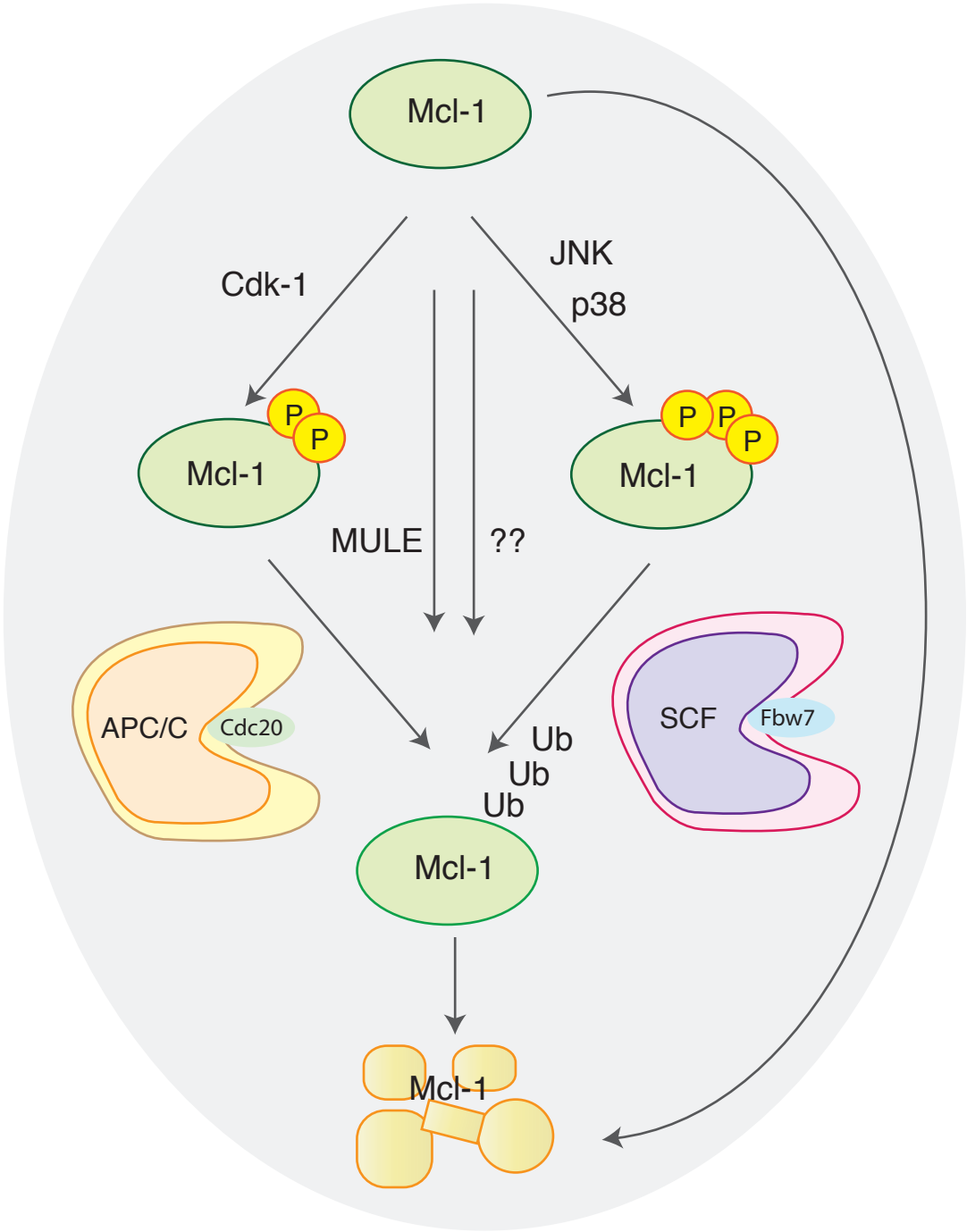

Figure 1.10. Mcl-1 protein during a mitotic arrest.
Mcl-1 undergoes mitotic phosphorylation by several kinases including mitotic kinase Cdk-1. Phosphorylated Mcl-1 can then interact with E3 ligases APC/C-Cdc20 and SCF-Fbw7, driving Mcl-1 degradation in mitosis. Other known mechanisms of Mcl-1 degradation in mitosis include E3 ligase MULE as well as ubiquitin-independent proteasome-mediated degradation of Mcl-1.

(Wertz et al., 2011). It was shown that these phosphorylations enhanced binding of Mcl-1 to Fbw7, another E3 ligase. Fbw7 forms the substrate recognition part of the E3 ligase SCF complex with Skp1 and Cul1 that mediates targeted ubiquitination of proteins for degradation (Welcker and Clurman, 2008). Additionally, inhibition of JNK and p38 enhanced phosphorylation and binding (Wertz et al., 2011). Other groups have shown loss of MULE also stabilises Mcl-1 in mitosis (Kawabata et al., 2012; Shi et al., 2011). The identification of several ligases that contribute to Mcl-1 degradation in mitosis suggests that there may be redundancy between the E3 ligases or cell-specific dependency on different mechanisms of targeted ubiquitination for Mcl-1 degradation.

1.6.5 Mcl-1 and mitotic death

Mcl-1 undergoes loss-of function changes during mitosis but do these changes translate into a phenotype in terms of cell fate? Indeed, Mcl-1 degradation during mitosis reduces the amount of Bak sequestered by Mcl-1, suggesting that this may increase the pool of free Bak able to engage with the mitochondria and instigating MOMP (Chu et al., 2012; Miller et al., 2013). In addition, Mcl-1 levels determine the sensitivity of Myeloma tumor cell lines and RPMI 8226 tumor xenografts in response to kinesin inhibitor ARRY-520 (Tunquist et al., 2010), although it is not clear at which point of the cell cycle Mcl-1 sensitizes cells to ARRY-520. More recently, Mcl-1 RNAi was performed on a panel of cell lines and time-lapse microscopy was used to analyse cell death. Loss of Mcl-1 sensitized cells to increased DiM to varying extents between cell lines in comparison to RNAi of other anti-apoptotic proteins (Shi et al., 2011). Furthermore, cell fate profiles of RKO cell transfected with Mcl-1 RNAi showed a reduction in the number of cells that slipped and an increase in the number of cells committing to DiM (Topham et al., 2015). Altogether, it is likely that loss of Mcl-1 increases the rate of mitotic apoptosis, as a greater pool of Bak and Bax are free to drive MOMP. However, the possibility that loss of Mcl-1 increases mitotic death due to the reduction in slippage signalling has not been eliminated. Furthermore, Mcl-1 degradation can be suppressed by ERK signalling (Ding et al., 2008). Superimposing MEK inhibition on top of anti-mitotics reduced slippage and increased DiM, which according to the competing networks model, suggests that destabilising Mcl-1 either accelerates DiM or delays slippage (Kawabata et al., 2012).

Although Mcl-1 levels fall during a mitotic arrest, Mcl-1 degradation is not always sufficient to drive DiM by itself (Chu et al., 2012). Although Mcl-1 is degraded during a mitotic arrest, there appears to be a level of redundancy between the Bcl-2 family proteins. Indeed, this was observed in RKO cells treated with either Mcl-1 or Bcl-xL RNAi. Although loss of Mcl-1 or Bcl-xL increased cell commitment to DiM or PmD respectively, loss of both proteins caused very rapid DiM (Topham et al., 2015). Copy number variation of Mcl-1 and Bcl-xL is a common occurrence in cancers and this may reflect the different dependencies cell lines have on individual members of the Bcl-2 family (Beroukhim et al., 2010).

Additionally, a few studies have analysed the extent to which the different E3 ligase mechanisms contribute to DiM. One group has reported that loss of MULE partially delays the time to DiM by Mcl-1 stabilisation (Kawabata et al., 2012). Conversely, inhibiting FBW7 reduces DiM and increases slippage (Wertz et al., 2011). This may reflect redundancy, cell line variation and/or 'belt and braces' protection to ensure that an overly protracted mitosis sensitizes cells to undergo apoptosis (Topham and Taylor, 2013). Despite identification of an interaction between Mcl-1 and Cdc20, the effect of APC/C-Cdc20 on DiM is unknown. This is in part because the APC/C-Cdc20 is also required for Cyclin B1 degradation and therefore slippage, making interpretation difficult.

1.6.6 Mcl-1 protein involvement in mitotic slippage and network cross-talk

The association of Mcl-1 with Cdc20 indicates that Mcl-1 may also influence APC/C-Cdc20 activity and thus affect Cyclin B1 degradation and mitotic exit (Harley et al., 2010). This points towards the existence of cross-talk between the mitotic slippage and DiM pathways. Indeed, the concept of network cross-talk is not novel, as several members of the slippage pathway have been implicated in apoptotic signalling. As described in Chapter 1.4, Cdk1 phosphorylates and alters the function of various pro- and anti-apoptotic members of the apoptotic machinery (Allan and Clarke, 2007; Chu et al., 2012; Harley et al., 2010; Terrano et al., 2010). In addition, Bim is targeted for degradation by APC/C-Cdc20 (Wan et al., 2014). However, the net effect of either Cdk1 or APC/C-Cdc20 activity on DiM is unclear, as one cannot inhibit Cdk1 without causing mitotic exit (including both mitotic slippage and mitotic division, making it

difficult to study. Additionally, loss of MCC disassembly factor p31^{comet} (see Chapter 1.2.6) increases apoptosis (Díaz-Martínez et al., 2014). As p31^{comet} is important for ensuring efficient mitotic exit through MCC disassembly, a simple explanation for this is that the increase in apoptosis is merely due to inhibition of mitotic exit (Westhorpe et al., 2011). However, when compared to loss of Cdc20, which also inhibits mitotic exit, the time to mitotic death upon loss of p31^{comet} is accelerated (Díaz-Martínez et al., 2014). This either suggests that either loss of Cdc20 delays apoptosis through inhibition of Mcl-1 degradation, or that p31^{comet} accelerates apoptotic signalling through an unknown mechanism. Conversely, loss of apoptotic effectors Bak and Bax delays slippage (Díaz-Martínez et al., 2014). Understanding the nature of this cross-talk may allow us to better understand patient responses to anti-mitotic drugs and therefore be able to predict patient responses and perhaps propose new treatments that utilise this cross-talk in order to accelerate DiM signalling and extend slippage signalling.

The existence of the competing networks and cross-talk makes functional analysis of the contribution of protein factors towards the various fates difficult to interpret. It is therefore important to carefully select model systems whereby one can directly analyse the effect on one network without interference from the other network. In this thesis, I selected DLD1 cells in order to analyse changes to slippage rates, as these cells predominantly slip out of mitosis following treatment with Eg5 inhibitor AZ138 (Gascoigne and Taylor, 2008). Conversely I used an RKO cell line expressing a stabilised form of Cyclin B1 (Cyclin B1 R42A) in order to analyse changes to the rate of DiM.

1.7 Aims

By activating the SAC and enforcing a prolonged mitotic arrest in cell culture, anti-mitotic drugs can suppress the proliferation of cancer cells. The links between a mitotic arrest and how cells commit to death are not fully characterised, but it is clear that the apoptotic network plays a large role in mediating this response. Evidence suggests that Mcl-1 depletion by RNAi increases the abundance of mitotic death in some cell populations. However, as previously mentioned, due to the presence of mitotic slippage it is unknown whether this increase in DiM is caused by an acceleration in DiM signalling or simply an extension in the time it takes to degrade Cyclin B1 to undertake mitotic slippage. To conclusively distinguish between these two possibilities my first aim was to create a cell line (RKO cells expressing a stabilised form of Cyclin B1, Cyclin B1 R42A) that would inhibit slippage such that the rate of DiM could be directly measured in response to changes in Mcl-1 protein levels.

The observed association between Mcl-1 and Cdc20 by Harley et al in 2010 raised an intriguing possibility that this interaction could affect cell fate in two ways (Harley et al., 2010). Firstly by targeting Mcl-1 for degradation, the APC/C-Cdc20 could sensitise cells to apoptosis. Secondly by affecting the ability of Cyclin B1 to bind the APC/C-Cdc20 complex, Mcl-1 could influence the rate of mitotic slippage. Using the RKO Cyclin B1 R42A cell line to measure the rate of DiM and DLD-1 cells to measure the rate of mitotic slippage, I investigated the effect this interaction has on both DiM and slippage. In addition, several high profile papers have highlighted the requirement for other E3 ligase mechanisms that contribute to Mcl-1 degradation during mitosis (Shi et al., 2011; Wertz et al., 2011). Using the RKO Cyclin B1 R42A cell line to directly measure the rate of DiM, I attempted to analyse the importance of these individual E3 ligase mechanisms in the context of Mcl-1 degradation and DiM as well as identify any redundancy that exists between the different mechanisms.

The cytotoxic effect of anti-mitotic drugs is not limited to DiM but also to how they influence cells following mitotic exit. Recently, it was shown that loss of Mcl-1 increased the number of γH2.AX foci in mitotic cells, while increasing the amount of Mcl-1 both reduced the DNA-damage response in the subsequent interphase and increased the number of cells

progressing to S phase, suggesting that Mcl-1 protein may be required for the post-mitotic response (Colin et al., 2015). If this is the case, Mcl-1 degradation may also serve as a post-mitotic death timer and may help explain why mitotic duration can also influence the post-mitotic response. To test this, I create a cell system by which mitotic duration can be controlled and tested the influence of both mitotic duration and Mcl-1 protein levels on the post-mitotic response.

2 Chapter 2: Materials and Methods

2.1 Cell Biology

Cell Culture

The cell lines used in this thesis include DLD-1, RKO, HeLa, HCT-116, HT29, H1703, DLD-1 LacZeo/TO, RKO LacZeo/TO and DLD-1 myc-Tir1 LacZeo/TO (for origin and seeding density see Table 2.1). The LacZeo/TO cell lines had a flip-recombinase target (FRT) containing-construct stably integrated into the genome and grown up through clonal selection under selection in Zeocin™ (Themofisher) as described previously (Girdler et al., 2006; Tighe et al., 2004; Topham et al., 2015). For work using the AID-auxin system, the DLD-1 LacZeo cell line containing OsTir-6xMyc construct inserted through retroviral transfection was kindly donated by Dr. Andrew Holland (Holland et al., 2012). All cell lines were cultured in Dubecco's Modified Eagles Medium (DMEM) supplemented with 10 % heat-inactivated fetal bovine serum (FBS)(Gibco), 2 mM glutamine (Sigma), 100 U/ml penicillin and 100 U/ml streptomycin (Sigma) in an incubator set at 37 °C and 5 % CO_2. Cells were passaged by an initial wash step with Dulbecco's Phosphate Buffered Saline (PBS) (Sigma) followed by incubation for 5 minutes with 1-2 mls of 10 X Trypsin-EDTA (Sigma) diluted in PBS. The trypsin was neutralized by DMEM and cell density was measured using a haemocytometer.

Cell Line	**96 Well**	**96 Well**	**24 Well**	**24 Well**	**6 Well**
Thymidine 2 mM	Yes		Yes		
RKO (plus derivatives)	12	9	18	15	20
DLD-1 (plus derivatives)	7.5	5	12	10	13
HeLa	n/a	8	n/a	15	n/a
HCT-116	n/a	9	n/a	15	n/a
HT29	n/a	9	n/a	15	n/a
H1703	n/a	9	n/a	15	n/a

Table 2.1 Cell plating density. Numbers are represented to the power of 1 X 10^4 cells/ml.

Drug Treatments

Powdered drugs were solubilised in dimethyl sulfoxide (DMSO) to the indicated stock concentration and stored at the temperature indicated in Table 2.2. Before cell treatment, all drugs were diluted to the required concentration in DMEM. Thymidine was initially dissolved in PBS and filtered using a PES syringe filter (pore size 0.45 µm) (Whatman™) before dilution into DMEM.

Drug	**Source**	**Stock Concentration**	**Storage (°C)**	**Final Concentration**
AZ138	Astra Zeneca (Gift) (Gascoigne)	10 mM	-20	1 µM
MG132	Calbiochem	20 mM	-20	20 µM
Nocodazole	Sigma	5 mg/ml	-20	0.66 µM
Taxol	Sigma	10 mM	-20	0.1 µM
IAA	Sigma	500 mM	-20	500 µM
proTAME	Peakdale	20 mM	-80	As indicated
Apcin	R & D Systems	100 mM	-20	As indicated
AZ3146	Astra Zeneca (Gift)	10 mM	-20	2 µM
Cycloheximide	Sigma	10 mg/ml	-20	30 µg/ml
Tetracycline	Sigma	1 mg/ml	-20	1 µg/ml

Table 2.2 Drug concentrations

Stable cell line generation

Generation of DLD-1 and RKO cell lines expressing tet-inducible exogenous protein was performed using the Flp-In™ system (Invitrogen). The Flp-In™ T-Rex System creates cell lines expressing exogenous proteins from the same genomic locus (Invitrogen, 2010). This system makes use of a Flp recombinase that catalyses recombination reactions between two FRT sites. Briefly, cells were stably transfected with pFRT/LacZeo plasmid, which introduces an FRT site as well as the Zeocin™ selection marker under the control of an SV40 promoter. This is followed by Zeocin selection and single colony expansion. Both RKO and DLD-1 LacZeo/TO had been previously generated in the lab (Girdler et al., 2006; Tighe et al., 2004; Topham et al., 2015).

Plasmids containing GFP-tagged and/or AID-tagged Mcl-1 and Cyclin B1 genes under the control of a *cis* tetO containing-CMV promoter sequence were co-transfected with pOG44 encoding Flp recombinase under the control of a constitutively active CMV promoter into the

LacZeo cell lines using Lipofectamine and Lipofectamine Plus reagent (Thermofisher). The Flp recombinase catalyses a recombination reaction between the FRT site on the LacZeo cassette stably integrated in the genome and the FRT site on the plasmid containing the tagged gene of interest allowing integration of the tetracycline-inducible gene into the FRT site (O'Gorman et al., 1991).The mixtures were incubated at room temperature in DMEM minus both FBS and antibiotics for a further 15 minutes to allow DNA-lipid complexes to form. Regular DMEM media was replaced with DMEM media not containing FBS or antibiotics and transfection mixtures were transferred into each well. Transfections were terminated 3 hours later by the addition of DMEM fully supplemented as above plus additional FBS. After 24 hours, transfected wells were expanded into 2 x 10 cm dishes and incubated for 24 hours. Cells were put under antibiotic selection by treatment with hygromycin B (80 µg/ml) (Roche) and Blastacidin (8 µg/ml) (Melford). Supplemented DMEM containing antibiotics were replaced every 4 days until cell colony formation. Colonies were pooled and expanded to form cell lines. To confirm cell line generation, cells were seeded into a 6-well plate (see table 2.1) and incubated at 37 °C for 24 hours before the addition of tetracycline (and IAA if required) for 24 hours. Following drug exposure, cells were trypisinised and spun down, resuspended and re-spun in 1 ml PBS before protein lysis using 100 µl 6 x SDS buffer (0.35 M Tris pH 6.8, 0.1 g/ml Sodium dodecyl sulfate, 93 mg/ml Dithiothreitol, 30 % Glycerol, 50 µg/ml Bromophenol Blue) for immunoblotting.

Transient Transfections

For transient plasmid transfections, cells were seeded onto a 24 well plate (Corning) for immunoblotting and a 24 well microclear plate (Ibidi) for time-lapse microscopy. Seeded cells were incubated for 24 hours before 0.5 µg plasmid transfection. Plasmids were incubated with serum-free media containing DhamaFECT 1 transfection reagent (Dhamacon) for 20 minutes. Supplemented DMEM was replaced by DMEM minus FBS and antibiotics. Following media replacement, the plasmid-lipid mixture was added to cells. To confirm transient transfection, each well was trypsinised, lysed by 50 µl 6 x SDS buffer and proteins were run on an SDS-PAGE gel for immunoblotting.

For siRNA transfections, the required siRNA (see Table 2.3) was diluted to 2 µM in 1x siRNA buffer (Dhamacon). In each well of a 96-well plate, 5 µl of the diluted siRNA mixture was added to 45 µl of DharmaFECT 1 transfection reagent reagent (Dhamacon) diluted in OPTI-MEM® (Gibco). Lipid-RNA mixtures were incubated at room temperature for 30 minutes. Cells were plated on top of the siRNA mixture using DMEM media minus antibiotics. Following 24 hour incubation at 37 °C, the transfection media was removed from the cells. Cells were washed in PBS and released into the drugs indicated for time-lapse microscopy. For immuno-blotting, 12 wells per condition were trypsinised, pooled, centrifuged and lysed in 100 µl 6x SDS buffer after 24-hour incubation with the relevant siRNAs to confirm knockdown.

siRNA	**Sequences (5'-3')**
Non-targeting	UGGUUUACAUGUCGACUAA, UGGUUUACAUGUUGUGUGA, UGGUUUACAUGUUUUCUGA, UGGUUUACAUGUUUUCCUA
Mcl-1	CGAAGGAAGUAUCGAAUUU, GAUUAUCUCUCGGUACCUU, GAAGGUGGCAUCAGGAAUG, GGUUUGGCAUAUCUAAUAA
Bcl-xL	GGACAGCAUAUCAGAGCUU, GAAAUGACCAGACACUGAC, CCUACAAGCUUUCCCAGAA, UUAGUGAUGUGGAAGAGAA
Cdc20	CGGAAGACCUGCCGUUACA, GGGCCGAACUCCUGGCAAA, GAUCAAAGAGGGCAACUAC, CAGAACAGACUGAAAGUAC
Bak	CGACAUCAACCGACGCUAU, UAUGAGUACUUCACCAAGA, GACGGCAGCUCGCCAUCAU, AAUCAUGACUCCCAAGGGU
Bax	UGGGCUGGAUCCAAGACCA, CUGAGCAGAUCAUGAAGAC, ACAUGUUUUCUGACGGCAA, GUGCCGGAACUGAUCAGAA
Fbw7	GGGCACCAGUCGUUAACAA, GUGAGUGGAUCUCUUGAUA, GGAGUUGUGUGGCGGAUCA, CAACAACGACGCCGAAUUA
MULE (HUWE1)	GCAAAGAAAUGGAUAUCAA, GGAAGAGGCUAAAUGUCUA, UAACAUCAAUUGUCCACUU, GAAAUGGAUAUCAAACGUA

Table 2.3 siRNA Sequences

2.2 Molecular Biology

DNA plasmid vectors containing the pcDNA5- and pLNCX2- backbones are stored in 50 % glycerol at -80 °C. Table 2.4 describes the cloning strategy to create the vectors used in this thesis. The AID tag was inserted into the pcDNA5/FRT/TO/GFP vector using a SalI restriction site at the N-terminus that fused to the digested XhoI site, removing the existence of both sites. Furthermore, the AID-tag was PCR amplified with primers such that the C-terminus contained restriction sites for XhoI, BamHI and NotI for cloning of target genes into the C-terminus.

Vector	Production
pcDNA5-FRT-TO-Cyclin B1 R42A-GFP	Made previously by K.Gascogine
pcDNA5-FRT-TO-GFP-AID	PCR amplify fragment, SalI/NotI digestion
pcDNA5-FRT-TO-GFP-AID-Cyclin B1 WT	XhoI/NotI digestion. Fragment already in-house
pcDNA5-FRT-TO-GFP-AID-Cyclin B1 R42A	XhoI/NotI digestion. Fragment already in-house
pcDNA5-FRT-TO-GFP-AID-Mcl-1 WT	PCR amplify fragment, BamHI/ApaI digestion. Fragment already in-house
pcDNA5-FRT-TO-GFP-AID-Mcl-1 RALA	PCR amplify fragment, BamHI/ApaI digestion. Fragment already in-house
pcDNA5-FRT-TO-GFP-Mcl-1 WT	Made previously by C.Topham
pcDNA5-FRT-TO-GFP-Mcl-1 RALA	Made previously by C.Topham
pLNCX2-mCherry	Made previously by K.Gascogine
pLNCX2-90aaMcl-1 WT-mCherry	PCR amplify fragment, XhoI/BamHI digestion
pLNCX2-90aaMcl-1 RALA-mCherry	PCR amplify fragment, XhoI/BamHI digestion

Table 2.4 Molecular Cloning

Polymerase Chain Reaction

DNA fragment genes were amplified using Q5® High-Fidelity DNA Polymerase. The reaction was set up as the following: 0.3 µg vector DNA, 0.2 mM each primer (see table 2.5), 8 mM dNTPs (Bioline), 10x Q5 reaction buffer, 200 U Q5® High-fidelity DNA Polymerase and dH_2O. Cycling conditions performed by a Geneamp® PCR System 2700 (Applied Biosystems) are specified in table 2.6.

Restriction Digest

Restriction digestion reactions were used to 1) digest plasmids for ligation and to 2) confirm plasmid identification. For digestion of PCR products, PCR products were purified using the QIAquick® PCR Purification kit (Qiagen). Briefly, 10 x CutSmart® Buffer, DNA (all 30µl eluted from PCR purification reaction, 3 µg of vector, 0.3 µg for test digest), 20 U enzyme (see table 2.4) (NewEnglandBiolabs) were added to a tube and incubated at 37°C either overnight for ligation reactions or for 90 minutes for a test digest.

Restriction site-gene of interest	Sequences (5'-3')
BamHI-Mcl-1-ApaI	**F** ATATGGATCCTTTGGCCTCAAAAGAAACGCG **R** ATATGGGCCCCTATCTTATTAGATATGCCAA
BamHI-mMcl-1-ApaI	**F** ATATGGATCCTTTGGCCTGCGGAGAAACGCG **R** ATATGGGCCCCTATCTTATTAGATATGCCAG
XhoI-90aaMcl-1-BamHI	**F** ATATCTCGAGGACGGGTCACTACCCTCGACGCCG **R** ATATGGATCCCAACGATTTCACATCGTCTTCGTT
SaI-AID-Xho1/BamHI/NotI	**F** ATATGTCGACGGCAGTGTCGAGCTGAATCTGA GGGAG **R** ATATGCGGCCGCGGATCCCTCGAGAGCTCTGC TCTTGCACTTCTC
MULE (qPCR)	**F** GGGGTTATGACCCAAGAGGT **R** CCCATCTCGAGACTCCTCTG
GAPDH (qPCR)	**F** CCACCCATGGCAAATTCCATGGCA **R** TCTAGACGGCAGGTCAGGTCCACC
Sequencing Primers	
GFP	**F** CATGGTCCTGCTGGAGTTCGTG
CMV	**F** CGCAAATGGGCGGTAGGCGTG
pcDNA5 Reverse	**R** TAGAAGGCACAGTCGAGG

Table 2.5 Primer sequences

Time	Temperature	Cycles
30 Secs	98 °C	
20 Secs	98 °C	X 32
30 Secs	55 °C (Cyclin B1, Mcl-1, 90aa fragments) 65 °C (mMcl-1)	
2 Mins	72 °C	
5 Mins	72 °C	
Store	4 °C	

Table 2.6 Polymerase Chain Reaction Conditions

Gel electrophoresis

Gel electrophoresis was used to confirm the amplification of a gene using PCR, to confirm existence of the correct plasmid via restriction digest reactions and to isolate digested vector and insert for ligation. For the first two functions, agarose (Bioline) was dissolved into TBE buffer (88mM Tris, 88nM Boric Acid, 2 mM EDTA, pH 8.2) such that the final concentration of gel was 1 % agarose. For the later function, Microsieve Clone LM agarose (Flowgen Bioscience) was used and set at 4 °C. Samples were mixed with a DNA dye (50 % glycerol, 10 % bromophenol blue, 10 % xylene blue) and ran in TBE buffer within the gel using a Biorad

Minisub® CELL GT (Biorad). Gels were stained with ethidium bromide and DNA was visualized using a hand-held UV lamp (UVP). The DNA fragments required for ligation were removed from the gel using stainless steel surgical blades (Swann-Morton).

DNA Ligation

Following excision from agarose gel, the gel slices containing DNA fragments were heated to 55 °C for 10 minutes to melt the agarose. In a separate tube, 1 µl of the vector backbone gel mixture was mixed with 7 µl of the insert gel mixture with 1 µl 10 x T4 DNA Ligase reaction buffer (NewEnglandBiolabs). The gel mixture was left on ice to solidify before the addition of 1 µl T4 DNA Ligase (400 U/µl) (NewEnglandBiolabs) on top of the gel mixture and incubated at room temperature for 90 minutes. Following incubation, 40 µl dH_2O was added to the reaction and the tubes were placed on a 55 °C heat block for a further 10 minutes.

Bacterial Transformation and Plasmid Isolation

XL1 Blue *Escherichia Coli* competent cells were thawed after storage at -80 °C and placed on ice. Bacteria (50 µl) and the vector-insert gel mixture (10 µl) were combined in a separate tube, placed on ice for 20 minutes and heat-shocked for 90 seconds at 42 °C. Transformed bacteria were spread onto agar plates containing carbenicillin (100 µg/ml). Plates were incubated at 37 °C overnight. Single colonies were picked and placed into a liquid culture of Luria Broth (Invitrogen) containing ampicillin (25 µg/ml). Following overnight growth at 37 °C in a shaking incubator, replicated plasmids were isolated and purified using QIAprep® spin miniprep kit (Qiagen) and stored at -20 °C. For long-term storage, bacterial cultures were mixed 50:50 with glycerol and placed at -80 °C.

DNA Sequencing

DNA Sequencing was performed in the University Core Sequencing Facility. DNA samples were prepared for sequencing using the BigDye® Terminator Sequencing Kit (Applied Biosystems). The sequencing reaction consisted of 6 pmol primer (see table 2.6 for sequences), 1 µg DNA, 5 x BigDye® Terminator Sequencing Buffer and 1 µl BigDye® Terminator Sequencing Kit (both Applied Biosystems). DNA amplification was performed using the following cycle times

25: 96 °C for 10 seconds, 50 °C for 5 seconds and 60 °C for 4 minutes. Amplified DNA was precipitated on ice for 15 minutes with 8.5 mM NaAc pH 4.8, 70 % EtOH, and 9 µg/ml GlycoBlue (Ambion). Precipitated pellet was pelleted by centrifugation and air-dried for sequencing.

2.3 Protein analysis

Bradford assay

For equal loading of protein between cell lines a Bradford assay was performed in order to quantify the amount of protein in the lysate. Briefly, 150 µl of Bradford solution (Sigma) was added to a clear 96-well plate (BD Falcon™). To each solution, 2 µl of sample was added and left to rest for 20 minutes before measurement. A protein standard curve was set up using a purified BSA substance (NewEnglandBiolabs) and diluted in duplicate to concentrations between 0.75-10 µg. Detection of protein was performed on a Synergy HT microplate reader (Biotek) at 595 nm. Concentration of protein was calculated based on standard curve measurements of BSA and 8 µg of each lysate was loaded onto an SDS-PAGE gel.

SDS-PAGE

All proteins were denatured for 5 minutes at 100 °C in 6 x SDS buffer Resolution of proteins was achieved with either a 12 % acrylamide gel for Mcl-1 and Bcl-xL blots and 10 % gel for immuno-blotting of all other proteins (see Table 2.7 for reagents). A Precision Plus Protein™ Dual Color standard (Biorad) was used a a marker ladder. In 1 x running buffer (25 mM Tris, 200 mM glycine, 0.1 % (w/v) SDS), a current of 80 V was applied for 1 hour using a Hoefer™ SE260 vertical electrophoresis unit (Amersham Biosciences) followed by an application of 120 V until resolve of proteins had reached completion.

Immunoblotting

Polyacrylamide gels containing resolved proteins were electro-blotted onto Immobilion-P membranes (Millipore) using a Mini-PROTEAN® Tetra System (Bio-Rad) in 1 x transfer buffer (25 mM Tris, 190 mM glycine, 0.1 % (w/v) SDS, 20 % methanol) at 300 Å for 75 minutes. The membrane was initially soaked in methanol. To minimalise non-specific antibody binding, the

protein-coated membrane was blocked for 30 minutes in 5 % milk (Marvel) in TBST (100 mM Tris, 150 mM NaCl, 0.1 % (v/v) Tween-20, pH 7.5) for 30 minutes prior to overnight incubation at 4 °C with the primary antibodies indicated diluted in TBST/milk (see table 2.8). Unbound primary antibody was washed off membranes with 3 x TBST on a rocking platform. Following TBST washes, blots were incubated with the relevant horseradish-peroxidase-conjugated secondary antibody (see table 2.8). Detectable signal was produced by the addition of EZ-ECL Chemiluminescence Reagents (Biological Industries) and developed on a Biospectrum® 500 imaging system (UVP). For weaker signals, Luminata™ Forte Western HRP Substrate (Millipore) was used as a substrate. Images were processed on VisionWorks®LS (UVP).

Regent (per gel)	**Resolving Gel (ml)**		**Stacking Gel (ml)**
	10 %	12 %	
H_2O	6.1	5.1	5.7
1.5 M Tris pH 8.8	3.75	3.75	n/a
Tris 0.5 M pH 6.8	n/a	n/a	2.5
Acrylamide (30 %)	5	6	1.7
10 % (v/v) SDS	0.15	0.15	0.1
10 % (v/v) APS	0.15	0.15	0.1
TEMED	0.015	0.015	0.01

Table 2.7 SDS-PAGE Buffers

Coimmunoprecipation

For immunoprecipation of exogenous GFP-tagged proteins, a GST-GFP-binder protein was used (Rothbauer et al., 2008). Previously, the ORF encoding a GFP-binder had been cloned into pGEX-4T3 then transformed into *E.coli* strain BL21. The GST-GFP-binder fusion protein was then induced with IPTG purified using Glutathione sepharose beads (Amintra), eluted using soluble glutathione then dialysed. Prior to co-immunoprecipitation, cells were plated into four 10 cm dishes per condition and treated with 1 µg/ml tetracycline overnight to induce expression of GFP-tagged proteins once the cells have reached roughly 70 % confluency. Cell plates were trypisised, pooled and lysed in lysis buffer (0.1 % Triton X-100, 100 mM NaCl, 10 mM Tris pH7.4, 1 mM EDTA, 1mM EGTA, 20 mM β-glycerol, 10 mM NaF, cOmplete™, Mini, EDTA-free Proteasome inhibitor Cocktail tablet (Roche)). Insoluble proteins were removed by centrifugation at 4 °C. To extract GFP-tagged proteins, Glutathione magnetic bead slurry (50 %) was pre-washed twice in lysis buffer and added to the lysate along with 30 µg of GST-GFP-binder

protein. The bead-lysis mixture was put under rotation at 4 °C for three hours. The beads were washed five times in lysis buffer to remove any unspecific protein binding. To elute and denature the proteins bound to the beads, 6X SDS sample buffer was added to the beads and the samples were boiled for 5 minutes at 100°C. For the input sample, 5 % of the original lysis was taken.

Antibody Target	Host	Source	Concentration
Primary Antibodies			
Anti-Cyclin B1	Mouse	Millipore	1/1500
Anti-Tao1	Sheep	(Westhorpe et al., 2010)	1/1500
Anti-Mcl-1	Rabbit	Santa-Cruz	1/800
Anti-Bcl-xL	Rabbit	Cell Signalling	1/800
Anti-Myc (tag) 4A6	Mouse	Millipore	1/5000
Anti-Bak	Mouse	Calbiochem	1/800
Anti-Bax	Rabbit	Santa-Cruz	1/800
Anti-Cdc20	Mouse	Santa-Cruz	1/2000
Anti-FBW7	Rabbit	Bethyl	1/800
Anti-α-tubulin	Mouse	(Woods et al., 1989)	1/300
Anti-Aurora A	Sheep	(Girdler et al., 2006)	1/1000
Secondary Antibodies			
Anti-mouse HRP	Goat	Zymed	1/2000
Anti-rabbit HRP	Goat	Zymed	1/2000
Anti-sheep HRP	Rabbit	Zymed	1/2000
Anti-sheep-Cy2	Rabbit	Stratech	1/1000
Anti-mouse-Cy3	Goat	Stratech	1/1000

Table 2.8 Antibodies

2.4 Microscopy

Time-lapse microscopy

Cells were plated and transfected 24 hours prior to addition of anti-mitotic drugs and subsequent time-lapse imaging. Cells were seeded onto a microclear 96 well plate (Greiner). For the majority of the time-lapse imaging experiments, cells were maintained at 37 °C and 5 % CO_2 and phase-contrast images were taken within an IncuCyte ZOOM® (EssenBioSciences) using a 20x objective for the times indicated. Once trained, real-time confluency measurements were performed using the IncuCyte ZOOM® software. For confluency measurements, an average across 4 images per well were taken and represented as percentage change from t=0. To

determine mitotic fate and timing, MPEG-4 image sequences were generated and analysed manually (50 cells per condition from duplicate wells). Figure 2.1 displays images depicting what defines the various mitotic cell fates. Zero hours represents when imaging started unless indicated otherwise. Cell fate profiles were drawn on Graphpad Prism 6 (Gascoigne and Taylor, 2008). For real-time measurement of apoptosis, IncuCyte™ 96-Well Kinetic Caspase-3/7 reagent was added to the media at a final concentration of 5 μM and the number of green fluorescent entities was counted by IncuCyte ZOOM® software (EssenBioSciences).

Fluorescent time-lapse microscopy.

For transient transfections of the mCherry-Mcl-1 fragments and fluorescent tracking of AID-tagged proteins, live cell tracking of fluorescent cells was performed on an Axiovert 200 microscope (Zeiss) enclosed by a control chamber (Solvent) where cells were maintained at 37 °C and a continuous flow of CO_2. Images were taken every 10 minutes using a CoolSNAP HQ camera (Photometrics). Images were viewed on Metamorph® software. Cells were seeded into a 24 well microclear plate (Ibidi). The n number of cells are as indicated. Cell fluorescence was determined at each time point using integrated pixel intensity within a defined region of choice. Each fluorescence measurement was normalised against background fluorescence at each time point.

Immunofluorescence

Cells were washed with PBS and fixed in 100 % MeOH for 20 minutes at -20 °C. Fixed coverslips were washed in PBS/T (PBS with 0.1 % (v/v) Triton X-100) and incubated with PBS/T for 20 minutes at room temperature. Primary antibodies were diluted to the appropriate dilution with PBS/T and added to the coverslips for 30 minutes at room temperature. Unbound antibodies were washed off coverslips using three PBS/T washes before coverslips were incubated with the appropriate secondary antibodies (see table 2.8) for 30 minutes at room temperature in the dark. Unbound secondary antibodies were washed off the coverslips using three PBS/T washes. Coverslips were inverted and put on top of a glass slide containing a drop of mounting media (90 % glycerol, 20 mM Tris pH 9.2). An Axioskop 2 microscope (Zeiss) with a

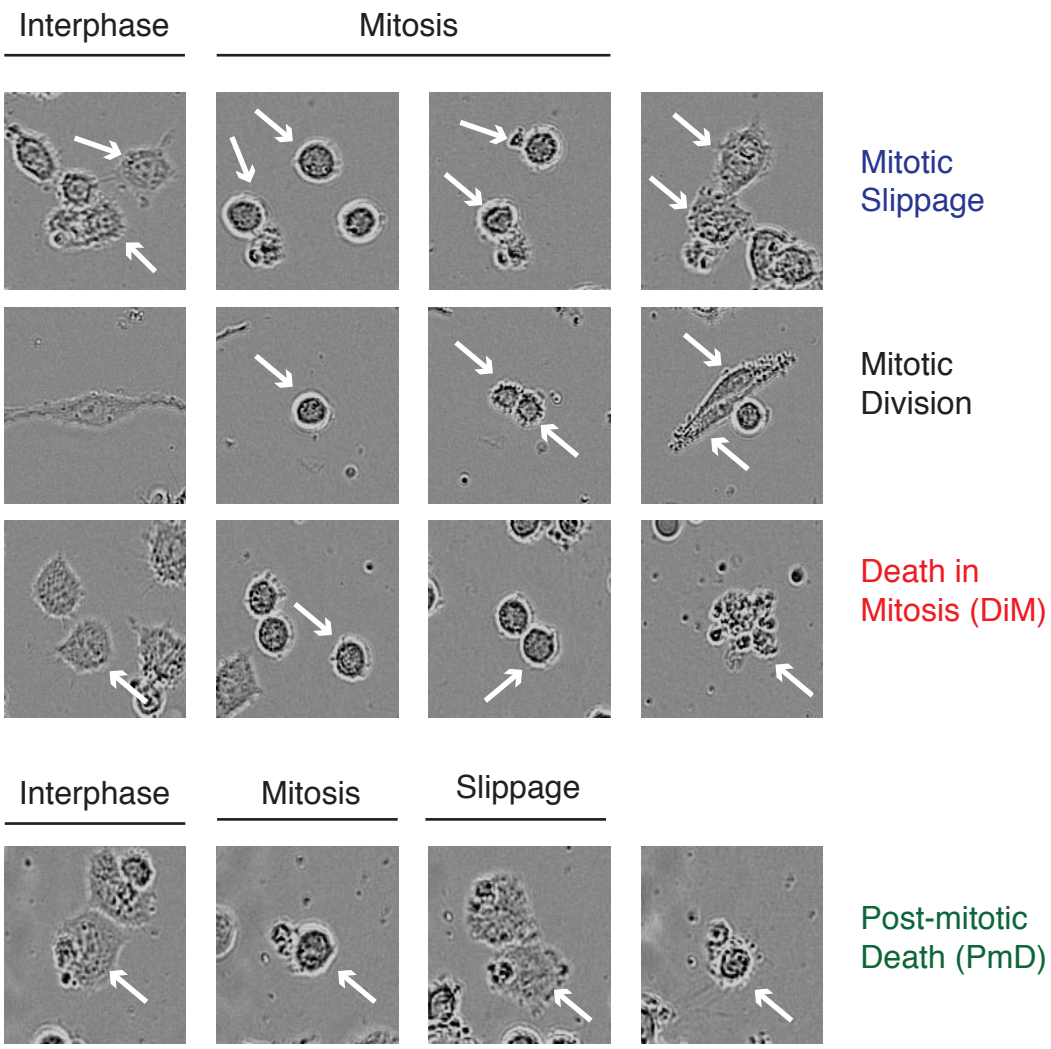

Figure 2.1. Definition of mitotic fates. Cell fate profiles were generated by the analysis of phase time-laspe images of RKO cells treated with taxol as above. The point of mitotic slippage is defined as the flattening down of the cell without division into two daughter cells. Mitotic division is defined as the point the cell separates into two and flattens down onto the plate. Death in mitosis (DiM) and post-mitotic death (PmD) are defined as the point of cell death in mitosis and interphase, respectively.

100x objective was used to image cells and images were taken using a CoolSNAP HQ CCD camera (Photometrics). Images were analysed on Metamorph® software.

2.5 RNA analysis

RNA extraction

Following trypsinisation and centrifugation, cells were homogenized in 1 ml TRIzol® for 5 minutes before the addition of 0.2 ml chloroform. The chloroform-phenol mixtures were shaken vigorously for 15 seconds and incubated at room temperature for 2 minutes before centrifugation at 4 °C at 12,000 x g for 15 minutes. The top aqueous phase was removed, and the RNA was precipitated out of solution using 0.5 ml 100 % isopropanol at room temperature for 10 minutes before centrifugation for 10 minutes at 4 °C at 12,000 x g to pellet the RNA. The RNA pellet was washed with 1 ml 75 % ethanol, and re-pelleted. Finally, RNA was resuspended in RNase-free water and incubated for one hour with DNase enzyme and stored at -80 °C until use.

cDNA Synthesis

Total RNA (1 µg) was incubated at 70°C for 10 minutes with the following: 0.83 mM dNTPs and 0.29 µM random hexamers (Qiagen) for primer annealing. The mixture was chilled on ice before the addition of Reverse Transcriptase (100 Units) (Qiagen) and RNase inhibitor (20 Units) (Qiagen), RT buffer (Qiagen) and dH_2O. Tubes were incubated at the following temperatures: room temperature for 10 minutes, 37 °C for 50 minutes and 88 °C for 10 minutes.

Quantitiative PCR (qPCR)

For specific gene amplification, 0.5 µl of the synthesized cDNA (see above) was mixed with SYBR® Green (Qiagen), 1 µM each primer (for sequences, see table 2.6) and dH_2O. Cycling conditions were as followed: 8 minutes at 95 °C followed by 40 cycles of 30 seconds at 95 °C, 30 seconds at 58 °C and 45 seconds at 72 °C. Analysis was performed on an Mx3000P qPCR System (Agilent Technologies). Fold changes were calculated using the delta CT method.

2.6 Flow Cytometry

Cells were plated into a 6-well plate at 15 x10^4 cells/ml and treated with drugs indicated. Both the cell media and trypsinised cells were collected into a tube and centrifuged at 12,000 rpm for 5 mins. Pelleted cells were washed in PBS and re-suspended with 150 µl PBS before drop-wise fixation of the cells with 350 µl 100 % ethanol. Fixed cells were stored at -20 °C for at least 16 hours. Cells were again pelleted by centrifugation and washed with PBS. To measure DNA content, pelleted cells were re-suspended in 40 µg/ml propidium iodide and 50 µg/ml RNase A diluted in PBS for at least 1 hour. Cell populations stained with propidium iodide were analysed on a BD Biosciences LSR Fortessa.

2.7 Statistical Tests

Cumulative frequency plots and statistical analyses (non-parametric Mann-Whitney U tests and correlation analysis) were performed on Graphpad Prism 6. Box-and-whisker plots show the mean and the interquartile ranges. Error bars represent standard deviation.

3 Chapter 3: The role of Mcl-1 in mitotic death

3.1 Introduction

Loss of Mcl-1 increases cell death in mitosis (DiM) in response to anti-mitotics (Shi et al., 2011; Topham et al., 2015; Tunquist et al., 2010). Whilst it seems likely that Mcl-1 loss increases the rate of pro-apoptotic signalling in mitosis, it is also possible that the increase in death is caused by the suppression of mitotic slippage by loss of Mcl-1. To distinguish between these two possibilities I would require a model system that was able to (1) uniformly commit to DiM in response to anti-mitotics so the rate of mitotic death could be directly measured and (2) degrade Mcl-1 in order to analyse the contribution of changes in Mcl-1 levels to DiM. The colon carcinoma cell line, RKO, predominantly undergoes mitotic death in response to a variety of anti-mitotic drugs (Gascoigne and Taylor, 2008). One way to inhibit residual slippage in this cell line is to express a stabilised form of Cyclin B1. This mutation, Cyclin B1 R42A, destroys the RxxL D-box motif of Cyclin B1 that is recognised by APC/C-Cdc20 (Holloway et al., 1993; Sivakumar and Gorbsky, 2015). High expression of Cyclin B1 R42A in mammalian cells results in a sustained metaphase-like arrest, where sister chromatids remain bound together (Hagting et al., 2002; Wolf et al., 2006). At low expression sister chromatids separate but mitotic exit is inhibited owing to re-activation of the spindle assembly checkpoint due to inefficient degradation of the mutant Cyclin B1 R42A protein (Clijsters et al., 2014; Hagting et al., 2002; Wolf et al., 2006). In this Chapter I generate this cell line and use it to directly measure time to mitotic death when modulating Mcl-1 levels.

3.2 Mitotic Mcl-1 degradation is proteasome-dependent in RKO cells.

In order to study the kinetics of mitotic death I first wanted to determine whether Mcl-1 levels were reduced in RKO cells during mitosis. Cells were synchronised overnight by thymidine treatment before being released into 0.1 μM taxol (Figure 3.1A). Flow cytometry analysis of RKO cells following thymidine treatment shows an increase in cells in S phase compared to asynchronous controls (Figure 3.1B, left and middle panels). To observe Mcl-1 levels during this

time-course protein samples were taken every 2 hours following a 10-hour incubation in taxol. The immunoblot (Figure 3.1C) shows that in interphase Mcl-1 runs as a
single band of approximately 37 kDa. Following 10 hour treatment with taxol, when the majority of cells are in a mitotic arrest- (Figure 3.1B, right panel), a higher molecular band was also observed which corresponds to the mitosis-specific phosphorylation of Mcl-1 at T92 and S64 (Harley et al., 2010; Kobayashi et al., 2007). However, the levels of both forms of Mcl-1 are reduced during the course of a mitotic arrest when compared to the protein levels of loading control protein Tao1, that is unaffected in a mitotic arrest (Westhorpe et al., 2010). Mcl-1 protein levels had decreased significantly compared to the original 10-hour level after 16 hours taxol treatment. Consistent with previous observations, Mcl-1 is degraded in RKO cells during a prolonged mitotic arrest induced by taxol treatment.

Many proteins are degraded via the proteasome, a large holoenzyme complex containing many enzymes that drive proteolysis. One way to inhibit proteasome-mediated degradation of proteins is treatment of cells with MG132; a small peptide that reversibly binds the proteasome, inhibiting the chymotrypic and post-acidic action of protein degradation (Vinitsky et al., 1992). To investigate whether Mcl-1 is degraded in a proteasome-dependent manner, RKO cells were synchronised in S phase with thymidine and released into taxol for the times indicated. As addition of MG132 blocks mitotic entry, cells were treated with MG132 10-hours after thymidine release into taxol when cells had already entered mitosis (Rapino et al., 2013). Consistent with previous observations, Mcl-1 protein levels reduced during the mitotic arrest in the absence of MG132 (Figure 3.1D,left panel). In contrast, Mcl-1 was not lost in the mitotic population treated with MG132 (Figure 3.1D, right panel). In fact, the levels of both forms of Mcl-1 appear to increase upon the addition of MG132, which may suggest that Mcl-1 is getting synthesised during the mitotic arrest.

Mitotic degradation of several proteins including Cyclin B1, APC/C co-factor Cdc20 and pro-apoptotic protein Bim are also mediated through the ubiquitin-proteasome pathway (Glotzer et al., 1991; Nilsson et al., 2008; Wan et al., 2014). In the absence of MG132, Cyclin B1 protein levels remained constant, consistent with slow Cyclin B1 degradation in RKO cells observed with a Cyclin B1 fluorescent reporter (Gascoigne and Taylor, 2008). Protein levels of Bim were.

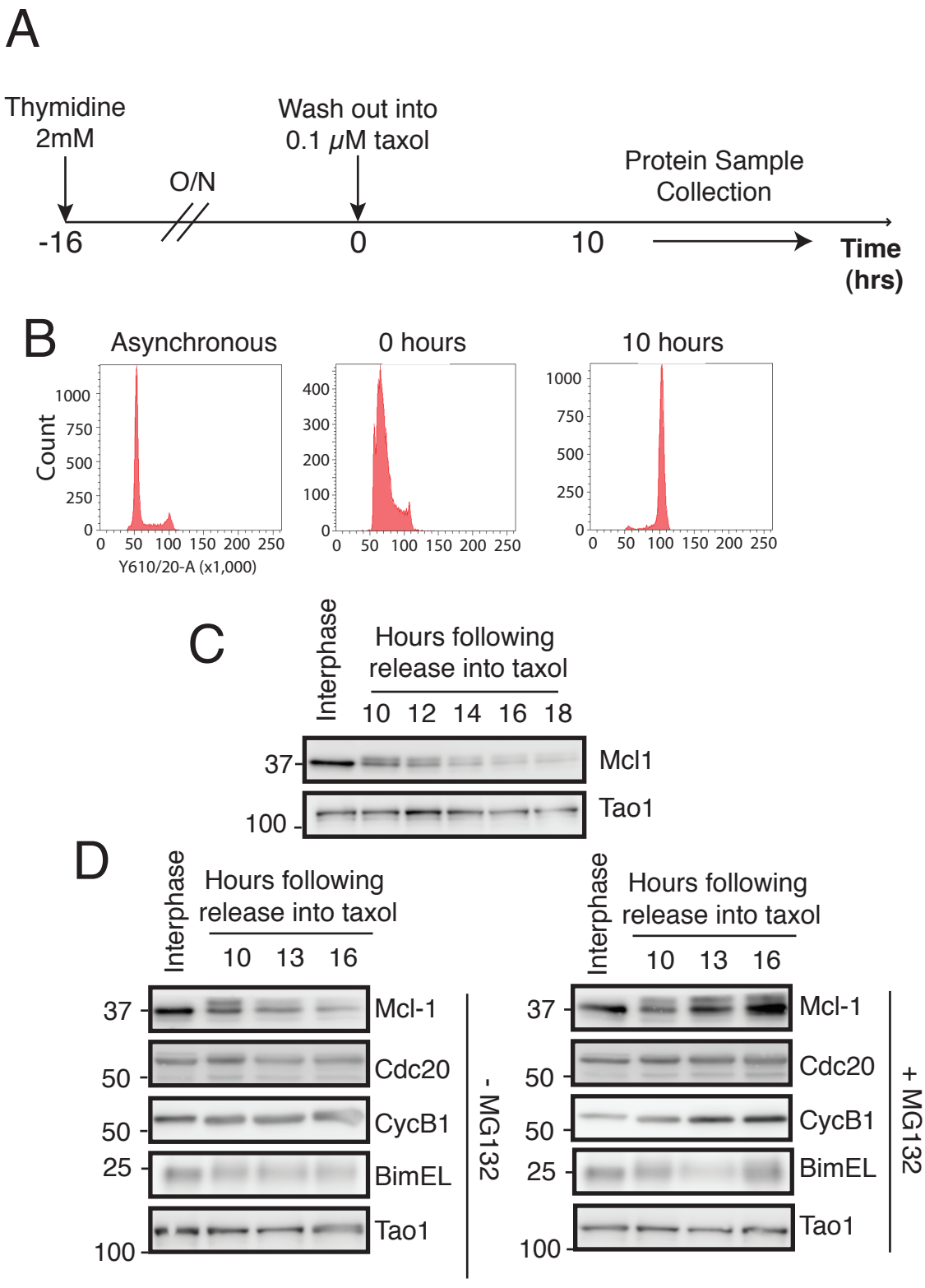

Figure 3.1 Proteasome-mediated loss of Mcl-1 in mitotic RKO cells.
(A) Timeline schematic of experimental procedure for protein sample collection of mitotic RKO cells.
(B) Flow cytometry profile of DNA content in cells treated with thymidine overnight followed by 10 hour taxol treatment.
(C) Immunoblot of Mcl-1 protein levels at times indicated following thymidine release into taxol. Tao1 protein levels were used as a loading control.
(D) Immunoblot of Mcl-1, Cdc20, Cyclin B1 and Bim in RKO cells during the course of a mitotic arrest with or without treatment with the proteasome inhibitor MG132 10 hours following wash-out of thymidine into taxol. Time-points of cell lysis are as indicated.

slightly reduced in all time-course samples in comparison with the interphase population, but no decline over time was observed. Upon MG132 addition, Cyclin B1 levels increased upon which is in line with the notion that Cyclin B1 protein is synthesised during a mitotic arrest (Mena et al., 2010)Addition of MG132 also appeared to increase Bim levels at the later time point of 16 hours, while Cdc20 protein levels remained constant with or without MG132 treatment in mitotic populations. Overall, the most pronounced effect on protein levels upon addition of MG132 was with Mcl-1, confirming that Mcl-1 degradation depends on proteasome activity.

3.3 Generation and characterisation of a cell line (RKO GFP-Cyclin B1 R42A) to directly study the rate of DiM.

The proteasome inhibitor MG132 appeared to have the greatest effect on Mcl-1 levels during a mitotic arrest. Consequently I wanted to investigate the net effect MG132 treatment would have on the rate of DiM. However, the limitation of this approach is that the proteasome also affects the rate of slippage as Cyclin B1 degradation is also abolished (Clute and Pines, 1999). Based on the independent networks model, any change in mitotic death might just be a hallmark of an inhibition of slippage. Therefore, I set out to express a stabilised form of Cyclin B1 (Cyclin B1 R42A) in order to create a model system to directly measure DiM by blocking mitotic slippage.

Constitutive expression of this form of Cyclin B1 is highly detrimental for proliferating cells, as it would interfere with normal cell division. Therefore, I wanted to control the expression of Cyclin B1 R42A gene until it was required for experimental purposes. One way to accomplish this is to put the Cyclin B1 R42A gene expression under the control of a tetracycline-inducible promoter. The tetracycline system is based on a naturally occurring tetracycline-sensitive operon in *Escherichia coli* (Gossen and Bujardt, 1992). Briefly, the operon requires a *trans* rtetR protein that binds to a *cis* tetO element downstream of the promoter region of the gene of interest, hindering the transactivation activity of the promoter. Cell lines stably expressing rtetR had been made previously in the lab. The tetR protein interacts and binds tetracycline when added and this interaction alleviates its interaction with TetO, thus relieving repression on the gene promoter and activating gene expression.

An inducible RKO GFP-Cyclin B1 R42A cell line was created using the Flp-In™ T-Rex System (see methods). Upon addition of tetracycline, expression of the exogenous GFP-Cyclin B1 R42A protein was induced (Figure 3.2A). The expression levels of the exogenous protein (approximately ~80 kDa) appear equal to the endogenous (approximately 55 kDa). Subsequently, I performed time-lapse microscopy on the RKO GFP-Cyclin B1 R42A cell line to determine if this cell line was able to efficiently block mitotic exit either by itself or in combination with 0.1 μM taxol. In the untreated cell population, all cells completed mitosis within 45 minutes and 66 % underwent 3 or more mitoses (Figure 3.2B, left panel). In contrast, upon addition of tetracycline, 80 % of cells now arrested in mitosis for longer than two hours, 50 % of which were unable to overcome the mitotic arrest induced by expression of the GFP-Cyclin B1 R42A protein and eventually commit to DiM, with 34 % and 16 % undertaking mitotic division and mitotic slippage respectively (Figure 3.2B, second panel). As mentioned in Chapter 3.1, different expression levels of Cyclin B1 R42A can cause different phenotypes and heterogenous expression between cells within the population that may account for intraline cell fate variation. Following mitotic exit, cells undertook a variety of post-mitotic responses: of those that exited mitosis, 16 % died in the subsequent interphase, 44 % entered a second mitosis and 40 % remained in interphase. This indicates that although the stabilised GFP-Cyclin B1 R42A protein is able to delay mitotic exit, its expression alone cannot fully block mitotic exit. Although expression of the GFP-Cyclin B1 R42A mutant protein alone did not fully abolish mitotic exit, I tested whether expression of the protein would abolish mitotic slippage when the SAC was superimposed by taxol treatment. Consistent with previous studies of wild type RKO cells, addition of 0.1 μM taxol alone caused 84 % of cells to commit to DiM (Figure 3.2B, third panel) (Gascoigne and Taylor, 2008; Topham et al., 2015). Co-treatment of tetracycline and 0.1 μM taxol caused 100 % of cells to remain in mitosis and commit to DiM with an average time to death of 15.4 hours (Figure 3.3B, fourth panel). These cell fate profiles confirmed that the Cyclin B1 R42A cells could be used as a model system to measure rates of DiM in response to taxol treatment.

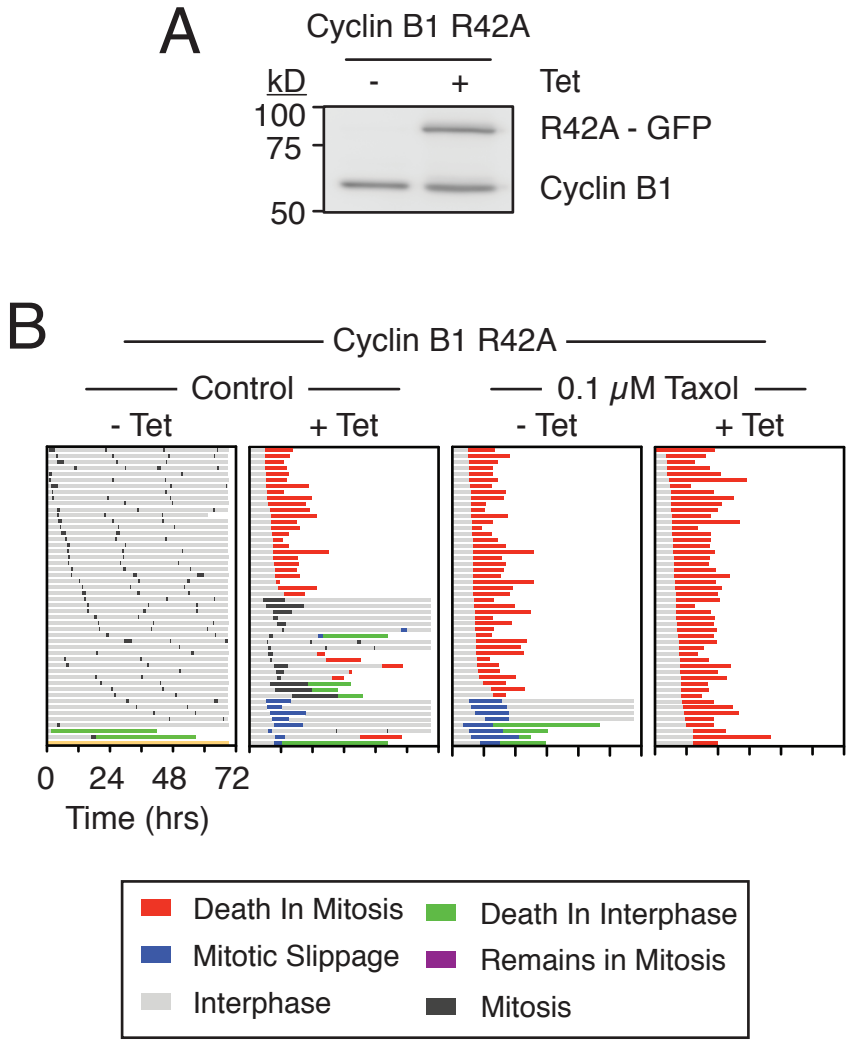

Figure 3.2 Generation and characterisation of RKO GFP-Cyclin B1 R42A cells.
(A) Immunoblot showing endogenous and exogenous Cyclin B1 protein upon tetracycline induction.
(B) Cell fate profiles of RKO GFP-Cyclin B1 R42A cells upon tetracycline induction with or without taxol treatment. n=50.

3.4 Investigating the effect of Mcl-1 depletion on DiM in RKO GFP-Cyclin B1 R42A cells.

In Chapter 3.3 I described a model cell system in which the timing of mitotic death could be directly measured. To determine if the rate of DiM in this cell line was responsive to changes in Mcl-1 levels. I analysed the effect of Mcl-1 depletion on the rate of DiM in the RKO GFP-Cyclin B1 R42A cells in response to taxol treatment by reverse-transfecting cells with either non-targeting or Mcl-1 siRNA. Immunoblotting confirmed the loss of Mcl-1 in Mcl-1 siRNA transfected RKO cells 24 hours after oligonucleotide transfection (Figure 3.3A). Subsequently, RKO GFP-Cyclin B1 R42A cells depleted of Mcl-1 were subjected to the taxol and tetracycline combination. In comparison to the non-targeting and un-transfected populations, Mcl-1 depleted cells committed to DiM at a faster rate, with 50 % of cells committing to DiM by 4.42 hours compared to 13.26 and 14.36 hours on average in the non-targeting and un-transfected populations respectively (Figure 3.3B). This suggests that by accelerating loss of Mcl-1, RKO cells accelerate commitment to DiM.

3.5 Analysing the effect of proteasome-mediated Mcl-1 degradation on DiM.

After observing that the RKO GFP-Cyclin B1 R42A cell line was responsive to Mcl-1 depletion, I chose to test the effect of Mcl-1 stabilisation in this cell line. As shown in Figure 3.1C, addition of MG132 stabilised Mcl-1 in mitosis. To test the effect of MG132 on DiM, cells were treated with the drug 10-hours after taxol addition. Addition of MG132 delayed DiM from an average of 15.5 hours to 25.8 hours (Figure 3.4A). Additionally, there also appeared to be a large degree of variability within the cell population in terms of mitotic death timing. This could be caused by the length of time that each cell had been in mitosis for prior to MG132 addition; cells that had been in mitosis for longer before MG132 addition having already degraded proteins that may contribute to the rate of DiM. To investigate this, I categorised the individual cells into two groups: cells that had either been in mitosis for more than or for less than 2.5 hours preceding MG132 treatment. Although both categories of cells delayed DiM in comparison to the untreated

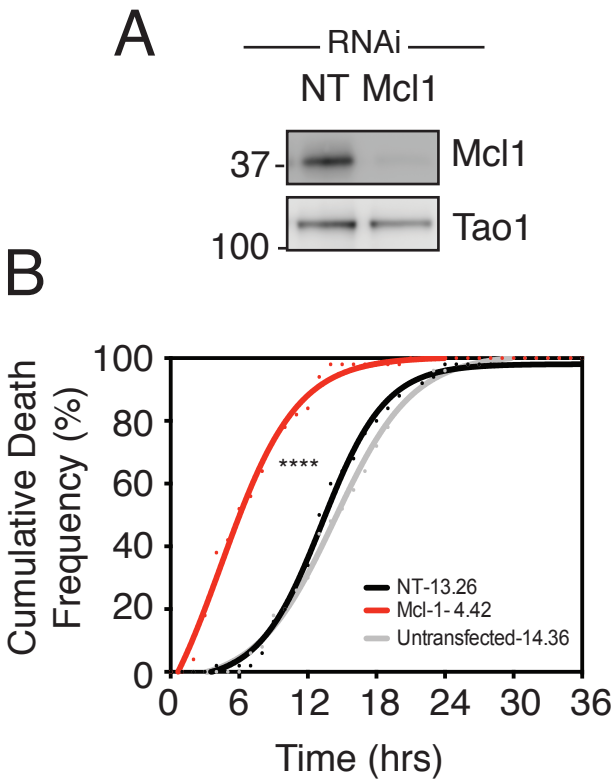

Figure 3.3 Consequence of Mcl-1 depletion on DiM in RKO GFP-Cyclin B1 R42A cells.
(A) Immunoblot of Mcl-1 protein levels following transfection with siRNAs targeting Mcl-1 or non-targeting control. Protein lysates were collected 24 hours following transfection. Tao1 protein levels are used as a loading control.
(B) Cumulative frequency graph of mitotic death following transfection with siRNAs targeting Mcl-1 or non-targeting control. n=50. Mann Whitney U test, **** $p < 0.0001$.

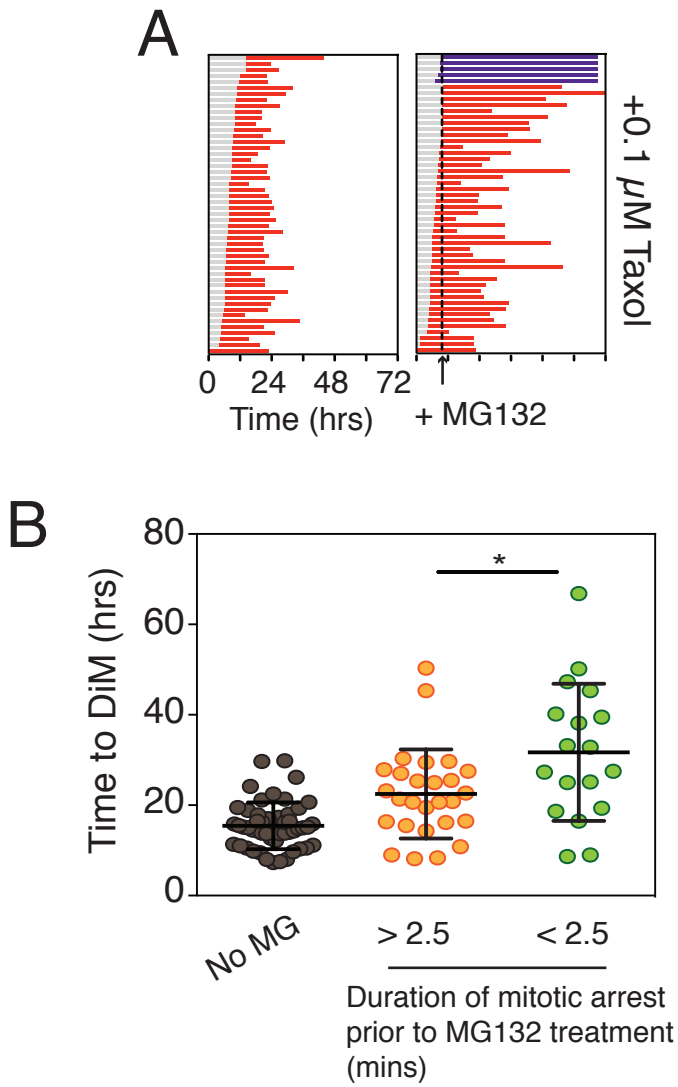

Figure 3.4 Effect of proteasome inhibition on DiM in RKO GFP-Cyclin B1 R42A cells.
(A) Cell fate profiles of RKO GFP-Cyclin B1 R42A cells treated with taxol and tetracycline. At 10 hours MG132 was added. The line represents the point at which MG132 was added to the cell population n=50
(B) The data presented in Figure 3.4A plotted as time-to-death from mitotic entry in RKO GFP-Cyclin B1 R42A cells treated with taxol, tetracycline and MG132 at 10 hours. Cells within the MG132-treated population were sub-catagorised based on mitotic duration prior to the addition of MG132. Mann Whitney U test, * $p < 0.05$

control population, the fraction of cells that had been in a mitotic arrest for only 2.5 hours or less prior to MG132 treatment delayed death significantly longer than those that had been in mitosis for longer (Figure 3.4B). Thus far, I can conclude from this that proteasome-mediated proteolysis sensitises cells to DiM.

However, inhibition of the proteasome is also inhibits degradation of a number of proteins during a mitotic arrest (Figure 3.1C) (Glotzer et al., 1991; Nilsson et al., 2008; Wan et al., 2014) To test if the effect of MG132 on DiM was specific to Mcl-1 stabilisation, Mcl-1 depleted cells were also treated with MG132. Immunoblotting showed efficient loss of Mcl-1 following siRNA transfection that increased upon MG132 treatment although the Mcl-1 levels were below that of the non-targeted untreated population (Figure 3.5A). Importantly, this increase was substantially less than the non-targeting population treated with MG132 relative to the Tao1 loading control.

To determine the effect on DiM, cells were again tracked by time-lapse microscopy. However, to counteract the possibility that endogenous protein had already been degraded before the addition of MG132 as shown in Chapter 3.4, only cells that had been in mitosis for less than 2.5 hours were analysed. The addition of MG132 to control cells transfected with NT siRNA delayed DiM by 23.1 hours: from 10.2 hours to 31.2 hours (Figure 3.5B, 3.5C, left panels). As described previously, cells transfected with siRNA targeting Mcl-1 underwent DiM faster with an average time of 3.47 hours (Figure 3.5B). Strikingly, addition of MG132 did not induce a significant delay to DiM in Mcl-1 depleted cells, with an average time to DiM of 4.0 hours. Importantly, there was no significant difference between the time to DiM in Mcl-1 depleted cells with or without MG132 treatment (Figure 3.5B, 3.5C, middle panel). Additionally, to ensure that the lack of delay by MG132 in Mcl-1-depleted cells was not simply because cells had committed to DiM before addition of MG132 due to an acceleration of pro-apoptotic signalling, Bcl-xL siRNA was used as an additional control. The immunoblot for Bcl-xL displays an additional band in the mitotic lysates, consistent with phosphorylation of Bcl-xL in mitosis at Serine 62 (Figure 3.5A)(Upreti et al., 2008b). Loss of Bcl-xL accelerated mitosis by 3.83 hours but like the non-targeting population, MG132 treatment delayed the average time to death by 19.3 hours to 25.7 hours (Figure 3.5B, 3.5C, right panel).

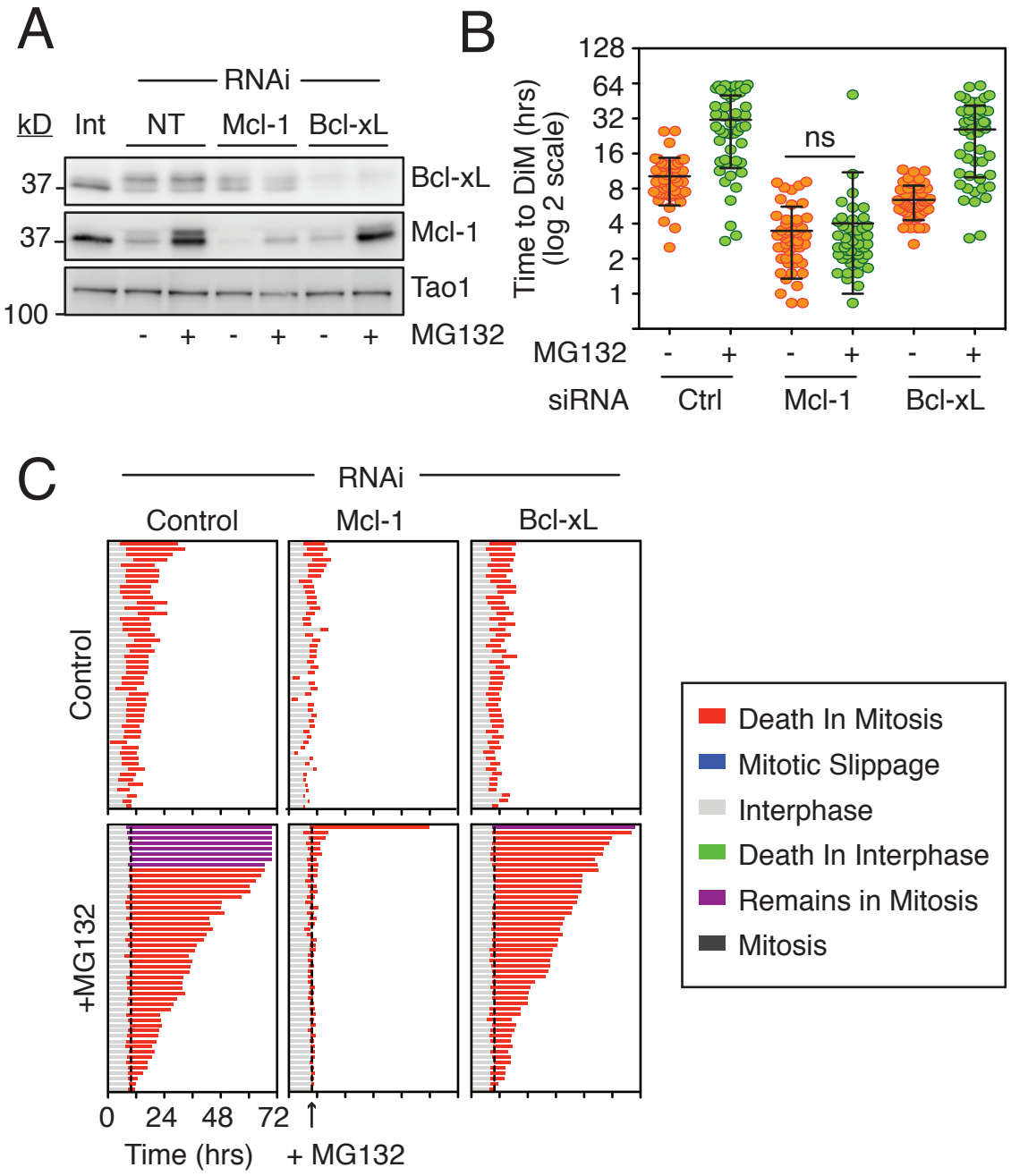

Figure 3.5 Effect of proteasome-mediated Mcl-1 degradation on DiM in RKO GFP-Cyclin B1 R42A cells.
(A) Immunoblot of Mcl-1 and Bcl-xL protein levels of RKO GFP-Cyclin B1 R42A cells following 24 hour transfection with siRNAs targeting the indicated proteins before treatment with taxol, tetracycline and MG132 (after 10 hours). Lysates were collected 16 hours following drug treatment.
(B) Time-to-DiM from mitotic entry of RKO GFP-Cyclin B1 R42A cells treated as indicated in Figure 3.5A. Mann Whitney U test, ns $p > 0.05$.
(C) Cell fate profiles of RKO GFP-Cyclin B1 R42A cells treated reated as indicated in Figure 3.5A.

Put together, I can conclude that the dynamics of Mcl-1 degradation contribute to the sensitisation of these cells.

3.6 Investigating the effect of protein synthesis on Mcl-1 degradation and DiM.

As described previously (Chapter 3.2), upon addition of MG132, Mcl-1 protein levels were not just stabilised but increased during the course of a mitotic arrest. This suggests that Mcl-1 is being synthesised *de novo* during the course of a mitotic arrest. To test this I took lysates from mitotic cell populations during a mitotic arrest induced by treatment with taxol with or without the translational inhibitor cycloheximide. Cycloheximide inhibits the ability of the ribosome to move along the mRNA strand, thus blocking translational elongation (Schneider-Poetsch et al., 2010). As cycloheximide has a universal effect on gene expression I added the drug 10 hours after the start of taxol treatment. Addition of cycloheximide to RKO GFP-Cyclin B1 R42A cells dramatically accelerated Mcl-1 loss during a mitotic arrest (Figure 3.6A). This indicates that Mcl-1 is being synthesised during a mitotic arrest.

Cells treated with cycloheximide were imaged and analysed by time-lapse microscopy. As with the previous MG132 experiment, cell analysis was filtered so that only cells that had entered mitosis within 2.5 hours were quantified. Addition of cycloheximide increased mitotic slippage from 4 % to 26 % (Figure 3.6B). The increase in slippage is likely to be caused by inhibition of *de novo* Cyclin B1 synthesis in mitosis and therefore accelerated loss in Cyclin B1 protein levels resulting in slippage (Mena et al., 2010). Furthermore, time to DiM was accelerated from 15.2 to 9.2 hours in the cycloheximide-treated population (Figure 3.6C). It is possible that the decrease in the average time to DiM could be attributed to accelerated slippage that 'masked' cells that would have taken longer to commit to apoptosis. However, 31 cells (62 %) of the untreated population took longer than 13.1 hours to commit to apoptosis whereas only one cell within the cycloheximide-treated population underwent death-in-mitosis by this point and so this seems unlikely. Together, this suggests that inhibition of translation by cycloheximide accelerates DiM, and this may be attributed to Mcl-1 synthesis.

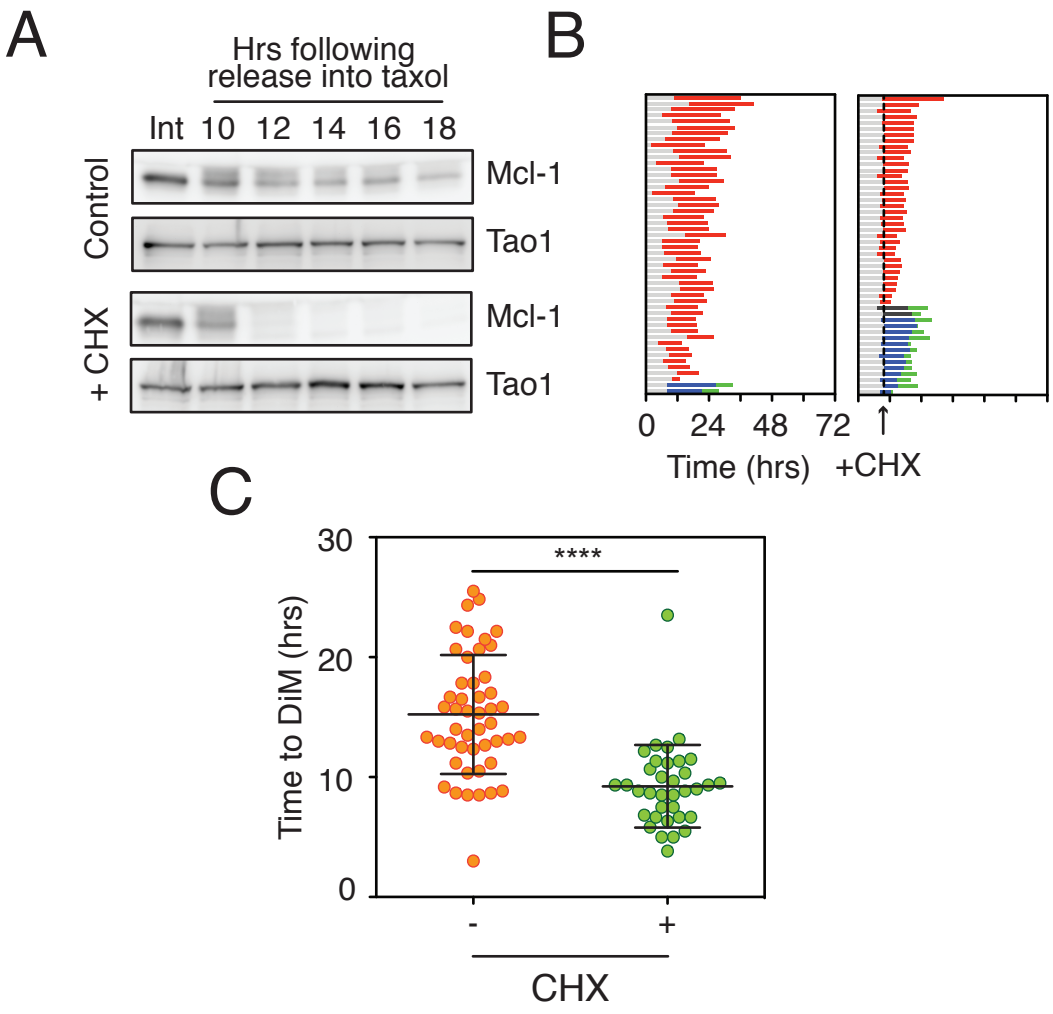

Figure 3.6 Effect of translational inhibitor cycloheximide on DiM and Mcl-1 protein in RKO GFP-Cyclin B1 R42A cells.
(A) Immunoblot of Mcl-1 levels in RKO GFP-Cyclin B1 R42A cells treated with taxol and cycloheximide.
(B) Cell fate profiles of cells treated with tetracycline and taxol. The black line indicates the point at which cycloheximide is added.
(C) Quantification of the time to DiM in the cell populations from Figure 3.6B. Mann Whitney U test, **** $p < 0.0001$

3.7 Summary

In this Chapter I generated a RKO GFP-Cyclin B1 R42A cell line that reduces slippage when treated with taxol. Using this system I have directly measured the time to DiM of cells in response to modulating levels of Mcl-1 and shown that Mcl-1 degradation during a mitotic arrest induced by taxol contributes to apoptosis in mitosis. As previously described, this indicates that (1) the rate of Mcl-1 degradation and (2) the duration of the mitotic arrest in order to degrade Mcl-1 likely to be important factors contributing to cell fate following exposure with anti-mitotic drugs (Huang et al., 2009; Sakurikar et al., 2012). In Chapter 6 I aimed to explore the later point by assessing the contribution of Mcl-1 degradation in a slippage-prone cell line and investigating the effect that increased mitotic duration has on overall survival in response to anti-mitotic drugs. Additionally I have shown that Mcl-1 is synthesised in mitosis and that this may be a factor in determining the rate of sensitivity to anti-mitotic drugs. Moreover, I have shown that proteasome inhibitor MG132 significantly delays time to mitotic death in RKO cells by stabilising Mcl-1. This was an interesting observation as it shows that the net effect of protein degradation is to sensitise RKO cells to apoptosis. This may be a cell-line specific phenomenon and may depend on the factors that dictate the degradation rates of proteins that could vary between cell lines.

The RKO GFP-Cyclin B1 R42A cell line provides a model system in which to study Mcl-1 degradation in mitosis as it efficiently degrades Mcl-1 and suppresses slippage so that time to death can be directly measured and in Chapter 4 I use this system to explore factors that contribute to Mcl-1 degradation in mitosis.

4 Chapter 4: The role of Mcl-1 degradation mechanisms on mitotic death

4.1 Introduction

The RKO GFP-Cyclin B1 R42A cell line generated in Chapter 3 provides an intrinsic system upon which to directly study the kinetics of DiM. Using this system I have shown that the rate of DiM can be controlled by changes to the Mcl-1 protein in mitosis. Here, using this system, I analyse the contribution of several known E3 ligase mechanisms to Mcl-1 degradation and DiM. Firstly, although an interaction between the mitotic E3 ligase complex APC/C-Cdc20 and Mcl-1 has been identified, no functional data exists on the contribution of this interaction to DiM. I take several approaches in order to assess the contribution of the APC/C-Cdc20 with regards to its interaction with Mcl-1 on DiM. Firstly I use Cdc20 RNAi and small molecule inhibitors in order to suppress APC/C-Cdc20 activity and measure time to DiM in the RKO GFP-Cyclin B1 R42A cell line. Secondly, I use a more direct approach by mutating the D-box-like degron in Mcl-1 to see if that has an effect on Mcl-1 protein stability and DiM. Finally, I analyse the extent to which APC/C-Cdc20 other E3 ligase mechanisms contribute in order to assess the relevant importance of each in the net effect of Mcl-1 degradation and DiM.

4.2 Analysing the effect of Cdc20 depletion on DiM.

In order to study the effect of the APC/C-Cdc20 on DiM, I decided to first concentrate on repressing the function of this complex and analysing the effect on DiM. To achieve this, RKO GFP-Cyclin B1 R42A cells were transfected with either non-targeting or Cdc20 siRNAs and protein lysates were obtained 24 hours later. Immunoblotting showed that Cdc20 levels were reduced in the Cdc20 RNAi cell population (Figure 4.1A).

To observe the effect of Cdc20 loss on DiM, RKO GFP-Cyclin B1 R42A cells were firstly transfected with non-targeting or Cdc20 siRNAs as well as treatment with thymidine in order to inhibit mitotic entry and arrest induced purely through loss of Cdc20. Cells were then

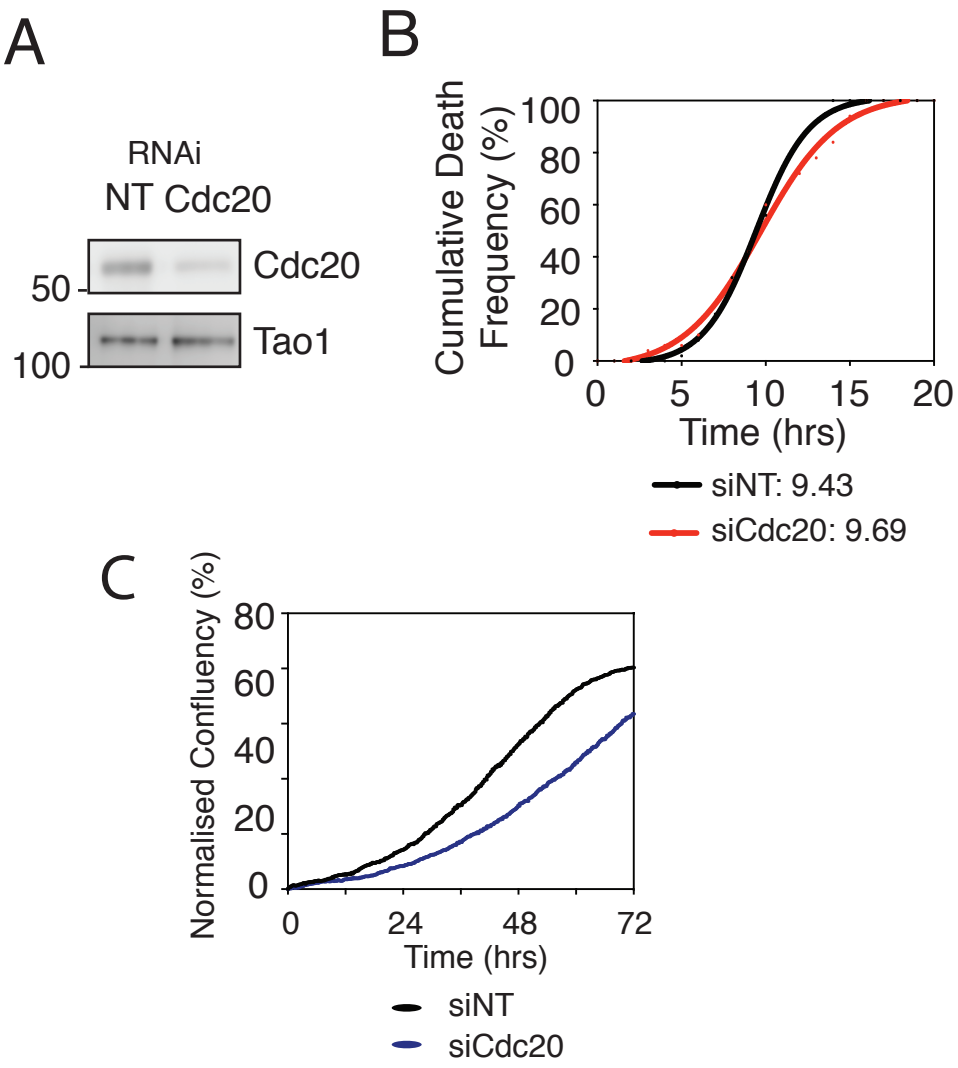

Figure 4.1 Effect of Cdc20 depletion on DiM in RKO GFP-Cyclin B1 R42A cells.
(A) Immunoblot of Cdc20 levels in RKO GFP-Cyclin B1 R42A cells following transfection with siRNAs targeting either Cdc20 or non-targeting control for 24 hours.
(B) Cumulative frequency graph of mitotic death of RKO GFP-Cyclin B1 R42A cells transfected with siRNAs targeting either Cdc20 or non-targeting control and treated with taxol and tetracycline.
(C) Normalised confluency of cells transfected with siRNAs targeting Cdc20 or a non-targeting control.

released into 0.1 μM taxol and tetracycline to induce the GFP-Cyclin B1 R42A protein and imaged (Figure 4.1B). The control non-targeting population underwent DiM with an average time of 9.43 hours. Upon taxol addition, Cdc20 depleted cells underwent DiM with a similar timing to the non-targeting population of 9.69 hours, thereby suggesting that Cdc20 suppression, and therefore APC/C-Cdc20 activity, has no effect on DiM. However, it was possible that suppression of APC/C-Cdc20 by Cdc20 RNAi was not penetrant enough to efficiently suppress APC/C-Cdc20 activity and mitotic exit. To test this, untreated cells were transfected with siRNAs targeting Cdc20 and confluency was measured using the IncuCyte® software that is based on the surface area taken up by cells within the image (Figure 4.1C.). If Cdc20 RNAi was efficiently blocking mitotic exit then one would have expected that cell confluency would remain the same over time as cells would be stuck in a mitotic arrest. The non-targeting population grew normally, with a continual upwards curve over time during the course of the experiment. However, in the cell population transfected with siRNAs targeting Cdc20, confluency was still increasing over the time-course experiment, albeit slightly slower than the non-targeting population, suggesting that Cdc20 RNAi was not sufficiently suppressing APC/C-Cdc20 activity.

4.3 Examining the effect of APC/C inhibitors proTAME and Apcin on mitotic exit.

As Cdc20 depletion by RNAi did not effectively halt cell growth, Cdc20 RNAi could not be used as a way to analyse the effect of APC/C-Cdc20 activity on DiM. Another way to block APC/C-Cdc20 activity is by treating RKO GFP-Cyclin B1 R42A cells with small molecule inhibitors of APC/C. ProTAME acts as a competitor of Cdc20 for the APC/C and Apcin fits into the D-box site inhibiting interactions between Cdc20 and D-box containing substrates (Lara-Gonzalez and Taylor, 2012; Sackton et al., 2014; Zeng et al., 2010). It hs been previously shown that proTAME and Apcin synergise to block mitotic exit (Sackton et al., 2014).

In order to find the lowest concentration combination of Apcin and proTAME that sufficiently blocks the APC/C, I performed serial dilutions of both drugs based on the concentration range known to delay mitotic progression in RPE cells (Sackton et al., 2014; Zeng et al., 2010). To evaluate the ability of the drugs to induce a mitotic arrest I took advantage of the

IncuCyte® software to measure confluency. As a mitotic cell takes up less surface area than a flattened-down interphase cell, I could use the confluency data over a time-course to determine drug concentrations that caused a mitotic arrest. In the untreated population, cell confluency steadily grew until 45.6 hours when confluency plateaued as the cells had covered over 99 % of the plate (Figure 4.2A). This graph shape was identical in cell populations treated with Apcin alone upto 100 μM, suggesting that Apcin by itself is not a potent inhibitor of APC/C activity (Figure 4.2A, top row). Equally, addition of proTAME upto 4 μM had little effect on confluency. However, when proTAME concentrations were increased to 8 μM or over, the confluency rate was decreased. At 15 μM, the cell population took 57.6 hours to reach 50 % confluency in comparison to the untreated population that took 20.2 hours (Figure 4.2A, left column).

To investigate the effect of this combination of drugs further, I generated cell fate profiles for each drug by itself and in combination. In the untreated population, 86 % completed 3 mitoses with an average time of 35.4 minutes (Figure 4.2B, left panel). Similarly when cells were treated with 25 μM Apcin, 90 % cells also completed 3 mitoses with an average time of 34.8 minutes (Figure 4.2B, second panel). When cells were treated with 15 μM proTAME, mitotic exit was blocked in 46 % of cells that eventually undertook DiM in an average time of 12.5 hours (Figure 4.2B, third panel). Only 66 % of the population treated with proTAME arrested in mitosis for longer than 3 hours. When cells are co-treated with 25 μM Apcin and 10 μM proTAME, 94 % of cells arrest in mitosis for 3 hours or longer. However, only 78 % of cells undergo DiM with an average time to death of 13.6 hours, with the rest able to complete mitosis (Figure 4.2B, right panel). Interestingly, cells that are able to complete mitosis despite addition of APC/C inhibitors are able to complete on average 2 more rounds of cell division. These subsequent rounds of mitosis are not delayed and cells complete these on an average of 48 minutes. This is possibly indicative of the life span of drug activity caused by either drug excretion or efficient drug metabolism. Altogether, this data shows that this combination of APC/C inhibitors can sufficiently inhibit mitotic exit and thus APC/C-Cdc20 activity.

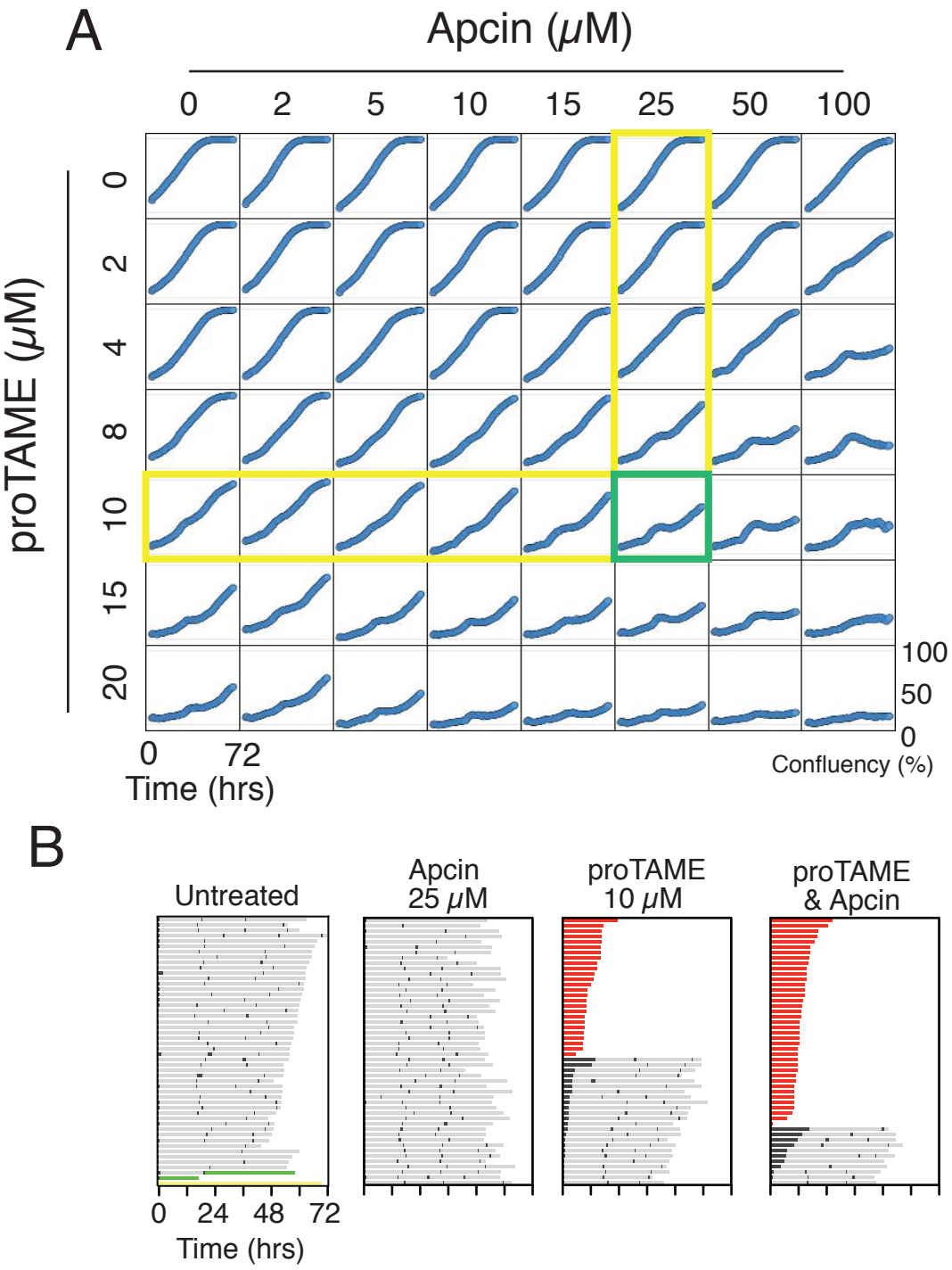

Figure 4.2. Characterisation of APC/C inhibitors proTAME and Apcin.
(A) Confluency graphs of RKO GFP-Cyclin B1 R42A cells over the course of 72 hours after treatment with the two inhibitors at the concentrations indicated.
(B) Cell fate profiles of cells treated with the indicated concentrations of proTAME and Apcin. T=0 represents time of mitotic entry.

4.4 Exploring the effect of SAC override on the mitotic arrest induced by co-treatment of proTAME and Apcin.

I have established the concentration combination of Apcin and proTAME that could sufficiently block mitotic exit. However, the prolonged block in mitotic exit caused by Apcin/proTAME combination over time might not be caused directly by inhibition of APC/C-Cdc20 activity. Following a prolonged mitotic arrest induced by proTAME, sister chromatids prematurely separate, a process known as cohesion fatigue (Lara-Gonzalez and Taylor, 2012). The initiation of cohesion fatigue reduces kinetochore-microtubule tension, which in turn re-activates the SAC (Daum et al., 2011; Stevens et al., 2011). Therefore, it is possible that the block in mitotic arrest caused by the Apcin/proTAME combination is then only sustained over time by SAC activation instead of APC/C-Cdc20 inhibition. To eliminate this possibility, I wanted to see if overriding the SAC would have any effect on the mitotic arrest induced by Apcin and proTAME.

To override the SAC I used an Mps1 inhibitor, AZ3146 (Hewitt et al., 2010). Mps1 is a spindle checkpoint protein whose catalytic activity is required to recruit Mad2 to the kinetochore (Hewitt et al., 2010; Weiss and Winey, 1996). The untreated control population grew normally with an average time of 41.6 minutes to complete mitosis (Figure 4.3A top left, 4.3B, top left panel). Addition of AZ3146 to uninduced RKO GFP-Cyclin B1 R42A cells had a significant effect on cell growth as cell confluency plateaued at 58 % (Figure 4.3A, top right). Cell fate profile of this population showed that inhibition of Mps1 caused cells to exit mitosis with a slightly faster average time of 30.6 minutes, indicative of SAC override (Figure 4.3B, top right panel). Additionally, 42 % underwent post-mitotic death (PmD) following completion of one mitosis (Figure 4.3B, top right panel). Of the cells that did not commit to PmD, only 66 % entered a second mitosis, suggesting that the cells were delayed in G1. As aneuploidy is characteristic of inhibition of Mps1 activity, the large degree of PmD could be explained by the post-mitotic response mechanisms to aneuploidy in this cell line.(Jelluma et al., 2008a, 2008b) When inhibition of Mps1 by the addition of AZ3146 was imposed on top of the combination of APC/C-Cdc20 inhibitors, there was no obvious effect on confluency in comparison to the APC/C-Cdc20 inhibitors by themselves (Figure 4.3A, bottom bands). In addition, there was no difference in the

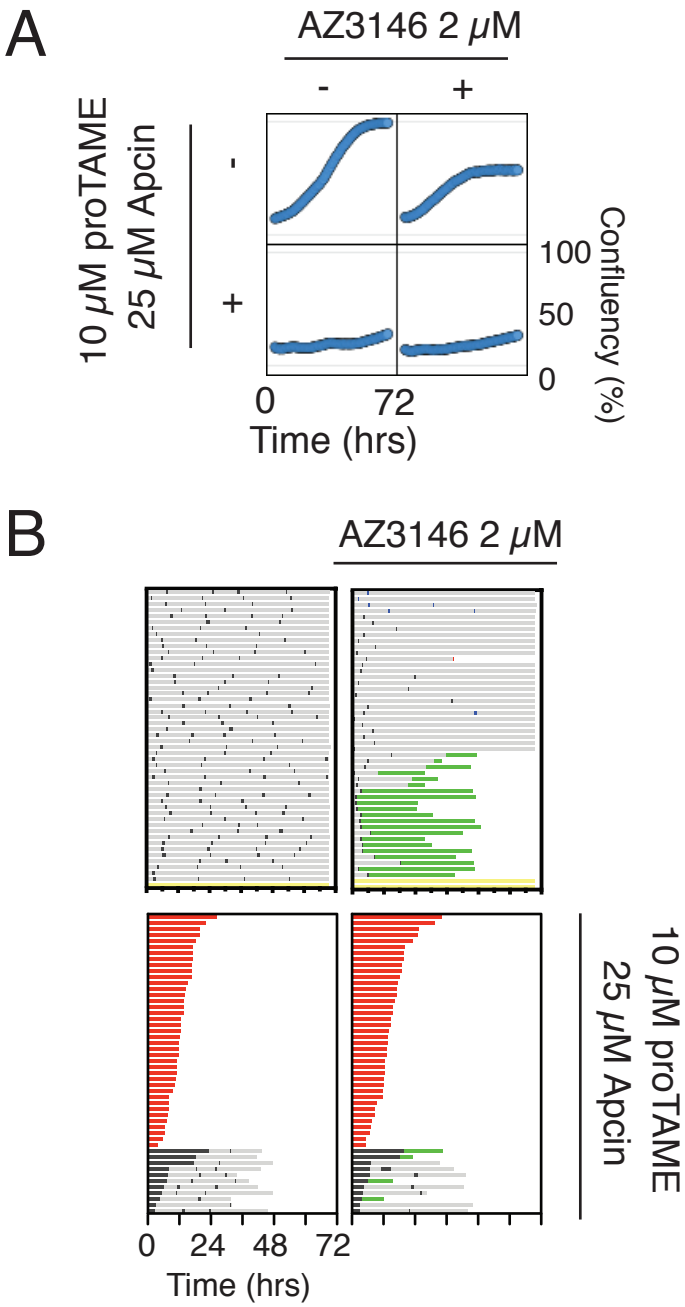

Figure 4.3 Effect of spindle checkpoint override on RKO GFP-Cyclin B1 R42A cells treated with Apcin and proTAME.
(A) Confluency graphs of RKO GFP-Cyclin B1 R42A cells over the course of 48 hours after treatment with the three inhibitors indicated.
(B) Cell fate profiles treated with the indicated combinations of drugs. T=0 represents time of mitotic entry.

percentage of cells that were arrested in mitosis for over three hours (98 % vs 96 %) or the number of cells that were unable to exit mitosis and undergo DiM (78 % versus 78 %) (Figure 4.3B, bottom panels). Moreover, there was no significant difference in the time to DiM between the populations. Similarly to addition of AZ3146 by itself, of the cells that could escape the mitotic arrest, 36.4 % underwent PmD. Put together, this indicates that the prolonged mitotic arrest induced by co-treatment of Apcin and proTAME is independent of cohesion fatigue and SAC reactivation.

4.5 Analysing the effect of Apcin and proTAME on DiM.

Once it was established that the Apcin/proTAME co-treatment on RKO cells was sufficient to inhibit APC/C-Cdc20 activity, I co-treated these cells with the APC/C-Cdc20 inhibitors in combination with 0.1 μM taxol and tetracycline for induction of GFP-Cyclin B1 R42A protein to investigate the effect inhibition of APC/C-Cdc20 would have on the time to DiM. Co-treatment of RKO GFP-Cyclin B1 R42A cells caused cells to undergo DiM in an average time of 8.25 hours (Figure 4.4A). When cells were also treated with 25 μM Apcin and 10 μM proTAME, the time to DiM was unaffected (8.91 hours). Additionally, co-treatment of cells with another combination of Apcin/proTAME, 5 μM and 15 μM respectively, also had no effect on the time to DiM, with cells dying in mitosis in an average time of 8.63 hours.

In addition, the effect of the APC/C-Cdc20 inhibitor combination on mitotic Mcl-1 degradation was analysed. RKO GFP-Cyclin B1 R42A cells were treated with the APC/C inhibitors, 0.1 μM taxol and tetracycline and protein lysate samples were taken 16 hours later (Figure 4.4B). This time point was chosen as Mcl-1 protein had been sufficiently degraded in response to taxol (Figure 3.1B). For a positive control of inefficient Mcl-1 degradation in mitosis, MG132 was added after 10 hours drug exposure. Immunoblotting showed that in comparison to MG132, Mcl-1 levels were reduced in the mitotic population (Figure 4.4C, lanes 1,4). The addition of Apcin/proTAME had no effect on Mcl-1 levels in comparison to the control, suggesting that Mcl-1 degradation was unaffected upon inhibition of APC/C-Cdc20 (Figure 4.4C, lane 2,3). Together, this indicates that the APC/C-Cdc20 complex does not contribute to DiM and Mcl-1 degradation.

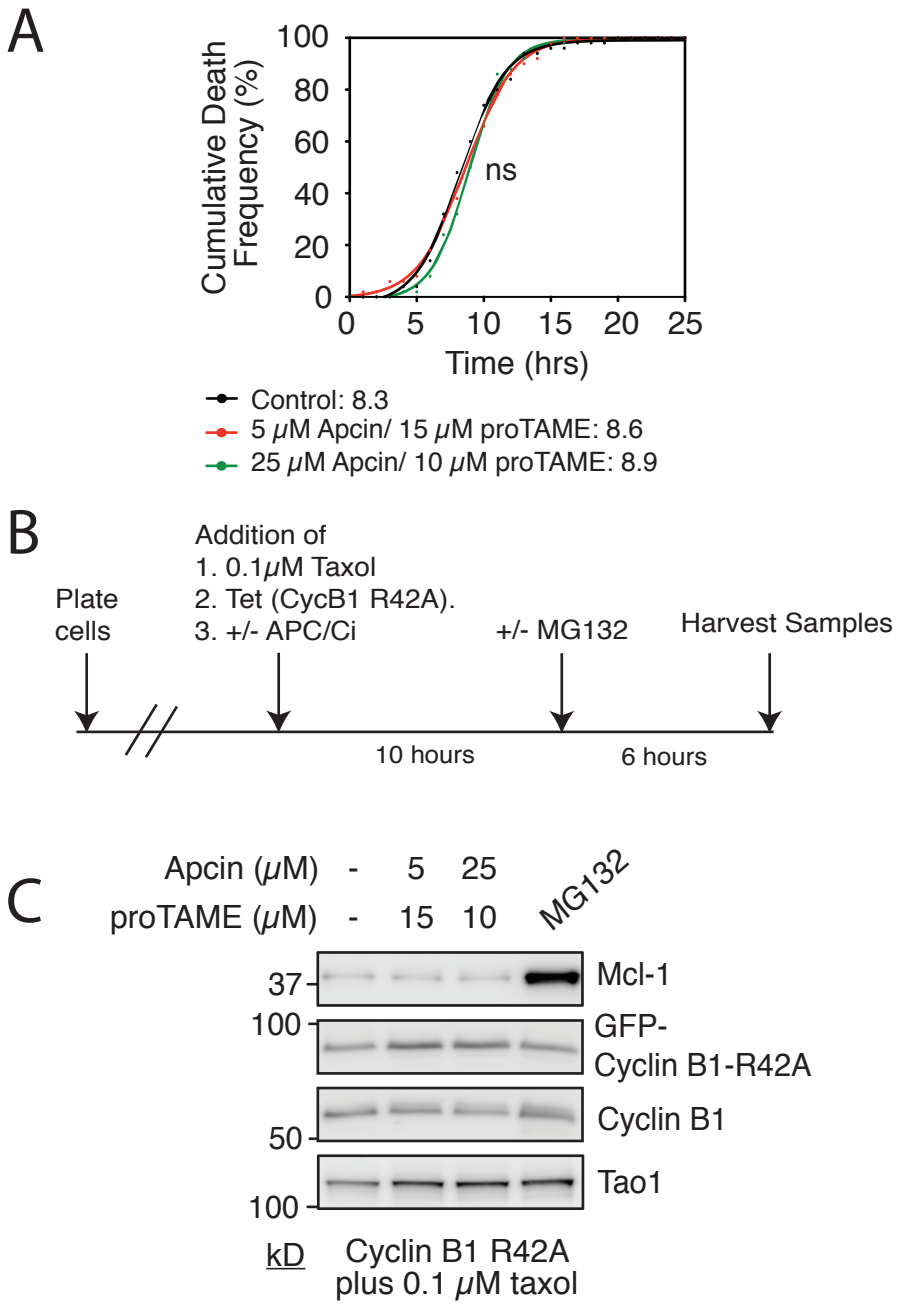

Figure 4.4 Effect of Apcin and proTAME on DiM and mitotic Mcl-1 protein levels in RKO GFP-Cyclin B1 R42A cells.
(A) Cumulative frequency graph of the time to mitotic death of RKO GFP-Cyclin B1 R42A cells treated with tetracycline, taxol and the APC/C inhibitors indicated.
(B) Timeline schematic of experiment to collect protein samples.
(C) Immunoblot of Mcl-1 and Cyclin B1 proteins treated with the drug regiment shown in Figure 4.4B.

4.6 Investigating the effect of APC/C-Cdc20, SCF-Fbw7 and MULE inhibition on the DiM.

Although inhibition of the APC/C-Cdc20 complex has no effect on mitotic death, I explored the possibility that redundancy with other E3 ligases may be compensating for loss of APC/C-Cdc20 activity. As mentioned in the introduction, other E3-ligases have been implicated in the targeted degradation of Mcl-1 during mitosis including the SCF complex (through substrate recognition by subunit Fbw7) and the MULE complex (Shi et al., 2011; Wertz et al., 2011). To identify any redundancy between APC/C-Cdc20 and SCF-Fbw7, RKO GFP-Cyclin B1 R42A cells were transfected with siRNAs targeting Fbw7 followed by co-treatment with taxol, tetracycline and the proTAME/Apcin drug combination. When time to DiM was measured, there was no significant difference in the average time to death in cells treated with the APC/C inhibitors with Fbw7 RNAi (13.28 hours versus 11.11 hours) (Figure 4.5A). In addition, Mcl-1 levels following 16-hour drug exposure were analysed by immunoblotting. Co-treatment with proTAME, Apcin and Fbw7 RNAi did not stabilise Mcl-1 in mitosis (Figure 4.5B). Therefore, inhibition of both APC/C-Cdc20 and SCF-Fbw7 had no effect on DiM or Mcl-1 degradation.

Finally, I combined inhibition of SCF-Fbw7 by RNAi and APC/C-Cdc20 by treatment with proTAME and Apcin with transfection of siRNAs inhibiting MULE. Gene expression analysis by RT-PCR confirmed a gene expression decrease to 33 % of MULE mRNA compared to the non-targeting population (Figure 4.6A). Upon suppression of the activity of all three E3 ligases by either small molecule inhibitors or siRNA transfection, there was no significant change in the time to DiM of RKO GFP-Cyclin B1 R42A cells treated with taxol and tetracycline (Figure 4.6B). Immunoblotting showed that inhibition of MULE gene expression also had no effect on mitotic Mcl-1 degradation (Figure 4.6C) Altogether this implies that the three mechanisms previously shown to be important for Mcl-1 degradation do not appear to be necessary for Mcl-1 loss or DiM in this context.

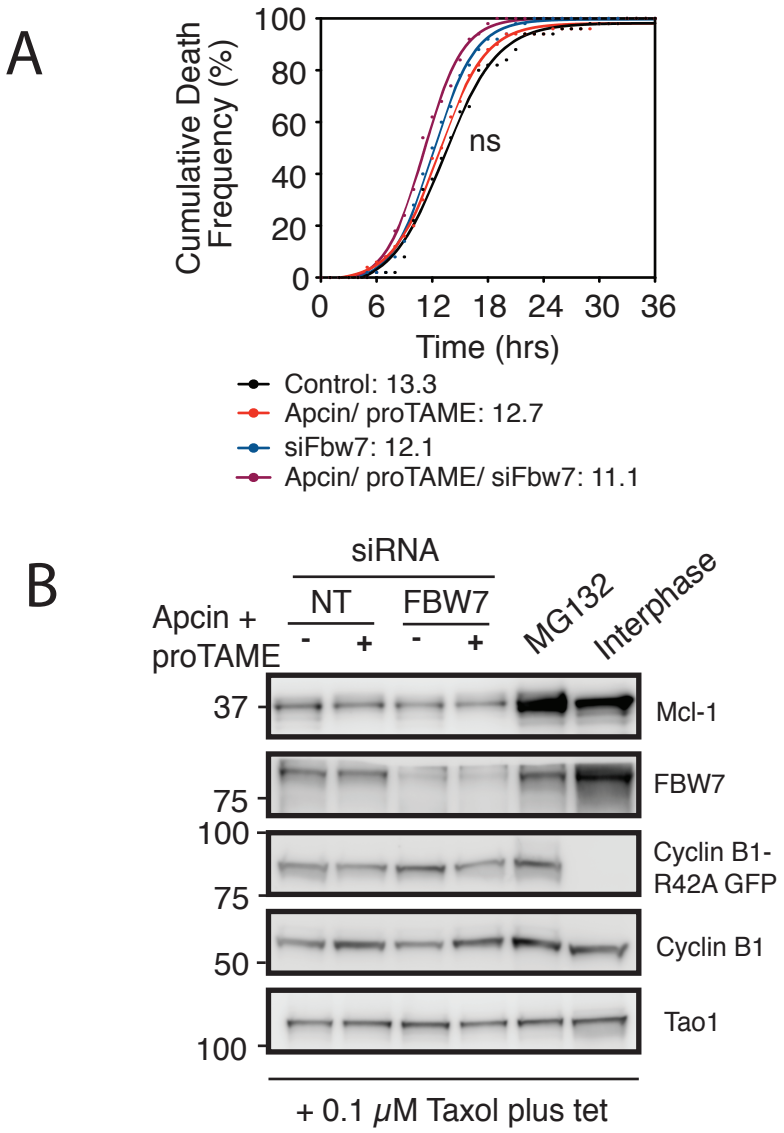

Figure 4.5 Effect of Fbw7 depletion, Apcin and proTAME on DiM in RKO GFP-Cyclin B1 R42A cells.
(A) Cumulative frequency graph of the time to mitotic death of RKO GFP-Cyclin B1 R42A cells transfected with siRNAs targeting Fbw7 24 hours prior to the addition of taxol, tetracycline and the APC/C inhibitors indicated.
(B) Immunoblot of Fbw7, Mcl-1 and Cyclin B1 protein levels in RKO GFP-Cyclin B1 R42A cells transfected with siRNAs targeting Fbw7 24 hours prior to the addition of taxol, tetracycline and the APC/C inhibitors indicated. Protein lysates were collected 16 hours following drug treatment.

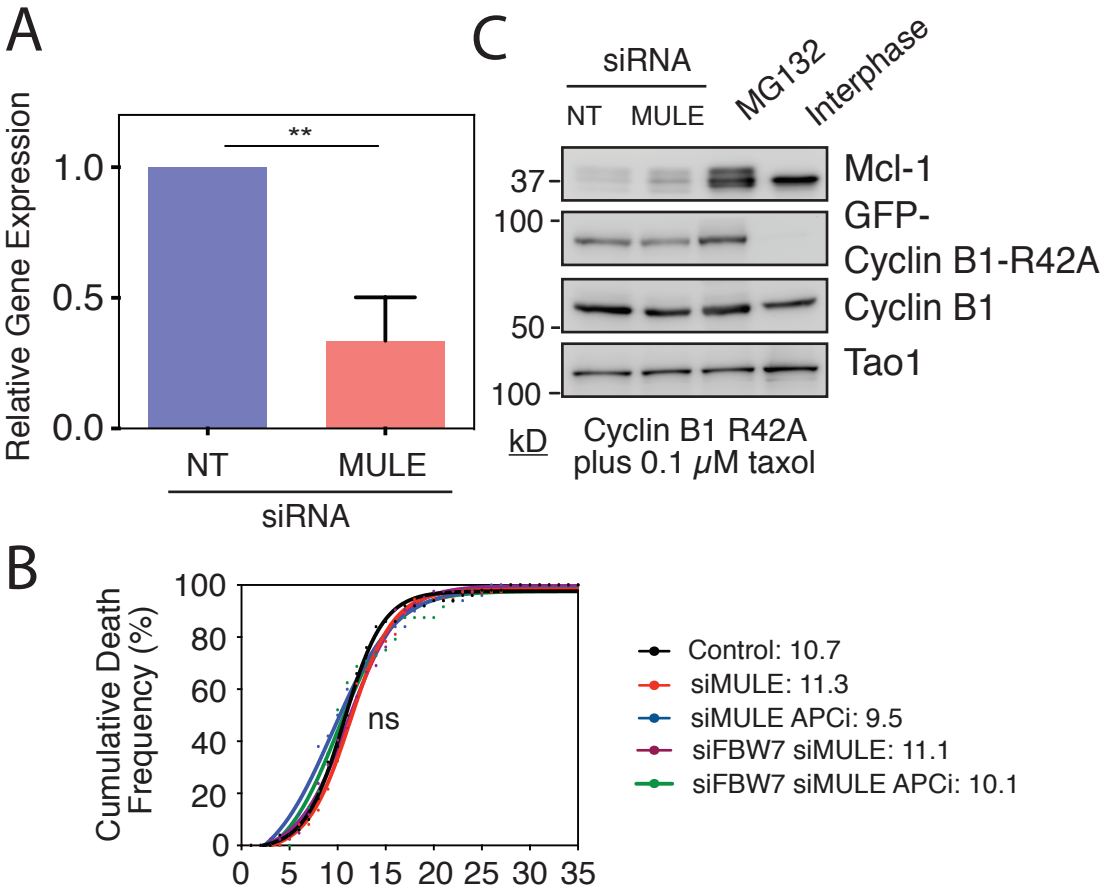

Figure 4.6 Effect of Fbw7 depletion, MULE depletion, Apcin and proTAME on DiM in RKO GFP-Cyclin B1 R42A cells.
(A) Relative gene expression of MULE and non-targeting mRNA following transfection of siRNA for 24 hours targeting MULE or non-targeting control.
(B) Cumulative frequency graph of the time to mitotic death of RKO GFP-Cyclin B1 R42A cells transfected with siRNAs targeting Fbw7 24 hours prior to the addition of taxol, tetracycline and the APC/C inhibitors indicated.
(C) Immunoblot of Mcl-1 and Cyclin B1 protein levels in RKO GFP-Cyclin B1 R42A cells transfected with siRNAs targeting Fbw7 24 hours prior to the addition of taxol, tetracycline and the APC/C inhibitors indicated. Protein lysates were collected 16 hours following drug treatment.

4.7 Exploring the effect of over-expressing Mcl-1 wild type and D-box-like mutant Mcl-1 protein on DiM.

I have so far shown that suppression of APC/C-Cdc20, SCF-FBW7 and MULE has no significant effect on Mcl-1 degradation and the time to DiM. However, it is possible that the use of siRNA transfections or small molecule inhibitors were not penetrant enough to sufficiently suppress E3 ligase activity on Mcl-1. A more direct approach to test this is by mutating residues in Mcl-1 that are recognised by the E3 ligase machinery for ubiquitination. For this I concentrated on the RxxL D-box motif that resides in Mcl-1 at residues 207-210. As mentioned previously, the RxxL motif is contained within substrates recognised by the APC/C-Cdc20 complex for degradation such as Cyclin B1 and Securin (Glotzer et al., 1991; Pines, 2011). Previously it was shown in U2OS cells that expression of a Mcl-1 form with a double mutation in the RxxL motif, where arginine 207 and leucine 210 in the RXXL motif are mutated to alanine, was more stable in a mitotic arrest (Figure 4.7A) (Harley et al., 2010). To see if this mutant form of Mcl-1 (named Mcl-1 RALA) has an effect on DiM, I created tetracycline-inducible RKO stable cell lines expressing either the wild type Mcl-1 protein (Mcl-1 WT) or the RxxL mutant form (Mcl-1 RALA) fused to GFP and treated these stable cell lines with taxol.

Immunoblotting of Mcl-1 shows that upon tetracycline addition, the GFP-Mcl-1 proteins are expressed at a higher molecular weight of ~75 kDa (Figure 4.7A). When compared to endogenous Mcl-1 that was also used as a loading control, the exogenous protein was expressed at slightly reduced levels in comparison to endogenous Mcl-1 protein. Importantly, both Mcl-1 WT and Mcl-1 RALA are expressed at similar levels and as such can be used for comparison. Following taxol treatment, 78 % and 86 % of cells underwent DiM in the control Mcl-1 WT and Mcl-1 RALA cell lines respectively (Figure 4.7B, left panels). Additionally, time to DiM was similar in both populations with an average time to DiM of 13.1 hours (Mcl-1 WT) and 12.7 hours (Mcl-1 RALA) (Figure 4.7C). Co-treatment with tetracycline delayed time to DiM by 5.3 hours (Mcl-1 WT) and 3.2 hours (Mcl-1 RALA) to 18.4 hours and 15.9 hours, respectively. Additionally, mitotic slippage was reduced in cells expressing GFP-Mcl-1 WT protein from 22 % to 14 %, whereas mitotic slippage was increased in cells expressing GFP-Mcl-1 RALA protein from 12 % to 22 % (Figure 4.7B, right panels). Importantly, there was no significant difference

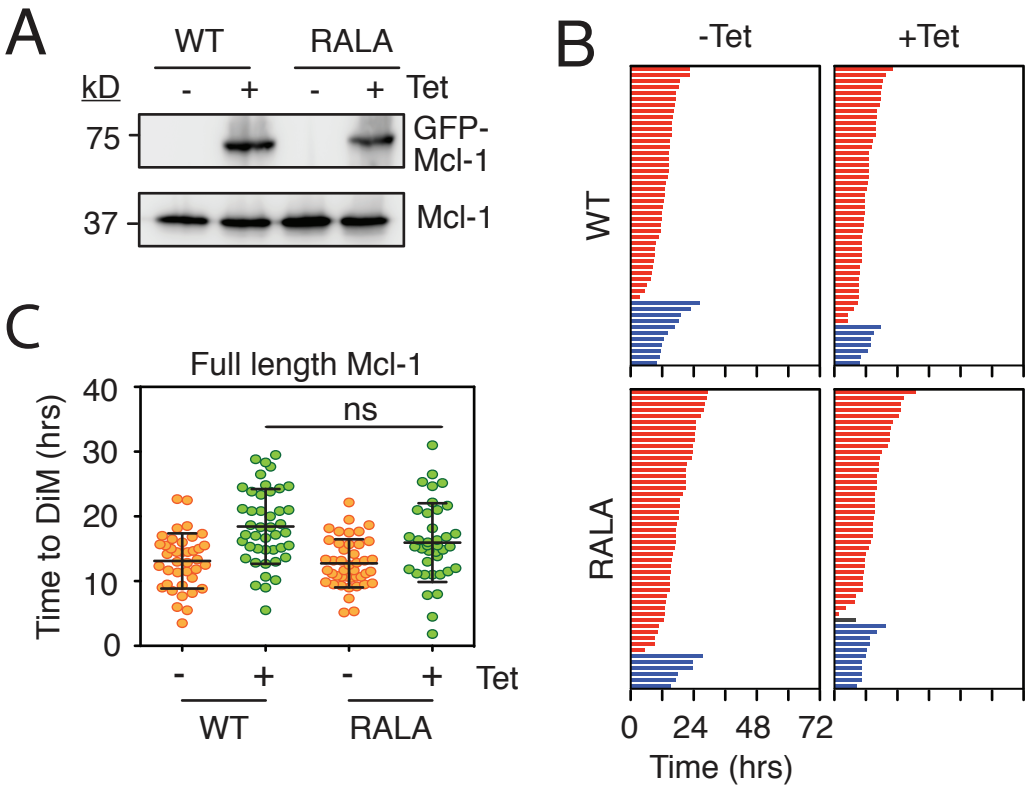

Figure 4.7 Generation and Characterisation of RKO cell lines stably expressing either GFP-Mcl-1 WT or GFP-Mcl-1 RALA mutant.
(A) Immunoblot of exogenous and endogenous Mcl-1 protein levels in the RKO GFP-Mcl-1 lines following treatment with tetracycline for 24 hours.
(B) Cell fate profiles of the RKO GFP-Mcl-1 cell lines treated with tetracycline and taxol.
(C) Quantification of time to DiM in cell populations in Figure 6.1B. T=0 represents time of mitotic entry.

between the times to DiM in cells expressing Mcl-1 WT versus cells expressing Mcl-1 RALA. This suggests that the RALA mutation in Mcl-1 does not have a significant effect on DiM. Moreover, it provides further evidence to highlight the insignificance of the Mcl-1-APC/C-Cdc20 interaction.

4.8 Analysing the effect of transiently transfecting in fragments of Mcl-1 containing the D-box-like motif.

It is possible that the GFP-tagged Mcl-1 RALA did not have a greater effect on DiM compared to expression of the wild type GFP-tagged Mcl-1 protein as the stable expression of the exogenous Mcl-1 protein was not high enough observe a detectable change in the time to DiM. To test this specifically, I overexpressed an 90 amino acid fragment encompassing the D-box like motif (amino acids 157-246) that may compete with Mcl-1 specifically for APC/C-Cdc20 binding via the putative D-box (Figure 4.8A). This approach is conceptually similar to the experiment that laid the foundation for the discovery of Securin whereby addition of a fragment of Cyclin B1 containing the D-box to *Xenopus* egg extracts competed endogenous Cyclin and Securin away from APC/C-Cdc20, thereby inhibiting mitotic exit and anaphase onset (Holloway et al., 1993). To perform overexpression analysis, the 90 amino acid fragment of Mcl-1 was fused to a Myc-tagged mCherry reporter (Gascoigne and Taylor, 2008), transiently transfected into the RKO GFP-Cyclin B1 R42A cell line and the time to DiM was measured. Immunoblotting using a Myc-tag antibody confirmed the success of the transient transfection (Figure 4.8B). Furthermore, I measured the time to DiM specifically in fluorescing cells as these were clearly expressing the fragment-mCherry fusion protein (Figure 4.9A). Furthermore, as the transfection protocol caused many cells to undergo interphase death, I selectively analysed cells healthy enough to commit to mitosis. Transfected cells were treated with taxol and tetracycline and imaged. In the mCherry control population, cells underwent DiM with a T_{50} of 14.2 hours (Figure 4.9B, black line), a time consistent with an un-transfected cell population. Overexpressing the 90aa fragment of Mcl-1 extended the T_{50} to 19.3 hours. Furthermore, expression of a Mcl-1 fragment containing the RALA double mutation did not extend the time to DiM, but reduced the

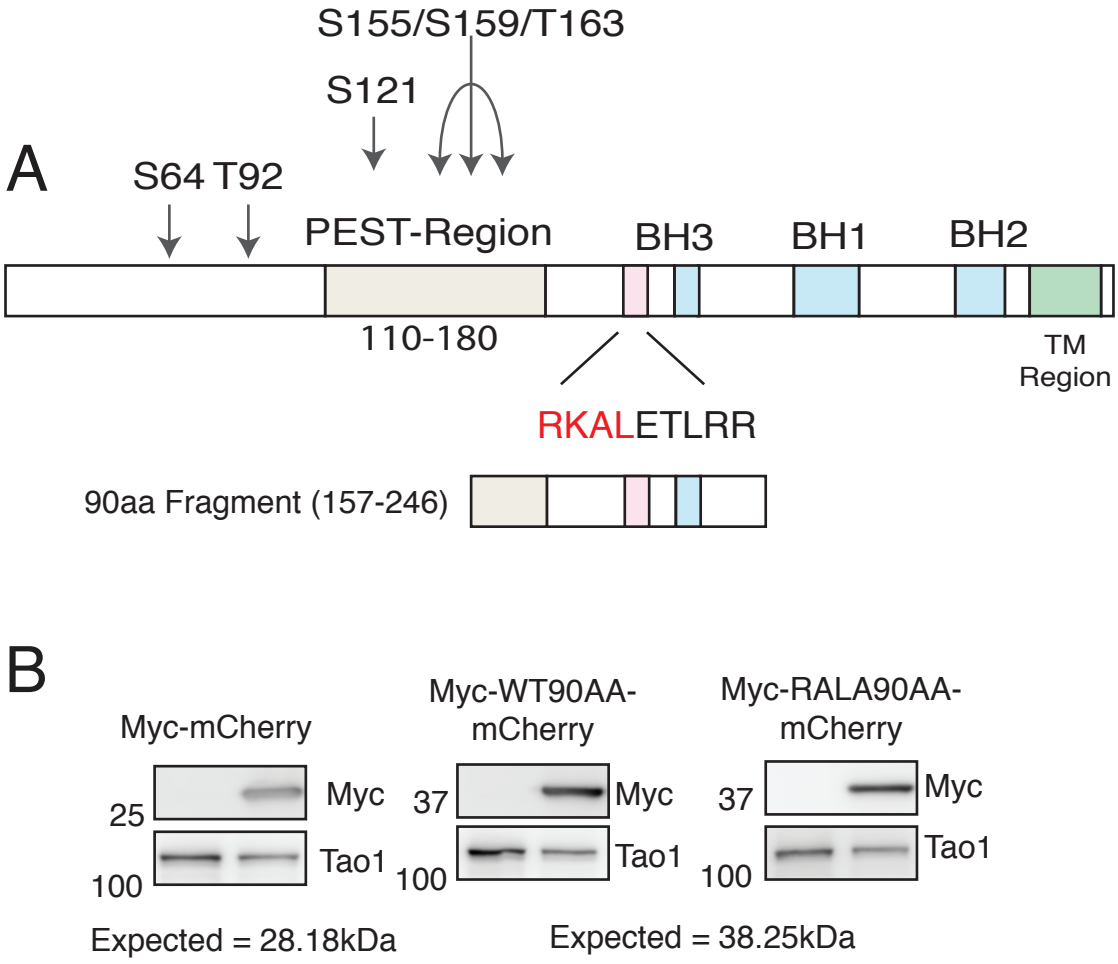

Figure 4.8 Transient expression of a 90aa fragment of Mcl-1.
(A) Schematic of the Mcl-1 gene and the 90aa fragment.
(B) Immunoblot of Myc protein levels in cells transciently transfected with a pLPCX plasmid containing a myc-tagged 90aa fragment of Mcl-1 fused to mCherry. Lysates were obtained 24 hours following transfection. Tao1 protein levels were used as a loading control.

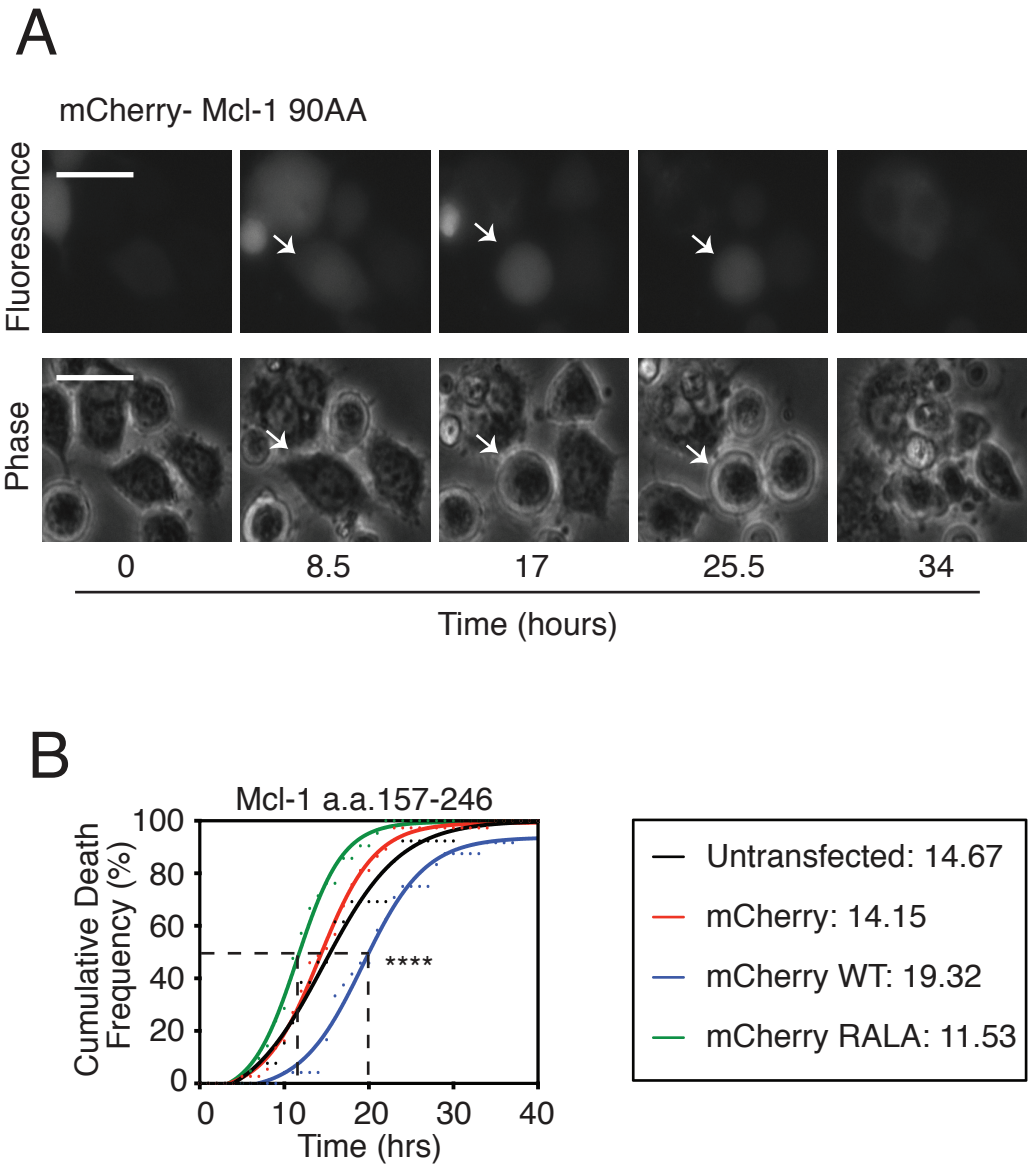

Figure 4.9 Effect of transient expression of a 90aa fragment of Mcl-1 on DiM in RKO GFP-Cyclin B1 R42A cells.

(A) Red fluorescence and phase images of RKO Cyclin B1 R42A cells transciently transfected with an a 90aa fragment of Mcl-1 fused to mCherry and treated with taxol. The arrow indicates a tracked mitotic fluorescent cell.

(B) Immunoblot of Myc protein levels in cells transciently transfected with a pLPCX plasmid containing a myc-tagged 90aa fragment of Mcl-1 fused to mCherry. Lysates were obtained 24 hours following transfection. Tao1 protein levels were used as a loading control. Untransfected n=28, mCherry n=37, mCherry WT n=24, mCherry RALA n=21 for three independent experiments.

time to DiM to an average of 11.5 hours (Figure 4.9B, green line). This suggests that overexpressing this fragment oversaturates the APC/C, thus inhibiting any APC/C-Cdc20-Mcl-1 association that may contribute to death in mitosis.

4.9 Summary

Although the association between APC/C-Cdc20 and Mcl-1 had been previously identified and it has been noted that the APC/C-Cdc20 complex contributes to DiM, functional experiments have been difficult to interpret due to the presence of mitotic slippage. Using the RKO Cyclin B1 R42A cells, this Chapter primarily aimed to analyse the functional effect of the potential APC/C-Cdc20-Mcl-1 interaction on DiM through two approaches. Firstly, by inhibiting APC/C-Cdc20 action by Cdc20 depletion or by small molecule inhibitors proTAME and Apcin. Secondly, by mutating the D-box-like motif on Mcl-1 thought to be required for the interaction with the APC/C-Cdc20 complex. Using these methods, it appears that the APC/C-Cdc20 complex has no obvious overall effect on the rate of DiM. Additionally, by transiently overexpressing Mcl-1 fragments containing the RxxL mutation, it does appear that the this potential route of interaction between Mcl-1 and the APC/C-Cdc20 complex may have a functional effect. However, when the full length protein is stably expressed at lower levels, there was no functional effect between expression of Mcl-1 WT and Mcl-1 RALA. The later experiment using stable expression reflects better the physiological state, meaning that it may be more relevant.

I reasoned that E3 ligase redundancy may explain why APC/C-Cdc20 inhibition did not have an effect on DiM. Inhibition of other E3 ligases previously identified to contribute to Mcl-1 degradation and the response to anti-mitotic drugs (namely SCF-Fbw7 and MULE) by siRNA of MULE and Fbw7 in combination with APC/C-Cdc20 inhibition also had no effect on the time to DiM. One plausible reason for this is that like Cdc20 RNAi, the siRNA knockdown is not effective enough to show a functional effect. Additionally, this could be indicative of a novel targeted degradation mechanism or a non-targeted degradation mechanism. In addition, the discrepancy between these results and those previously published may be explained by cell line variation for the dependency of different E3 ligase mechanisms or alternative degradation mechanisms. In the next chapter I analyse the effect of Mcl-1 protein in a slippage-prone cell line.

5 Chapter 5: The role of Mcl-1 in mitotic slippage.

5.1 Introduction

In the previous chapters I explored the role of Mcl-1 degradation in DiM in the context of RKO cells as this was a model cell line in which to study the rate of mitotic death. Unlike death-prone RKO cells, slippage-prone cell lines are mostly able to escape a mitotic arrest. The first aim of this chapter is to explore the role of Mcl-1 in a slippage prone cell line, DLD-1, both in terms of efficiency of degradation and the dependency on Mcl-1 for survival in a prolonged mitotic arrest.

Secondly, even though I was unable to find any functional role of the APC/C-Cdc20 complex, specifically in regards to its identified association with Mcl-1, towards DiM in the RKO cell line, it is possible that this interaction may influence the rate of slippage by competing with Cyclin B1 for binding to the APC/C-Cdc20 complex. To do this, I determined whether modulation of Mcl-1 levels impacted on the rate of mitotic slippage in DLD-1 cells treated with Eg5 inhibitor AZ138 (Gascoigne and Taylor, 2008).

5.2 Analysing the effect of Mcl-1 depletion in DLD-1 cells treated with Eg5 inhibitor AZ138.

It has been previously suggested that slippage-prone cell lines do not degrade Mcl-1, which causes suppression of DiM in response to anti-mitotic drugs (Sakurikar et al., 2014). After choosing DLD-1 cells as a representative cell line for slippage, I firstly checked to see if Mcl-1 was being degraded efficiently. Using the same protocol as for RKO cells, I synchronised DLD-1 cells by an overnight single thymidine block before release into 1 μM AZ138. Protein samples were taken every 2 hours following a 10-hour incubation in AZ138. Immunoblotting showed no obvious decline in Mcl-1 levels during this time period (Figure 5.1A). This suggests that like other slippage-prone cell lines previously analysed, it is possible that DLD-1 cells do not degrade Mcl-1. However, to check whether this negative result was not just an artifact of ineffective thymidine synchronisation of DLD-1 cells, DLD-1 cells were synchronised in mitosis by the addition of

AZ138 for 4 hours followed by a mitotic shake-off and re-plating mitotic cells back into AZ138. Using this different synchronisation protocol, Mcl-1 loss was visible in DLD-1 cells (Figure 5.1B). Mcl-1 protein levels had decreased compared to the original 10-hour level after 16 hours incubation with AZ138. This confirms that Mcl-1 can be degraded in DLD-1 cells and more importantly, a slippage-prone cell line.

In RKO cells, loss of Mcl-1 contributes to DiM. However, even though it appears that Mcl-1 is degraded in DLD-1 cells, it is plausible that Mcl-1 degradation is not having as big an effect on DiM. To investigate whether accelerated Mcl-1 loss in DLD-1 cells influences the amount of DiM, DLD-1 cells were transfected with either non-targeting or Mcl-1 siRNA (Figure 5.1C). Upon addition with 1 μM AZ138 DLD-1 cells were tracked by time-lapse microscopy and cell fate was analysed. In the non-targeting cell population, 80 % of cells committed to mitotic slippage, with 20 % committing to DiM with an average time of 16.3 hours (Figure 5.1D, top left panel). Of the cells that exited mitosis, 10 % underwent PmD, 15 % entered a second mitosis and the rest remained in interphase until the end of the experiment. Similarly in the Mcl-1 depleted cells, 74 % and 26 % of cells underwent mitotic slippage and DiM respectively (Figure 5.1D, top right panel). Although loss of Mcl-1 accelerated DiM by 5.4 hours to 11.0 hours, this suggests that in the DLD-1 cell line, Mcl-1 degradation had no effect on DiM. However, 62 % of the cells that exited mitosis underwent PmD, a 52 % increase in comparison to the non-targeting cell population. This indicates that in this cell line, Mcl-1 is required to inhibit post-mitotic death.

As Mcl-1 is not particularly important for DiM in DLD-1 cells, I hypothesised that the cell line was more dependent on a different member of the anti-apoptotic family of Bcl-2 proteins that could compensate for loss of Mcl-1 during a mitotic arrest. To test this idea, I transfected cells with siRNA targeting anti-apoptotic protein Bcl-xL (Figure 5.1D, bottom panels). When Bcl-xL depleted cells were treated with 1 μM AZ138, all cells now underwent DiM with an average time of 6.3 hours, suggesting that this cell line is dependent on Bcl-xL in a mitotic arrest.

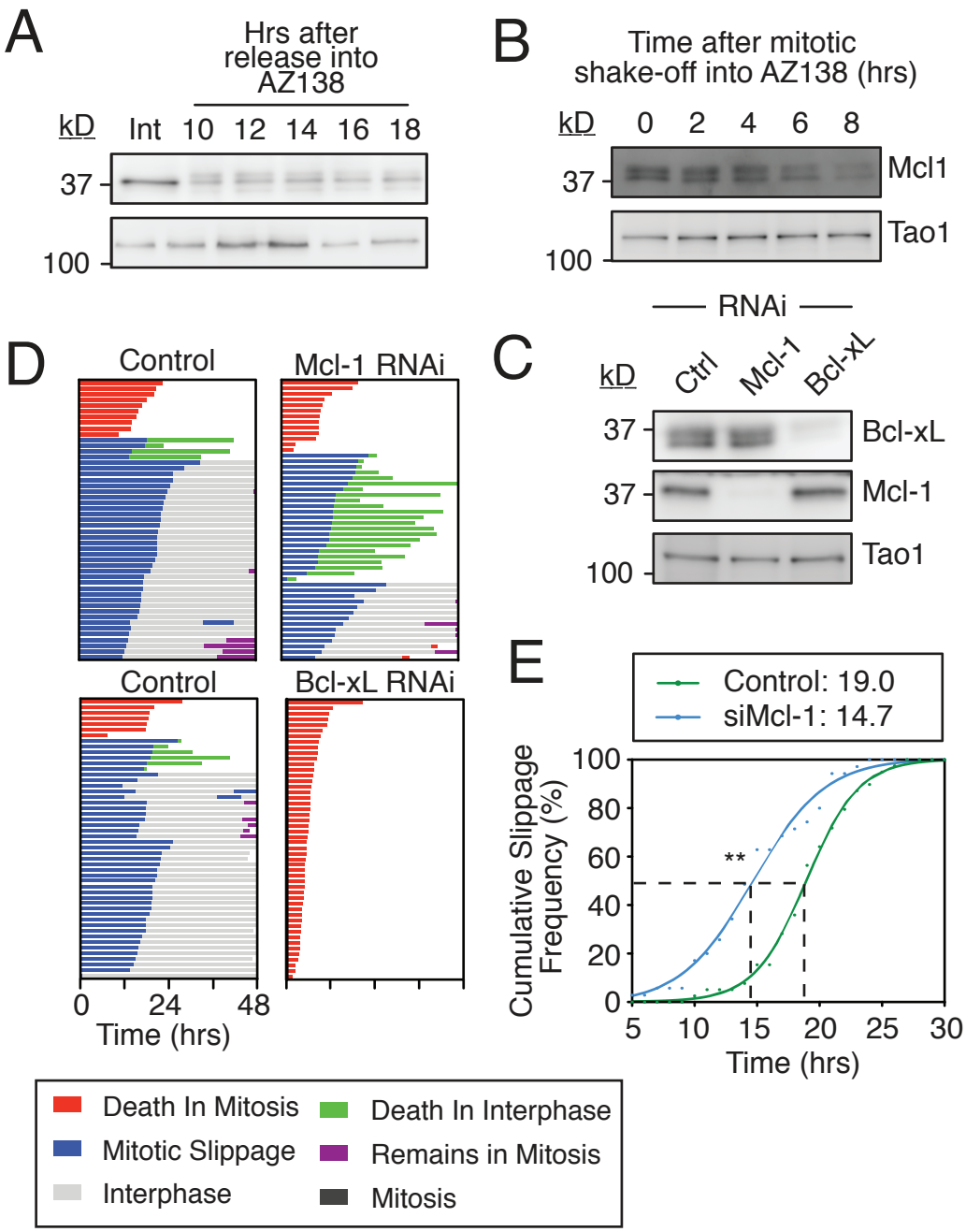

Figure 5.1 Effect of Mcl-1 depletion in slippage-prone DLD-1 cells.
(A) Immunoblot of Mcl-1 protein levels in DLD-1 cells treated with AZ138 for the times indicated.
(B) Immunoblot of Mcl-1 protein levels in DLD-1 cells treated with AZ138 for 5 hours followed by a mitotic shake-off.
(C) Immunoblot of DLD-1 cells transfected with siRNAs targeting Mcl-1, Bcl-xL or a non-targeting control. Lysates were taken 24 hours following transfection.
(D) Cell fate profiles of DLD-1 cells transfected with siRNAs targeting Mcl-1, Bcl-xL or a non-targeting contro and treated with AZ138. T=0 represents time of mitotic entry.
(E) Cumulative frequency graph of mitotic slippage undertaken by DLD-1 cells transfected with either Mcl-1 or non-targeting control siRNA for 24 hours before treatment with AZ138. Mann Whitney U test, ** $p < 0.0001$

5.3 Investigating the effect Mcl-1 protein levels have on mitotic slippage.

Loss of Mcl-1 has very little effect on DiM as all cells are able to slip out of mitosis. This provided a way to address the second hypothesis regarding the Cdc20-Mcl-1 association and mitotic slippage. I hypothesised that loss of Mcl-1 would reduce any competition between the Cyclin B1 and Mcl-1 for the APC/C-Cdc20 complex, thereby accelerating the rate of Cyclin B1 loss and mitotic slippage. Interestingly, when the time to mitotic slippage data was re-plotted as cumulative frequency of slippage, it appears that loss of Mcl-1 accelerated the rate of mitotic slippage (Figure 5.1E). Non-targeting cells exited mitosis with an average time of 19.0 hours whereas Mcl-1 depleted cells exited mitosis with an average time of 14.7 hours; an acceleration of 4.3 hours.

Following this, I investigated what effect an increased amount of Mcl-1 protein would have on the rate of slippage. I generated a DLD-1 cell line expressing GFP-Mcl-1 upon addition of tetracycline. Immunoblotting showed that upon 0.2 or 0.5 μg/ml tetracycline, exogenous GFP-Mcl-1 was expressed at similar levels to the exogenous (Figure 5.2A). Note that the higher molecular weight band is due to the presence of an additional AID tag. DLD-1 GFP-Mcl-1 WT cells were then treated with 1 μM AZ138 and the time to mitotic slippage was plotted as cumulative slippage frequency (Figure 5.2B). In the control population, cells slipped out of mitosis with an average time of 20.59 hours. Upon tetracycline addition, the average time to mitotic slippage was increased by 3.7 hours to 24.3 hours. This indicates that the Mcl-1 protein levels can influence the rate of mitotic slippage.

In Chapter 4, I showed that the APC/C-Cdc20-Mcl-1 interaction had no effect on DiM and Mcl-1 degradation in RKO cells. However, as Mcl-1 protein appears to influence mitotic slippage by potentially interacting with components that affect the rate of slippage, I asked whether Mcl-1 was perhaps interfering with mitotic slippage through the association with Cdc20. To do this I also generated a DLD-1 cell line expressing the RALA mutant form (containing a mutation in the RxxL D-box-like motif recognised by APC/C-Cdc20) of Mcl-1 attached to GFP upon tetracycline addition. As with the DLD-1 GFP-Mcl-1 WT-expressing cell line, GFP-Mcl-1-

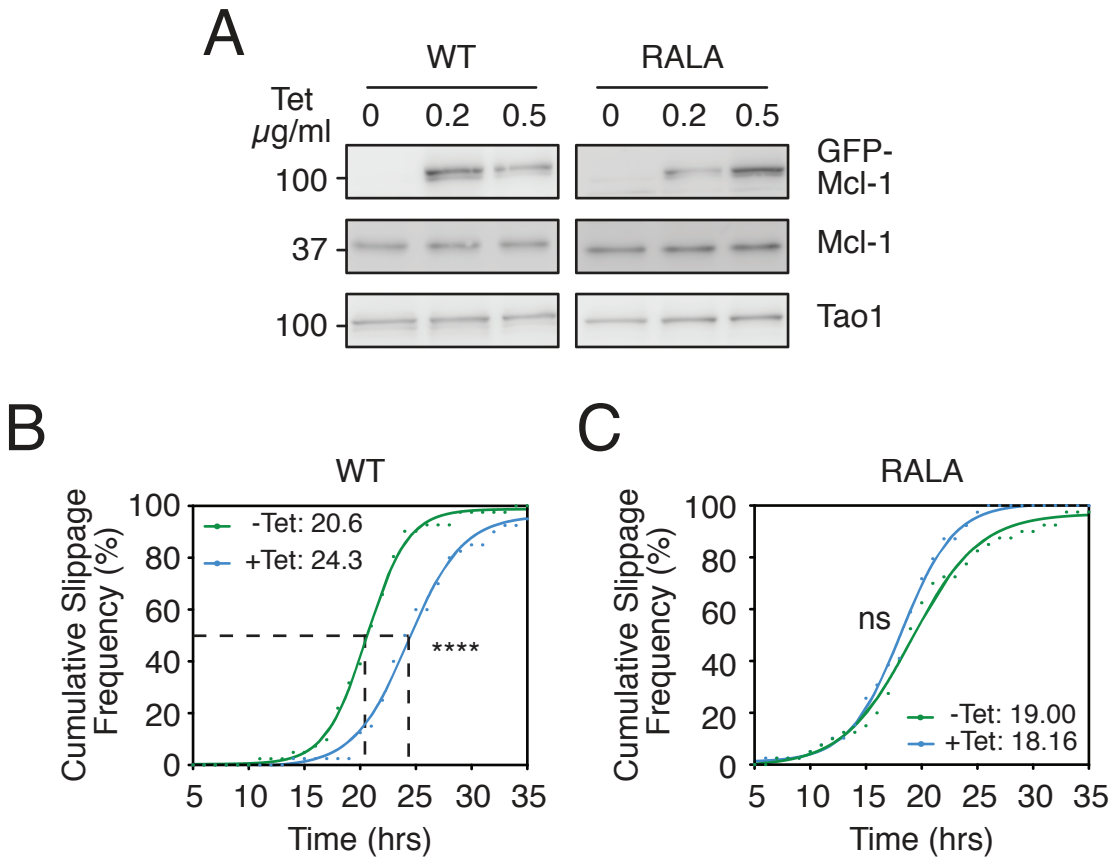

Figure 5.2 Generation and characterisation of DLD-1 cells stably expressing either GFP-Mcl-1 WT or GFP-Mcl-1 RALA mutant.
(A) Immunoblot of Mcl-1 exogenous and endogenous protein following tetracycline treatment for 24 hours in DLD-1 Mcl-1 cell lines.
(B) + (C) Cumulative frequency graph of mitotic slippage of DLD1 GFP-Mcl-1 cell lines following treatment with AZ138 and tetracycline. Mann Whitney U test, **** $p < 0.0001$, ns $p > 0.05$.

RALA was expressed in DLD-1 cells following addition of 0.2 and 0.5 µg/ml tetracycline at a similar level to the endogenous Mcl-1 protein (Figure 5.2A). Following treatment with 1 µM AZ138, control DLD-1 cells exited mitosis with an average time of 19.00 hours (Figure 5.2C). This time, addition of tetracycline to induce the DLD-1-GFP-Mcl-1-RALA protein had no significant effect on time to mitotic slippage and cells exited with an average time of 18.16 hours. This suggests that Mcl-1 protein interferes with mitotic slippage through its putative D-box like RxxL motif. As mentioned above, although no effect on DiM was observed, it is possible that Mcl-1 influences slippage rates by competing with Cyclin B1 for the APC/C.

5.4 Examining the effect that co-depletion of Mcl-1, Bak and Bax has on mitotic slippage.

I have shown that the levels of Mcl-1 influence slippage. Next, I used this knowledge to help explain a recent observation in the literature, namely that depletion of Bak and Bax delays slippage (Díaz-Martínez et al., 2014). It was proposed that Bak and Bax influence the rate of slippage indirectly through reduction in energy levels and translation via mitochondrial dynamics. Specifically, a reduction in translation suppresses Cyclin B1 synthesis, causing faster loss of Cyclin B1 and mitotic exit. However, as Mcl-1 can bind both Bak and Bax, I can alternatively suggest that loss of Bak and Bax increases the amount of Mcl-1 able to engage with the mitotic slippage machinery, thus slowing down Cyclin B1 degradation and mitotic slippage.

To test this, I first performed a immunopreciptation of GFP-Mcl-1 to confirm that Mcl-1 can bind to both Bak and Bax in DLD-1 cells. Following overnight tetracycline induction in DLD-1 GFP-Mcl-1 WT cells, I incubated the cell lysates with a ‘GFP-binder’ protein and glutathione beads. This GFP-binder protein originates from a single chain llama antibody generated using a GFP fragment. The GFP-binder gene was previously cloned into a vector such that the expressed binder protein as fused to a Glutathione S-Transferase (GST) tag so that it can attach to glutathione beads. Immunoblotting of Mcl-1 showed successful pull down of the exogenous GFP-Mcl-1 protein upon tetracycline addition (Figure 5.3A). Although endogenous Mcl-1 was detected in the 5 % input sample, Mcl-1 was not detected in the immunoprecipation reaction, thus serving as a good negative control. Both Bak and Bax could be detected in the

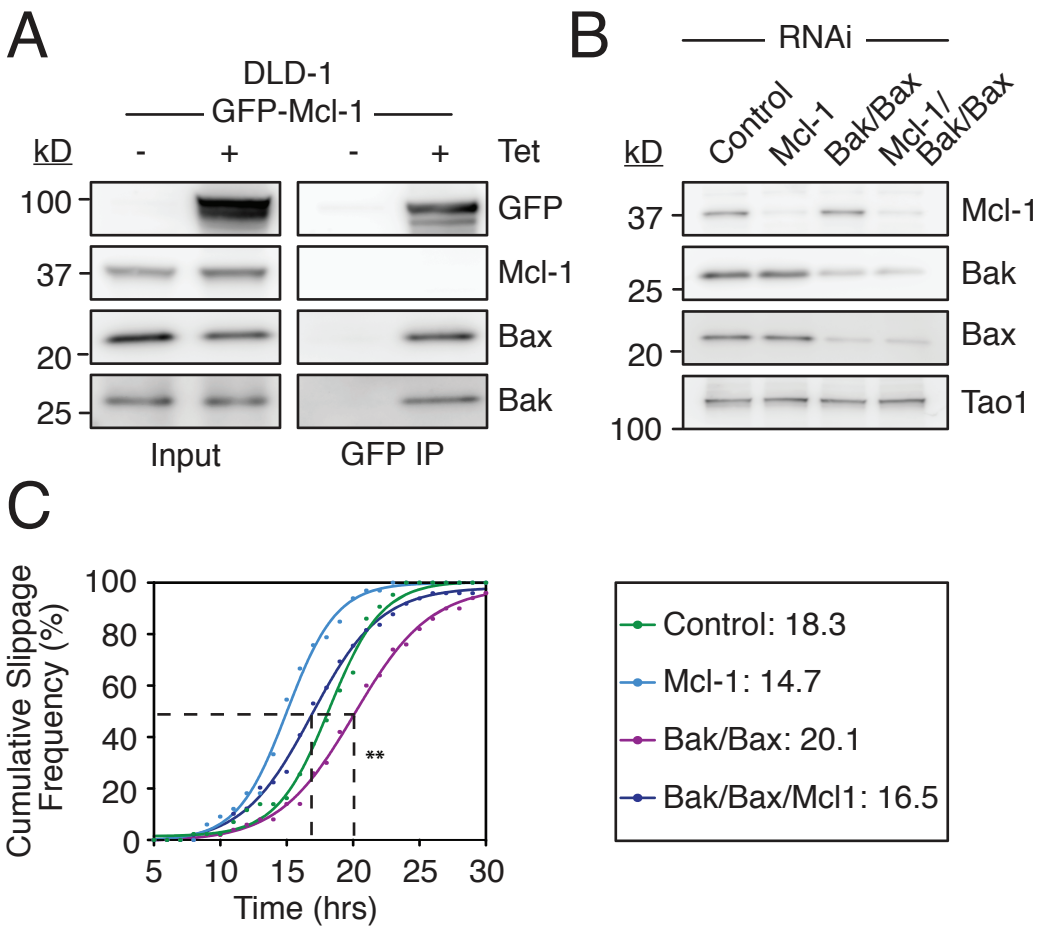

Figure 5.3 Effect of Mcl-1, Bak and Bax depletion on mitotic slippage in DLD-1 cells.
(A) Immunoblot of GFP, Mcl-1, Bak and Bax following immunoprecipation of DLD-1 GFP-Mcl-1 WT cell line lysate with a GFP binder protein. Cells were treated with tetracycline to express GFP-Mcl-1 WT.
(B) Immunoblot of Mcl-1, Bak and Bax levels following transfection of siRNAs targeting the indicated proteins.
(C) Cumulative frequency of mitotic slippage in response to AZ138 and co-depletion of proteins indicated by RNAi. Mann Whitney U test, ** $p < 0.01$

immunopreciptated tetracycline-treated sample, confirming that Mcl-1 may bind both proteins in DLD-1 cells. It should be noted however that this may not be entirely conclusive as the detergent used to lyse cells in this thesis (Triton X-100) may cause unspecific dimerization between Bcl-2 family members that may not complete reflect the situation in vivo (Hsu and Youle 1997, Hsu and Youle 1998).

Next I investigated the effect of Bak/Bax depletion on the time to mitotic slippage in DLD-1 cells using RNAi. Immunoblotting confirmed that Bak and Bax proteins were lost upon transfection with the relevant siRNAs (Figure 5.3B). Cells were then treated with 1 μM AZ138 and imaged (Figure 5.3C). In the non-targeting population, cells slipped out of mitosis with an average time of 18.3 hours. Consistent with previous literature, depletion of Bak and Bax delayed slippage by 1.8 hours to an average time of 20.1 hours.

To see whether the delayed slippage caused by Bak and Bax could be caused by an increase in free Mcl-1, I co-transfected siRNAs targeting Mcl-1 with siRNAs targeting Bak and Bax (Figure 5.3B, C). Consistent with my earlier data, Mcl-1 depleted cells accelerated slippage by 3.6 hours to an average time of 14.7 hours. Importantly, depleting Mcl-1 in Bak/Bax RNAi cells rescued the delayed time to slippage with an average of 16.5 hours, suggesting that the extended mitotic slippage time caused by Bak/Bax depletion may be dependent on Mcl-1. Although not conclusive, this provides evidence for the simpler explanation connecting members of the apoptotic network to slippage signalling.

5.5 Analysing the effect of Mcl-1 depletion on normal mitotic timing.

I have shown that the levels of Mcl-1 influence the rate of mitotic slippage during a prolonged mitotic arrest. This effect of Mcl-1 may only be apparent during a prolonged mitotic arrest as Cyclin B1 degradation is slower due to inhibition of the APC/C-Cdc20 by the MCC complex, meaning any changes to the rate of Cyclin B1 are easily identified. To see if Mcl-1 could effect the rate of Cyclin B1 degradation in a situation when APC/C-Cdc20 inhibition is alleviated (i.e. in anaphase), I transfected DLD-1 cells with siRNAs targeting Mcl-1 and imaged the dividing population of cells without addition of an anti-mitotic drug (Figure 5.4A). In the non-

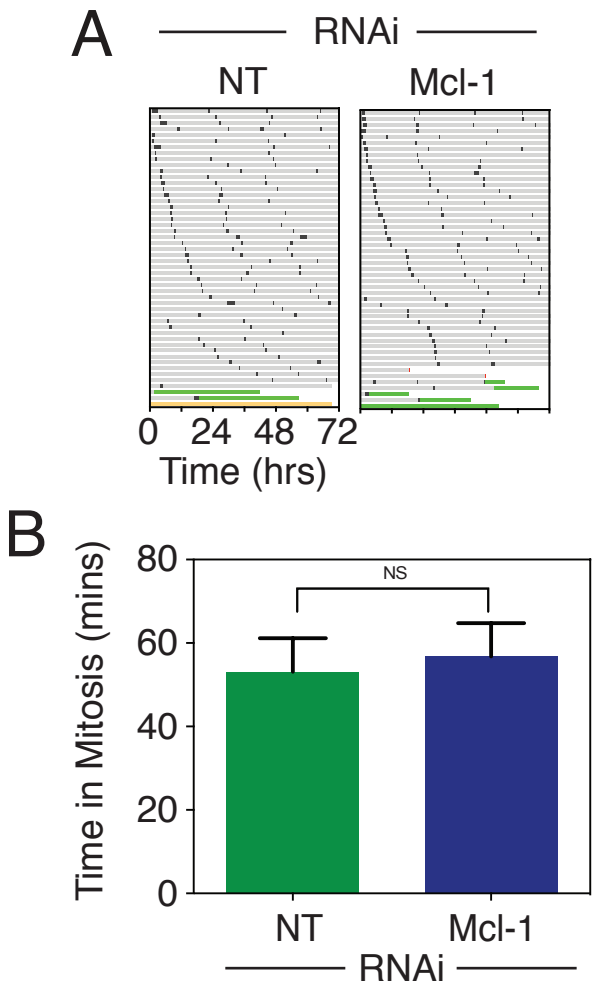

Figure 5.4 Effect of Mcl-1 on normal mitotic timing in DLD-1 cells.
(A) Cell fate profiles of DLD-1 cells transfected with siRNAs targeting Mcl-1 or non-targeting control.
(B) Quantification of mitotic timing in cells ttransfected with siRNAs targeting Mcl-1 or non-targeting control. Mann-Whitney U test, ns $p > 0.05$.

targeting control population, 92 % of cells underwent two or more mitoses during the 72-hour time period. Similarly, in Mcl-1 depleted cells, 86 % underwent two or more mitoses. In addition, there was no large increase in cell death in the Mcl-1 depleted cell population. Importantly, when the time in mitosis was measured, there was no significant difference in mitotic timing between the non-targeting population and the Mcl-1 depleted population (Figure 5.4B). Put together, this suggests that although Mcl-1 affects mitotic slippage timing, the effect is only apparent under situations when Cyclin B1 degradation is constrained such as a mitotic arrest induced by SAC activation.

5.6 Investigating the effect of overexpressing Mcl-1 on both mitotic slippage and DiM in parallel.

Thus far, I have used RKO GFP-Cyclin B1 R42A cells and DLD-1 cells to study the rate of DiM and mitotic slippage respectively. This is a reflection on extensive inter-line variation observed in cancer cell lines in response to anti-mitotics (Gascoigne and Taylor, 2008). In Chapter 3, I showed that modulating Mcl-1 levels affected the rate of DiM in RKO cells and in this Chapter I have shown that Mcl-1 levels influenced slippage, suggesting that Mcl-1 has the ability to affect both networks at the same time. To test this possibility, I re-tuned the DLD-1 experimental system so that the cell line underwent a combination of DiM and mitotic slippage. For this I used a high concentration of nocodazole (6.6 μM). When I treated the DLD-1 cells with 6.6 μM nocodazole, 36 % cells committed to mitotic slippage and 64 % of cells underwent DiM, possibly caused by super-activation of the SAC leading to greater inhibition of APC/C-Cdc20 activity (Figure 5.5A, top left panel). To test the effect of increased Mcl-1 levels I added tetracycline to induce expression of the GFP-Mcl-1 WT protein (Figure 5.5A, top right panel). Expression of the Mcl-1 protein increased time to DiM from an average of 23.2 hours to 33.2 hours, thereby showing that Mcl-1 levels can affect DiM in a slippage-prone cell line (Figure 5.5B). Furthermore, the time to PmD was extended from 10.3 hours to 27.1 hours, thus confirming the earlier Mcl-1 RNAi data suggesting that Mcl-1 is required for post-mitotic survival in this cell line (Figure 5.5C). As DiM was delayed in the cells expressing GFP-Mcl-1 WT one may have expected to observe an increase in slippage as suggested by the competing networks

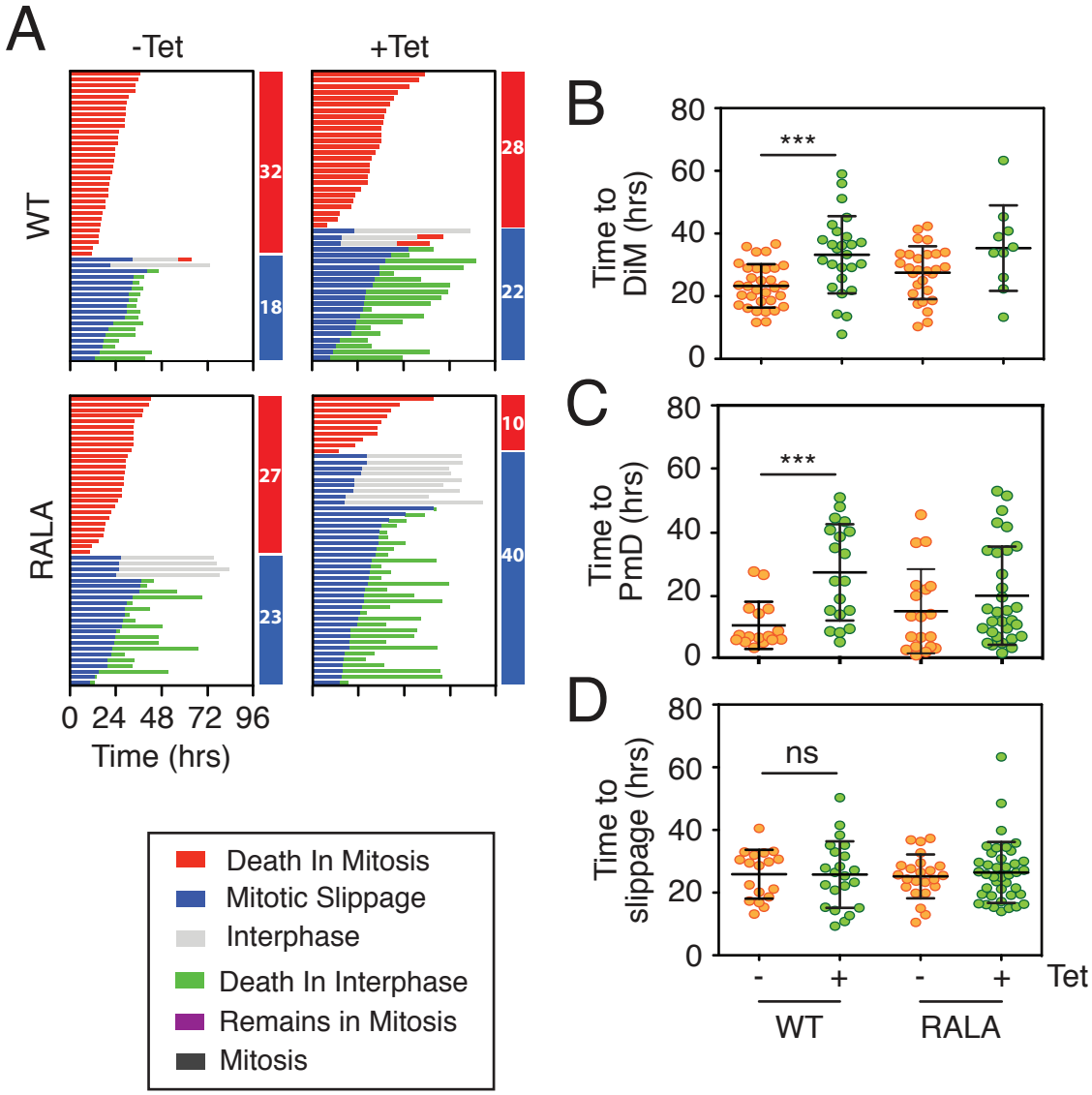

Figure 5.5 Treating DLD-1 cells expressing GFP-Mcl-1 WT or GFP-Mcl-1 RALA mutant with a high concentration of nocodazole.
(A) Cell fate profiles of DLD-1 Mcl-1 WT and RALA mutant treated with 6.6 μM nocodazole and tetracycline in order to induce the exogenous protein. T=0 represents time of mitotic entry.
(B,C,D) Time in mitosis before the cells in each population in Figure 5.5A undertake either death in mitosis (B), post-mitotic death (C) and mitotic slippage (D). Mann Whitney U test, *** $p < 0.001$, ns $p > 0.05$.

model (Gascoigne and Taylor, 2008). However, only 44 % committed to mitotic slippage in the GFP-Mcl-1 WT expressing cells, corresponding to an insignificant 8 % increase (Figure 5.5A, top right panel.). One explanation for this is that mitotic slippage is also delayed, consistent with the results in Chapter 5.4. However, of the cells that exited mitosis, the time to slippage was unaffected upon expression of GFP-Mcl-1 WT (Figure 5.5D).

To test this further I also treated GFP-Mcl-1 RALA cells with tetracycline to express the exogenous Mcl-1 protein. Again, both DiM and PmD were delayed on average by 7.9 hours and 4.9 hours, respectively, indicating that the mutant Mcl-1 RALA protein was not defunct in its anti-apoptotic ability (Figure 5.5B, C). In contrast to expression of GFP-Mcl-1 WT, expression of GFP-Mcl-1 RALA increased slippage from 48 % to 80 % (Figure 5.5A, bottom panels). As expression of the GFP-Mcl-1 RALA protein has no significant effect on the rate of mitotic slippage (Figure 5.2C, 5.5D), I can deduce that the increase in slippage is caused by the increase in the time to DiM and that the increase was not apparent on expression of the GFP-Mcl-1 WT protein because slippage was also delayed. This indicates that Mcl-1 can influence both sides of the competing networks model at the same time.

5.7 Exploring the effect of Mcl-1 depletion on mitotic slippage in RKO cells overexpressing Bcl-xL.

I have shown that modulating the levels of Mcl-1 in mitosis influences the rate of slippage in DLD-1 cells. In order to see if this effect can be recapitulated in the death-prone RKO cell line, I needed to tune the RKO cells so that they would predominantly commit to slippage so that slippage rates could be directly measured. Recently it was shown that tetracycline induction of exogenous Bcl-xL in RKO cells switched RKO cells from DiM to slippage in response to taxol treatment (Topham et al., 2015). Overexpressing Bcl-xL suppresses the dependency of the RKO cells for Mcl-1 and so I can use this cell line as a way to measure slippage in response to Mcl-1 RNAi.

To use this as a model system, I needed to use a concentration of tetracycline that could induce a dominant slippage phenotype. Additionally, in order to directly compare slippage rates, I

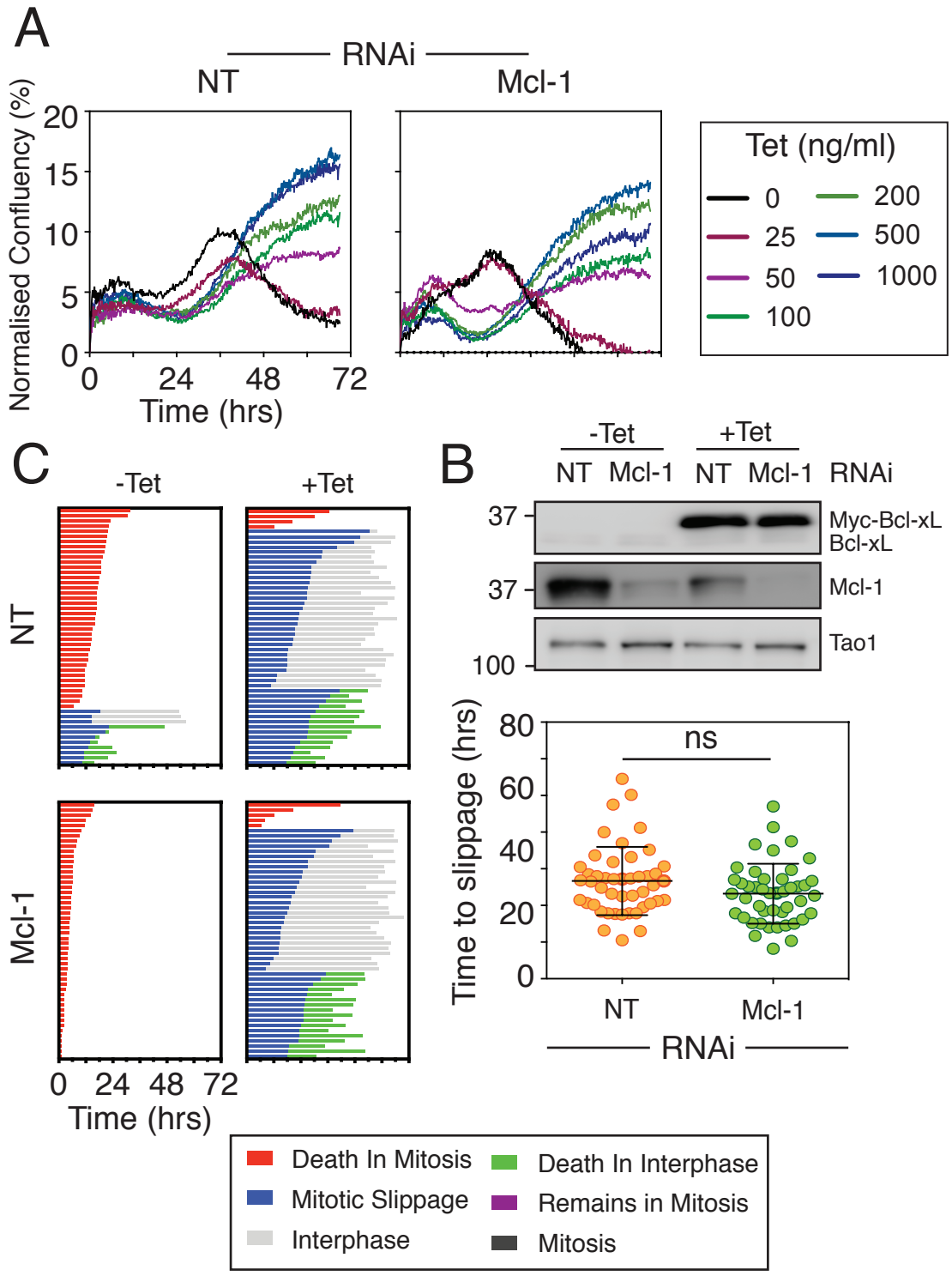

Figure 5.6 Effect of Mcl-1 depletion on mitotic slippage in RKO cells stably overexpressing Bcl-xL.

(A) Cell confluency over time of RKO Myc-Bcl-xL cells tranfected overnight with either non-targeting or Mcl-1 siRNAs. Following transfection, cells were treated with 0.1 μM taxol and tetracycline at the indicated concentrations.
(B) Immunoblot of RKO Myc-Bcl-xL cells transfected overnight with either non-targeting or Mcl-1 siRNA and treated with 500 ng/ml tetracycline for 6 hours.
(C) Cell fate profile and time to slippage of non-targeting or Mcl-1 depleted RKO Myc-Bcl-xL cells treated with 500ng/ml tetracycline and 0.1 μM taxol. Mann-Whitney U test, ns $p > 0.05$. T=0 represents time of mitotic entry.

also needed to ensure that loss of Mcl-1 had no effect on the abundance of slippage and DiM. I transfected RKO Myc-Bcl-xL cells with siRNAs targeting Mcl-1 before performing a serial dilution of tetracycline and co-treating cells with tetracycline and taxol. I used confluency as a read-out for the abundance of mitotic slippage within the population. In the non-targeting control cells, the non-induced population confluency peaked at 10 % above the t=0 time point at 37 hours and decreased to 2.5 %, indicating that the population was undertaking a large amount of cell death in response to taxol (Figure 5.6A, left panel). However, upon addition of either 500 or 1000 ng/ml tetracycline, cell confluency reaches the highest (15-16 % normalised) at 72 hours. From the confluency data, I looked more specifically at the effect of 500 ng/ml tetracycline had on the cell line when co-treated with taxol. Immunoblotting showed that this concentration induced Myc-Bcl-xL expression many times above the expression of the endogenous Bcl-xL protein in this cell line (Figure 5.6B). In line with the confluency data, 78 % of the control population underwent DiM in response to taxol treatment, whereas only 8 % of the population co-treated with 500 ng/ml tetracycline committed to DiM due to Bcl-xL overexpression (Figure 5.6C, top panels). Consistent with previous data, DiM was accelerated from 16.6 hours to 5.3 hours in response to Mcl-1 RNAi in cells treated with taxol only (Figure 5.6C, left panels). Furthermore, Mcl-1 RNAi increased DiM in the control population from 78 % to 100 %. Upon addition of 500 ng/ml tetracycline to induce the Bcl-xL protein in cells depleted in Mcl-1, there was no difference in the number of cells that committed to slippage, showing that Bcl-xL overexpression was sufficient to overcome the loss of Mcl-1 by RNAi (Figure 5.6C, bottom right panel). Moreover, there was only a slight increase in the number of cells undertaking PmD (16 cells versus 15 cells). However, when the time to slippage was compared, although Mcl-1 depleted cells underwent slippage on average 3.4 hours faster than the control population, there was no significant difference between the two populations, thus suggesting that in this context, Mcl-1 protein levels have no effect on mitotic slippage (Figure 5.6C). This indicates that Mcl-1 effect on mitotic slippage may not necessarily be a universal phenomenon.

5.8 Investigating the functional effect of variable levels of Mcl-1 and Bcl-xL proteins in slippage-prone and death-prone cell lines.

In Chapter 5.2 I show that slippage-prone DLD-1 cells are dependent on Bcl-xL to survive a mitotic arrest induced by AZ138. As DLD-1 cells are also able to degrade Mcl-1, one could hypothesise that a differentiating factor between DiM-prone and slippage-prone cell lines is the ability of the apoptotic network to cope with the loss of Mcl-1. This may in part depend on the dependency for Mcl-1 as opposed to other Bcl-2 family proteins due to the expression levels. To investigate the variability of protein expression of Bcl-xL and Mcl-1 I took protein lysates from 6 different cell lines: four DiM prone cell lines (HeLa, RKO, HT29 and H1703) and two slippage-prone cell lines (DLD-1 and HCT-116) (Figure 5.7). Immunoblotting of the six cell lines showed variability in the expression of both Mcl-1 and Bcl-xL in all cell lines in comparison to the protein control Tao1 (Figure 5.8). Both slippage prone cell lines had relatively low levels of Mcl-1 in comparison to the DiM-prone cell lines. However, both these cell lines expressed Bcl-xL, thus suggesting that these cell lines are dependent on Bcl-xL (Figure 5.8 lanes 1 and 3). This explains why Mcl-1 loss has no effect on DiM in DLD-1 cells and why Bcl-xL depletion causes a dramatic shift to DiM (Figure 5.1D). Of the four DiM-prone cell lines, two of the cell lines (HeLa and H1703 lung cell line) express little/no protein levels of Bcl-xL and are therefore likely to be dependent on Mcl-1. RKO and HT29 death-prone cell lines have a mixture of both and so the Bcl-2 protein dependency is harder to predict (Figure 5.8 lanes 4 and 5).

To confirm the predictions regarding dependency on Mcl-1 and Bcl-xL, I transfected into these cell lines siRNAs targeting Mcl-1 and Bcl-xL and performed time-lapse microscopy to see the comparative effect loss of each of these proteins had on the cell fate in each of the cell lines. Immunoblotting confirmed efficient knockdown of Mcl-1 and Bcl-xL in all cell lines (Figure 5.9). As a way to measure real-time apoptosis cells were treated with a dye that fluoresces upon caspase 3/7-enzyme activation and the number of fluorescent spots were counted in each image taken every 10 minutes. Although DLD-1 and HCT116 are slippage-prone cell lines, caspase 3/7 becomes activated after approximately 35 and 20 hours in the non-targeting populations (Figure 5.10, top panels). In both slippage-prone cell lines, knockdown of Mcl-1 had no significant effect on the amount of caspase 3/7 accumulation, explaining why loss of Mcl-1 does not increase

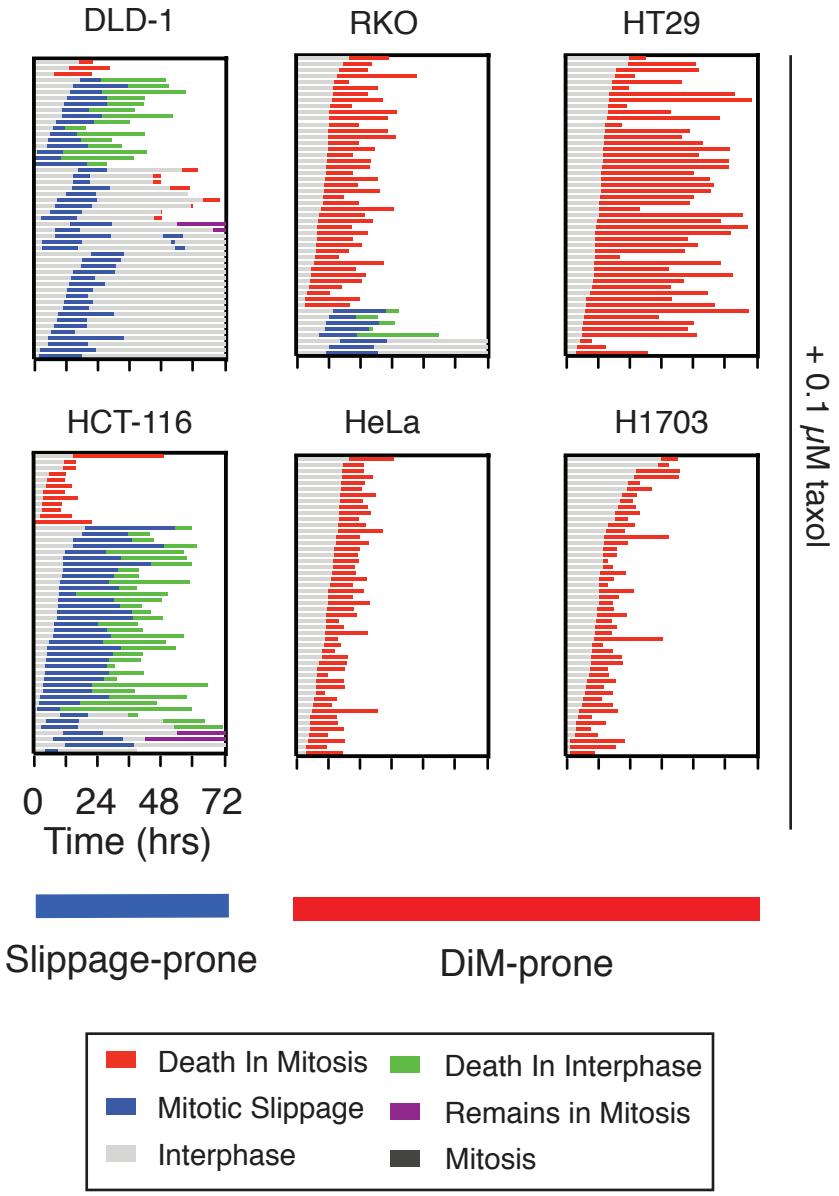

Figure 5.7 Responses of different slippage-prone and DiM-prone cell lines to taxol.
Cell fate profiles of the indicated cell lines treated with 0.1 μM taxol

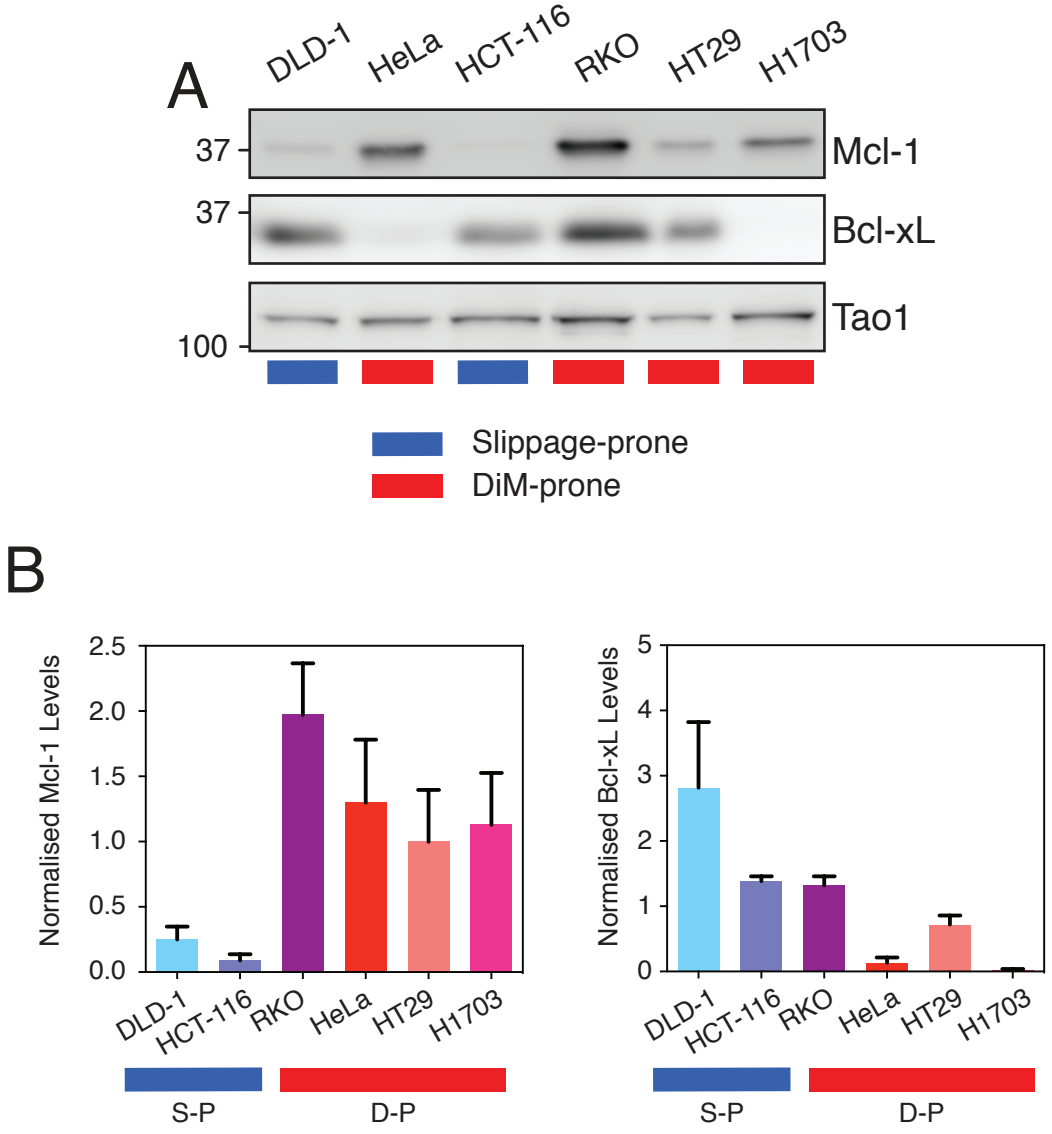

Figure 5.8 Relative expression levels of Mcl-1 and Bcl-xL in different cell lines.
(A) Immunoblot of the levels of Mcl-1 and Bcl-xL protein in the lysates of six cell lines indcated. A Bradford assay was performed to enable equal loading of 8 μg.
(B) Quantification of 3 x immunoblots shown in Figure 5.8A.

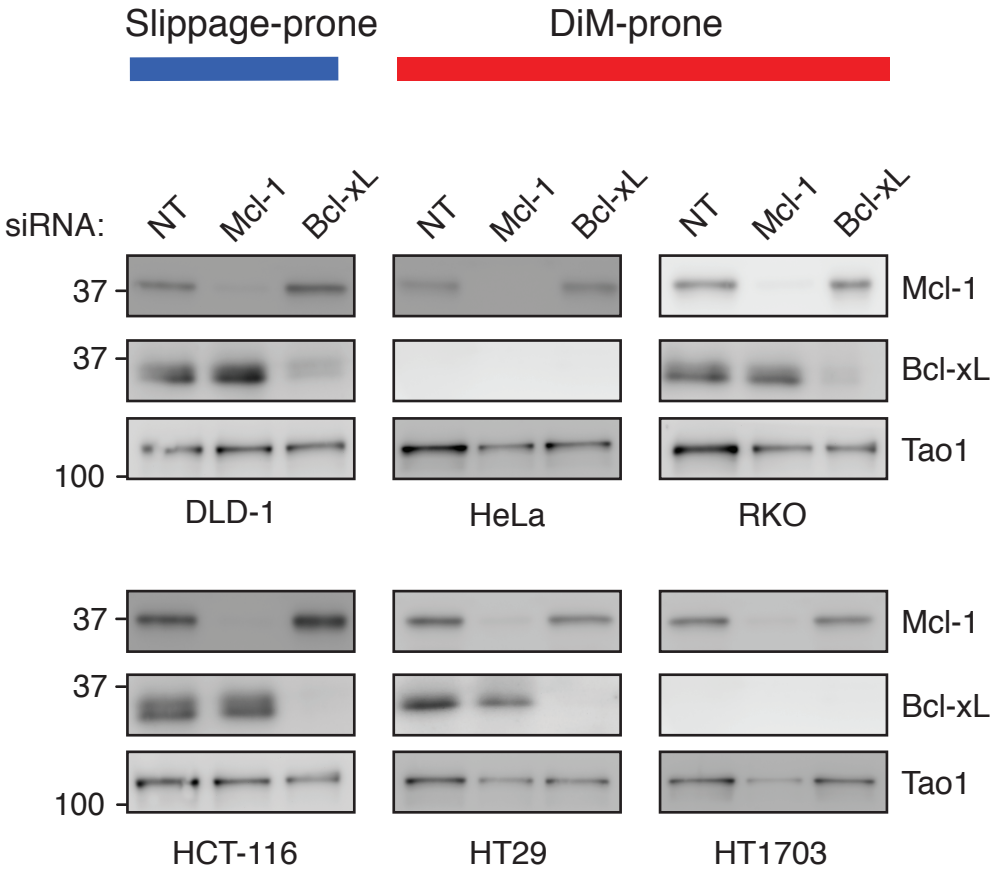

Figure 5.9 Mcl-1 and Bcl-xL depletion in different cell lines.
Immunoblot of Mcl-1 and Bcl-xL in the cell lines indicated. Lysates were collected 24 hours following siRNA tranfection of cells targeting either Mcl-1, Bcl-xL or non-targeting control.

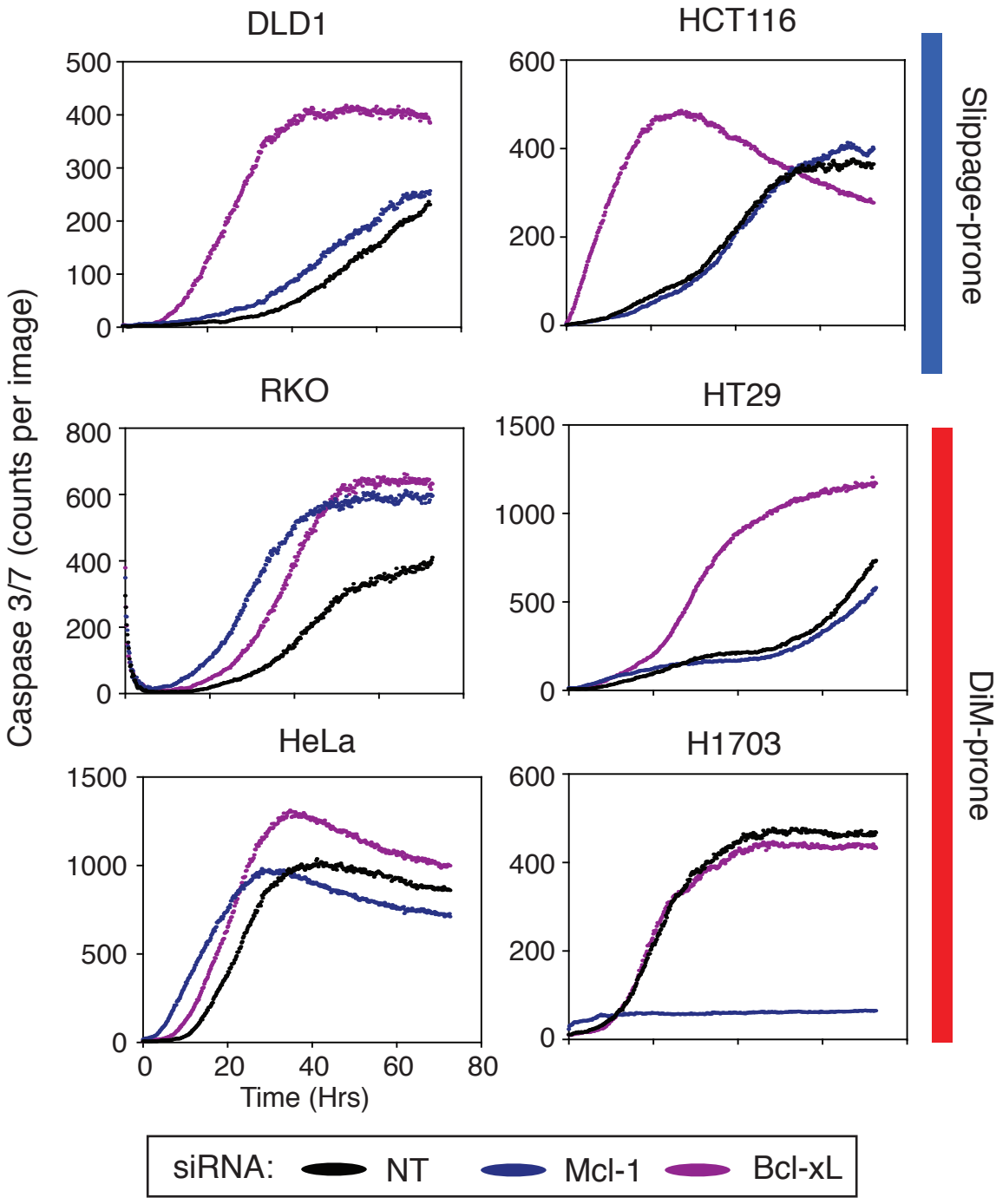

Figure 5.10 Response of different cell lines treated with taxol to Mcl-1 and Bcl-xL depletion.
Different cell lines (indicated) were transfected overnight with siRNAs targeting Mcl-1, Bcl-xL and non-targeting control. The number of cells with activated caspase 3/7 per image are measured using a caspase 3/7 fluorescent dye.

DiM. However, loss of Bcl-xL in both cell lines had a very significant effect as caspase 3/7 activation occurred immediately following the addition of taxol. These results are in line with the high expression levels of Bcl-xL versus Mcl-1 in these cell lines (Figure 5.8). This indicates that slippage-prone cell lines are very dependent on Bcl-xL and are therefore unlikely to respond to loss of Mcl-1 during a mitotic arrest.In the death-prone cell lines, initiation of caspase 3/7 activation occurred faster than the slippage-prone cell populations in 3 out of 4 cell populations (RKO: 20 hours, HeLa: 10 hours, H1703: 10 hours) (Figure 5.10 bottom panels). Loss of Mcl-1 accelerated caspase 3/7 activation in both RKO and HeLa cell lines (Figure 5.10 bottom right panels). Furthermore, loss of Mcl-1 in the H1703 cell line caused uniform cell death before the beginning of the experiment, showing that this cell line is completely dependent on Mcl-1 for survival. This is again consistent with the high expression levels of Mcl-1 compared to Bcl-xL in this cell line (Figure 5.8). One exception is the death-prone HT29 cell line which displayed accelerated death only upon loss of Bcl-xL but not Mcl-1 which mirrors the response of the slippage-prone cell lines (Figure 5.10 middle right panel). However, this cell line takes much longer to commit to DiM compared with the other DiM-prone cell lines (35.8 hours versus and average time to DiM of less than 17 hours for the other 3 cell lines); an indication that Mcl-1 degradation does not affect the apoptotic balance in this cell line. Instead, the DiM-response of this cell line is likely to be caused by slow slippage kinetics as previously described (Gascoigne and Taylor, 2008). Put together, this suggests that DiM-prone cell lines have a greater dependency on Mcl-1 for survival, which may explain why they are sensitive to DiM due to loss of Mcl-1 during a protracted mitosis.

5.9 Summary

In the previous chapter it was observed that the APC/C-Cdc20-Mcl-1 association previously identified had no effect on DiM. In this chapter, analysis of mitotic slippage showed that it might have an effect on the rate of Cyclin B1 degradation. However, as loss of Mcl-1 in RKO cells expressing Bcl-xL had no effect on the rate of slippage, it is possible that this association is not a universal phenomenon and so the general significance of this may be minimal.

In this chapter I also show that Mcl-1 loss has little effect on DiM in a slippage prone cell line. This is caused by expression levels and therefore dependency of slippage-prone cell lines for Bcl-xL. This may also in help differentiate and predict death-prone and slippage-prone cell lines on a molecular level. However, despite not having an effect on DiM, loss of Mcl-1 has an effect on post-mitotic survival, indicating that it may also act as a post-mitotic death timer. In the final chapter I explore whether prolonging the mitotic arrest, thereby providing more time for Mcl-1 loss, can affect the post-mitotic response.

6 Chapter 6: The role of Mcl-1 in post-mitotic fate.

6.1 Introduction

In Chapter 3 I showed that degradation of Mcl-1 contributed to death in mitosis (DiM) in death-prone RKO cells and in Chapter 5 I observed that depletion of Mcl-1 increased the number of cells committing to post-mitotic death (PmD) following mitotic slippage, indicating that Mcl-1 has a survival role in both DiM and PmD. As previously shown, Mcl-1 is degraded during a prolonged mitotic arrest in slippage-prone DLD-1 cells (Figure 5.1B). I therefore postulated that if the mitotic arrest induced by the Eg5 inhibitor AZ138 was stalled for a longer period of time, DLD-1 cells would have more time to degrade Mcl-1 and subsequently commit to post-mitotic death (PmD), thereby making Mcl-1 degradation a contributor to the post-mitotic death timer. To indirectly achieve this, I aimed to analyse the effect of mitotic duration on post-mitotic death.

The concept of mitotic duration influencing the post-mitotic response is not novel. Although others have shown that mitotic duration correlates with decreased cell viability, thereby supporting a model whereby a death-signal accumulates during a mitotic arrest which then persists into the next cell cycle, the point at which these cells eventually commit to death (PmD or DiM in the next mitosis) is not well defined (Colin et al., 2015; Zhu et al., 2014). Here I use single-cell time-lapse analysis to differentiate between interphase and mitotic death when mitotic duration is artificially increased.

6.2 Correlation analysis between time to mitotic exit and post-mitotic death in DLD-1 cells.

Mitotic duration has an effect on post-mitotic cell cycle arrest and post-mitotic survival (Colin et al., 2015; Uetake and Sluder, 2010; Zhu et al., 2014). To investigate whether mitotic duration impacts on the kinetics of post-mitotic death I plotted the time in mitosis versus the time to PmD of DLD-1 Mcl-1 WT and Mcl-1 RALA cells previously treated with 6.6 μM nocodazole and tetracycline as there were enough cells committing to PmD in these populations in which to analyse (Figure 5.4, Figure 6.1). Two out of the four scatter plots show a significant correlation

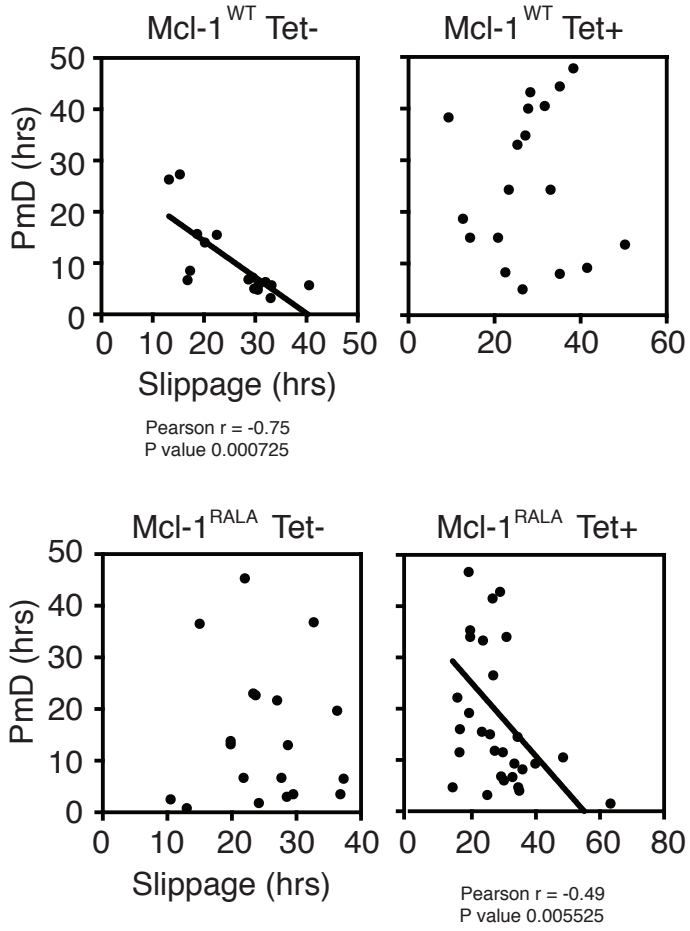

Figure 6.1 Correlation analysis between time to mitotic exit and time to post-mitotic death in DLD-1 GFP-Mcl-1 cell lines.
(A) Correlation analysis of time to mitotic exit versus time to post-mitotic death in individual DLD-1 GFP-Mcl-1 cells treated with 1 μg/ml tetracycline and 6.6 μM nocodazole as analysed in Figure 5.5.

between the two variables. The negative Pearson R values for the uninduced Mcl-1 WT and induced Mcl-1 RALA populations of -0.75 and -0.49 suggest a negative correlation between time to slippage and time to PmD; the longer a cell remains in mitosis before it exits, the faster it will commit to death in the subsequent interphase (Figure 6.1, top left panel and bottom right panel). However, the induced Mcl-1 WT and the uninduced Mcl-1 RALA populations did not show any correlation between mitotic duration and time to post-mitotic death (Figure 6.1, top right panel and bottom left panel). This may be caused in part on the small number of slipped cells analysed in this experiment. Although I could not draw any strong conclusions, the data does support the idea that a prolonged mitotic duration does appear to have an effect on the post-mitotic response.

6.3 Generation of DLD-1 cells expressing Cyclin B1 wild type and Cyclin B1 R42A-AID under the control of the AID-auxin system.

Although the data in Chapter 6.2 suggests a connection between mitotic duration and PmD, I wanted to test this relationship more directly. To achieve this I created a model cell system which could:

1. Induce a longer mitotic arrest by suppressing mitotic slippage
2. Control the timing of mitotic slippage.

In Chapter 3 I created a RKO cell line unable to commit to mitotic slippage by expressing a stabilised form of Cyclin B1, Cyclin B1 R42A. Expression of this protein in DLD-1 cells would therefore induce a prolonged mitotic arrest by suppressing slippage. In order to satisfy the second criterion, I expressed Cyclin B1 R42A fused to an auxin-inducible degron (AID) tag which causes its rapid degradation upon addition of a family derivative of the plant hormone auxin, indole-3-acetic acid (IAA). So, by adding a controllable-degradation tag to Cyclin B1 R42A, one can cause its degradation at will, thus controlling mitotic slippage.

The components of the AID-auxin system were identified in plants as a way to rapidly degrade short-term transcriptional repressors (Figure 6.2)(Hayashi, 2012). Upon addition to cells, IAA mediates ubiquitination of AID-tagged proteins via the SCF E3 ligase complex. IAA binds both Tir1, an F-box protein subunit of the SCF and a protein containing an AID tag, putting

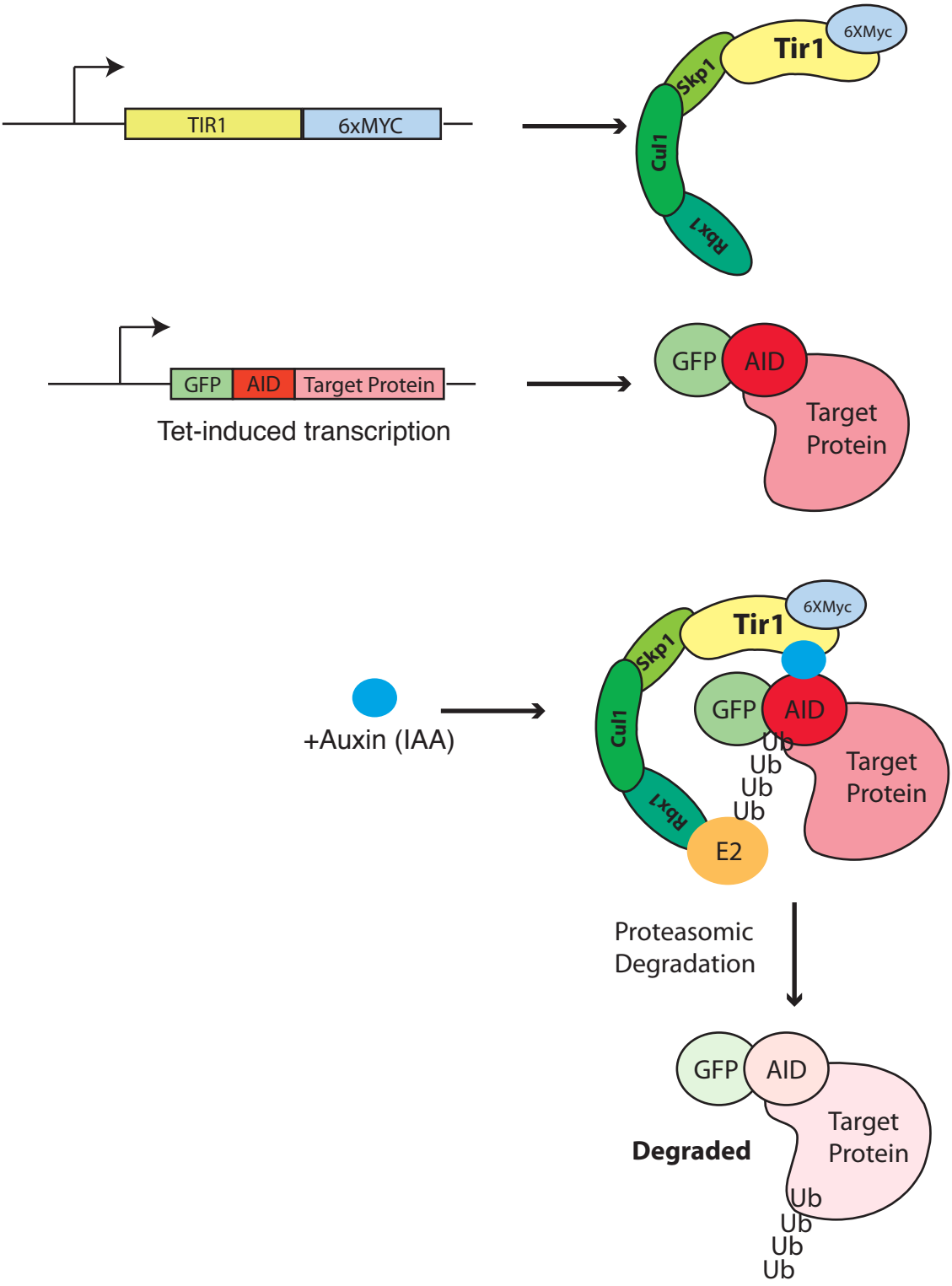

Figure 6.2 The AID-auxin system.
The AID-auxin system requires expression of two components: the Tir1 F-box protein that binds to the E3 ligase SCF complex and the target protein fused to an AID tag. Addition of IAA brings the two protein complexes toegther. With the help of an E2 protein, the AID-tagged target protein is rapidly ubiquitinated and degraded via the proteasome

the two proteins into close proximity (Nishimura et al., 2009). This allows the transfer of ubiquitin from an E2 conjugating enzyme to the AID-tagged target substrate and subsequent proteasome-mediated degradation. As both Tir1 and AID-containing substrates are not present in mammalian cells, the AID system has been used to rapidly and reversibly degrade a variety of specific proteins in both yeast and mammalian cells by exogenously expressing the Tir1 protein which binds to the mammalian SCF complex and the protein of interest fused to an AID-tag (Holland et al., 2012; Morawska and Ulrich, 2013; Nishimura et al., 2009).

6.4 Characterisation of the DLD-1 GFP-AID-Cyclin B1 cell lines.

Using the Flp-In™ T-Rex System, GFP-AID tagged Cyclin B1 genes (GFP-AID-Cyclin B1) were stably integrated into the genome of DLD-1 myc-Tir1 cells (Holland et al., 2012). Immunoblotting for Cyclin B1 and GFP showed that upon addition of tetracycline, exogenous GFP-AID-Cyclin B1 WT and GFP-AID-Cyclin B1 R42A proteins were expressed at slightly lower levels when compared to the endogenous Cyclin B1 protein (Figure 6.3). Importantly, upon co-treatment with 500 μM IAA, exogenous Cyclin B1 protein is lost, indicating that the expressed AID-tagged Cyclin B1 proteins are being rapidly turned-over by IAA-mediated degradation.

Having shown that I can degrade GFP-AID tagged Cyclin B1 I aimed to test whether the AID-auxin system could revert the phenotype exerted by expression of Cyclin B1 *in vivo*. Cells were synchronised with a single overnight thymidine block then released into media with or without the drugs and filmed single cells using time-lapse microscopy. Uninduced DLD-1 GFP-AID-Cyclin B1 WT cells undertook two or more divisions during the 48 hour time period (86 %) (Figure 6.4A, top left panel) with an average time in mitosis of 37.8 minutes (Figure 6.4B). Expression of wild-type Cyclin B1 upon the addition of tetracycline to the non-drug population had no obvious effect on proliferation as 94 % of cells were able to complete two divisions (Figure 6.4A, top middle panel). However, the average mitotic duration was increased by 17.4 minutes to 55.2 minutes, possibly caused by the requirement to degrade more Cyclin B1 protein during anaphase (Figure 6.4B). Upon addition of Eg5 inhibitor AZ138, the majority (90 %) of control uninduced DLD-1 GFP-AID-Cyclin B1 cells underwent slippage with an average time of 14.0 hours (Figure 6.4A, bottom left panel). This is similar response to wild type DLD-1 cells

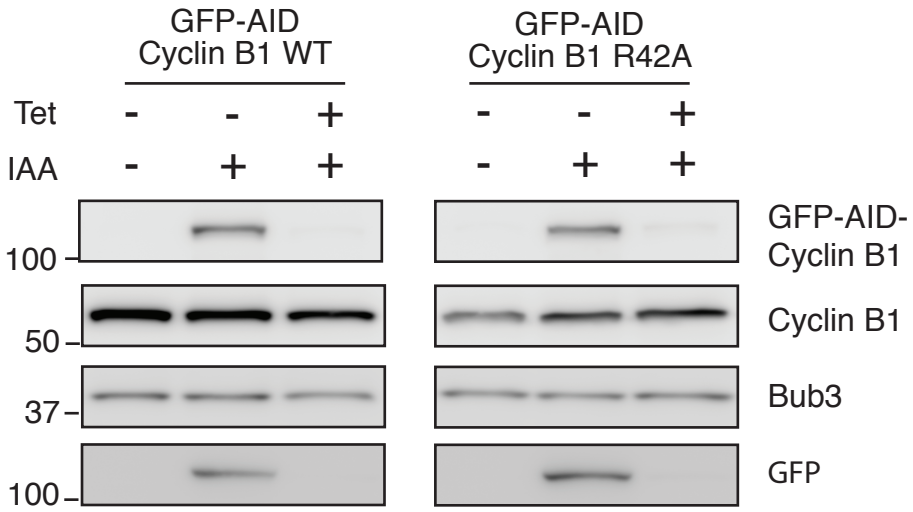

Figure 6.3 Generation of DLD-1 cells stably expressing GFP-AID-Cyclin B1 protein.
Immunoblot of Cyclin B1 and GFP protein levels in DLD-1 GFP-AID-Cyclin B1 WT and DLD-1 GFP-AID-Cyclin B1 R42A cells after 24 hour treatment with 1 μg/ml tetracycline and 500 μM IAA. Bub3 is used as a loading control.

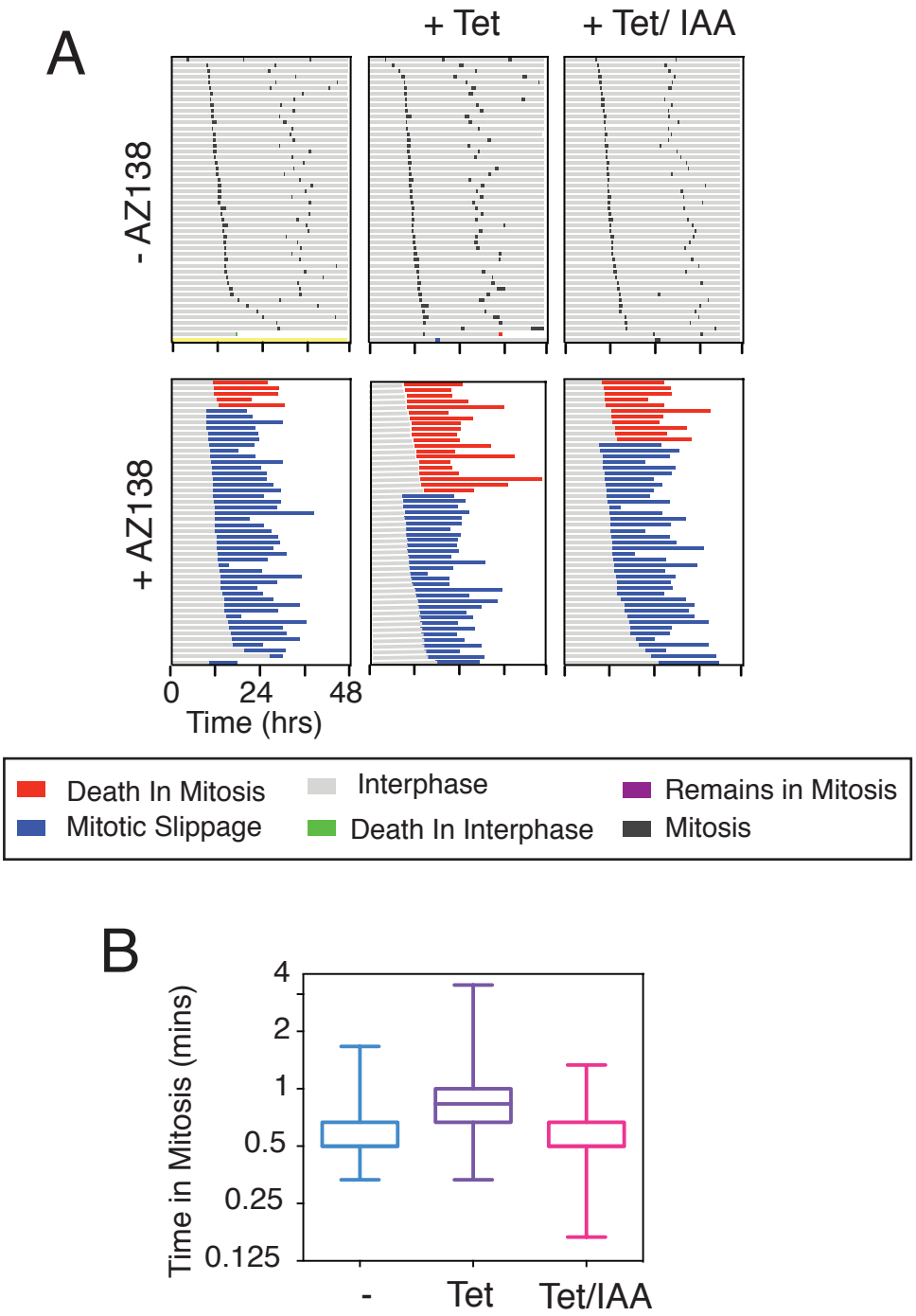

Figure 6.4 Characterisation of the DLD-1 GFP-AID-Cyclin B1 WT cell line.
(A) Cell fate profiles of DLD-1 GFP-AID-Cyclin B1 WT cells treated with 1 µM AZ138, 1 µg/ml tetracycline and 500 µM IAA where indicated. Cells were imaged using time-lapse microscopy.
(B) Quantification of the time to regular mitotic division in DLD-1 GFP-AID-Cyclin B1 WT cells treated with 1 µg/ml tetracycline and 500 µM IAA.

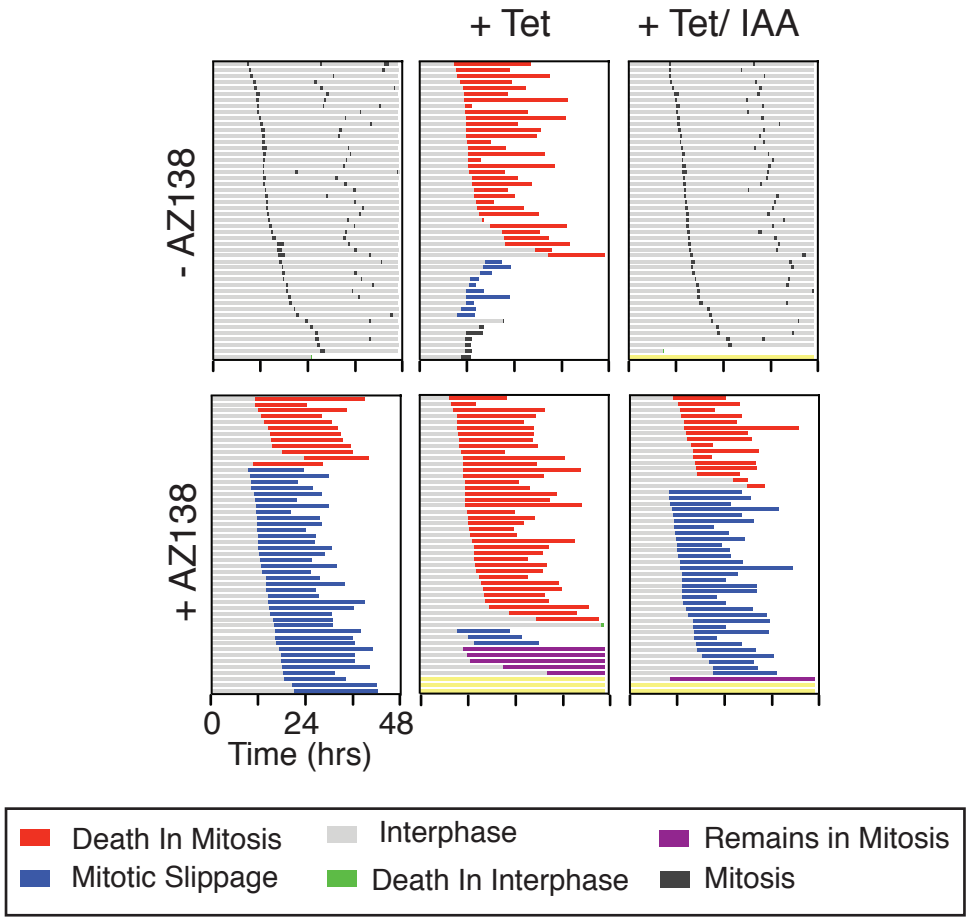

Figure 6.5 Characterisation of the DLD-1 GFP-AID-Cyclin B1 R42A cell line.
Cell fate profiles of DLD-1 GFP-AID-Cyclin B1 R42A cells treated with 1 µM AZ138, 1 µg/ml tetracycline and 500 µM IAA where indicated. Cells were imaged using time-lapse microscopy.

(Figure 5.1D). Although the time to slippage or DiM is unaffected, expression of GFP-AID-Cyclin B1 WT caused an increase in DiM to 40 %, presumably as slippage was suppressed due to an increase in Cyclin B1 protein. Altogether this shows that the exogenous Cyclin B1 WT protein is functioning as expected with the GFP-AID tag. Importantly, co-treatment of tetracycline and IAA with or without the presence of AZ138 resulted in the DLD-1 cells reverting to their original phenotypes, showing that the Cyclin B1 AID-auxin system has a functional effect (Figure 6.4A right panels).

The same characterisation was also performed on the DLD-1 GFP-AID-Cyclin B1 R42A cells. Untreated DLD-1 GFP-AID-Cyclin B1 R42A cells undertook two divisions during the 48 hour time period (76 %) with a mitotic average time of 42.3 minutes (Figure 6.5A, top left panel). In contrast to Cyclin B1 WT-induced cells, expression of GFP-AID-Cyclin B1 R42A protein caused 84 % of cells to arrest in mitosis for longer than two hours (Figure 6.5A, top middle panel). Only 14 % of cells could commit to a normal mitotic division, with 20 % committing to mitotic slippage and 66 % undertaking DiM as they were unable to escape the mitotic arrest. These cell fate profiles mirror the characterisation of the RKO cell line expressing GFP-Cyclin B1 R42A (Figure 3.3). Upon addition of AZ138, the number of cells unable to exit mitosis increased to 86 %, with 76 % of cells committing to DiM with an average time of 18.1 hours (Figure 6.5A, bottom middle panel). Again, addition of IAA to the DLD-1 GFP-AID-Cyclin B1 R42A reversed the effect and cells reverted to the original cell fate phenotypes (Figure 6.5A, right panels). This shows that I have a model cell system that can force cells to remain in a mitotic arrest under the control of the AID-auxin system.

6.5 Time-course fluorescence analysis of GFP-AID-Cyclin B1 R42A upon addition of IAA.

I generated cell lines expressing AID-tagged Cyclin B1 R42A in order to control mitotic duration. However, the AID-auxin system has been shown to degrade different target proteins at different rates (Holland et al., 2012). To investigate the kinetics of AID-tagged Cyclin B1 degradation and how this corresponds to the kinetics of mitotic exit, I used single-cell fluorescence time-lapse microscopy to determine the rate of GFP loss upon IAA addition. DLD-1

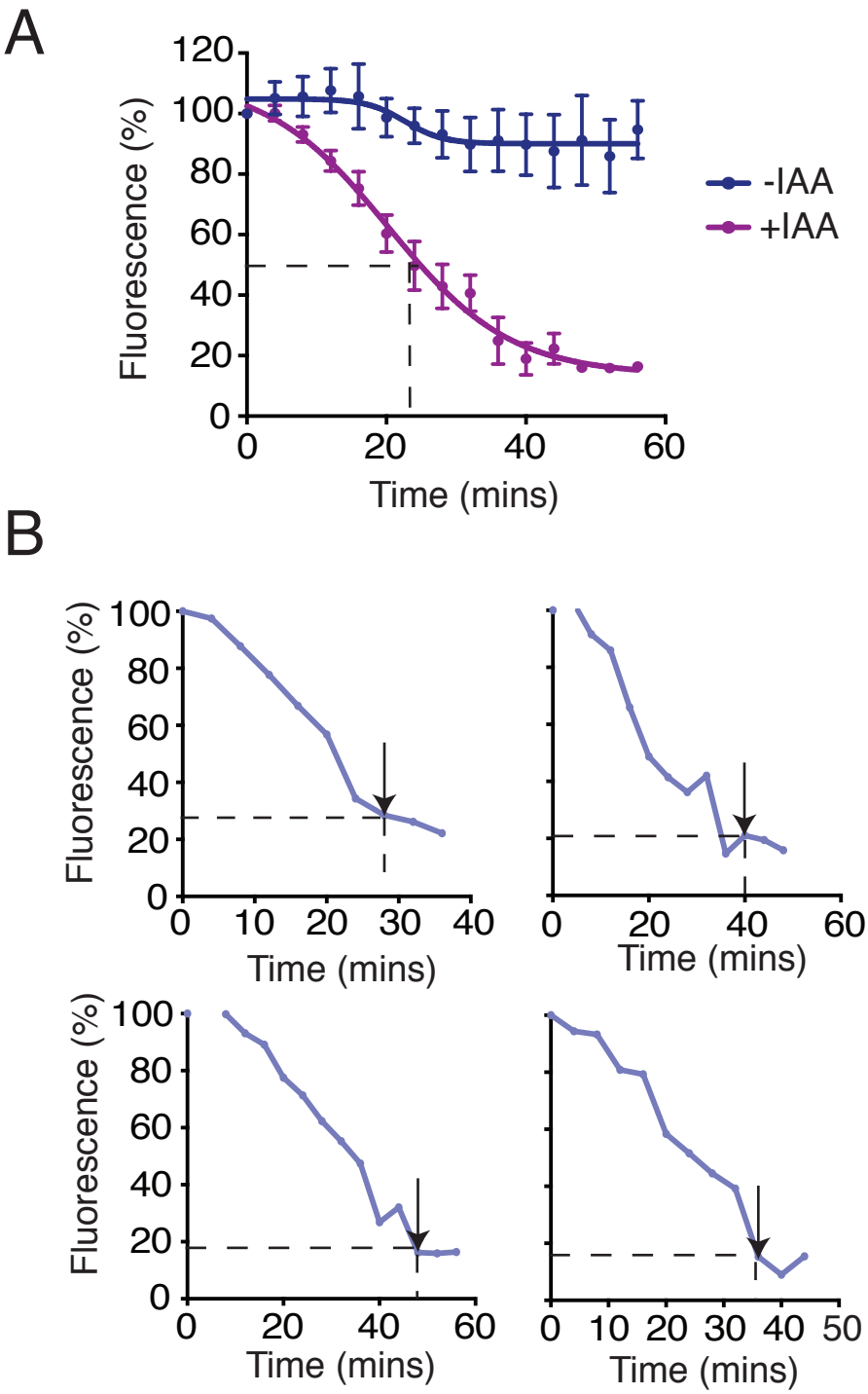

Figure 6.6 Tracking degradation kinetics of GFP-AID-Cyclin B1 R42A protein using fluorescence microscopy.
(A) Average fluorescence intensity of DLD-1 GFP-AID-Cyclin B1 cells over the course of an hour following IAA treatment. Cells were first treated with tetracycline for 6 hours prior to imaging to induce the GFP-AID-Cyclin B1 protein. Error bars represent standard error. n=4 per condition.
(B) Fluorescence intensity of individual mitotic DLD1 GFP-Cyclin B1 R42A cells following the addition of IAA at t=0. The arrows dep-ict the time-point at which the cell divides.

GFP-AID-Cyclin B1 R42A cells were treated with tetracycline for 6 hours to induce expression of the GFP-AID-Cyclin B1 protein and force a mitotic arrest in some cells. At this point, IAA was added to the media and fluorescent cells that had arrested in mitosis were imaged (classed as t=0). Images were taken every 4 minutes over the course of 1 hour. Fluorescence measurements of control mitotic cells that were not treated with IAA remained relatively level with a small reduction of fluorescence of 5.3 % on average by the end of the experiment (Figure 6.6A). In contrast, addition of IAA caused a rapid decrease in GFP expression with average fluorescence levels reduced to just 16.4 %. On average, the half life of the protein was roughly 22 minutes which is consistent with the degradation of other AID-tagged proteins (Han et al., 2013; Holland et al., 2012; Nishimura et al., 2009).

In order to analyse the kinetics of mitotic division following IAA addition, phase images were also taken. Mitotic cells divided on average 35.8 minutes following the addition of IAA (Figure 6.6B). Conversely, mitotic cells that were not treated with IAA were unable to exit mitosis (data not shown). Moreover, cells completed cell division after GFP fluorescence was reduced to 21.3 % on average. This shows that mitotic exit can occur rapidly after the degradation of GFP-AID-Cyclin B1 R42A protein. Put together, I have created and characterised a system that can control the mitotic time to exit through the rapid degradation of exogenous Cyclin B1 R42A protein that can be used to investigate the effect of time to mitotic slippage on post-mitotic death.

6.6 Investigating the effect that mitotic duration has on post-mitotic death.

Having generated and characterised the DLD-1 GFP-AID-Cyclin B1 R42A cell line I can now directly compare the post-mitotic response when mitotic duration is changed under the control of the Cyclin B1 R42A AID-auxin system. The aim of this experiment was to add IAA at different times during a protracted mitosis in order to induce slippage at different times for comparison using time-lapse microscopy. To do this, time points for comparison needed to be chosen. Based on the independent networks model (Chapter 1.3.2), If cells are arrested in mitosis for too long, the DiM signal has enough time to reach the threshold and cells commit to DiM as seen in the DLD-1 Cyclin B1 R42A cells treated with tetracycline and AZ138 only (Figure

6.5A, bottom middle panel). This means that the longer time point has to be before the point at which many cells undertake DiM in order to obtain enough cells that have undertaken mitotic slippage to analyse the post-mitotic response. Following thymidine release, the majority of cells had naturally slipped out of mitosis by 30 hours and so delaying IAA treatment until this time point would further prolong the mitotic arrest. Additionally, by 30 hours less than 50 % of the cells expressing GFP-AID-Cyclin B1 R42A in response to AZ138 had committed to DiM, meaning that this time point would provide enough “slipped” cells in which to assess the post-mitotic response (Figure 6.5A, bottom middle panel). As an IAA control to induce a short arrest for comparison, I chose 20 hours because at this point, none of the control DLD-1 Cyclin B1 R42A cells had committed to slippage by this point as endogenous protein had not yet been degraded (Figure 6.5A, bottom left panel). Addition of IAA at this time point meant that cells can then exit mitosis naturally through endogenous degradation of Cyclin B1.

Cell fate profiling was used to characterise these cell populations in response to the Eg5 inhibitor AZ138 (Figure 6.7A). Consistent with earlier results, 88 % of the control population underwent slippage in an average time of 14.8 hours (Figure 6.7A, top left panel). Consistently, expression of Cyclin B1 upon tetracycline treatment caused 70 % of cells to commit to DiM with 30 % undertaking mitotic slippage (Figure 6.7A, top middle panel). This phenotype was reversed upon co-treatment with IAA (Figure 6.7A, top right panel). When IAA was added 20 hours post-thymidine release, 96 % of cells underwent mitotic slippage at an average time of 15.5 hours; a time that was not-significant with both the non-induced and the tetracycline/IAA control cell populations (Figure 6.7A bottom left panel, 6.8B). On average, these cells exited mitosis 6.9 hours after IAA addition. This at first seemed inconsistent as the fluorescence kinetics analysis suggested cells could undergo mitotic exit after 35.8 minutes (Figure 6.6B). However, this is likely to reflect on the fact that endogenous Cyclin B1 had not yet fallen beneath a level to cause mitotic exit upon IAA addition. Addition of IAA at 30 hours post-thymidine release caused 84 % of cells to slip out of mitosis at a significantly delayed average time of 20.6 hours compared to controls (Figure 6.7A, bottom right panel, 6.7B). Additionally, cells were able to exit mitosis 2.4 hours after IAA addition presumably because by this time, endogenous Cyclin B1 had already been degraded and so cells were now dependent on the exogenous GFP-AID-Cyclin B1 R42A

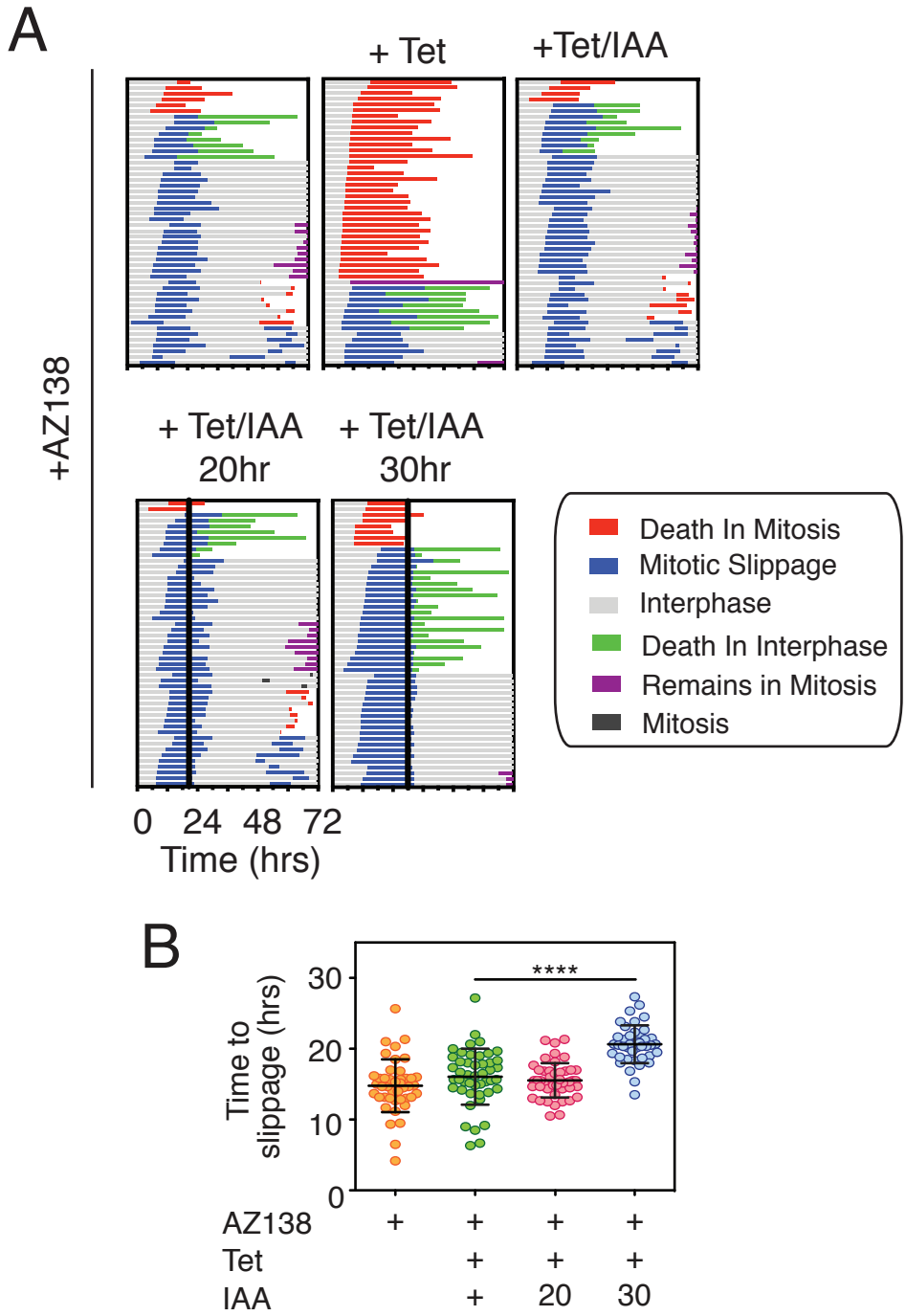

Figure 6.7 Analysing post-mitotic fate following changes to the time to mitotic slippage.
(A) Cell profiles of DLD-1 GFP-AID-Cyclin B1 R42A cells treated with 1 µM AZ138, 1 µg/ml tetracycline and 500 µM IAA.
(B) Graph quantifying time to mitotic slippage in DLD-1 GFP-AID-Cyclin B1 cells from Figure 6.7a.

protein, and therefore under the control of IAA. Therefore, these time points (20 and 30 hours) were used to compare differences in the post-mitotic response.

To analyse the post-mitotic response I looked at the proportion of cells committing to mitotic exit that eventually undertook death in the subsequent interphase. Following exit, 17 % and 20 % of the control uninduced and tetracycline/IAA cell populations committed to PmD (Figure 6.7A, top panels). Furthermore, a similar effect was observed in the IAA 20 hour cell population, where 17 % undertook PmD, 60 % entered a second mitosis and the rest remained in interphase (Figure 6.7A, bottom left panel). However, in the IAA 30 hour population, the percentage of cells that committed to PmD following mitotic slippage increased to 52 %, with only 7 % able to enter a second mitosis (Figure 6.7A, bottom right panel). Put together, this experiment elegantly confirms the hypothesis regarding the association between mitotic duration and post-mitotic death in the subsequent interphase.

6.7 Analysing the co-functional effect of mitotic duration and Mcl-1 loss on the post-mitotic response.

Prolonging the mitotic arrest using the Cyclin B1 R42A AID-auxin system has led to 44 % of cells committing to PmD (Figure 6.7A, bottom right panel). This is very similar number to the 46 % of cells committing to PmD in Mcl-1-depleted DLD-1 cells (Figure 5.1). These observations add fuel to the notion that the PmD caused in cells forced to remain in a mitotic arrest for longer is due to a reduction in Mcl-1 levels. If this is true, one may expect that loss of Mcl-1 in the IAA 20-hour treated population may mirror the effect of prolonging mitotic duration by Cyclin B1 R42A expression. To test these hypotheses DLD-1 GFP-AID-Cyclin B1 R42A cells were treated with thymidine and transfected with siRNAs targeting Mcl-1 before treatment with AZ138, tetracycline and IAA at 20 and 30 hours post thymidine release. Immunoblotting confirmed knockdown of both Mcl-1 24 hours after siRNA transfections (Figure 6.8A).

Cells were imaged using time-lapse microscopy and the number of cells undertaking each post-mitotic fate was quantified (Figure 6.8B). Consistently, 22 % of control cells with IAA treatment at 20 hours committed to PmD, which was increased to 51 % in cells treated with IAA

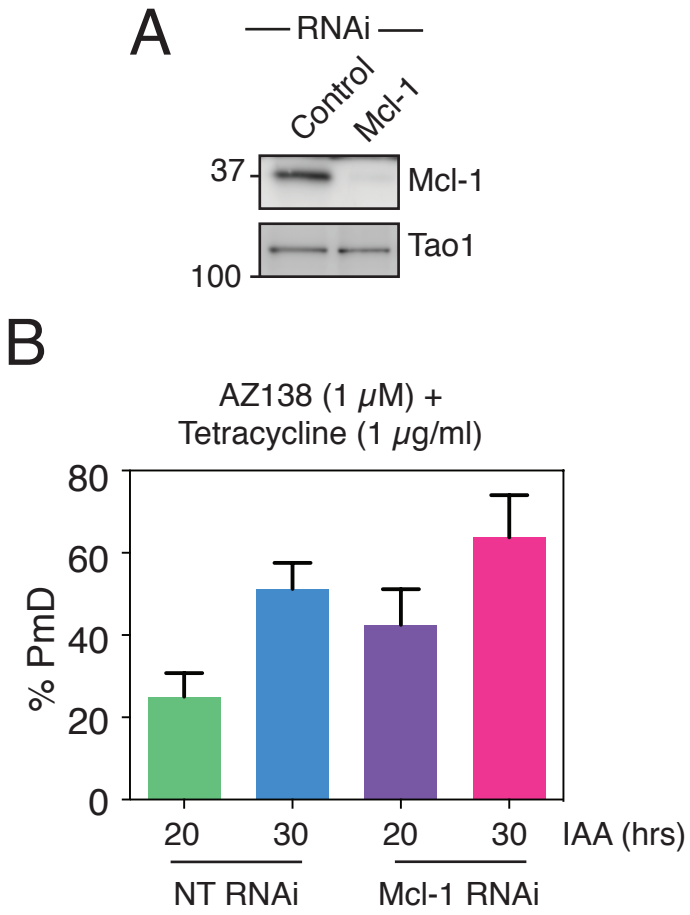

Figure 6.8 Effect of Mcl-1 depletion and mitotic duration on post-mitotic death.
(A) Immunoblot of Mcl-1 levels 24 hours following siRNA tranfections targeting the indicated proteins in DLD-1 GFP-AID-Cyclin B1 R42A cells.
(B) Bar graph representing the proportion of DLD-1 GFP-AID-Cyclin B1 R42A cells undertaking PmD in response to co-treatment with 1 μM AZ138, 1 μg/ml tetracycline and 500 μM IAA at the indicated times following 24 hour siRNA transfections targeting the indicated proteins. n=20x4 per condition

at 30 hours post-thymidine release. Loss of Mcl-1 in the IAA 20 population increased the number of cells that committed to PmD by 17.5 % to 42.5 %, a phenotype consistent with previous Mcl-1 knockdown data. However, Mcl-1 RNAi did not completely restore PmD to the level of the control IAA 30 hour population (42.5 % versus 51 %), indicating that other factors may play a role. Furthermore, depletion of Mcl-1 further increased the amount of PmD in cells treated with IAA at 30 hours from 51.3 % to 63.8 %. This indicates that Mcl-1 loss during a further prolonged mitosis can further enhance PmD.

6.8 Summary

In this chapter I have generated and characterised a Cyclin B1 R42A AID-auxin cell system that can be used to control mitotic duration and mitotic slippage. Using this system I have concluded through direct analysis of populations undertaking mitotic slippage at different times that increasing mitotic duration increases PmD. Firstly, this supports the notion that an accumulated 'death' signal over time in a prolonged mitotic arrest causes PmD rather an a *de novo* apoptotic signal upon mitotic exit. Using the knowledge that loss of Mcl-1 increases PmD, I hypothesised that the shift in the apoptotic network towards pro-death through the degradation of Mcl-1 over time contributed to the increased PmD. Although loss of Mcl-1 does contribute to PmD, it appears that Mcl-1 degradation is not the only accumulative factor required for PmD and is therefore not necessarily the definitive post-mitotic death timer. However, this may be due to the fact that Mcl-1 protein expression is not fully lost by this time.

7 Chapter 7: Discussion

7.1 Mcl-1 and the response to anti-mitotics

Since the acknowledgement that there is extensive interline and intraline variation in the response to anti-mitotic drugs in cell culture, substantial effort has gone into understanding the underlying factors that drive such intrinsic diversity. As proposed by the competing networks model, these factors contribute to the rates of mitotic slippage and death-in-mitosis (DiM) that accumulate during a prolonged mitotic arrest. Whereas the rate of mitotic slippage is ultimately determined by the factors that influence the rate of Cyclin B1 degradation, the rate of DiM is governed by the balance between the pro-apoptotic pathway and expression of anti-apoptotic players. These two rates combine to determine the sensitivity of cancer cells to anti-mitotic agents. Thus, further understanding the determinants of this interplay may help explain the differential responses seen in cells when treated with anti-mitotics.

Many groups have shown that the two rates are governed by differential post-translational modifications to key players in both networks. For the apoptotic network, these modifications have been described as 'priming' the network to accumulating death signals during a prolonged mitosis (Wang et al., 2014). Most of these studies looking at the rate of DiM have been functional studies using phosopho-mutant forms of the apoptotic proteins. Relevant to this work, both phosphorylation of Bcl-xL and Mcl-1 have been shown to affect the rates of DiM. Phosphorylation of Mcl-1 in mitosis increases death whereas phosphorylation of Bcl-xL suppresses apoptosis (Bah et al., 2014; Harley et al., 2010). Conversely, phosphorylation of pro-apoptotic protein Bid sensitises cells to death (Wang et al., 2014). These post translational modifications appear especially vital when one considers that non-genetic factors are the major cause of heterogeneous responses to anti-mitotics (Gascoigne and Taylor, 2008). In addition to phosphorylation, another main determinate of protein activity is regulation of its turnover. Importantly, Mcl-1 degradation is an observed phenomenon that occurs during a protracted mitosis that results in a shift in the balance between pro-apoptotic and Bcl-2 family anti-apoptotic factors. Proof of this is found by depleting Mcl-1 which results in increased DiM and a decrease

in slippage (Shi et al., 2011; Topham et al., 2015; Tunquist et al., 2010). Further support that Mcl-1 is a plays a critical role in overall survival in response to anti-mitotic drugs was given by Caspase 3/7 reporter dye that confirms acceleration of death following Mcl-1 depletion in various cell lines. By looking at single-cell time-lapse imaging it has been possible to pinpoint the dependency on Mcl-1 for survival at specific stages in the cell cycle. To do this I first created a system using RKO cells expressing a more stable isoform of Cyclin B1 (R42A). This allowed the direct measurement of the rate of DiM to a higher degree of accuracy than previously shown. In Chapter 3, I found that induced loss of Mcl-1 accelerates the rate of DiM when cells were exposed to a high dose of taxol (0.1 μM). This indicated that Mcl-1 degradation could act as a DiM sensitiser. Additionally, time-lapse analysis of DLD-1 cells treated with an Eg5 inhibitor, AZ138, showed that Mcl-1 depletion had little effect on DiM, but increased PmD showing that Mcl-1 is required at both these points in the cell cycle (Figure 7.1).

The loss of Mcl-1 is therefore important in mediating cell death in response to anti-mitotics. The ability of Mcl-1 loss to drive the apoptotic process may therefore depend on the efficiency of Mcl-1 degradation. This idea was proposed in Sakurikar *et al* who showed inefficient degradation of Mcl-1 during slippage-conditions (Sakurikar et al., 2014). Although it appears in this thesis that Mcl-1 is degraded in both death-prone RKO and slippage-prone cell lines, immunoblotting methods do not provide enough resolution for a direct comparison. Another way to test this idea would be the endogenous tagging of Mcl-1 with a fluorescent reporter using knock in-CRISPR methods in different cell lines in order to compare the cell line-specific rates of Mcl-1 degradation. If this is indeed the case then understanding the factors that contribute to the rate of Mcl-1 degradation may have greater importance in understanding cell fate.

7.2 Factors affecting Mcl-1 loss during mitosis.

Several proteins are degraded during a prolonged mitotic arrest. Using the pan proteasome inhibitor MG132, I have shown that the net effect of protein degradation during mitosis is to sensitise cells to apoptosis, with Mcl-1 as a target for proteasome degradation. This doesn't rule out the possibility that degradation of other Mcl-1 regulators are not important (for example, Noxa) (Haschka et al., 2015). However, ultimately I show that the downstream effect of

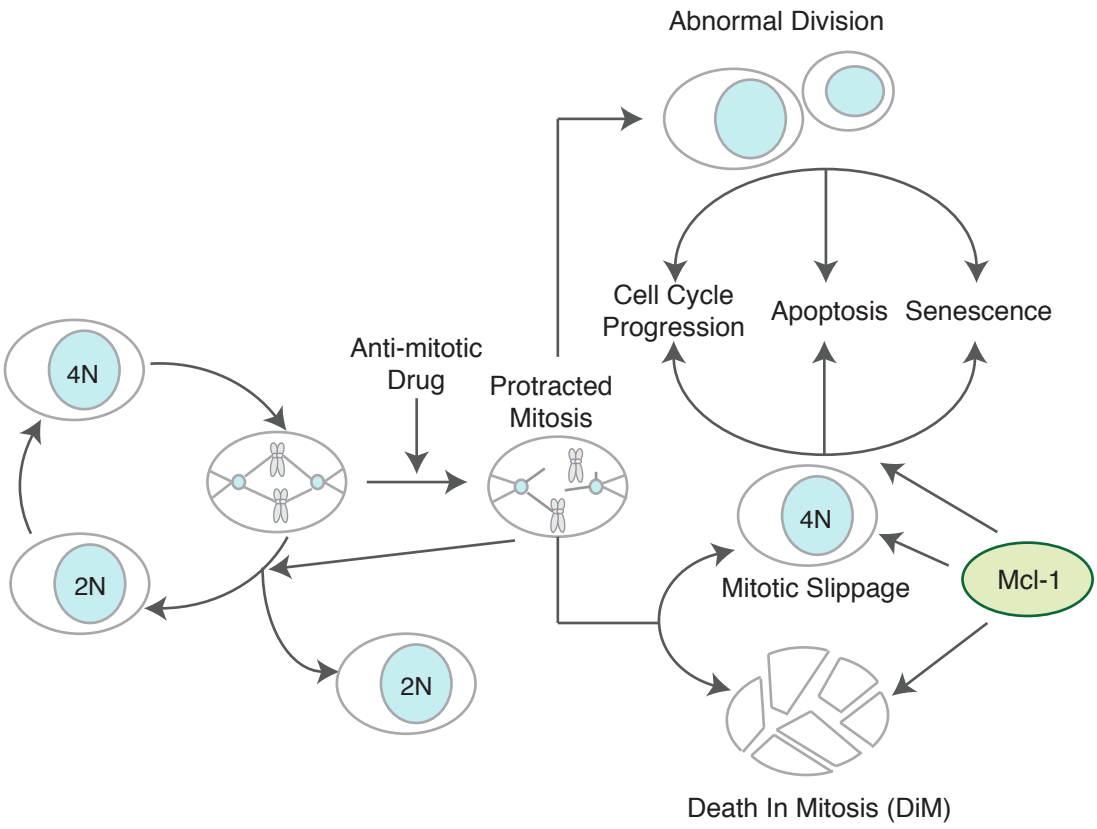

Figure 7.1 Mcl-1 as an important mediator of mitotic fate. This thesis has provided data to show that Mcl-1 loss during mitosis influences the ability of the cell to undertake death in mitosis (DiM) and death in interphase post-slippage (PmD). Mcl-1 can also dictate the rate of slippage. Therefore Mcl-1 can mediate the cell fate response to a protracted mitosis both in mitosis and interphase.

protein degradation on the rate of DiM is through loss of Mcl-1 activity via the proteasome. This further highlights the importance of Mcl-1 as a primary anti-apoptotic factor during a prolonged mitosis.

The ubiquitin-proteasome pathway provides a quick, efficient and targeted way to degrade important proteins (Pines and Lindon, 2005). To understand this process in mitosis I exploited the fact that the time to DiM in the RKO GFP-Cyclin B1 R42A cell line depended in part on the rate of Mcl-1 degradation in order to expose the dependency of different E3 ligase mechanisms on Mcl-1 degradation and therefore DiM. APC/C-Cdc20, SCF-Fbw7 and MULE E3 ligase complexes have all been previously identified in the literature as mechanisms of Mcl-1 degradation in mitosis (Harley et al., 2010; Shi et al., 2011; Wertz et al., 2011). However, a combination of siRNAs and small molecule inhibitors suppressing the activity of all three ligase mechanisms had little effect on Mcl-1 degradation and DiM. One obvious explanation for the inconsistencies between previous research and this data is that degradation of Mcl-1 is not a singular linear mechanism. Whilst a function of each E3 ligase in Mcl-1 degradation is not ruled out, it suggests that any functional role each ligase has can be compensated for by an alternative degradation system. Furthermore, different cell lines may vary in the dependency for different degradation mechanisms as well as contain mutations in the Mcl-1 protein that may affect the ability of Mcl-1 to bind members of each E3 ligase complex. Finally, suppression of gene expression using RNAi may not be penetrant enough to see an effect. One conclusive way to fully inhibit activity is through the creation of a knockout cell line using CRISPR methods. To further address the later point, a more direct approach to delve further into the potential functional role of the APC/C-Cdc20-Mcl-1 interaction was used. By stably expressing Mcl-1 containing mutations in the D-box like motif, I showed that the D-box has no additional effect on the time to DiM. This certainly contradicts the idea proposed in the Harley *et al* paper that showed that the mutating RxxL motif increased Mcl-1 stability that then should have translated into an increase in the time to DiM. This discrepancy could be caused by cell line variation or possible differences in experimental procedures. It is also possible that Mcl-1 binding and polyubiquitination by the APC/C-Cdc20 is not completely dependent on the D-box like motif. Indeed, Mcl-1 contains both an IR tail that may promote binding with tetratricopeptide repeat

(TPR)-containing subunits of the APC/C and a TEK site that was proposed to provide a platform for transfer of the first ubiquitin molecule onto a substrate (Benanti and Toczyski, 2008; Harley et al., 2010; Jin et al., 2008). Either way, this does cast a level of doubt onto the significance of past findings. All together, this pointed towards either a novel degradation mechanism such as sumoylation-mediated proteasome degradation or proteasomal degradation independent of the E1-E2-E3 ubiquitin pathway. Additionally, this may provide evidence that supports the notion of non-targeted proteasome degradation of Mcl-1 (Stewart et al., 2010). One way to test this is to compare the time to DiM following expression of another mutant form of Mcl-1 with all its lysines mutated to expression of Mcl-1 wild type. If there is no difference in the time to DiM following expression of the mutant form then one would add more caution onto the importance of the E3 ligase-mediated mechanism of Mcl-1 degradation and suggest that the dynamic reduction in Mcl-1 protein levels could be a passive process caused by reduction in overall protein synthesis in mitosis (Konrad, 1963).

The levels of Mcl-1 during a mitotic arrest are based on the rate of synthesis as well as the rate of degradation. As transcription and translation is largely suppressed in mitosis, it seemed unlikely that protein synthesis of Mcl-1 in mitosis would have a significant effect. However, using the translational inhibitor cycloheximide, I have now added Mcl-1 to the list of proteins that are synthesised in mitosis including Cdc20 and Cyclin B1. Addition of cycloheximide accelerated DiM in line with the phenotype observed with Mcl-1 RNAi, suggesting that the accelerated DiM is due to accelerated loss in overall Mcl-1 levels. Additionally, the fact that Mcl-1 is synthesised in mitosis may have provided an alternative hypothesis regarding the effect of cycloheximide on mitotic slippage. Treatment of cells with cycloheximide accelerates the rate of mitotic slippage. This is recapitulated in the RKO GFP-Cyclin B1 R42A cells as cycloheximide increases slippage. This is currently attributed to inhibition of *de novo* Cyclin B1 protein synthesis. As I have also shown that Mcl-1 depletion accelerates slippage, I hypothesised whether the cycloheximide slippage phenotype was caused by its effect on Mcl-1 levels. However, Mcl-1 depletion with RNAi did not show a similar effect on mitotic slippage in this context, thus ruling out this possibility (Figure 3.5, 3.7).

7.3 APC/C-Cdc20 and DiM.

The APC/C-Cdc20 complex is best known for mediating Cyclin B1 degradation, making it a major factor in mitotic progression. However, it is now known that the repertoire of binding-partners and catalytic substrates not only expands to other mitotic mediators but also to members of the apoptotic network. Specifically, Cdc20 is associated to both pro-apoptotic protein Bim and Mcl-1, suggesting that the APC/C-Cdc20 has some function in regulating apoptosis. As these two proteins are clearly antagonistic to one another, it was unclear what net effect the APC/C-Cdc20 has on DiM. APC/C-Cdc20 activity has been linked to apoptosis as increased DiM is observed in Cdc20-depleted cells treated with anti-mitotics (Huang et al., 2009; Sakurikar et al., 2012). However, whether the increased DiM is caused by accelerated DiM signalling or merely just a block on mitotic slippage was unknown.

I used RKO cells expressing Cyclin B1 R42A as a way to enable the analysis of the role of APC/C-Cdc20 in DiM through the use of small molecule inhibitors proTAME and Apcin and Cdc20 RNAi. I showed that the proTAME/Apcin combination efficiently inhibited normal mitotic exit, which is in line with suppression of APC/C-Cdc20 mediated degradation of Cyclin B1. However, co-treatment had no effect on the time to DiM, indicating that the net effect of APC-Cdc20-mediated degradation of protein members of the apoptotic network is insignificant. This could be explained by the antagonistic effect the APC/C-Cdc20 has on Mcl-1 and Bim, but no changes to the rate of Mcl-1 degradation were observed.

One caveat to these experiments is that despite identification of an association between APC/C-Cdc20 and apoptotic member proteins, protein degradation by the APC/C may not be entirely dependent on the interaction between Cdc20 and proteins containing the D-box motif. An example of this is Nek2a whose degradation is unaffected upon loss of Cdc20 by RNAi (Boekhout and Wolthuis, 2015). In which case, the use of Cdc20 RNAi and the small molecule inhibitors that suppress Cdc20 binding and/or D-box-containing proteins to the complex may be ineffective in inhibiting binding and catalysis of apoptotic proteins. However, this is unlikely to be the case for Bim that specifically interacts with the WD40 repeat motif of Cdc20(Wan et al., 2014). Inhibiting other potential binding sites of the APC/C complex through either the

development of novel APC/C inhibitors or knockdown of various APC/C subunits such as Apc3 that can bind substrates containing a C-terminal MR or IR motif tails (present on Mcl-1) independently of Cdc20 binding (Hayes et al., 2006; Kraft et al., 2005), may uncover the dependency on other sites for binding of APC/C substrates.

7.4 Mcl-1 and network 'cross-talk'.

When the competing networks model was first formulated in 2008 (in the Taylor lab), it proposed that the DiM and mitotic slippage networks were independent (Gascoigne and Taylor, 2008). Further to this, another group measured the time to slippage and DiM separately by using a pan-caspase inhibitor or Cdc20 RNAi respectively and used simulated predictive modeling to support the notion of independent networks (Huang et al., 2010). Additionally, this model was further supported by the recent discovery that transcription factor Myc was a major determinant of mitotic cell fate (Topham et al., 2015). Expression of Myc drives DiM in response to anti-mitotic drugs through the up-regulation of several pro-apoptotic BH3-only proteins (Bim, Bid and Noxa) and down-regulation of the anti-apoptotic protein Bcl-xL. Whilst loss of Myc increases mitotic slippage through a delay in DiM, slippage rates are unaffected, thus showing that a major shift in the expression of many apoptotic proteins has no obvious effect on the rate of mitotic slippage.

However as mentioned in the introduction, members of the slippage network can interact with various proteins within the apoptotic network. For example, the Cyclin B1/Cdk1 complex has been shown to phosphorylate Caspase 9, Bcl-xL and Mcl-1 (Allan and Clarke, 2007; Chu et al., 2012; Harley et al., 2010; Terrano et al., 2010). From this one may predict that the gradual loss of Cyclin B1 by APC/C-Cdc20-mediated targeted degradation would also dynamically change the Cdk1-dependent phosphorylation status of the above apoptotic factors, thus affecting the rate of DiM. However, upon mitotic exit, Cyclin B1/Cdk1 kinase activity is counteracted by feed-forward activation of phosphatases driven by loss of inhibitory Cyclin B1/Cdk-1 phosphorylations and therefore it is unlikely that loss of Cyclin B1/Cdk-1 activity is gradual despite the continual loss of Cyclin B1 and is thereby unlikely to have an effect on the apoptotic network (Grallert et al, 2015; Medema and Lindqvist, 2011; Dohadwala et al, 1994). In addition to Cyclin B1, the

APC/C-Cdc20 complex targets Bim for degradation in mitosis (Wan et al., 2014). This may suggest that the rate of APC/C-Cdc20 activity is able to mediate the rates of both mitotic slippage and DiM. Put together, the molecular associations previously identified highlights the possibility of cross-talk between the networks. Recently this notion was supported with functional data by Diaz-Martinez *et al* who showed that suppression of the MCC disassembly factor $p31^{comet}$ accelerated the rate of DiM in comparison to Cdc20 RNAi, thereby showing that a factor that can influence Cyclin B1 degradation by regulation of the MCC-APC/C interaction can also influence slippage. Equally, they observed that co-depletion of Bak and Bax delayed mitotic slippage showing in converse that the levels of apoptotic factors can influence the rate of mitotic slippage (Díaz-Martínez et al., 2014). If indeed there is network cross-talk, then interpretation of functional data regarding the effect of members of either network becomes complicated as manipulating one network may impact on the rate of the other. Despite this, there have been occasions when results have been misinterpreted as network cross-talk. For example, it has been suggested that the SAC activates apoptosis as checkpoint override resulted in decreased death. However, this is explained simply by checkpoint override driving a cell out of mitosis, thereby reducing DiM. Therefore, one must be cautious when concluding a result as network cross-talk unless all simplified explanations have been exhausted.

For this thesis, I optimised the cell conditions such that each network could be analysed separately: RKO GFP-Cyclin B1 R42A cells treated with taxol to study DiM and DLD-1 cells treated with AZ138 to study mitotic slippage. Additionally, cell fate profiles generated from the time-lapse microscopy have allowed the effect of both networks to be observed when required. Using these model systems, I demonstrated that Mcl-1 protein levels can influence the rates of both DiM and slippage. Furthermore, I have shown that mutating the D-box-like motif inhibits the ability of Mcl-1 to delay slippage. Based on prior research identifying an interaction between Mcl-1 and Cdc20, the data supports a notion that Mcl-1 delays slippage through substrate competition with Cyclin B1 for the APC/C-Cdc20. This at first glance not only supports the notion of network cross-talk but also suggests that Mcl-1 is a central protein in this cross-talk. However, in the RKO GFP-Cyclin B1 R42A cells, inhibition of APC/C-Cdc20 has no effect on Mcl-1 degradation or DiM, suggesting that the supposed APC/C-Cdc20-Mcl-1 interaction is

unidirectional. It is possible that the ability of Mcl-1 to bind the APC/C may differ between cell lines, a notion supported by the fact that loss of Mcl-1 did not have a significant effect in RKO cells over-expressing Bcl-xL (Figure 5.6). To test this idea, the Mcl-1-Cdc20 interaction identified using immunoprecipitation would be required to be replicated in other cell lines. Despite this, the ability of Mcl-1 to influence slippage may be an epiphenomenon that arises during a prolonged mitotic arrest due to the presence of an RxxL motif that serves as a weak D-box allowing it to engage APC/C-Cdc20 in a non-regulated manner. The idea that Mcl-1 passively influences the rate of Cyclin B1 degradation by APC/C-Cdc20 is further supported by the fact that Mcl-1 depletion has no obvious effect on normal mitotic timing.

This idea can help explain other recent observations in the literature that describes 'cross-talk' between the two networks. Firstly, the observation that loss of $p31^{comet}$ accelerates DiM (Diaz-Martinez et al 2014). As $p31^{comet}$ is a disassembly factor for the MCC and therefore acts as a SAC silencer, one could propose that $p31^{comet}$ causes super-stabilisation of the MCC onto APC/C-Cdc20, thus inhibiting the ability of Cyclin B1 to engage with the APC/C, causing an acceleration in Mcl-1 degradation and DiM. However, this idea is contradicted by the data presented in Chapter 4 that argues against any physiological importance for APC/C-Cdc20 mediated degradation of Mcl-1, potentially due to novel degradation mechanisms. However, the cell line used in the previous study, U2OS cells, may be more dependent on the APC/C-Cdc20 complex for Mcl-1 degradation. Importantly, the Mcl-1 mCherry fragment experiment did show that the RxxL motif had a role to play in the time to DiM when overexpressed, so the role of APC/C-Cdc20 has not been ruled out entirely. Secondly, I have shown that loss of Mcl-1 rescues the delay in slippage caused by co-depletion of Bak and Bax. Loss of Bak and Bax alleviates Mcl-1 binding, creating a greater pool of Mcl-1 able to engage with other binding partners such as the APC/C-Cdc20 complex, thereby causing a delay in Cyclin B1 degradation and mitotic slippage. All together this argues against the proposal of direct cross-talk signalling between the two networks, but rather that passive network interference is occurring. The presence of network interference also highlights the need to create assays that isolate either network when studying the molecular components within each network.

7.5 Mcl-1 and the post-mitotic response

Mitotic slippage leads to the formation of cells with abnormal tetraploid genomes that tend to be eliminated by cell cycle arrest and death. However, how the apoptotic network responds to mitotic slippage is largely unexplored. First, using the Cyclin B1 R42A auxin-AID system, I showed directly that prolonging a mitotic arrest leads to increased cell death post-slippage. This suggests that dynamic changes in a mitotic arrest can sensitise cells to death (Figure 7.2). This could be through either modifications to the apoptotic network, thus softening the response to apoptotic stimuli or an accumulation of stress signaling such as DNA damage (Orth et al, 2012). As Mcl-1 levels drop during mitosis, it is conceivable that the network becomes more sensitised to apoptotic stimuli over time, such that in the presence of any apoptotic stimuli, whether in mitosis or the subsequent interphase, the network is more responsive to apoptosis under situations when Mcl-1 protection was required for survival. It is equally conceivable that the level of damage and apoptotic stimuli accumulates over time that drives apoptosis in a mitotic-duration dependent manner. Although these both reflect on the correlation between mitotic duration and apoptosis in Chapter 6, it is important to remember that interphase mitochondria are not as well 'primed' for apoptosis as mitotic mitochondria and so the death threshold may raise as cells exit mitosis (Rieder and Maiato 2004). This could mean that the damage accumulated during mitosis drives a large death signal post-mitosis. This seems plausible as DNA damage signaling through p53 is only active in interphase (Minn et al, 1996). However, loss of Mcl-1 during mitosis may cause mitochondria to be more responsive to apoptosis in the subsequent interphase. Both of these explanations may contribute to the mitotic duration-induced PmD. Whilst this does argue for the accumulative model, it does not rule out that a *de novo* cell death signal upon mitotic exit, such as the formation of micronuclei, contributes to the post-mitotic response (Crasta et al., 2012; Zhang et al., 2015; Zhu et al., 2014).

As I showed that Mcl-1 could be degraded in a slippage-prone cell line and that Mcl-1 depletion resulted in increased PmD, I tested the possibility that the increased PmD observed when further prolonging a mitotic arrest was caused by Mcl-1 loss over time in a mitotic arrest. However Mcl-1 loss did not fully mirror the level of PmD caused by forcing cells to remain in

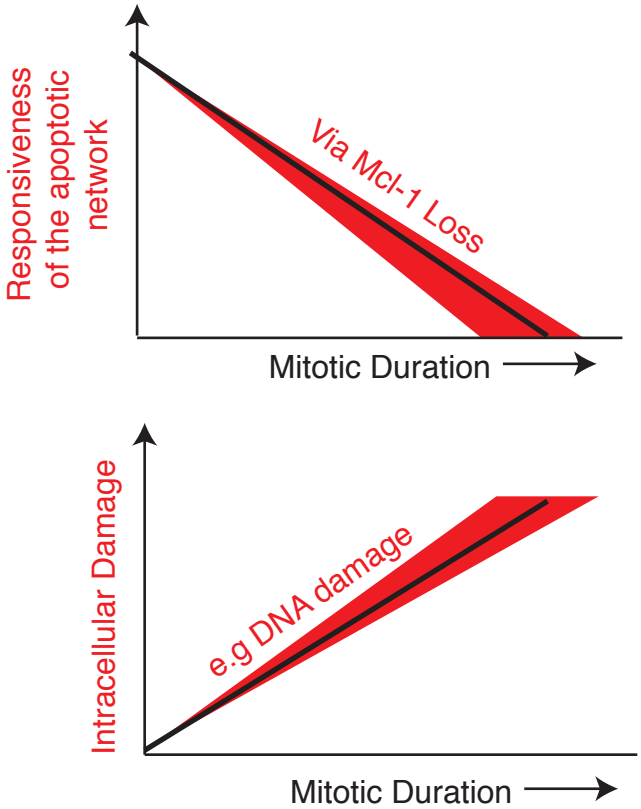

Figure 7.2 Factors contributing to the mitotic duration-induced post-mitotic death. Over the course of a mitotic arrest, dynamic Mcl-1 loss may make the apoptotic network more responsive to apoptotic stimuli such that the longer a cell remains in mitosis, the more responsive the network may be to apoptotic stimuli in the subsequent interphase. Equally, over a protacted mitosis intracellular damage may accumulate such as DNA damage that can be only responded to in the subsequent interphase. The longer the mitotic arrest, the greater the level of damage that the cell has to respond to in the subsequent interphase.

mitosis for longer. This shows that although loss of Mcl-1 can sensitise cells to PmD, potentially through accumulation of DNA damage (Colin et al., 2015), Mcl-1 degradation may not be solely responsible for the accumulative death signal in mitosis. Other accumulative signals are likely to come in the form of stress stimuli such as oxidative/proteosomic stress. These stresses then signal to the apoptotic machinery that shift the balance towards death over time which impacts in the subsequent interphase.

7.6 Mcl-1 as a therapeutic target.

I showed that Mcl-1 is an important determinate in the sensitivity between cell lines to induced apoptosis in mitosis. In addition I found that Mcl-1 post-translational degradation can lead to accelerated DiM and PmD. This increased sensitivity to mitotic inhibitors when combined with depleted Mcl-1 reaffirms the possibility of combinatorial therapies. Mcl-1 depletion decreases the threshold at which apoptosis is triggered however this appears most apparent in the cell lines that are dependent on Mcl-1, partly due to elevated protein expression. Consequently this would require pre-screening of patients to identify those that would have the most therapeutic benefit with the proposed combination such as cancers with increased Mcl-1 levels. Although Mcl-1 dependency may only account for a fraction of the patients receiving anti-mitotic drugs the benefits could still be substantial. This dependency may come from increased expression of the gene or from cell lines that are less efficient at degrading Mcl-1 during mitosis. Indeed, mutations in Fbw7 have been shown to affect the efficiency of Mcl-1 degradation, resulting in increased sensitivity to anti-mitotics (Wertz et al., 2011). Thus suggesting that E3 ligase mutations may also be used to stratify patients into those that are more resistant to anti-mitotic agents due to inefficient Mcl-1 degradation. However, the data presented in this thesis suggest that E3 ligase dependency, specifically of those already identified, is not universal. Moreover, stratified patients receiving combination with anti-mitotics may show improved overall drug tolerance by decreasing the drug dose burden that causes severe side effects, such as peripheral neuropathy and liver damage.

To this end, much work has gone into developing small molecule inhibitors specifically targeting Mcl-1 (Belmar and Fesik, 2015). The rational of using Mcl-1 specific inhibitors versus

other pan BH3 inhibitors such as obatoclax is that pre-screening for high Mcl-1 dependency in the tumour may lead to preferential targeting and therefore decreased off target effects. Recently a small molecule inhibitor (A-1210477) has been tested *in vitro* that disrupts the Mcl-Bim interaction (Leverson et al., 2015). Inhibition of Mcl-1 with A-1210477 induces apoptosis in cell lines specifically dependent on Mcl-1. Furthermore, in combination with Navitoclax (Bcl-2/Bcl-xL inhibitor), A-1210477 causes synergistic cell death (Leverson et al., 2015). As Navitoclax is able to synergize with anti-mitotics in cell lines more dependent on Bcl-2/Bcl-xL, this lends further support that Mcl-1 small molecule inhibitors should also synergise with anti-mitotic drugs in cell lines dependent on Mcl-1 (Shi et al., 2011).

Dependency on Mcl-1 was observed in many cancers containing a genetic amplification of the genomic region of Mcl-1 (Beroukhim et al., 2010). Dependency on Mcl-1 will also depend on (1) the levels and activity of other Bcl-2 pro-survival factors and (2) the levels and activity of the pro-death factors including the BH3-only proteins as well as Bak and Bax. Indeed many of these factors change during mitosis either by degradation (Bim and Noxa) or phosphorylation (Bid, Bcl-xL) (Haschka et al., 2015; Poruchynsky et al., 1998; Wan et al., 2014; Wang et al., 2014). The first of these points was partially addressed by comparing the levels of Mcl-1 and Bcl-xL in two slippage-prone cell lines and four death-prone cell lines. In both the slippage-prone cell lines, the relative level of Bcl-xL protein appeared greater than the amount of Mcl-1 protein, whereas the death-prone cell lines appeared to have a relatively equal amount of both proteins or a greater amount of Mcl-1. The high Bcl-xL/Mcl-1 ratio may explain why slippage-prone cell lines are able to cope with the loss of Mcl-1 in mitosis as Bcl-xL compensates for the reduction in pro-survival activity. In support of this, depletion of Bcl-xL significantly sensitised slippage-prone cell lines DLD-1 and HCT-116 to anti-mitotics as opposed to depletion of Mcl-1. This result has also been seen in a separate study looking at the slippage-prone breast cancer cell line MDA-MB-231 (Bah et al., 2014). However, this is not the case with the Mcl-1 high DiM prone cell lines where Bcl-xL depletion only has a significant effect on one cell line, suggesting that Bcl-xL cannot effectively compensate for the loss of Mcl-1 in DiM-prone cell lines. This is similar to the situation found in a drug screen that discovered that low Bcl-xL expression compared to Mcl-1 resulted in increased sensitivity to repressing Mcl-1 function (Wei et al., 2012). This balance of Bcl-2 family proteins as

shown here in relation to the relative levels of Mcl-1 and Bcl-xL that may serve as predictors of cell response to anti-mitotic agents (Figure 7.3). This model is as yet incomplete as the apoptotic balance also depends on the levels and activity of the pro-death factors, including the BH3-only proteins as well as Bak/Bax, many of which have been shown to change during mitosis. In addition, other anti-apoptotic proteins could provide redundancy in place of Bcl-xL. Although there appears to be no obvious role of Bcl-2 or Bcl-w in regulating DiM in response to anti-mitotics, it does not mean that another member of the Bcl-2 family, namely A1, is involved in the response (Li et al., 2005; Shi et al., 2011). This situation is likely to be far less simple in tumours as the activity of apoptotic factors within cells can be regulated by extracellular signals that derive from the stroma and other neighbouring cells. For example, Mcl-1 can be regulated by JNK, Gsk-1 and Erk-1, either functionally or in the ability to engage with the degradation machinery, which themselves are often regulated by extracellular signaling pathways (Ding et al., 2008; Domina et al., 2004; Inoshita et al., 2002; Kobayashi et al., 2007; Kodama et al., 2009; Maurer et al., 2006; Morel et al., 2009). However, these pathways may also be manipulated to sensitise cells to anti-mitotics through the influence on members of the apoptotic network. For instance, inhibition of MEK to cells treated with anti-mitotic vincristine accelerates Mcl-1 loss in mitosis as well as sensitising the cells to DiM although whether this is causative remains unclear (Kawabata et al., 2012). Although this may prove effective, the apoptotic network contains a large level of redundancy and it is the fine-tuning of the apoptotic balance that ultimately decides the net output of the system. The responsiveness of the system to apoptosis using the various BH3 peptides and measuring MOMP as utilized by the BH3-prolifing, is currently being used to predict sensitivity to chemotherapy, optimal drug dosage and treatment identification from patient samples grown in culture (Monetro et al 2015).

Genetic amplification of many members of the Bcl-2 family has been widely observed in the development of many cancers (Beroukhim et al., 2010). To appreciate how variations in their ratios impact on DiM it would be essential to analyse specific Bcl-2 amplified cell lines. Indeed, genetic amplifications of Bcl-2 family members may be one of the true determinants of patient outcome in response to anti-mitotics, as well as providing an explanation for the heterogeneous

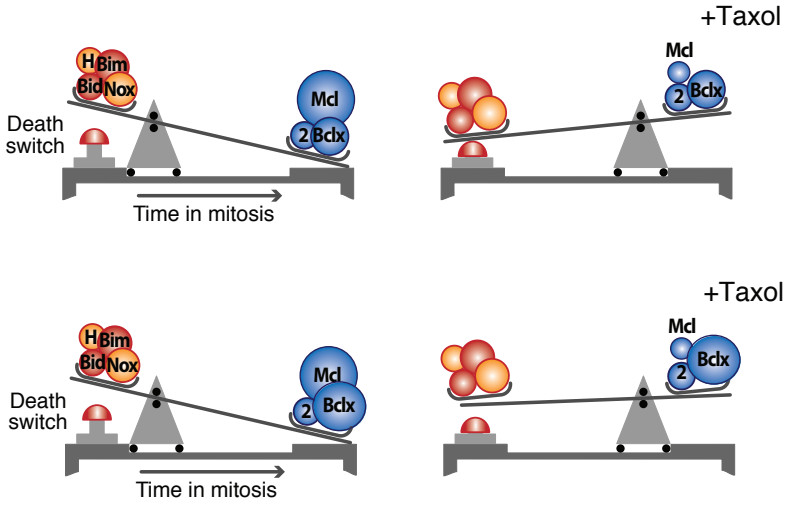

Figure 7.3 The Mcl-1/Bcl-xL balance. The irreversible switch to death is dictated by the balance of pro- and anti-apoptotic factors. During a prolonged mitotic arrest, Mcl-1 is degraded, forcing the balance towards cell death. However, if the levels of other Bcl-2 family proteins are high they are able to compensate for the loss of Mcl-1 and block death in mitosis. Adapted from Topham et al 2015.

responses observed between cell lines in culture. Consequently, prescreening for the levels of Mcl-1 and Bcl-xL may indicate whether the cancer will react in a DiM-prone or slippage-prone manner due to its dependency for Mcl-1 which gets lost during a prolonged mitosis. Secondly this suggests that these predictions may form a rational basis for trialing combination therapies of anti-mitotic drugs with the relevant Bcl-xL/Mcl-1 inhibitor for a more efficacious result. This may indeed also result in lower concentrations of both drugs, thus reducing drug side-effects.

7.7 Concluding remarks

This thesis has first served to highlight the importance of Mcl-1 degradation in providing sensitivity to anti-mitotic drugs in both mitosis and interphase, as well as showing that cell lines have different dependency on Mcl-1 and Bcl-xL for survival. A more in-depth analysis on the correlation between the levels of the Bcl-2 family protein members and the response to anti-mitotic drugs in cell culture and patient samples will be required. This thesis also casts doubt over the simplicity/targeted nature of the mechanisms of Mcl-1 degradation previously proposed and suggests that more analysis in different cell lines is required in order to dissect the importance of each degradation mechanism. Finally, although an interaction between the APC/C cofactor Cdc20 complex and Mcl-1 has been previously identified, this thesis shows that the significance of this is likely to be minimal and only through an indirect effect on mitotic slippage (network interference).

8 References

Acquaviva, C., Herzog, F., Kraft, C., and Pines, J. (2004). The anaphase promoting complex/cyclosome is recruited to centromeres by the spindle assembly checkpoint. Nat. Cell Biol. *6*, 892–898.

Adams, J.M., and Cory, S. (2007). The Bcl-2 apoptotic switch in cancer development and therapy. Oncogene *26*, 1324–1337.

Agostinis, P., Derua, R., Sarno, S., Goris, J., and Merlevede, W. (1992). Specificity of the polycation-stimulated (type-2A) and ATP,Mg-dependent (type-1) protein phosphatases toward substrates phosphorylated by P34cdc2 kinase. Eur. J. Biochem. *205*, 241–248.

Akgul, C., Moulding, D.A., White, M.R., and Edwards, S.W. (2000). In vivo localisation and stability of human Mcl-1 using green fluorescent protein (GFP) fusion proteins. FEBS Lett. *478*, 72–76.

Allan, L.A., and Clarke, P.R. (2007). Phosphorylation of Caspase-9 by CDK1/Cyclin B1 Protects Mitotic Cells against Apoptosis. Mol. Cell *26*, 301–310.

Alushin, G.M., Lander, G.C., Kellogg, E.H., Zhang, R., Baker, D., and Nogales, E. (2014). High-Resolution Microtubule Structures Reveal the Structural Transitions in ab -Tubulin upon GTP Hydrolysis. Cell *157*, 1117–1129.

Álvarez-Fernández, M., Sánchez-Martínez, R., Sanz-Castillo, B., Gan, P.P., Sanz-Flores, M., Trakala, M., Ruiz-Torres, M., Lorca, T., Castro, A., and Malumbres, M. (2013). Greatwall is essential to prevent mitotic collapse after nuclear envelope breakdown in mammals. Proc. Natl. Acad. Sci. U. S. A. *110*, 17374–17379.

Andersen, J.L., Johnson, C.E., Freel, C.D., Parrish, A.B., Day, J.L., Buchakjian, M.R., Nutt, L.K., Thompson, J.W., Moseley, M.A., and Kornbluth, S. (2009). Restraint of apoptosis during mitosis through interdomain phosphorylation of caspase-2. EMBO J. *28*, 3216–3227.

Andreassen, P.R., Martineau, S.N., and Margolis, R.L. (1996). Chemical induction of mitotic checkpoint override in mammalian cells results in aneuploidy following a transient tetraploid state. Mutat. Res. *372*, 181–194.

Andreassen, P.R., Lohez, O.D., Lacroix, B., and Margolis, R.L. (2001a). Tetraploid State Induces p53-dependent Arrest of Nontransformed Mammalian Cells in G1. Mol Biol Cell *12*, 1315–1328.

Andreassen, P.R., Lacroix, B., Lohez, O.D., and Margolis, R.L. (2001b). Neither p21 WAF1 Nor 14-3-3 Prevents G 2 Progression to Mitotic Catastrophe in Human Colon Carcinoma Cells after DNA Damage , But p21 WAF1 Induces Stable G 1 Arrest in Resulting Tetraploid Cells 1. Cell Cycle *116*, 7660–7668.

Antonarakis, S.E., Lyle, R., Dermitzakis, E.T., Reymond, A., and Deutsch, S. (2004). Chromosome 21 and down syndrome: from genomics to pathophysiology. Nat. Rev. Genet. *5*, 725–738.

De Antoni, A., Pearson, C., Cimini, D., Canman, J., Sala, V., Nezi, L., Mapelli, M., Sironi, L., Faretta, M., Salmon, E., et al. (2005). The Mad1/Mad2 Complex as a template for Mad2 activation in the Spindle Assembly Checkpoint. Curr. Biol. *15*, 214–225.

Bah, N., Maillet, L., Ryan, J., Dubreil, S., Gautier, F., Letai, A., Juin, P., and Barillé-Nion, S. (2014). Bcl-xL controls a switch between cell death modes during mitotic arrest. Cell Death Dis. *5*, e1291.

Barford, D. (2015). Understanding the structural basis for controlling chromosome division. Philos. Trans. R. Soc. A *373*.

Belmar, J., and Fesik, S.W. (2015). Small molecule Mcl-1 inhibitors for the treatment of cancer. Pharmacol. Ther. *145*, 76–84.

Benanti, J., and Toczyski, D. (2008). Cdc20, an activator at last. Mol. Cell *32*, 460–461.

Beroukhim, R., Mermel, C.H., Porter, D., Wei, G., Raychaudhuri, S., Donovan, J., Barretina, J., Boehm, J.S., Dobson, J., Urashima, M., et al. (2010). The landscape of somatic copy-number alteration across human cancers. Nature *463*, 899–905.

Bieging, K.T., Mello, S.S., and Attardi, L.D. (2014). Unravelling mechanisms of p53-mediated tumour suppression. Nat. Rev. Cancer *14*, 359–370.

Blangy, A., Lane, H. a, D'Hérin, P., Harper, M., Kress, M., and Nigg, E. a (1995). Phosphorylation by p34cdc2 regulates spindle association of human Eg5, a kinesin-related motor essential for bipolar spindle formation in vivo. Cell *83*, 1159–1169.

Boekhout, M., and Wolthuis, R. (2015). Nek2A destruction marks APC/C activation at the prophase-to-prometaphase transition by spindle-checkpoint-restricted Cdc20. J. Cell Sci. *128*, 1639–1653.

Borel, F., Lohez, O.D., Lacroix, F.B., and Margolis, R.L. (2002). Multiple centrosomes arise from tetraploidy checkpoint failure and mitotic centrosome clusters in p53 and RB pocket protein-compromised cells. Proc. Natl. Acad. Sci. U. S. A. *99*, 9819–9824.

Bouillet, P., Metcalf, D., Huang, D.C., Tarlinton, D.M., Kay, T.W., Köntgen, F., Adams, J.M., and Strasser, A. (1999). Proapoptotic Bcl-2 relative Bim required for certain apoptotic responses, leukocyte homeostasis, and to preclude autoimmunity. Science (80-.). *286*, 1735–1738.

Brandeis, M., Rosewell, I., Carrington, M., Crompton, T., Jacobs, M. a, Kirk, J., Gannon, J., and Hunt, T. (1998). Cyclin B2-null mice develop normally and are fertile whereas cyclin B1-null mice die in utero. Proc. Natl. Acad. Sci. U. S. A. *95*, 4344–4349.

Breitenbuecher, F., Markova, B., Kasper, S., Carius, B., Stauder, T., Frank, D., Masson, K., Rönnstrand, L., Huber, C., Kindler, T., et al. (2009). A novel molecular mechanism of primary resistance to FLT3-kinase inhibitors in AML. Blood *113*, 4063–4073.

Brito, D.A., and Rieder, C.L. (2006). Mitotic checkpoint slippage in humans occurs via cyclin B destruction in the presence of an active checkpoint. Curr. Biol. *16*, 1194–1200.

Burger, A.M., and Seth, A.K. (2004). The ubiquitin-mediated protein degradation pathway in cancer: Therapeutic implications. Eur. J. Cancer *40*, 2217–2229.

Burgess, A., Vigneron, S., Brioudes, E., Labbé, J.-C., Lorca, T., and Castro, A. (2010). Loss of human Greatwall results in G2 arrest and multiple mitotic defects due to deregulation of the cyclin B-Cdc2/PP2A balance. Proc. Natl. Acad. Sci. U. S. A. *107*, 12564–12569.

Burrell, R., McGranahan, N., Bartek, J., and Swanton, C. (2013). The causes and consequences of genetic heterogeneity in cancer evolution. Nature *501*, 338–345.

Cancer Research UK No Title.

Castilho, P., Williams, B., Mochida, S., Zhao, Y., and Goldberg, M. (2010). The M Phase kinase Greatwall (Gwl) promotes inactivation of PP2A/B55(delta), a phosphatase directed against CDK phosphosites. Mol. Biol. Cell *21*, 4042–4056.

Certo, M., Del Gaizo Morre, V., Nishino, M., Wei, G.,Korsmeyer, S., Armstrong, S.A., and Letai, A. (2006) Mitochondria primed by death signals determine cellular addiction to antiapoptotic BCL2 family members. Cancer Cell *9* 351-365.

Cesare, A., Hayashi, M., Crabbe, L., and Karlseder, J. (2013). The Telomere deprotection response is functionally distinct from the Genomic DNA damage response. Mol. Cell *51*, 141–155.

Chang, J.C., Wooten, E.C., Tsimelzon, A., Hilsenbeck, S.G., Gutierrez, M.C., Elledge, R., Mohsin, S., Osborne, C.K., Chamness, G.C., Allred, D.C., et al. (2003). Mechanisms of disease gene expression profiling for the prediction of therapeutic response to docetaxel in patients with breast cancer. Lancet *362*, 362–369.

Chang, L., Zhang, Z., Yang, J., McLaughlin, S.H., and Barford, D. (2014). Molecular architecture and mechanism of the anaphase-promoting complex. Nature *17*, 13–17.

Chao, W.C.H., Kulkarni, K., Zhang, Z., Kong, E.H., and Barford, D. (2012). Structure of the mitotic checkpoint complex. Nature *484*, 208–213.

Chehab, N.H., Malikzay, A., Stavridi, E.S., and Halazonetis, T.D. (1999). Phosphorylation of Ser-20 mediates stabilization of human p53 in response to DNA damage. Proc. Natl. Acad. Sci. U. S. A. *96*, 13777–13782.

Chem, J.B., Motoyama, N., Wang, F., Roth, K.A., Sawa, H., Nakayama, K., Nakayama, K., Negishi, I., Senju, S., Zhang, Q., et al. (1995). Massive Cell Death of Immature Hematopoietic Cells and Neurons in Bcl-x-Deficient Mice. Science (80-.). *267*, 1506–1510.

Chen, L., Willis, S.N., Wei, A., Smith, B.J., Fletcher, J.I., Hinds, M.G., Colman, P.M., Day, C.L., Adams, J.M., and Huang, D.C.S. (2005). Differential targeting of prosurvival Bcl-2 proteins by their BH3-only ligands allows complementary apoptotic function. Mol. Cell *17*, 393–403.

Chipuk, J.E., Moldoveanu, T., Llambi, F., Parsons, M.J., and Green, D.R. (2010). The BCL-2 Family Reunion. Mol. Cell *37*, 299–310.

Chu, R., Terrano, D.T., and Chambers, T.C. (2012). Cdk1/cyclin B plays a key role in mitotic arrest-induced apoptosis by phosphorylation of Mcl-1, promoting its degradation and freeing Bak from sequestration. Biochem. Pharmacol. *83*, 199–206.

Clijsters, L., van Zon, W., Riet, B. Ter, Voets, E., Boekhout, M., Ogink, J., Rumpf-Kienzl, C., and Wolthuis, R.M.F. (2014). Inefficient degradation of cyclin B1 re-activates the spindle checkpoint right after sister chromatid disjunction. Cell Cycle *13*, 2370–2378.

Clute, P., and Pines (1999). Temporal and spatial control of cyclin B1 destruction in metaphase. Nat. Cell Biol. *1*, 82–87.

Colin, D.J., Hain, K.O., Allan, L.A., Clarke, P.R., and Clarke, P.R. (2015). Cellular responses to a prolonged delay in mitosis are determined by a DNA damage response controlled by Bcl-2 family proteins. Open Biol. *5*, 140156.

Collin, P., Nashchekina, O., Walker, R., and Pines, J (2013) The spindle assembly checkpoint works like a rheostat rather than a toggle switch. Nat Cell Biol *15* 1378-1385.

Crasta, K., Huang, P., Morgan, G., Winey, M., and Surana, U. (2006). Cdk1 regulates centrosome separation by restraining proteolysis of microtubule-associated proteins. EMBO J. *25*, 2551–2563.

Crasta, K., Ganem, N.J., Dagher, R., Lantermann, A.B., Ivanova, E. V., Pan, Y., Nezi, L., Protopopov, A., Chowdhury, D., and Pellman, D. (2012). DNA breaks and chromosome pulverization from errors in mitosis. Nature *482*, 53–58.

Cross, R.A., and McAinsh, A. (2014). Prime movers: the mechanochemistry of mitotic kinesins. Nat. Rev. Mol. Cell Biol. *15*, 257–271.

Cross, S.M., Sanchez, C.A., Morgan, C.A., Schimke, M.K., Ramel, S., Idzerda, R.L., Raskind, W.H., and Reid, B.J. (1995). A p53-dependent mouse spindle checkpoint. Science (80-.). *267*, 1353–1356.

Cuconati, A., Mukherjee, C., Perez, D., and White, E. (2003). DNA damage response and MCL-1 destruction initiate apoptosis in adenovirus-infected cells. Genes Dev. *17*, 2922–2932.

Daum, J.R., Potapova, T.A., Sivakumar, S., Daniel, J.J., Flynn, J.N., Rankin, S., and Gorbsky, G.J. (2011). Cohesion fatigue induces chromatid separation in cells delayed at metaphase. Curr. Biol. *21*, 1018–1024.

Day, C.L., Chen, L., Richardson, S.J., Harrison, P.J., Huang, D.C.S., and Hinds, M.G. (2005). Solution structure of prosurvival Mcl-1 and characterization of its binding by proapoptotic BH3-only ligands. J. Biol. Chem. *280*, 4738–4744.

Day, C.L., Smits, C., Fan, F.C., Lee, E.F., Fairlie, W.D., and Hinds, M.G. (2008). Structure of the BH3 Domains from the p53-Inducible BH3-Only Proteins Noxa and Puma in Complex with Mcl-1. J. Mol. Biol. *380*, 958–971.

Deng, J., Carlson, N., Takeyama, K., Dal Cin, P., Shipp, M., and Letai, A. (2007) BH3 profiling identifies three distinct classes of apoptotic blocks to predict response to ABT-737 and conventional chemotherapeutic agents. Cancer Cell. *12* 171-185.

Deng, X., Gao, F., Flagg, T., and May, W.S. (2004). Mono- and multisite phosphorylation enhances Bcl2's antiapoptotic function and inhibition of cell cycle entry functions. Proc. Natl. Acad. Sci. U. S. A. *101*, 153–158.

Desai, A., and Mitchison, T.J. (1997). Microtubule polymerization dynamics. Annu. Rev. Cell Dev. Biol. *13*, 83–117.

Dessev, G., Iovcheva-Dessev, C., Bischoff, J.R., Beach, D., and Goldman, R. (1991). A complex containing p34cdc2 and cyclin B phosphorylates the nuclear lamina and disassembles nucli of clam oocytes in vitro. J. Cell Biol. *112*, 523–533.

Dewhurst, S.M., McGranahan, N., Burrell, R. a, Rowan, A.J., Grönroos, E., Endesfelder, D., Joshi, T., Mouradov, D., Gibbs, P., Ward, R.L., et al. (2014). Tolerance of whole-genome doubling propagates chromosomal instability and accelerates cancer genome evolution. Cancer Discov. *4*, 175–185.

Díaz-Martínez, L. a, Karamysheva, Z.N., Warrington, R., Li, B., Wei, S., Xie, X.-J., Roth, M.G., and Yu, H. (2014). Genome-wide siRNA screen reveals coupling between mitotic apoptosis and adaptation. EMBO J. *33*, 1960–1976.

Ding, Q., He, X., Hsu, J.-M., Xia, W., Chen, C.-T., Li, L.-Y., Lee, D.-F., Liu, J.-C., Zhong, Q., Wang, X., et al. (2007). Degradation of Mcl-1 by beta-TrCP mediates glycogen synthase kinase 3-induced tumor suppression and chemosensitization. Mol. Cell. Biol. *27*, 4006–4017.

Ding, Q., Huo, L., Yang, J.Y., Xia, W., Wei, Y., Liao, Y., Chang, C.J., Yang, Y., Lai, C.C., Lee, D.F., et al. (2008). Down-regulation of myeloid cell leukemia-1 through inhibiting Erk/Pin 1 pathway by sorafenib facilitates chemosensitization in breast cancer. Cancer Res. *68*, 6109–6117.

Dohadwala, M., da Cruz e Silva, EF., Hall, F., Williams, R., Carbonaro-Hall, D., Nairn, A., Greengard, P., and Berndt, N. (1994) Phosphorylation and inactivation of protein phosphatase 1 by cyclin-dependent kinases. Proc Natl Acad Sci USA. *91* 6408-6412

Doménech, E., Maestre, C., Esteban-Martínez, L., Partida, D., Pascual, R., Fernández-Miranda, G., Seco, E., Campos-Olivas, R., Pérez, M., Megias, D., et al. (2015). AMPK and PFKFB3 mediate glycolysis and survival in response to mitophagy during mitotic arrest. Nat. Cell Biol.

Domina, A.M., Vrana, J.A., Gregory, M.A., Hann, S.R., and Craig, R.W. (2004). MCL1 is phosphorylated in the PEST region and stabilized upon ERK activation in viable cells, and at additional sites with cytotoxic okadaic acid or taxol. Oncogene *23*, 5301–5315.

Dorstyn, L., Puccini, J., Wilson, C.H., Shalini, S., Nicola, M., Moore, S., and Kumar, S. (2012). Caspase-2 deficiency promotes aberrant DNA-damage response and genetic instability. Cell Death Differ. *19*, 1411–1411.

Du, L., Lyle, C.S., and Chambers, T.C. (2005). Characterization of vinblastine-induced Bcl-xL and Bcl-2 phosphorylation: evidence for a novel protein kinase and a coordinated phosphorylation/dephosphorylation cycle associated with apoptosis induction. Oncogene *24*, 107–117.

Dumontet, C., and Jordan, M.A. (2010). Microtubule-binding agents : a dynamic field of cancer therapeutics. Nat. Rev. Drug Discov. *9*, 790–803.

Elmore, S. (2012). Apoptosis: A Review of Programmed Cell Death. *29*, 997–1003.

Den Elzen, N., and Pines, J. (2001). Cyclin A is destroyed in prometaphase and can delay chromosome alignment and anaphase. J. Cell Biol. *153*, 121–135.

Enari, M., Sakahira, H., Yokoyama, H., Okawa, K., Iwamatsu, a, and Nagata, S. (1998). A caspase-activated DNase that degrades DNA during apoptosis, and its inhibitor ICAD. Nature *391*, 43–50.

Estey, M.P., Di Ciano-Oliveira, C., Froese, C.D., Fung, K.Y.Y., Steels, J.D., Litchfield, D.W., and Trimble, W.S. (2013). Mitotic regulation of SEPT9 protein by cyclin-dependent kinase 1 (Cdk1) and pin1 protein is important for the completion of cytokinesis. J. Biol. Chem. *288*, 30075–30086.

Fadeel, B., and Orrenius, S. (2005). Apoptosis: A basic biological phenomenon with wide-ranging implications in human disease. J. Intern. Med. *258*, 479–517.

Fang, G., Yu, H., and Kirschner, M.W. (1998). Direct binding of CDC20 protein family members activates the anaphase-promoting complex in mitosis and G1. Mol. Cell *2*, 163–171.

Finley, D. (2009). Recognition and processing of ubiquitin-protein conjugates by the proteasome. Annu. Rev. Biochem. *78*, 477–513.

Di Fiore, B., and Pines, J. (2010). How cyclin a destruction escapes the spindle assembly checkpoint. J. Cell Biol. *190*, 501–509.

Fleischer, B.E. Al (2006). Mcl-1 is an anti-apoptotic factor for human hepatocellular carcinoma. Int J Oncol *28*, 25–32.

Flemming, W. (1881). Studien uber Regeneration der Gewebe. Aus Dem Anat. Inst. Kiel *4-42, 60-6*.

Flores, M.L., Castilla, C., Ávila, R., Ruiz-Borrego, M., Sáez, C., and Japón, M. a. (2012). Paclitaxel sensitivity of breast cancer cells requires efficient mitotic arrest and disruption of Bcl-xL/Bak interaction. Breast Cancer Res. Treat. *133*, 917–928.

Foley, E.A., and Kapoor, T.M. (2013). Microtubule attachment and spindle assembly checkpoint signalling at the kinetochore. Nat. Rev. Mol. Cell Biol. *14*, 25–37.

Fry, A.M., Meraldi, P., and Nigg, E.A. (1998). A centrosomal function for the human Nek2 protein kinase, a member of the NIMA family of cell cycle regulators. EMBO J. *17*, 470–481.

Fujiwara, T., Bandi, M., Nitta, M., Ivanova, E. V, Bronson, R.T., and Pellman, D. (2005). Cytokinesis failure generating tetraploids promotes tumorigenesis in p53-null cells. Nature *437*, 1043–1047.

Garnett, M.J., Mansfeld, J., Godwin, C., Matsusaka, T., Wu, J., Russell, P., Pines, J., and Venkitaraman, A.R. (2009). UBE2S elongates ubiquitin chains on APC/C substrates to promote mitotic exit. Nat. Cell Biol. *11*, 1363–1369.

Gascoigne, K.E., and Taylor, S.S. (2008). Cancer cells display profound intra- and interline variation following prolonged exposure to antimitotic drugs. Cancer Cell *14*, 111–122.

Gascoigne, K.E., and Taylor, S.S. (2009). How do anti-mitotic drugs kill cancer cells? J. Cell Sci. *122*, 2579–2585.

Gazdar, A. (2009). Activating and resistance mutations of EGFR in non-small-cell lung cancer: role in clinical response to EGFR tyrosine kinase inhibitors. Oncogene *28*, 1–14.

Geley, S., Kramer, E., Gieffers, C., Gannon, J., Peters, J.M., and Hunt, T. (2001). Anaphase-promoting complex/cyclosome-dependent proteolysis of human cyclin A starts at the beginning of mitosis and is not subject to the spindle assembly checkpoint. J. Cell Biol. *153*, 137–147.

Gerecitano, J.F., Stephenson, J.J., Lewis, N.L., Osmukhina, A., Li, J., Wu, K., You, Z., Huszar, D., Skolnik, J.M., and Schwartz, G.K. (2013). A Phase i trial of the kinesin spindle protein (Eg5) inhibitor AZD4877 in patients with solid and lymphoid malignancies. Invest. New Drugs *31*, 355–362.

Germain, M., and Duronio, V. (2007). The N terminus of the anti-apoptotic BCL-2 homologue MCL-1 regulates its localization and function. J. Biol. Chem. *282*, 32233–32242.

Girdler, F., Gascoigne, K.E., Eyers, P.A., Hartmuth, S., Crafter, C., Foote, K.M., Keen, N.J., and Taylor, S.S. (2006). Validating Aurora B as an anti-cancer drug target. J. Cell Sci. *119*, 3664–3675.

Glotzer, M., Murray, A., and Kirschner, M. (1991). Cyclin is degraded by the ubiquitin pathway. Nature *349*, 132–138.

Glück, S., Ross, J.S., Royce, M., McKenna, E.F., Perou, C.M., Avisar, E., and Wu, L. (2012). TP53 genomics predict higher clinical and pathologic tumor response in operable early-stage breast cancer treated with docetaxel-capecitabine ± Trastuzumab. Breast Cancer Res. Treat. *132*, 781–791.

Godek, K.M., Kabeche, L., and Compton, D. a. (2014). Regulation of kinetochore–microtubule attachments through homeostatic control during mitosis. Nat. Rev. Mol. Cell Biol. *16*, 57–64.

Golan, A., Yudkovsky, Y., and Hershko, A. (2002). The cyclin-ubiquitin ligase activity of cyclosome/APC is jointly activated by protein kinases Cdk1-cyclin B and Plk. J. Biol. Chem. *277*, 15552–15557.

Gossen, M., and Bujardt, H. (1992). Tight control of gene expression in mammalian cells by tetracycline-responsive promoters. Proc. Natl. Acad. Sci. U. S. A. *89*, 5547–5551.

Grallert, A., Boke, E., Hagting, A., Hodgson, B., Connolly, Y., Griffiths, J., Smith, D., Pines, J., and Hagan, I. (2015) A PP1-PP2A phosphatase relay controls mitotic progression. Nature. *517* 94-98.

Hagting, A., Den Elzen, N., Vodermaier, H.C., Waizenegger, I.C., Peters, J.-M., and Pines, J. (2002). Human securin proteolysis is controlled by the spindle checkpoint and reveals when the APC/C switches from activation by Cdc20 to Cdh1. J. Cell Biol. *157*, 1125–1137.

Haldar, S., Jena, N., and Croce, C.M. (1995). Inactivation of Bcl-2 by phosphorylation. Proc. Natl. Acad. Sci. U. S. A. *92*, 4507–4511.

Han, J.S., Holland, A.J., Fachinetti, D., Kulukian, A., Cetin, B., and Cleveland, D.W. (2013). Catalytic assembly of the mitotic checkpoint inhibitor BubR1-Cdc20 by a Mad2-induced functional Switch in Cdc20. Mol. Cell *51*, 92–104.

Hanahan, D., and Weinberg, R.A. (2000). The hallmarks of cancer. Cell *100*, 57–70.

Harley, M.E., Allan, L.A., Sanderson, H.S., and Clarke, P.R. (2010). Phosphorylation of Mcl-1 by CDK1-cyclin B1 initiates its Cdc20-dependent destruction during mitotic arrest. EMBO J. *29*, 2407–2420.

Harvey, M., Sands, A., Weiss, M., Hefi, M., Wiseman, R., Pantazis, P., Giovanella, B., Tainsky, M., Bradley, A., and Donehower, L. (1993). In vitro growth characteristics of embryo fibroblasts isolated from p53-deficient mice. Oncogene *8*, 2457–2467.

Haschka, M.D., Soratroi, C., Kirschnek, S., Hacker, G., Hilbe, R., Geley, S., Villunger, A., and Fava, L.L. (2015). The NOXA-MCL1-BIM axis defines lifespan on extended mitotic arrest. Nat. Commun. *6*, 1–13.

Haupt, Y., Maya, R., Kazaz, A., and Oren, M. (1997). Mdm2 promotes the rapid degradation of p53. Nature *431*, 296–299.

Hayashi, K.I. (2012). The interaction and integration of auxin signaling components. Plant Cell Physiol. *53*, 965–975.

Hayashi, M., Cesare, A., Fitzpatrick, J., Denchi, E.L., and Karlseder, J. (2012). A telomere-dependent DNA damage checkpoint induced by prolonged mitotic arrest. Nat. Struct. Mol. Biol. *19*, 387–395.

Hayashi, M.T., Cesare, A.J., Rivera, T., and Karlseder, J. (2015). Cell death during crisis is mediated by mitotic telomere deprotection. Nature *522*, 492–496.

Hayes, M.J., Kimata, Y., Wattam, S.L., Lindon, C., Mao, G., Yamano, H., and Fry, A.M. (2006). Early mitotic degradation of Nek2A depends on Cdc20-independent interaction with the APC/C. Nat. Cell Biol. *8*, 607–614.

He, J., Chao, W.C.H., Zhang, Z., Yang, J., Cronin, N., and Barford, D. (2013). Insights into degron recognition by APC/C coactivators from the structure of an Acm1-Cdh1 complex. Mol. Cell *50*, 649–660.

Henson, E.S., Hu, X., and Gibson, S.B. (2006). Herceptin sensitizes ErbB2-overexpressing cells to apoptosis by reducing antiapoptotic Mcl-1 expression. Clin. Cancer Res. *12*, 845–853.

Hershko, A. (2005). The ubiquitin system for protein degradation and some of its roles in the control of the cell division cycle. Cell Death Differ. *12*, 1191–1197.

Hershko, A., Heller, H., Elias, S., and Ciechanover, A. (1983). Components of Ubiquitin-Protein Ligase System. J. Biol. Chem. *258*, 8206–8214.

Hewitt, L., Tighe, A., Santaguida, S., White, A.M., Jones, C.D., Musacchio, A., Green, S., and Taylor, S.S. (2010). Sustained Mps1 activity is required in mitosis to recruit O-Mad2 to the Mad1-C-Mad2 core complex. J. Cell Biol. *190*, 25–34.

Higgins, J,. (2013) Chromosome segregation:learning to let go. Curr Biol *23* R883-885

Ho, L.H., Read, S.H., Dorstyn, L., Lambrusco, L., and Kumar, S. (2008). Caspase-2 is required for cell death induced by cytoskeletal disruption. Oncogene *27*, 3393–3404.

Hochegger, H., Takeda, S., and Hunt, T. (2008). Cyclin-dependent kinases and cell-cycle transitions : does one fit all ? Nat. Rev. Mol. Cell Biol. *9*, 910–916.

Holland, A.J., Fachinetti, D., Han, J.S., and Cleveland, D.W. (2012). Inducible, reversible system for the rapid and complete degradation of proteins in mammalian cells. Proc. Natl. Acad. Sci. U. S. A. *109*, E3350–E3357.

Hollebecque, a., Deutsch, E., Massard, C., Gomez-Roca, C., Bahleda, R., Ribrag, V., Bourgier, C., Lazar, V., Lacroix, L., Gazzah, a., et al. (2013). A phase I, dose-escalation study of the Eg5-inhibitor EMD 534085 in patients with advanced solid tumors or lymphoma. Invest. New Drugs *31*, 1530–1538.

Holloway, S.L., Glotzer, M., King, R.W., and Murray, A.W. (1993). Anaphase Is Initiated by Proteolysis Rather Than by the Inactivation of Maturation-Promoting Factor. Cell *73*, 1393–1402.

Hoyt, M.A., Totis, L., and Roberts, B.T. (1991). S. cerevisiae genes required for cell cycle arrest in response to loss of microtubule function. Cell *66*, 507–517.

Hsu, Y., and Youle, R. (1997) Nonionic detergents induce dimerization among members of the Bcl-2 family. J Biol Chem. *272* 13829-13834

Hsu, Y., and Youle, R. (1998) Bax in murine thymus is a soluable monomeric protein that displays differential detergent-induced conformations. J Biol Chem. *273* 10777-10783

Huang, H.-C., Mitchison, T.J., and Shi, J. (2010). Stochastic competition between mechanistically independent slippage and death pathways determines cell fate during mitotic arrest. PLoS One *5*, e15724.

Huang, H.C., Shi, J., Orth, J.D., and Mitchison, T.J. (2009). Evidence that Mitotic Exit Is a Better Cancer Therapeutic Target Than Spindle Assembly. Cancer Cell *16*, 347–358.

Hwang, a., Maity, a., McKenna, W.G., and Muschel, R.J. (1995). Cell cycle-dependent regulation of the cyclin B1 promoter. J. Biol. Chem. *270*, 28419–28424.

Inoshita, S., Takeda, K., Hatai, T., Terada, Y., Sano, M., Hata, J., Umezawa, A., and Ichijo, H. (2002). Phosphorylation and inactivation of myeloid cell leukemia 1 by JNK in response to oxidative stress. J. Biol. Chem. *277*, 43730–43734.

Inuzuka, H., Shaik, S., Onoyama, I., Gao, D., Tseng, A., Maser, R.S., Zhai, B., Wan, L., Gutierrez, A., Lau, A.W., et al. (2011). SCF(FBW7) regulates cellular apoptosis by targeting MCL1 for ubiquitylation and destruction. Nature *471*, 104–109.

Invitrogen (2010). Flp-In System.

Irniger, S., Piatti, S., Michaelis, C., and Nasmyth, K. (1995). Genes involved in sister chromatid separation are needed for B-type cyclin proteolysis in budding yeast. Cell *81*, 269–278.

Jeffrey, P.D., Russo, A.A., Polyak, K., Gibbs, E., Hurwitz, J., Massagué, J., and Pavletich, N.P. (1995). Mechanism of CDK activation revealed by the structure of a cyclinA-CDK2 complex. Nature *376*, 313–320.

Jelluma, N., Brenkman, A.B., van den Broek, N.J.F., Cruijsen, C.W. a, van Osch, M.H.J., Lens, S.M. a, Medema, R.H., and Kops, G.J.P.L. (2008a). Mps1 Phosphorylates Borealin to Control Aurora B Activity and Chromosome Alignment. Cell *132*, 233–246.

Jelluma, N., Brenkman, A.B., McLeod, I., Yates, J.R., Cleveland, D.W., Medema, R.H., and Kops, G.J.P.L. (2008b). Chromosomal instability by inefficient Mps1 auto-activation due to a weakened mitotic checkpoint and lagging chromosomes. PLoS One *3*, 1–8.

Jin, L., Williamson, A., Banerjee, S., Philipp, I., and Rape, M. (2008). Mechanism of Ubiquitin-Chain Formation by the Human Anaphase-Promoting Complex. Cell *133*, 653–665.

Jones, R., Vuky, J., Elliott, T., Mead, G., Arranz, J.A., Chester, J., Chowdhury, S., Dudek, A.Z., Müller-Mattheis, V., Grimm, M.O., et al. (2013). Phase II study to assess the efficacy, safety and tolerability of the mitotic spindle kinesin inhibitor AZD4877 in patients with recurrent advanced urothelial cancer. Invest. New Drugs *31*, 1001–1007.

Jordan, M.A., and Wilson, L. (2004). Microtubules as a target for anticancer drugs. Nat. Rev. Cancer *4*, 253–265.

Jordan, M., Toso, R.J., Thrower, D., and Wilson, L. (1993). Mechanism of mitotic block and inhibition of cell proliferation by taxol at low concentrations. Proc. Natl. Acad. Sci. U. S. A. *90*, 9552–9556.

Jordan, M.A., Thrower, D., and Wilson, L. (1991). Mechanism of Inhibition of Cell Proliferation by Vinca Alkaloids Mechanism of Inhibition of Cell Proliferation by Vinca Alkaloids. Cancer Res. *51*, 2212–2222.

Jordan, M.A., Wendell, K., Gardiner, S., Derry, W.B., Copp, H., and Wilson, L. (1996). Mitotic Block Induced in HeLa Cells by Low Concentrations of Paclitaxel (Taxol) Results in Abnormal Mitotic Exit and Apoptotic Cell Death Mitotic Block Induced in HeLa Cells by Low Concentrations of Paclitaxel (Taxol) Results in Abnormal Mitotic Exit. Cancer Res. *56*, 816–825.

Kapitein, L., Peterman, E., Kwok, B., Kim, J., Kapoor, T., and Schmidt, C. (2005). The bipolar mitotic kinesin Eg5 moves on both microtubules that it crosslinks. Nature *435*, 114–118.

Kastan, M.B., Onyekwere, O., Sidransky, D., Vogelstein, B., and Craig, R.W. (1991). Participation of p53 protein in the cellular response to DNA damage. Cancer Res. *51*, 6304–6311.

Kastan, M.B., Zhan, Q., el-Deiry, W.S., Carrier, F., Jacks, T., Walsh, W. V, Plunkett, B.S., Vogelstein, B., and Fornace, a J. (1992). A mammalian cell cycle checkpoint pathway utilizing p53 and GADD45 is defective in ataxia-telangiectasia. Cell *71*, 587–597.

Kawabata, T., Tanimura, S., Asai, K., Kawasaki, R., Matsumaru, Y., and Kohno, M. (2012). Up-regulation of pro-apoptotic protein Bim and down-regulation of anti-apoptotic protein Mcl-1 cooperatively mediate enhanced tumor cell death induced by the combination of ERK kinase (MEK) inhibitor and microtubule inhibitor. J. Biol. Chem. *287*, 10289–10300.

King, R.W., Peters, J.M., Tugendreich, S., Rolfe, M., Hieter, P., and Kirschner, M.W. (1995). A 20S complex containing CDC27 and CDC16 catalyzes the mitosis-specific conjugation of ubiquitin to cyclin B. Cell *81*, 279–288.

King, R.W., Glotzer, M., and Kirschner, M.W. (1996). Mutagenic Analysis of the Destruction Signal of Mitotic Cyclins and Structural Characterization of Ubiquitinated Intermediates. Mol. Biol. Cell *7*, 1343–1357.

Kobayashi, S., Lee, S.H., Meng, X.W., Mott, J.L., Bronk, S.F., Werneburg, N.W., Craig, R.W., Kaufmann, S.H., and Gores, G.J. (2007). Serine 64 phosphorylation enhances the antiapoptotic function of Mcl-1. J. Biol. Chem. *282*, 18407–18417.

Kodama, Y., Taura, K., Miura, K., Schnabl, B., Osawa, Y., and Brenner, D.A. (2009). Antiapoptotic Effect of c-Jun N-terminal Kinase-1 through Mcl-1 Stabilization in TNF-Induced Hepatocyte Apoptosis. Gastroenterology *136*, 1423–1434.

Komlodi-Pasztor, E., Sackett, D., Wilkerson, J., and Fojo, T. (2011). Mitosis is not a key target of microtubule agents in patient tumors. Nat. Rev. Clin. Oncol. *8*, 244–250.

Konrad, C.G. (1963). Protein Synthesis and Rna Synthesis During Mitosis in Animal Cells. J. Cell Biol. *19*, 267–277.

Kozopas, K.M., Yang, T.A.O., Buchan, H.L., Zhou, P., and Craig, R.W. (1993). MCLI , a gene expressed in programmed myeloid cell differentiation , has sequence similarity to BCL2. Proc. Natl. Acad. Sci. U. S. A. *90*, 3516–3520.

Kracikova, M., Akiri, G., George, A., Sachidanandam, R., and Aaronson, S.A. (2013). A threshold mechanism mediates p53 cell fate decision between growth arrest and apoptosis. Cell Death Differ. *20*, 576–588.

Kraft, C., Herzog, F., Gieffers, C., Mechtler, K., Hagting, A., Pines, J., and Peters, J.M. (2003). Mitotic regulation of the human anaphase-promoting complex by phosphorylation. EMBO J. *22*, 6598–6609.

Kraft, C., Vodermaier, H.C., Maurer-Stroh, S., Eisenhaber, F., and Peters, J.M. (2005). The WD40 propeller domain of Cdh1 functions as a destruction box receptor for APC/C substrates. Mol. Cell *18*, 543–553.

Krajewski, S., Bodrug, S., Krajewska, M., Shabaik, A., Gascoyne, R., Berean, K., and Reed, J.C. (1995). Immunohistochemical analysis of Mcl-1 protein in human tissues. Differential regulation of Mcl-1 and Bcl-2 protein production suggests a unique role for Mcl-1 in control of programmed cell death in vivo. Am. J. Pathol. *146*, 1309–1319.

Kramer, E.R., Gieffers, C., Hölzl, G., Hengstschläger, M., and Peters, J.M. (1998). Activation of the human anaphase-promoting complex by proteins of the CDC20/Fizzy family. Curr. Biol. *8*, 1207–1210.

Kramer, E.R., Scheuringer, N., Podtelejnikov, a V, Mann, M., and Peters, J.M. (2000). Mitotic regulation of the APC activator proteins CDC20 and CDH1. Mol. Biol. Cell *11*, 1555–1569.

Kubbutat, N., Jones, S., and Vousden, K. (1997). Regulation of p53 stability by Mdm2. Nature *387*, 299–303.

Kuerbitz, S.J., Plunkett, B.S., Walsh, W. V, and Kastan, M.B. (1992). Wild-type p53 is a cell cycle checkpoint determinant following irradiation. Proc. Natl. Acad. Sci. U. S. A. *89*, 7491–7495.

Kutuk, O., and Letai, A. (2008). Alteration of the Mitochondrial Apoptotic Pathway Is Key to Acquired Paclitaxel Resistance and Can Be Reversed by ABT-737. Cancer Res. 7985–7995.

Kutuk, O., and Letai, A. (2010). Displacement of Bim by Bmf and Puma rather than increase in Bim level mediates paclitaxel-induced apoptosis in breast cancer cells. Cell Death Differ. *17*, 1624–1635.

Lampson, M.A., and Cheeseman, I.M. (2011). Sensing centromere tension: Aurora B and the regulation of kinetochore function. Trends Cell Biol. *21*, 133–140.

Lampson, M.A., Renduchitala, K., Khodjakov, A., and Kapoor, T.M. (2004). Correcting improper chromosome-spindle attachments during cell division. Nat. Cell Biol. *6*, 232–237.

Lanni, J.S., and Jacks, T. (1998). Characterization of the p53-dependent postmitotic checkpoint following spindle disruption. Mol. Cell. Biol. *18*, 1055–1064.

Lara-Gonzalez, P., and Taylor, S.S. (2012). Cohesion fatigue explains why pharmacological inhibition of the APC/C induces a spindle checkpoint-dependent mitotic arrest. PLoS One *7*, e49041.

Lara-Gonzalez, P., Scott, M.I.F., Diez, M., Sen, O., and Taylor, S.S. (2011). BubR1 blocks substrate recruitment to the APC/C in a KEN-box-dependent manner. J. Cell Sci. *124*, 4332–4345.

Lara-Gonzalez, P., Westhorpe, F.G., and Taylor, S.S. (2012). The Spindle Assembly Checkpoint. Curr. Biol. *22*, R966–R980.

Lengauer, C., Kinzler, K., and Vogelstein, B. (1998). Genetic instabilities in human cancers. Nature *396*, 643–649.

Lens, S.M.A., Voest, E.E., and Medema, R.H. (2010). Shared and separate functions of in cancer. Nat. Rev. Cancer *10*, 825–841.

Di Leonardo, A., Khan, S.H., Linke, S.P., Greco, V., and Sedita, G. (1997). DNA replication in the presence of mitotic spindel inhibitors in human and mouse fibroblasts lacking either p53 or pRb function. Cancer Res. *57*, 1013–1019.

Leverson, J.D., Zhang, H., Chen, J., Tahir, S.K., Phillips, D.C., Xue, J., Nimmer, P., Jin, S., Smith, M., Xiao, Y., et al. (2015). Potent and selective small-molecule MCL-1 inhibitors demonstrate on-target cancer cell killing activity as single agents and in combination with ABT-263 (navitoclax). Cell Death Dis. *6*, e1590.

Li, R., and Murray, A.W. (1991). Feedback control of mitosis in budding yeast. Cell *66*, 519–531.

Li, Y., and Benezra, R. (1996). Identification of a human mitotic checkpoint gene: hsMAD2. Science *274*, 246–248.

Li, R., Moudgil, T., Ross, H.J., and Hu, H.-M. (2005). Apoptosis of non-small-cell lung cancer cell lines after paclitaxel treatment involves the BH3-only proapoptotic protein Bim. Cell Death Differ. *12*, 292–303.

Lindqvist, A., Rodríguez-Bravo, V., and Medema, R.H. (2009). The decision to enter mitosis: feedback and redundancy in the mitotic entry network. J. Cell Biol. *185*, 193–202.

Liu, D., Vader, G., Vromans, M., Lampson, M., and Lens, S. (2009). Sensing Chromosome Bi-Orientation by Spacial Separation of Aurora B Kinase from Kinetochore Substrates. Science (80-.). *323*, 1350–1353.

Liu, X., Kim, C.N., Yang, J., Jemmerson, R., and Wang, X. (1996). Induction of apoptotic program in cell-free extracts: Requirement for dATP and cytochrome c. Cell *86*, 147–157.

Lohka, M.J., Hayes, M.K., and Maller, J.L. (1988). Purification of maturation-promoting factor, an intracellular regulator of early mitotic events. Proc. Natl. Acad. Sci. U. S. A. *85*, 3009–3013.

Lolli, G., and Johnson, L. (2005). CAK-Cyclin-dependent activating kinase. Cell Cycle *4*, 572–577.

Luciano, F., Jacquel, A., Colosetti, P., Herrant, M., Cagnol, S., Pages, G., and Auberger, P. (2003). Phosphorylation of Bim-EL by Erk1/2 on serine 69 promotes its degradation via the proteasome pathway and regulates its proapoptotic function. Oncogene *22*, 6785–6793.

Manchado, E., Guillamot, M., de Cárcer, G., Eguren, M., Trickey, M., García-Higuera, I., Moreno, S., Yamano, H., Cañamero, M., and Malumbres, M. (2010). Targeting Mitotic Exit Leads to Tumor Regression In Vivo: Modulation by Cdk1, Mastl, and the PP2A/B55α,δ Phosphatase. Cancer Cell *18*, 641–654.

Mansfeld, J., Collin, P., Collins, M.O., Choudhary, J.S., and Pines, J. (2011). APC15 drives the turnover of MCC-CDC20 to make the spindle assembly checkpoint responsive to kinetochore attachment. Nat. Cell Biol. *13*, 1234–1243.

Margolis, R.L., Lohez, O.D., and Andreassen, P.R. (2003). G1 tetraploidy checkpoint and the suppression of tumorigenesis. J. Cell. Biochem. *88*, 673–683.

Markman, M. (2008). Antineoplastic agents in the management of ovarian cancer: current status and emerging therapeutic strategies. Trends Pharmacol. Sci. *29*, 515–519.

Maurer, U., Charvet, C., Wagman, A.S., Dejardin, E., and Green, D.R. (2006). Glycogen synthase kinase-3 regulates mitochondrial outer membrane permeabilization and apoptosis by destabilization of MCL-1. Mol. Cell *21*, 749–760.

Mayer, T.U., Kapoor, T.M., Haggarty, S.J., King, R.W., Schreiber, S.L., and Mitchison, T.J. (1999). Small molecule inhibitor of mitotic spindle bipolarity identified in a phenotype-based screen. Science (80-.). *286*, 971–974.

Medema, R ., and Lindqvist, A., (2011) Boosting and suppressing mitotic phosphorylation. Trends Biochem Sci. *36* 578-584

Mena, A.L., Lam, E.W.-F., and Chatterjee, S. (2010). Sustained spindle-assembly checkpoint response requires de novo transcription and translation of cyclin B1. PLoS One *5*, e13037.

Miller, A. V., Hicks, M. a., Nakajima, W., Richardson, A.C., Windle, J.J., and Harada, H. (2013). Paclitaxel-Induced Apoptosis Is BAK-Dependent, but BAX and BIM-Independent in Breast Tumor. PLoS One *8*, 1–9.

Millman, S.E., and Pagano, M. (2011). MCL1 meets its end during mitotic arrest. EMBO Rep. *12*, 384–385.

Minn, A.J., Boise, L.H., and Thompson, C.B. (1996). Expression of Bcl-x(L) and loss of p53 can cooperate to overcome a cell cycle checkpoint induced by mitotic spindle damage. Genes Dev. *10*, 2621–2631.

Minshull, J., Blow, J.J., and Hunt, T. (1989). Translation of cyclin mRNA is necessary for extracts of activated xenopus eggs to enter mitosis. Cell *56*, 947–956.

Mitchison, T.J. (2012). The proliferation rate paradox in antimitotic chemotherapy. Mol. Biol. Cell *23*, 1–6.

Mochida, S., Ikeo, S., Gannon, J., and Hunt, T. (2009). Regulated activity of PP2A-B55 delta is crucial for controlling entry into and exit from mitosis in Xenopus egg extracts. EMBO J. *28*, 2777–2785.

Momand, J., Zambetti, G., Olson, D., George, D., and Levine, A. (1992). The mdm-2 oncogene product forms a complex with the p53 protein and inhi- bits p53-mediated transactivation.pdf.crdownload. Cell *69*, 1237–1245.

Montero, J., Sarosiek, K., DeAngelo, J., Maertens, O., Ryan, J., Ercan, D., Piao, H., Horowitz, N., Berkowitz, R., Matulonis, U., et al (2015) Drug-induced death signnaling strategy rapidly predicts cancer response to chemotherapy. Cell *160* 977-989

Morawska, M., and Ulrich, H.D. (2013). An expanded tool kit for the auxin-inducible degron system in budding yeast. 341–351.

Morel, C., Carlson, S.M., White, F.M., and Davis, R.J. (2009). Mcl-1 integrates the opposing actions of signaling pathways that mediate survival and apoptosis. Mol. Cell. Biol. *29*, 3845–3852.

Nakajima, W., Hicks, M. a, Tanaka, N., Krystal, G.W., and Harada, H. (2014). Noxa determines localization and stability of MCL-1 and consequently ABT-737 sensitivity in small cell lung cancer. Cell Death Dis. *5*, e1052.

Nakano, K., and Vousden, K.H. (2001). PUMA, a novel proapoptotic gene, is induced by p53. Mol. Cell *7*, 683–694.

Nigg, E. (1995). Cyclin-dependent protein kinases: key regulators of the eukaryotic cell cycle. Bioessays *17*, 471–480.

Nijhawan, D., Fang, M., Traer, E., Zhong, Q., Gao, W., Du, F., and Wang, X. (2003). Elimination of Mcl-1 is required for the initiation of apoptosis following ultraviolet irradiation. Genes Dev. *17*, 1475–1486.

Nilsson, J., Yekezare, M., Minshull, J., and Pines, J. (2008). The APC/C maintains the spindle assembly checkpoint by targeting Cdc20 for destruction. Nat. Cell Biol. *10*, 1411–1420.

Nishimura, K., Fukagawa, T., Takisawa, H., Kakimoto, T., and Kanemaki, M. (2009). An auxin-based degron system for the rapid depletion of proteins in nonplant cells. Nat. Methods *6*, 917–922.

Nogales, E., Wolf, S.G., Khan, I. a, Ludueña, R.F., and Downing, K.H. (1995). Structure of tubulin at 6.5 A and location of the taxol-binding site. Nature *375*, 424–427.

Nurse, P. (1990). Universal control mechanism regulating onset of M-phase. Nature *344*, 503–508.

O'Gorman, S., Fox, D.T., and Wahl, G.M. (1991). Recombinase-mediated gene activation and site-specific integration in mammalian cells. Science (80-.). *251*, 1351–1355.

Oda, E., Ohki, R., Murasawa, H., Nemoto, J., Shibue, T., Yamashita, T., Tokino, T., Taniguchi, T., and Tanaka, N. (2000). Noxa, a BH3-only member of the Bcl-2 family and candidate mediator of p53-induced apoptosis. Science (80-.). *288*, 1053–1058.

Oliner, J.D., Pietenpol, J.A., Thiagalingam, S., Gyuris, J., Kinzler, K.W., and Vogelstein, B. (1993). Oncoprotein MDM2 conceals the activation domain of tumour suppressor p53. Nature *362*, 857–860.

Oliveira, R.A., Hamilton, R.S., Pauli, A., Davis, I., and Nasmyth, K. (2010). Cohesin cleavage and Cdk inhibition trigger formation of daughter nuclei. Nat. Cell Biol. *12*, 185–192.

Oltersdorf, T., Elmore, S.W., Shoemaker, A.R., Armstrong, R.C., Augeri, D.J., Belli, B.A., Bruncko, M., Deckwerth, T.L., Dinges, J., Hajduk, P.J., et al. (2005). An inhibitor of Bcl-2 family proteins induces regression of solid tumours. Nature *435*, 677–681.

Orth, J.D., Loewer, A., Lahav, G., and Mitchison, T.J. (2012). Prolonged mitotic arrest triggers partial activation of apoptosis, resulting in DNA damage and p53 induction. Mol. Biol. Cell *23*, 567–576.

Pajk, B., Cufer, T., Canney, P., Ellis, P., Cameron, D., Blot, E., Vermorken, J., Coleman, R., Marreaud, S., Bogaerts, J., et al. (2008). Anti-tumor activity of capecitabine and vinorelbine in patients with anthracycline- and taxane-pretreated metastatic breast cancer: Findings from the EORTC 10001 randomized phase II trial. Breast *17*, 180–185.

Pfleger, C.M., and Kirschner, M.W. (2000). The KEN box: An APC recognition signal distinct from the D box targeted by Cdh1. Genes Dev. *14*, 655–665.

Pines (2011). Cubism and the cell cycle: the many faces of the APC/C. Nat. Rev. Mol. Cell Biol. *12*, 427–438.

Pines, J., and Lindon, C. (2005). Proteolysis: anytime, any place, anywhere? Nat. Cell Biol. *7*, 731–735.

Poruchynsky, M.S., Fojo, T., Wang, E.E., Rudin, C.M., and Blagosklonny, M. V (1998). Bcl-xL Is Phosphorylated in Malignant Cells following Microtubule Disruption. Cancer Res. *4*, 3331–3338.

Rapino, F., Naumann, I., and Fulda, S. (2013). Bortezomib antagonizes microtubule-interfering drug-induced apoptosis by inhibiting G2/M transition and MCL-1 degradation. Cell Death Dis. *4*, e925.

Rath, O., and Kozielski, F. (2012). Kinesins and cancer. Nat. Rev. Cancer *12*, 527–539.

Rattani, A., Vinod, P.K., Godwin, J., Wolna, M., Malumbres, M., Novak, B., and Nasmyth, K. (2014). Dependency of the Spindle Assembly Checkpoint on Cdk1 Renders the Anaphase Transition Irreversible. Curr. Biol. *24*, 630–637.

Reynolds, J.E., Yang, T., Qian, L., Jenkinson, J.D., Zhou, P., Eastman, A., and Craig, R.W. (1994). Mcl-1, a Member of the Bcl-2 Family, Delays Apoptosis Induced by c-Myc Overexpression in Chinese Hamster Ovary Cells. Cell *54*, 6348–6352.

Rieder, C.L., and Maiato, H. (2004). Stuck in Division or Passing through : What Happens When Cells Cannot Satisfy the Spindle Assembly Checkpoint. Dev. Cell *7*, 637–651.

Rieder, C.L., Schultz, A., Cole, R., and Sluder, G. (1994). Anaphase onset in vertebrate somatic cells is controlled by a checkpoint that monitors sister kinetochore attachment to the spindle. J. Cell Biol. *127*, 1301–1310.

Rinkenberger, J.L., Horning, S., Klocke, B., Roth, K., and Korsmeyer, S.J. (2000). Mcl-1 deficiency results in peri-implantation embryonic lethality. Genes Dev. *14*, 23–27.

Rogers, S., Wells, R., and Rechsteiner, M. (1986). Amino acid sequences common to rapidly degraded proteins: the PEST hypothesis. Science *234*, 364–368.

Rothbauer, U., Zolghadr, K., Muyldermans, S., Schepers, A., Cardoso, M.C., and Leonhardt, H. (2008). A versatile nanotrap for biochemical and functional studies with fluorescent fusion proteins. Mol. Cell. Proteomics *7*, 282–289.

Rusan, N.M., Fagerstrom, C.J., Yvon, A.M., and Wadsworth, P. (2001). Cell cycle-dependent changes in microtubule dynamics in living cells expressing green fluorescent protein-alpha tubulin. Mol. Biol. Cell *12*, 971–980.

Ryan, J., Letai, A. (2013) BH3 profiling in while cells by fluorimeter or FACS. Methods. *61*, 156-164

Sackton, K.L., Dimova, N., Zeng, X., Tian, W., Zhang, M., Sackton, T.B., Meaders, J., Pfaff, K.L., Sigoillot, F., Yu, H., et al. (2014). Synergistic blockade of mitotic exit by two chemical inhibitors of the APC/C. Nature *514*, 646–649.

Sakurikar, N., Eichhorn, J.M., and Chambers, T.C. (2012). Cyclin-dependent kinase-1 (Cdk1)/cyclin B1 dictates cell fate after mitotic arrest via phosphoregulation of antiapoptotic Bcl-2 proteins. J. Biol. Chem. *287*, 39193–39204.

Sakurikar, N., Eichhorn, J.M., Alford, S.E., and Chambers, T.C. (2014). Identification of a mitotic death signature in cancer cell lines. Cancer Lett. *343*, 232–238.

Santamaría, D., Barrière, C., Cerqueira, A., Hunt, S., Tardy, C., Newton, K., Cáceres, J.F., Dubus, P., Malumbres, M., and Barbacid, M. (2007). Cdk1 is sufficient to drive the mammalian cell cycle. Nature *448*, 811–815.

Saxton, W.M., Stemple, D.L., Leslie, R.J., Salmon, E.D., Zavortink, M., and McIntosh, J.R. (1984). Tubulin dynamics in cultured mammalian cells. J. Cell Biol. *99*, 2175–2186.

Schellenberg, B., Wang, P., Keeble, J.A., Rodriguez-Enriquez, R., Walker, S., Owens, T.W., Foster, F., Tanianis-Hughes, J., Brennan, K., Streuli, C.H., et al. (2013). Bax Exists in a Dynamic Equilibrium between the Cytosol and Mitochondria to Control Apoptotic Priming. Mol. Cell *49*, 959–971.

Schiff, P., Fant, J., and Horwitz, S. (1979). Promotion of microtubule assembly in vitro by taxol. Nature *277*, 665–667.

Schmitz, M.H., Held, M., Janssens, V., Hutchins, J.R., Hudecz, O., Ivanova, E., Goris, J., Trinkle-Mulcahy, L., Lamond, A.I., Poser, I., et al. (2010). Live-cell imaging RNAi screen identifies PP2A-B55alpha and importin-beta1 as key mitotic exit regulators in human cells. Nat. Cell Biol. *12*, 886–893.

Schneider-poetsch, T., Ju, J., Eyler, D.E., Dang, Y., Bhat, S., Merrick, W.C., Green, R., Shen, B., and Liu, J.O. (2010). Inhibition of Eukaryotic Translation Elongation by Cycloheximide and Lactimidomycin. Nat. Chem. Biol. *6*, 209–217.

Sedgwick, G.G., Hayward, D.G., Di Fiore, B., Pardo, M., Yu, L., Pines, J., and Nilsson, J. (2013). Mechanisms controlling the temporal degradation of Nek2A and Kif18A by the APC/C-Cdc20 complex. EMBO J. *32*, 303–314.

Shi, J., Orth, J.D., and Mitchison, T. (2008). Cell type variation in responses to antimitotic drugs that target microtubules and kinesin-5. Cancer Res. *68*, 3269–3276.

Shi, J., Zhou, Y., Huang, H.-C., and Mitchison, T.J. (2011). Navitoclax (ABT-263) accelerates apoptosis during drug-induced mitotic arrest by antagonizing Bcl-xL. Cancer Res. *71*, 4518–4526.

Shieh, S.Y., Ikeda, M., Taya, Y., and Prives, C. (1997). DNA damage-induced phosphorylation of p53 alleviates inhibition by MDM2. Cell *91*, 325–334.

Sivakumar, S., and Gorbsky, G.J. (2015). Spatiotemporal regulation of the anaphase-promoting complex in mitosis. Nat. Rev. Mol. Cell Biol. *16*, 82–94.

Song, L., Coppola, D., Livingston, S., Cress, W.D., Haura, E.B., Song, L., Coppola, D., Livingston, S., Cress, D., and Haura, E.B. (2005). Mcl-1 Regulates Survival and Sensitivity to Diverse Apoptotic Stimuli in human non-small cell lung cancer cells. Cancer Biol. Ther. *4*, 37–41.

Stegmeier, F., Rape, M., Draviam, V.M., Nalepa, G., Sowa, M.E., Ang, X.L., McDonald, E.R., Li, M.Z., Hannon, G.J., Sorger, P.K., et al. (2007). Anaphase initiation is regulated by antagonistic ubiquitination and deubiquitination activities. Nature *446*, 876–881.

Stevens, D., Gassmann, R., Oegema, K., and Desai, A. (2011). Uncoordinated loss of chromatid cohesion is a common outcome of extended metaphase arrest. PLoS One *6*.

Stewart, D.P., Koss, B., Bathina, M., Perciavalle, R.M., Bisanz, K., and Opferman, J.T. (2010). Ubiquitin-independent degradation of antiapoptotic MCL-1. Mol. Cell. Biol. *30*, 3099–3110.

Stickeler, E., Pils, D., Klar, M., Orlowsk-Volk, M., Zur Hausen, A., Jäger, M., Watermann, D., Gitsch, G., Zeillinger, R., and Tempfer, C.B. (2011). Basal-like molecular subtype and HER4 up-regulation and response to neoadjuvant chemotherapy in breast cancer. Oncol. Rep. *26*, 1037–1045.

Storchova, Z., and Pellman, D. (2004). From polyploidy to aneuploidy, genome instability and cancer. Nat. Rev. Mol. Cell Biol. *5*, 45–54.

Sudakin, V., Ganoth, D., Dahan, a, Heller, H., Hershko, J., Luca, F.C., Ruderman, J. V, and Hershko, a (1995). The cyclosome, a large complex containing cyclin-selective ubiquitin ligase activity, targets cyclins for destruction at the end of mitosis. Mol. Biol. Cell *6*, 185–197.

Sudakin, V., Chan, G.K.T., and Yen, T.J. (2001). Checkpoint inhibition of the APC/C in HeLa cells is mediated by a complex of BUBR1, BUB3, CDC20, and MAD2. J. Cell Biol. *154*, 925–936.

Swanton, C., Marani, M., Pardo, O., Warne, P.H., Kelly, G., Sahai, E., Elustondo, F., Chang, J., Temple, J., Ahmed, A. a., et al. (2007). Regulators of Mitotic Arrest and Ceramide Metabolism Are Determinants of Sensitivity to Paclitaxel and Other Chemotherapeutic Drugs. Cancer Cell *11*, 498–512.

Tan, T.T., Degenhardt, K., Nelson, D. a., Beaudoin, B., Nieves-Neira, W., Bouillet, P., Villunger, A., Adams, J.M., and White, E. (2005). Key roles of BIM-driven apoptosis in epithelial tumors and rational chemotherapy. Cancer Cell *7*, 227–238.

Tang, D., and Kidd, V.J. (1998). Cleavage of DFF-45/ICAD by multiple caspases is essential for its function during apoptosis. J. Biol. Chem. *273*, 28549–28552.

Tang, Y., Orth, J.D., Xie, T., and Mitchison, T.J. (2011). Rapid induction of apoptosis during Kinesin-5 inhibitor-induced mitotic arrest in HL60 cells. Cancer Lett. *310*, 15–24.

Taylor, S.S., and McKeon, F. (1997). Kinetochore localization of murine Bub1 is required for normal mitotic timing and checkpoint response to spindle damage. Cell *89*, 727–735.

Taylor, S.S., Ha, E., and McKeon, F. (1998). The human homologue of Bub3 is required for kinetochore localization of Bub1 and a Mad3/Bub1-related protein kinase. J. Cell Biol. *142*, 1–11.

Terrano, D.T., Upreti, M., and Chambers, T.C. (2010). Cyclin-dependent kinase 1-mediated Bcl-xL/Bcl-2 phosphorylation acts as a functional link coupling mitotic arrest and apoptosis. Mol. Cell. Biol. *30*, 640–656.

Thallinger, C., Wolschek, M.F., Maierhofer, H., Skvara, H., Pehamberger, H., Monia, B.P., Jansen, B., Wacheck, V., and Selzer, E. (2004). Mcl-1 is a novel therapeutic target for human sarcoma: Synergistic inhibition of human sarcoma xenotransplants by a combination of Mcl-1 antisense oligonucleotides with low-dose cyclophosphamide. Clin. Cancer Res. *10*, 4185–4191.

Thomas, L.W., Lam, C., and Edwards, S.W. (2010). Mcl-1 ; the molecular regulation of protein function. FEBS Lett. *584*, 2981–2989.

Thomas, L.W., Lam, C., Clark, R.E., White, M.R.H., Spiller, D.G., Moots, R.J., and Edwards, S.W. (2012). Serine 162, an Essential Residue for the Mitochondrial Localization, Stability and Anti-Apoptotic Function of Mcl-1. PLoS One *7*, 1–10.

Tighe, A., Johnson, V.L., and Taylor, S.S. (2004). Truncating APC mutations have dominant effects on proliferation , spindle checkpoint control , survival and chromosome stability. J. Cell Sci. *117*, 6339–6353.

Todt, F., Cakir, Z., Reichenbach, F., Emschermann, F., Kaiser, A., Ichim, G., Tait, S.W.G., Frank, S., Langer, H.F., and Edlich, F. (2015). Differential retrotranslocation of mitochondrial Bax and Bak. EMBO J. *34*, 67–80.

Tokumoto, T., Yamashita, M., Tokumoto, M., Katsu, Y., Horiguchi, R., Kajiura, H., and Nagahama, Y. (1997). Initiation of cyclin B degradation by the 26S proteasome upon egg activation. J. Cell Biol. *138*, 1313–1322.

Topham, C.H., and Taylor, S.S. (2013). Mitosis and apoptosis: how is the balance set? Curr. Opin. Cell Biol. *25*, 780–785.

Topham, C., Tighe, A., Ly, P., Bennett, A., Sloss, O., Nelson, L., Ridgway, R.A., Huels, D., Littler, S., Schandl, C., et al. (2015). MYC Is a Major Determinant of Mitotic Cell Fate. Cancer Cell *28*, 129–140.

Tsui, M., Xie, T., Orth, J.D., Carpenter, A.E., Rudnicki, S., Kim, S., Shamu, C.E., and Mitchison, T.J. (2009). An intermittent live cell imaging screen for siRNA enhancers and suppressors of a kinesin-5 inhibitor. PLoS One *4*, e7339.

Tunquist, B.J., Woessner, R.D., and Walker, D.H. (2010). Mcl-1 Stability Determines Mitotic Cell Fate of Human Multiple Myeloma Tumor Cells Treated with the Kinesin Spindle Protein Inhibitor ARRY-520. Mol. Cancer Ther. *9*, 2046–2057.

Uetake, Y., and Sluder, G. (2004). Cell cycle progression after cleavage failure: Mammalian somatic cells do not possess a “tetraploidy checkpoint.” J. Cell Biol. *165*, 609–615.

Uetake, Y., and Sluder, G. (2010). Prolonged prometaphase blocks daughter cell proliferation despite normal completion of mitosis. Curr. Biol. *20*, 1666–1671.

Uhlmann, F., Lottspeich, F., and Nasmyth, K. (1999). Sister-chromatid separation at anaphase onset is promoted by cleavage of the cohesin subunit Scc1. Nature *400*, 37–42.

Uhlmann, F., Wernic, D., Poupart, M. a, Koonin, E. V, and Nasmyth, K. (2000). Cleavage of cohesin by the CD clan protease separin triggers anaphase in yeast. Cell *103*, 375–386.

Upreti, M., Chu, R., Galitovskaya, E., Smart, S.K., and Chambers, T.C. (2008a). Key role for Bak activation and Bak-Bax interaction in the apoptotic response to vinblastine. Mol. Cancer Ther. *7*, 2224–2232.

Upreti, M., Galitovskaya, E., Chu, R., Tackett, A.J., Terrano, D.T., Granell, S., and Chambers, T.C. (2008b). Identification of the major phosphorylation site in Bcl-xL induced by microtubule inhibitors and analysis of its functional significance. J. Biol. Chem. *283*, 35517–35525.

Uzunova, K., Dye, B.T., Schutz, H., Ladurner, R., Petzold, G., Toyoda, Y., Jarvis, M.A., Brown, N.G., Poser, I., Novatchkova, M., et al. (2012). APC15 mediates CDC20 autoubiquitylation by APC/C(MCC) and disassembly of the mitotic checkpoint complex. Nat. Struct. Mol. Biol. *19*, 1116–1123.

Varetti, G., Guida, C., Santaguida, S., Chiroli, E., and Musacchio, A. (2011). Homeostatic control of mitotic arrest. Mol. Cell *44*, 710–720.

Vaux, D.L., Cory, S., and Adams, J.M. (1988). Bcl-2 gene promotes haemopoietic cell survival and cooperates with c-myc to immortalize pre-B cells. Nature *335*, 440–442.

Veis, D.J., Sorenson, C.M., Shutter, J.R., and Korsmeyer, S.J. (1993). Bcl-2-Deficient Mice Demonstrate Fulminant Lymphoid Apoptosis , Polycystic Kidneys , and Hypopigmented Hair. Cell *75*, 229–240.

Vinitsky, A., Michaud, C., Powers, J.C., and Orlowski, M. (1992). Inhibition of the Chymotrypsin-like Activity of the Pituitary Multicatalytic Proteinase Complex. Biochemistry *31*, 9421–9428.

Vodermaier, H.C., Gieffers, C., Maurer-Stroh, S., Eisenhaber, F., and Peters, J.-M. (2003). TPR Subunits of the Anaphase-Promoting Complex mediate binding to the activator protein CDH1. Curr. Biol. *13*, 1459–1468.

Voets, E., and Wolthuis, R. (2015). MASTL promotes cyclin B1 destruction by enforcing Cdc20-independent binding of cyclin B1 to the APC/C. Biol. Open *4*, 484–495.

Voets, E., and Wolthuis, R.M.F. (2010). MASTL is the human orthologue of Greatwall kinase that facilitates mitotic entry, anaphase and cytokinesis. Cell Cycle *9*, 3591–3601.

Wakui, H., Yamamoto, N., Nakamichi, S., Tamura, Y., Nokihara, H., Yamada, Y., and Tamura, T. (2014). Phase 1 and dose-finding study of patritumab (U3-1287), a human monoclonal antibody targeting HER3, in Japanese patients with advanced solid tumors. Cancer Chemother. Pharmacol. *73*, 511–516.

Wan, L., Tan, M., Yang, J., Inuzuka, H., Dai, X., Wu, T., Liu, J., Shaik, S., Chen, G., Deng, J., et al. (2014). APC(Cdc20) suppresses apoptosis through targeting Bim for ubiquitination and destruction. Dev. Cell *29*, 377–391.

Wang, P., Lindsay, J., Owens, T.W., Mularczyk, E.J., Warwood, S., Foster, F., Streuli, C.H., Brennan, K., and Gilmore, A.P. (2014). Phosphorylation of the proapoptotic BH3-only protein Bid primes mitochondria for apoptosis during mitotic arrest. Cell Rep. *7*, 661–671.

Wang, Y., Seemann, J., Pypaert, M., Shorter, J., and Warren, G. (2003). A direct role for GRASP65 as a mitotically regulated Golgi stacking factor. EMBO J. *22*, 3279–3290.

Wani, M., Taylor, H., Wall, M., Coggon, P., and McPhail, A. (1971). Plant antitumor agents. VI. The isolation and structure of taxol, a novel antileukemic and antitumor agent from Taxus brevifolia. J. Am. Chem. Soc. *93*, 2325–2327.

Weaver, B.A. (2014). How Taxol / paclitaxel kills cancer cells. Mol. Biol. Cell *25*, 2677–2681.

Weaver, B., and Cleveland, D.W. (2005). Decoding the links between mitosis, cancer, and chemotherapy: The mitotic checkpoint, adaptation, and cell death. Cancer Cell *8*, 7–12.

Weaver, B.A., and Cleveland, D.W. (2006). Does aneuploidy cause cancer? Curr. Opin. Cell Biol. *18*, 658–667.

Wei, G., Margolin, A.A., Haery, L., Brown, E., Cucolo, L., Julian, B., Shehata, S., Kung, A.L., Beroukhim, R., and Golub, T.R. (2012). Article Chemical Genomics Identifies and BCL-xL as a Predictor of MCL1 Dependency. Cancer Cell *21*, 547–562.

Wei, S.H., Dong, K., Lin, F., Wang, X., Li, B., Shen, J.J., Zhang, Q., Wang, R., and Zhang, H.Z. (2008). Inducing apoptosis and enhancing chemosensitivity to Gemcitabine via RNA interference targeting Mcl-1 gene in pancreatic carcinoma cell. Cancer Chemother. Pharmacol. *62*, 1055–1064.

Weinstein, J., Jacobsen, F.W., Hsu-Chen, J., Wu, T., and Baum, L.G. (1994). A novel mammalian protein, p55CDC, present in dividing cells is associated with protein kinase activity and has homology to the Saccharomyces cerevisiae cell division cycle proteins Cdc20 and Cdc4. Mol. Cell. Biol. *14*, 3350–3363.

Weiss, E., and Winey, M. (1996). The Saccharomyces cerevisiae Spindle Pole Body Duplication Gene MPS1\nIs Part of a Mitotic Checkpoint. J. Cell Biol. *132*, 111–123.

Welburn, J.P.I., Vleugel, M., Liu, D., Yates, J.R., Lampson, M.A., Fukagawa, T., and Cheeseman, I.M. (2010). Aurora B Phosphorylates Spatially Distinct Targets to Differentially Regulate the Kinetochore-Microtubule Interface. Mol. Cell *38*, 383–392.

Welcker, M., and Clurman, B.E. (2008). FBW7 ubiquitin ligase: a tumour suppressor at the crossroads of cell division, growth and differentiation. Nat. Rev. Cancer *8*, 83–93.

Wertz, I.E., Kusam, S., Lam, C., Okamoto, T., Sandoval, W., Anderson, D.J., Helgason, E., Ernst, J.A., Eby, M., Liu, J., et al. (2011). Sensitivity to antitubulin chemotherapeutics is regulated by MCL1 and FBW7. Nature *471*, 110–114.

Westhorpe, F.G., Diez, M.A., Gurden, M.D.J., Tighe, A., and Taylor, S.S. (2010). Re-evaluating the role of Tao1 in the spindle checkpoint. Chromosoma *119*, 371–379.

Westhorpe, F.G., Tighe, A., Lara-Gonzalez, P., and Taylor, S.S. (2011). p31comet-mediated extraction of Mad2 from the MCC promotes efficient mitotic exit. J. Cell Sci. *124*, 3905–3916.

Wheatley, S.P., Hinchcliffe, E.H., Glotzer, M., Hyman, a a, Sluder, G., and Wang, Y.L. (1997). CDK1 inactivation regulates anaphase spindle dynamics and cytokinesis in vivo. J. Cell Biol. *138*, 385–393.

Williamson, A., Wickliffe, K.E., Mellone, B.G., Song, L., Karpen, G.H., and Rape, M. (2009). Identification of a physiological E2 module for the human anaphase-promoting complex. Proc. Natl. Acad. Sci. U. S. A. *106*, 18213–18218.

Williamson, A., Banerjee, S., Zhu, X., Philipp, I., Iavarone, A.T., and Rape, M. (2011). Regulation of Ubiquitin Chain Initiation to Control the Timing of Substrate Degradation. Mol. Cell *42*, 744–757.

Willis, S.N., Chen, L., Dewson, G., Wei, A., Naik, E., Fletcher, J.I., Adams, J.M., and Huang, D.C.S. (2005). Proapoptotic Bak is sequestered by Mcl-1 and Bcl-xL, but not Bcl-2, until displaced by BH3-only proteins. Genes Dev. *19*, 1294–1305.

Wolf, F., Wandke, C., Isenberg, N., and Geley, S. (2006). Dose-dependent effects of stable cyclin B1 on progression through mitosis in human cells. EMBO J. *25*, 2802–2813.

Wolthuis, R., Clay-Farrace, L., van Zon, W., Yekezare, M., Koop, L., Ogink, J., Medema, R., and Pines, J. (2008). Cdc20 and Cks Direct the Spindle Checkpoint-Independent Destruction of Cyclin A. Mol. Cell *30*, 290–302.

Woods, a, Sherwin, T., Sasse, R., MacRae, T.H., Baines, a J., and Gull, K. (1989). Definition of individual components within the cytoskeleton of Trypanosoma brucei by a library of monoclonal antibodies. J. Cell Sci. *93 (Pt 3)*, 491–500.

Woods, C.M., Zhu, J., McQueney, P.A., Bollag, D., and Lazarides, E. (1995). Taxol-induced mitotic block triggers rapid onset of a p53-independent apoptotic pathway. Mol. Med. *1*, 506–526.

Wurzenberger, C., and Gerlich, D.W. (2011). Phosphatases: providing safe passage through mitotic exit. Nat. Rev. Mol. Cell Biol. *12*, 469–482.

Yu, J., Zhang, L., Hwang, P.M., Kinzler, K.W., and Vogelstein, B. (2001). PUMA induces the rapid apoptosis of colorectal cancer cells. Mol. Cell *7*, 673–682.

Zasadil, L.M., Andersen, K.A., Yeum, D., Rocque, G.B., Wilke, L.G., Tevaarwerk, A.J., Raines, R.T., Burkard, M.E., and Weaver, B.A. (2014). Cytotoxicity of Paclitaxel in Breast Cancer Is due to Chromosome Missegregation on Multipolar Spindles. Sci. Transl. Med. *6*, 1–10.

Zeng, X., Sigoillot, F., Gaur, S., Choi, S., Pfaff, K.L., Oh, D.-C., Hathaway, N., Dimova, N., Cuny, G.D., and King, R.W. (2010). Pharmacologic inhibition of the anaphase-promoting complex induces a spindle checkpoint-dependent mitotic arrest in the absence of spindle damage. Cancer Cell *18*, 382–395.

Zhai, Y., Kronebusch, P.J., Simon, P.M., and Borisy, G.G. (1996). Microtubule dynamics at the G2/M transition: Abrupt breakdown of cytoplasmic microtubules at nuclear envelope breakdown and implications for spindle morphogenesis. J. Cell Biol. *135*, 201–214.

Zhang, C.-Z., Spektor, A., Cornils, H., Francis, J.M., Jackson, E.K., Liu, S., Meyerson, M., and Pellman, D. (2015). Chromothripsis from DNA damage in micronuclei. Nature *522*, 179–184.

Zhong, Q., Gao, W., Du, F., and Wang, X. (2005). Mule/ARF-BP1, a BH3-only E3 ubiquitin ligase, catalyzes the polyubiquitination of Mcl-1 and regulates apoptosis. Cell *121*, 1085–1095.

Zhu, Y., Zhou, Y., and Shi, J. (2014). Post-slippage multinucleation renders cytotoxic variation in anti-mitotic drugs that target the microtubules or mitotic spindle. Cell Cycle *13*, 1756–1764.

Van Zon, W., Ogink, J., Ter Riet, B., Medema, R.H., Te Riele, H., and Wolthuis, R.M.F. (2010). The APC/C recruits cyclin B1-Cdk1-Cks in prometaphase before D box recognition to control mitotic exit. J. Cell Biol. *190*, 587–602.